PITTING CORROSION INITIATION IN AISI 316 AUSTENITIC STAINLESS STEEL

By

H. Quinones

Submitted for the degree of

Doctor of Philosophy

BRUNEL UNIVERSITY

METALLURGY DEPARTMENT

APRIL, 1980

ACKNOWLEDGEMENTS

I would like to thank Mr. D.E.J. Talbot for advice and encouragement during the course of the work and Professor C. Bodsworth for the provision of laboratory facilities.

I would like to express my appreciation of Dr. F. Rivero and his interest and encouragement and for making the time available for carrying out the research programme.

I would also like to acknowledge the financial support provided by *FONINVES*, Caracas, (Venezuela).

ABSTRACT

The initiation of pitting corrosion on AISI 316 stainless steel has been examined from a phenomenological viewpoint with emphasis on the role of the metal in this complex interaction. A modified potentiodynamic technique was used to prepare specimens corresponding with a series of different points on the anodic polarisation curve for the material in 0.05 M sulphuric acid alone and with additions of 0.1 M sodium chloride solutions. The specimens were subsequently examined using standard metallographic techniques. It was found that suitable pit nuclei , called 'pit sites', are manifest as a result of the initial interaction of the metal with the solution at the rest potential, (E_R), i.e.,at potentials far below the potential range in which catastrophic pitting processes normally occur. It was further found that these pit sites were manifest even in the absence of chloride ions for which there is no subsequent catastrophic pitting process. Estimation of pit site density (N_A) for the different stages of the E-i curve and the use of a simple stereological model permit a statistical interpretation of the localisation of the phenomenon to particular areas of the metal surface. The statistical argument is extended to show that the breakdown potential for chloride media is associated with the development of a catastrophic condition which does not apply if chloride ions are absent and it is deduced that the breakdown potential is essentially indeterminate.

CONTENTS

1. INTRODUCTION

The increased use of highly corrosion and oxidation resistant metallic materials has brought about a marked interest in understanding localised corrosion processes. These forms of metallic structure deterioration are the main type of failure observed in the service life of these materials and the main problem is that they appear unpredictably, a fact which poses a great difficulty in their control. The Corrosion Science framework, outlined briefly in chapter 2, seems to be insufficient for a basic understanding of these phenomena which is a fundamental requirement in developing the means to control them. Stainless steels are typical examples of special metallic materials which owe their applications to their outstanding corrosion resistance. They are complex systems from a metallurgical viewpoint and their main property is related to a complex phenomenon, i.e., the passivity phenomenon, which has been widely studied as can be appreciated from discussions developed in Chapters 3 and 4. Localised corrosion appears to be related to the breakdown of the passive state formed as the manifestation of the passivity phenomenon. However, these aspects of the metal-solution interaction are not fully understood as yet. It is quite surprising to find that one of the reasons for this inadequate understanding is the lack of phenomenological studies of these processes although a large volume of other work is reported in the literature, as illustrated throughout discussions developed in Chapter 4. It seems important to direct some effort towards approaching these problems from a phenomenological viewpoint to provide a preliminary basic understanding after which a theoretical framework can be proposed. It is only through a clear perception of the phenomenon that improved solutions to practical problems can be presented.

Chapters 5, 6 and 7 are the synthesis of a research work conducted within this context. Pitting corrosion has been selected for this study because it is the example par excellence of localised attack and moreover, there is a large volume of results from previous experimental work to draw upon to aid in interpretation. AISI 316 austenitic stainless steel was selected as the material on which the study was carried out because of its outstanding corrosion resistance to this particular type of localised corrosion.

2. BASIC ASPECTS OF CORROSION

The literature dealing with the fundamental aspects of corrosion and the different forms in which it is manifest is very extensive; excellent books are available which clearly discuss the concepts and theories involved. Nevertheless, it is important to review some principles to illustrate the complexity of the phenomenon and to define the framework for discussions developed later.

2.1 DEFINITION AND CLASSIFICATION

Corrosion is a complex subject born of the triumph of the industrial revolution which was characterised fundamentally by the use and commercialisation of metallic materials. Because of the nature of the phenomenon, it is difficult to define corrosion satisfactorily covering all factors involved. However, it is possible to specify what is or should be understood by corrosion but as Shreir[1] has pointed out the definition differs according to whether it is given in the context of corrosion science or corrosion engineering, as follows:

> Corrosion Science definition: the reaction of a solid with its environments.
>
> Corrosion Engineering definition: the reaction of an engineering constructional metal (material) with its environment with the consequent deterioration in properties of the metal (material).

Broadly speaking, corrosion reactions are classified into dry and wet reactions depending on whether water and its constituent

ions take part in the reaction. The term "Dry Corrosion" is applied to reactions between gases and metals characterised by oxidation of the metal and reduction of the non-metal (gas) on the same place at the metal/gas interface. Typically the gas phase is oxygen and its direct ionisation is an essential feature of the mechanism. The situation in wet corrosion reactions is different; the oxidation of the metal and the reduction of species in solution occur at different areas on the metal surface with the consequent development of an electronic current through the metal; the metal atoms are transformed to their hydrated ions and the oxygen, if involved in the process is ionised to hydroxyl ions through a complex mechanism in which the hydronium ion or water take part[2].

The present work is concerned mainly with a particular type of wet corrosion, considered from the corrosion science view point or definition. From now onwards, the term corrosion and corrosion reaction will be applied in this context unless stated otherwise.

2.2 THERMODYNAMICS AND CORROSION

One very important principle to bear in mind when working in corrosion science is that the system under study is in a state of non-equilibrium with its environment and therefore corrosion reactions appear as a manifestation of the path followed by the system towards its equilibrium. Classical thermodynamics deals with systems under equilibrium and its application predicts with certainty when a given system is in equilibrium or whether it will

react to conform with such a final state but does not provide any idea of for how long or by which path the system will change in reactions by which it reaches the equilibrium state. These two points are irrelevant to thermodynamics but they are the main concern of corrosion science for even if corrosion reactions appear unavoidable, an understanding of them allows better control of their occurrence. Nevertheless, thermodynamic reasoning in corrosion is characterised by the works of Nernst and Pourbaix. The former formulated an expression which relates the potential of a piece of metal with the activity of its ions in solution and the latter introduced a diagrammatic approach to show the stability regions of a metal and different possible compounds resulting from the metal-solution interaction as a function of the potential of the metal and the pH of the solution.

2.2.1 The Nernst Equation

Chemical reactions in which the resultant products exhibit different oxidation states from those of the reactants occur through electron transfer or electron exchange mechanisms (called electrochemical reactions). Advantage can be taken from this fact to produce electrical work, providing that there is a suitable physical separation of reactants as for instance in the case of a galvanic cell *. The Nernst equation formulation predicts that the maximum of electrical work available from such a system is equal to

* In general the term electrochemical cell is applied.

the change in Gibbs free energy for the chemical reaction

i.e.,

$$\Delta G = -n\ F\ E \qquad (1)$$

where ΔG is the change in free energy for the reaction, n is the number of electron moles transferred in the reaction, F is the Faraday constant and E is the electromotive force or potential difference between electrodes of the cell. From this expression, it is simple to derive the Nernst equation by applying it to the Van't Hoff isotherm

$$E = E^{\theta} - \frac{RT}{nF} \ln Q \qquad (2)$$

where R is the gas constant, T is the temperature, Q is the activity quotient of species in the reaction and E^{θ} is the electromotive force for the cell when the interacting species are in their standard states.

Although this equation is useful in predicting electromotive forces of galvanic cells and in calculating these values from thermodynamic data through its relation to ΔG, it has also been applied to situations in which its validity is open to question. Furthermore, when the Nernst equation was first available, early in this century it proved so useful in guiding the study of electrochemical reactions that it inhibited consideration of kinetic aspects which are now regarded as equally if not more important. Bockris and Reddy[3] described this phase in electrochemistry as the "Nernst hiatus".

The influence of this formulism in corrosion science was immediate because any corrosion reaction must involve oxidation

of the metal and reduction of a specie in solution with the consequent electron transfer between reactants and can be conceived as the result of the setting up of galvanic cells on the metal surface due to differences in concentration of species in solution, differences in composition of the metal at the surface or both.

2.2.2 Pourbaix Diagrams

Extensive application of the Nernst eqation is illustrated throughout the work of Pourbaix and his collaborators[4]. They have evaluated thermodynamic information for M/H_2O systems (metal/water) at $25^{o}C$ and their results are represented in the form of equilibrium diagrams having E, equilibrium potential versus standard hydrogen electrode (SHE), as ordinate and pH of the solution as abscissa. These diagrams show the region of stability for the different species referred to arbitrarily chosen activities, giving thus, an idea of the thermodynamic tendency of the changes which will take place when a metal is immersed in water under a prescribed condition of potential and pH. A particular meaning has been given to them in corrosion science which leads to a straightforward interpretation; the diagrams are divided into zones which correspond with:

Corrosion: representing all areas in which stable species are in solution; for delimitation of these regions a minimum activity of 10^{-6} has been chosen for ions in solution.

Inmunity: the area in which the metal is unaffected or stable.

Passivity: all areas in which the stable species are solids different from the metal, usually oxides and hydroxides, for if deposited on the metallic surface they would hinder the dissolution reaction of the metal.

It must be emphasised that these diagrams have serious limitations imposed by the assumptions made in their derivation and construction. Thus, strictly speaking the metal - water system exists only at pH = 7; at any other value of pH, different species from water must be introduced resulting in a more complex system with the possibility of forming species other than those predicted in the M- H_2O diagram. Furthermore a given value of pH can be prepared by different acids or bases and everyone of them might result in chemically different products e.g., in consequence, a diagram calculated on the assumption of variation of pH with sulphuric acid might not be valid when the same range of pH is produced with hydrochloric acid.

The stability of solids formed by dissolution of a metal aqueous solution follows a thermodynamic criterion which implies that the whole metal will be transformed to such a state; the fact that at certain stages of the reaction a particular situation might arise leading to its termination is neither explicit nor implicit in the thermodynamic framework, i.e., thermodynamics cannot account for the principle of passivity. Moreover, solids formed in aqueous solution can differ structurally from those formed in other conditions even if they are isomers; for example, in the case of iron it is well known that ferric oxide is non-existent as $Fe(CH)_3$; the product formed is usually represented by the formula $Fe_2O_3\ nH_2O$, and is described as a hydrated ferric oxide, but this formula does

not reveal the also well known fact that what is formed in solution is a colloid which has a very different structure from solid ferric oxide. This structural difference could result in different diagrams according to whether the calculated free-energy of formation is based on one or the other structures. Unfortunately, the chemistry of colloids is a very complex subject and in practice the description of the solid formed in aqueous solution is easier if the assumption of ferric oxide is made.

2.3 ELECTROCHEMISTRY AND CORROSION

Advances in studying corrosion reaction mechanisms are intimately connected with those made in electrochemistry because of the nature of the phenomena. Hence it seems necessary to summarise some basic aspects of this formulism.

2.3.1 The Electroneutrality Principle

This is a fundamental physical principle which can be stated as "In any given isolated system the total negative charge is equal to the total positive charge"; there are other equivalent statements of this natural law; thus for a system under the influence of an external field "The flux of negative charges must be equal to the flux of positive charges". The application of this principle to electrochemical reactions results in the equality of the rate of the oxidation process to that of the reduction process:

$$I_a = I_c \qquad (3)$$

where I is the current intensity and can be taken as a measure of the rate or flux of charges. In a general process with several electrodes involved:

$$\Sigma I_a = \Sigma I_c \qquad (4)$$

If the current densities are introduced as a measure of the flux of charges, the relation of equality is no longer fulfilled because the areas supporting different reactions can be different. From this situation it follows that a criterion for general dissolution or uniform corrosion is given by the relation:

$$\Sigma i_a = \Sigma i_c \qquad (5)$$

and for localised attack:

$$\Sigma i_a > \Sigma i_c \qquad (6)$$

2.3.2 The Metal-Solution Interface

The region in which a solution makes contact with a metal is called the metal solution interface. It has been one of the aspects of major interest in electrochemistry because any dissolution of the metal occurs by a charge transfer mechanism in this region. Even when there is no reaction a special situation exists at the interface, reflecting differences in nature between the two adjacent phases. Electrons are not free to move between the phases under the influence of electric fields in the classic sense, so that their dynamics are more complex and are better represented within the framework of

quantum mechanics. Different theoretical models have been proposed for the structure of the interface[6]. The commonly accepted representation is as in Fig. 1, which illustrates a rearrangement of charges in the neighbourhood of the metal surface, reflecting a compromise distribution of charges due to differences in the natures of the phases, e.g., differences in electron conductivity. In consequence, the interface is electrified and a potential difference ($\Delta \phi_e$) is built up across it which is intrinsic to the metal solution system. This potential difference ($\Delta \phi_e$) between the metal and the solution is not a measurable physical parameter because in the measuring procedure, a term of comparison or reference must be introduced, such as the standard hydrogen electrode (SHE), giving then a value $\Delta\phi = \Delta\phi_e - \Delta\phi SHE$ which is measurable but not separable into its component parts. The convention of assigning a value $\Delta\phi_{SHE} = 0$ does not improve our knowledge of $\Delta\phi_e$ though it is found to be convenient.

Remark: Most of the experimental evidence explained with this model is based on the particular interface of the mercury electrode which not only offers a clean and highly polarisable surface reducing the problem of charge leakage, i.e., there is no net reaction involved, but also presents a uniform and reproducible structure. Electrodes of other metals deviate from this almost ideal condition making the study of their interfaces very difficult.

2.3.3 The Butler-Volmer Equation

The metal-solution interface is not a static structure but is a dynamic equilibrium in which, due to the thermal energy of the system and the high field strength ($\Delta\phi_e$ acting over very short distances), there is a continual passage of electrons from the metal to ions in the interface and in the reverse direction, i.e., there are anodic and cathodic reactions occurring simultaneously with a net zero current.

$$i_a = i_c = i_o \qquad (7)$$

where i_o is called the equilibrium exchange current density.

A net current density will be produced when there is a change in potential either in the metal or in the solution, producing a departure from the equilibrium value previously reached ($\Delta\phi_e$). The amount by which the potential difference ($\Delta\phi$) departs from the equilibrium value ($\Delta\phi_e$) is called the overpotential (η). It has been shown[7] that in this condition the net current density is given by the expression:

$$i = i_o\{\exp(\overleftarrow{\alpha}\,\eta\,F/RT) - \exp(-\overrightarrow{\alpha}\,\eta\,F/RT)\} \qquad (8)$$

where $\overrightarrow{\alpha}$ and $\overleftarrow{\alpha}$ are parameters related to the mechanism of the reaction and called transfer coefficients. The arrows indicate whether the reaction is anodic ($\leftarrow$) or cathodic ($\rightarrow$). This expression is the simplified form of the Butler-Volmer equation which provides a theoretical tool for studying electrochemical reactions.

It must be emphasised that in deriving this equation some important assumptions have been made such as to consider the metal dissolution and metal deposition as separate anodic and cathodic reactions respectively, i.e.,

$$M \rightarrow M^{+} + e \qquad \text{anodic reaction} \qquad (9)$$

$$M^{+} + e \rightarrow M \qquad \text{cathodic reaction} \qquad (10)$$

which are possible but not necessarily the only process at the metal solution interface in the equilibrium condition. When a positive overpotential, for instance, is applied the anodic reaction is favoured; the reaction occurs only if there are other species in solution which can react accepting electrons to make the balance of charges within the system possible. In aqueous solutions this usually occurs by hydrogen evolution or oxygen reduction:

$$2\,H^{+} + 2e \rightarrow H_2 \qquad (11)$$

$$O_2 + 2H_2O + 4e \rightarrow 4OH^{-} \qquad (12)$$

The overall reaction is not just metal dissolution (equ. 9) but simultaneous metal dissolution and oxygen reduction or hydrogen ion reduction (eqns 9 + 11 or 12). All of these processes occurring on different areas of the metal surface or at separate electrodes have their own reaction mechanisms and a Butler-Volmer equation can be written for each of them:

$$i_a = i_{o,a}\{\exp(\overleftarrow{\alpha}_a\, n_a\, F/RT) - \exp(-\vec{\alpha}_a\, n_a\, F/RT)\} \qquad (13)$$

$$i_c = i_{o,c}\{ \exp (\overleftarrow{\alpha}_c \, n_c \, F/RT) - \exp (- \vec{\alpha}_c \, n_c \, F/RT)\} \quad (14)$$

Assuming uniform dissolution, the corrosion current density is defined by the identity:

$$i_{CORR} = i_a = i_c \quad (15)$$

which reveals that the corrosion rate depends on the kinetics and mechanism of the anodic and cathodic processes. Moreover, it occurs when the system is not at equilibrium, i.e., there is a significant net current when there is an overpotential. The anodic and cathodic reactions occur by several steps, the slowest of which determines the overall corrosion rate. Thus, if mass transport is the critical factor, it will be presumably more important in sustaining the cathodic reaction for which species from the solution have to make contact with the metal. The cathodic process will then depend on the diffusion rate of these species in solution towards the electrode, resulting eventually in a current density limit (i_L) for the cathodic reaction; hence the overall corrosion rate is cathodically controlled or more precisely diffusion controlled. On the other hand, if the anodic reaction is altered in one of its steps, either because metal ions do not diffuse towards the solution but are immediately hydrolysed and deposited over the metal surface or because the anodic products are not metal ions but metal oxide, then the overall process can be anodically controlled as it is in the case of a passivated metal.

3. BASIC ASPECTS OF STAINLESS STEELS

Resistance to oxidation and dissolution in acid media of iron-chromium alloys were observed since last century and works on their metallurgy and mechanical properties were reported in the 1900s[8]. But it was later in the 1920's that technical and economical reasons made possible the development of stainless steels, e.g. improvements in power generating plants required materials with combined oxidation resistance and good mechanical properties, expansion of chemical industries demanded high corrosion resistance materials, etc. H. Brearley had introduced in 1916 a 12-13% Cr. martensitic steel for cutlery in Sheffield, but it was in 1924 that the well known 18% Cr - 8%Ni. with 0.10-0.15%C. austenitic steel came out, also in Sheffield, as a development of a 0.25%C-20%Cr-7%Ni., steel introduced by Strauss in Germany; its excellent mechanical properties and high corrosion resistance established it as the prototype of stainless steels. Nowadays, the term stainless steel is applied to a wide range of chromium-bearing iron alloys with not less than 12%Cr. content, although other elements are commonly added to enhance certain desired properties. The main types are[9]:

Ferritic steels: which contain 15-30%Cr. low carbon content, no nickel and often some molybdenum, niobium or titanium. These are highly corrosion resistant, they exhibit little or no transformation and they are susceptible to grain coarsening on heating to high temperatures and to certain forms of embrittlement.

Martensitic steels: which contain 12-17%Cr and 0.1-1%C. These are austenitic at temperatures of 950-1000^{o}C. but transform to martensite on

cooling. Their high hardenability makes them air-hardenable which can lead to difficulty in softening them for machining and fabrication, particularly as they are frequently alloyed with molybdenum or vanadium to produce a high degree of tempering resistance.

Austenitic steels: which contain 18-25%Cr, 8-20%Ni and low carbon contents. These steels also often contain additions of molybdenum, niobium or titanium and are predominantly austenitic at all temperatures. The austenite may have varying degrees of stability with respect to the formation of martensite, being transformed by cold work at room temperatures for some compositions. Other compositions are stable at temperatures down to -196°C and are not transformed even after the most severe deformation.

Precipitation - hardenable steels: designed as a compromise to combine the strength of a martensitic steel with the corrosion resistance of an austenitic steel. They contain 14-17%Cr, some C, Ni, Mn, Si and selected additions from among Co, Ti, Cu Mo, Al. They are austenitic at the solution treatment temperature but have transformation temperatures which can be adjusted by various thermal and mechanical treatments so that they can be either metastable austenitic or martensitic at room temperature. The transformation to martensite together with other mechanisms can be utilised to introduce age-hardening by suitable subsequent thermal and mechanical manipulations.

Thus, stainless steels are complex systems containing not only iron, chromium and carbon but also selected elements as nickel, molybdenum, titanium, etc. Their phase relationships are difficult to represent comprehensively in temperature composition equilibrium diagrams because of the large number of degrees of freedom due to composition variables. However, the general principles of alloying can be appreciated from considerations of binary systems and projections of ternary or multi-dimensional phase diagrams.

3.1. THE IRON-CHROMIUM SYSTEM AND THE EFFECT OF FURTHER ALLOYING

The fundamental aspects of the physical metallurgy of stainless steels are derived from the Fe-Cr binary system as these are their essential constituents. The basic phases derive from the allotropic forms of iron, evident from the equilibrium diagram in Fig. 2. Between 1400 and 1539°C, pure iron exists crystallographically as body-centered cubic phase (BCC) whose solutions are called Ferrite. This highest temperature allotrope is often termed delta ferrite (δ). Between 910 and 1400°C, iron is face-centered cubic (FCC) and solutions of this allotrope are called austenite or gamma phase (γ). Below 910°C, iron once again becomes BCC and its structure is identified as alpha ferrite (α). The delta and alpha ferrites are physically indistinguishable but their chemistry may differ. The nomenclature serves to identify the conditions of formation.

The addition of chromium up to about 7% reduces the temperatures of both BCC $\rightleftharpoons$ FCC transformation points. Above 7%, the temperature interval over which austenite exists gradually decreases until, about 12 - 13% Cr, no transformation occurs and ferrite exists at all temperatures. Thus, the region of stability of γ solid solutions is confined to an enclosed area or γ-loop and chromium is said to be a ferrite-forming element. Between the γ-loop and the α-phase field there is a narrow transition region where an alloy will have both α and γ phases which, depending on the quench rate, may or may not be retained at room temperature. The location of the γ-loop in the Fe-Cr phase diagram has been carefully

studied by Baerlecken, Fischer and Lorentz[11]; they reported 840°C and 6.5%Cr for the lowest point in the γ-loop, the greatest width of the two phases field is at about 1,075°C and the complete enclosure is at about 11.5%Cr. Since the greatest expansion of the γ-region is to about 10.6%Cr, the two phases (α + γ) region is very narrow.

There is a second important zone at lower temperatures centered at about 45% Cr. An intermetallic compound, Fe-Cr containing one atom of iron with one atom of chromium, known as sigma phase (σ), is formed. Above 820°C, it dissolves back into the chromium-rich ferrite (α) phase. It is hard, non-magnetic and exists in a tetragonal structure. Pure sigma phase forms between 42 and 50% Cr while a duplex structure (α + σ) has been found[12] to form in alloys with as little as 25% and as much as 70% Cr., after prolonged exposure to temperatures between 500-800°C.

Carbon is a common element in all steels unavoidably introduced in the ironmaking and steelmaking processes. It imparts strength and hardness to iron alloys and modifies the Fe-Cr diagram in two respects. Firstly, it increases the stability region of gamma solutions shifting the limit of the loop to a higher chromium content and widening the duplex (α + γ) field. Carbon is said to be an austenite stabiliser; its effect is a maximum at 0.6%C at which the limits of these regions correspond to 18 and 27%Cr contents respectively, Fig. 3. The second effect is the formation of carbides which are complex compounds with the formulae $(Fe, Cr)_3C$, $(Fe, Cr)_{23}C_6$ and $(Fe, Cr)_7C_3$; they are usually indicated as K_0, K_1, K_2 respectively

in phase diagrams. Carbides can co-exist with ferrite even at high temperatures because of the low solubility of carbon in this phase. The $M_{23}C_6$ type in particular can have a detrimental effect due to the large number of metallic atoms required for its formation. This leads to a localised region impoverished in chromium resulting in loss of the corrosion resistance locally, e.g., intergranular corrosion of austenitic stainless steels.

The section of the Fe-Cr-C ternary system at 17%Cr is presented as a pseudo-binary Fe-C diagram in Fig. 4. This serves to illustrate the complexity of the behaviour of chromium steels during heat-treatment. Below 0.08%C, the steels are entirely ferritic and undergo no transformation at any temperature. In the range, 0.08-0.22%C, heating brings about partial transformation and produces a duplex ($\alpha + \gamma$) structure which after quenching becomes duplex martensitic-ferritic. Finally, above 0.22%C, the steels can be austenised and react normally to quenching treatments resulting in martensitic steels.

Another important element in stainless steels is nickel which, having a FCC structure, has the opposite effect to that of chromium when alloyed with iron[15]. Nickel is an austenite former and hence it produces an expansion of the γ-field when added to the Fe-Cr system; this can be appreciated from Fig. 5. There is also an increase in the stability of the σ-phase over a wider range of Cr-content and extending to higher temperatures.

The combined addition of nickel and carbon leads to a stable austenite phase at room temperature whose high ductility and formability make it the most widely used stainless steel. The influence of chromium on the minimum nickel content required for a stable austenitic structure in steels containing 0.1%C is shown in Fig. 6. The predominant place occupied by the combination 18%Cr-8%Ni as the prototype for austenitic stainless steels can be immediately appreciated because it minimises the expensive nickel addition.

Finally, there are some other elements which are present in small quantities. They can be grouped as:

i) Minor alloying elements, deliberately added to impart specific properties, e.g., molybdenum for improving oxidation and corrosion resistance, titanium and niobium for stabilising.

ii) Residual elements, which are not intentionally added and should be regarded as impurities inherited from the manufacturing process of steels; their effects are variable depending on the form they are present in, i.e.

solid solution,
metallic or non-metallic phases[17].

A systematic assessment of the phase relationships in such complex systems is impossible. However, the combined effect of all of these elements on the structure can be summarised in the well known Schaeffler diagram constructed by grouping the component elements ferritisers and austenitisers. Their relative effects are expressed on scales of equivalent chromium and nickel contents respectively, i.e.

$$\text{Ni equivalents} = \% \text{ Ni} + 30 \times \% \text{ C} + 0.5 \times \% \text{ Mn}$$

$$\text{Cr equivalents} = \% \text{ Cr} + \% \text{ Mo} + 1.5 \times \% \text{ Si} + 0.5 \times \% \text{ Nb}$$

Some other authors have proposed different coefficients and introduced other elements[18]; in any case, these diagrams should not be used to define precisely the phases present in wrought and cast steels but as an indication of the relative potency of the respective austenite and ferrite stabiliser or former.

The foregoing discussion has referred only to the essential features of the physical metallurgy of stainless steels. More complete analysis of the structure and possible transformations in these complex systems is given by Pickering[9, 19].

3.2. THE ESSENTIAL PROPERTY OF STAINLESS STEELS

The property which distinguishes stainless steels from other ferrous materials and makes them special is their outstanding corrosion resistance; their mechanical properties and formability characteristics can equal those of many other steels by suitable alloying but they are not their fundamental attributes[9, 19]. Apparently, there is an intrinsic nobility or stability of these alloys in air and water in contrast to iron and other steels which rust under the same conditions. However, they are not exempt from undergoing corrosion reactions in certain conditions and these are difficult problems to face without a prior understanding of the meaning of 'stainless'. This, in turn, has been the subject of a long discussion in corrosion science particularly since it was realised that the normal behaviour of stainless steels is the

same as the abnormal behaviour of iron in the special case of exposure to fuming nitric acid where a peculiar phenomenon called passivity occurs. Iron dissolves readily in sulphuric acid, but the reaction in nitric acid depends on the conditions of the acid, if it is dilute there is a vigorous dissolution, but the reaction ceases after a few seconds if it is saturated with nitrogen dioxide. Thus, the passivity phenomenon is the cessation of dissolution of a metal/alloy under conditions in which thermodynamically there is a driving force for the reaction to occur[20]. Actually, there is a decrease in the dissolution rate to such an extent that it appears as if there is no reaction. This situation is clearly different from those in which the reaction is not produced simply because it is not favoured thermodynamically and the metal is said to be inert, e.g., in the case of gold in dilute acids.

To appreciate that the behaviour of stainless steels is a manifestation of the passivity phenomenon, but to a different degree, it is convenient to consider the electrified metal-solution interface as an electrical device and study its response under different electrical conditions. It was only when the voltage-current characteristics* for these electro-chemical systems were available that a clear view of the passivity phenomenon was possible[21]. These curves are determined with the aid of electronic equipment, e.g. potentiostat, galvanostat; or studying the dissolution rates of metals in solutions with different redox potentials. It has been shown elsewhere[22] that these different procedures lead to equivalent results, i.e., the polarisation can be produced either with natural chemical processes or artificially.

*Also known as polarisation curves.

The general shape of these E-i curves is as illustrated in Fig. 7, its relevant features can be summarised as follows:

i. Applications of low potentials (over potentials), at the metal-solution interface, result in current densities which correspond with metal dissolution; the interface works as an electrical conductor following not Ohm's law but a Butler-Volmer relation (equ. 8). This region is called the activity zone.

ii. The current density does not increase monotonously by further increments in potential, as would be expected, but decreases instead to a very small value which remains constant over a range of overpotentials, i.e., the interface acts as a poor conductor. This region is called the passive zone or passivity area in contrast to the initial behaviour.

iii. The interface becomes again an electrical conductor at very high over potentials. This is called transpassive zone.

iv. The active-passive transition occurs at a particular point in the curve, being characterised by particular values of potential and current density which are denoted passivation potential (Epp) and critical current density (i_{CRI}). The potential at which the minimum current density is reached is called Flade potential (E_F); some authors[24] interpret it as the potential for the onset of full passivity.

The explanation of the behaviour of iron in acids is now straightforward: the redox potential of iron ($E^{\ominus}_{Fe^{2+}/Fe^{o}}$) is -0.440 volts and that of sulphuric acid is near that of the SHE; therefore when iron is immersed in this acid the overpotential built up on the Fe/acid interface corresponds to a value in the activity region and dissolution occurs. In the case of fuming nitric acid, the redox potential is +1.07 volts which corresponds to the reduction of nitrogen dioxide; the overpotential at the interface is now in the passive region and the dissolution reaction of the metal occurs at a very low rate.

Stainless steels produce the same type of E-i characteristics in acids as shown in Fig. 8, where the E-i curve for a 18%Cr-8%Ni austenitic stainless steel is compared with those of iron, chromium and nickel. It is apparent that all of these materials behave in the same way and their differences are in degrees. Chromium exhibits the lowest Epp value and though its i_{CRI} is not also the lowest its current density in the passive region is extremely low, as a matter of fact, the normal behaviour of chromium is that of a noble metal. The steel exhibits a low passivation potential and a very low value of i_{CRI} which is about 10^{-4} the value for Fe and 10^{-2} of that for Cr, these values make it readily passivating over a range of 1 volt. It is this fact which lies at the root of the corrosion resistance of this material. The alloying of iron with chromium is manifest then in lowering the values of Epp, E_F and i_{CRI}; this is better appreciated from table I[26] and the data from it plotted in Fig. 9. The effect on the value of E_F becomes important for chromium contents above 12% which turns out to be the criterion generally accepted as implying that the material is stainless. Moreover, additions of nickel improve the ease with which these alloys are passivated by lowering still more the values of i_{CRI} and E_F, as illustrated in this table for 18% Cr - 8%Ni, with i_{CRI} = 2 mA/cm^2 and E_F = -0.10 volts (SHE scale), compared with i_{CRI} = 11 mA/cm^2 for the binary of 18%Cr. In this way, the property of stainless steels, i.e., excellent corrosion resistance, is a consequence of their ability to become passive.

It must be emphasised that passivity is not restricted to iron and iron-alloys, it appears to be a more general and fundamental phenomenon of the behaviour of metallic materials. According to

Tomashov[27], metals can be arranged in decreasing order of degree of passivity as follows: Zr, Ti, Ta, Nb, Al, Cr, Be, Mo, Mg, Ni, Co, Fe, Mn, Zn, Cd, Sn, Pb, Cu. The widespread occurrence of the phenomenon and its intimate connection with corrosion are the reasons for the enormous interest in understanding the passivating mechanism, as will be discussed in the next chapter.

3.3. CORROSION OF STAINLESS STEELS

General corrosion is produced when the entire surface of the metal or alloy exposed to the solution is attacked uniformly. This can result in severe losses of material but it is nevertheless the least dangerous type of corrosion since the attack is reflected in a uniform reduction in thickness of the material and can generally be predicted. The conditions in which it occurs are identifiable with those of the active or transpassive regions of the voltage-current curve. Hence, it is reduced to a minimum when passivity is established over the material surface. Stainless steels show an excellent resistance to this type of corrosion but care must be taken to ensure that the conditions correspond to those of the passive region. This can be illustrated by considering a ferritic steel (18%Cr type AISI 430) and two austenitic steels (18% Cr-8%Ni type AISI 304 and 18%Cr - 10%Ni - 3%Mo type AISI 316)[28] whose anodic polarisation curves are shown in Fig. 10. In a moderately oxidising electrolyte such as 20% HNO_3 at 90°C, all of them will be passive and the corrosion rate will be below 0.1mm/yr, but if the electrolyte is strongly oxidising, e.g. 99% HNO_3 at 40°C, then the corrosion potential will lie in the transpassive region and the corrosion rate will be more than 1mm/yr. An intermediate

situation occurs in the case of 5% H_2SO_4 at room temperatures. The type 316 steel will be passive and its corrosion rate will be below 0.1mm/yr; the type 430 steel will dissolve at a rate exceeding 1mm/yr; finally for the type 304 steel the passivity and corrosion rate are determined by the aeration of the acid; if the acid is air-saturated, passivity will be established because that solution will yield a diffusion-controlled current density limit of 100$\mu A/cm^2$ but if it is less than this value the steel will be active as illustrated in Fig. 10; therefore the corrosion rate will be somewhere between 0.1mm/yr and 1mm/yr depending on the degree of aeration.

Austenitic-steels are the most widely used and a great deal of the work reported in the literature refers to this type. Ferritic steels show higher i_{CRI} but improvements are made by alloying with molybdenum[29]. Martensitic steels are the least corrosion resistant because the fabrication of these alloys requires heat treatments to optimise the mechanical properties by precipitating phases resulting in depletion of the chromium and molybdenum content of the matrix. In general, it is often assumed that the behaviours of martensitic steels are similar to those of ferritic steels but this assumption is probably not justified for the reason just given.

Passivity is a complex phenomenon induced by the confluence of several factors, not yet fully understood; variations or fluctuations of any of these variables can be responsible for disturbing the metastable passive state, yielding place to the thermodynamically favoured reaction, i.e., metal dissolution. This often occurs locally

in which case the large cathodic area (passive area) sustains or enhances a high dissolution rate on the small anodic area, resulting in severe damage to the material. This is a contributory cause of intergranular, crevice, pitting and stress-corrosion-cracking which are different manifestations of localised corrosion. This classification is then based on the morphology of the damage rather than on the principles involved in the phenomena. The diversity of materials and conditions in which they have been observed introduce such a degree of complexity that an assessment of the corrosion mechanisms is rendered very difficult.

3.3.1. Intergranular Corrosion

In this type of corrosion the attack is concentrated at the grain boundaries leading to loss of strength and essential embrittlement or disintegration of the steel. It is symptomatic in this kind of corrosion that alloy components segregate or new phases precipitate preferentially at grain boundaries. The typical example is that of carbide precipitation in austenitic stainless steels which occurs when they are heat-treated in the range of 500-800^{o}C*, either for relieving stresses introduced by cold work or as the result of cooling after welding. The subsequent corrosion is known as weld decay.

The commonly accepted mechanism explains the phenomenon in terms of differential diffusion rates of the solutes[30]. Thus, when the steel is in that range of temperatures, carbon in the vicinity of the grain boundaries will diffuse towards the boundaries

*Annealed steels in this range of temperatures are denoted sensitised.

and these combine with chromium to produce chromium carbides type $Cr_{23}C_6$. Chromium diffuses more slowly because it is a substitutional solute and these carbides bind considerable quantities of chromium, thereby depleting the base metal of chromium close to the grain boundaries to such an extent that these areas are below the minimum 12% required for protective passivation. When the steel is immersed in an aggressive solution, selective dissolution will result in the areas alongside the grain boundaries. The severity of the attack will be determined by the extent of the precipitation, being more severe when the carbides form a network structure.

Ferritic and martensitic stainless steels are also susceptible to this kind of corrosion though not necessarily through carbide precipitation, e.g., the sigma phase may have the same effect. The duplex ($\alpha + \gamma$) steels are more resistant than the austenite due to the fact that the chromium-rich δ-ferrite, which is also present alongside the grain boundaries, provides most of the chromium for the carbides and therefore does not suffer the critical impoverishment of austenite.

The E-i curves of sensitised austenitic steels usually show higher values of i_{CRI}, E_F and i_{pass} as compared with those of the same but unsensitised materials. It has been shown[31] that all of these changes are due to preferential dissolution at the grain boundaries, being more severe when the steel is in the active region. It is interesting to observe that the increase in i_{pass}, even if small in absolute terms, is very

important and is mainly due to the intergranular attack.

This form of corrosion is minimised[32] by reduction of carbon content, or alloying with elements which form more stable carbides than that of chromium such as Ti, Nb; or selecting more suitable temperature ranges for heat-treatments if practicable. These remedies are not as straightforward as they may appear. Reduced carbon content is associated with some loss of strength and imposes a requirement for increased nickel contents to preserve the stable austenitic structure.

3.3.2. Crevice Corrosion

This type of corrosion occurs inside crevices and under shielded areas of a metal surface, e.g., bolted joints; where a stagnant solution may develop concentration gradients, with respect to the unshielded area, which result in concentration cells. Usually, this form of corrosion is exemplified by the effect of differential aeration because oxygen is the most common oxidising agent[33]. To maintain the passive state, sufficient concentrations of oxygen are required but its diffusion to crevices or shielded areas is sluggish or restricted; eventually the passivity breaks down and the corrosion potential of these areas will be in the active region of the E-i curve; resulting then in an active/passive cell, i.e., a galvanic effect with the anode inside the crevice and the cathode on the passivated free surface of the steel. This kind of

attack is more severe in solutions of chloride ion in which case it displays similar phenomenology to pitting corrosion, i.e. E-i curves show a reduction of the passive region. The experimental phenomena cannot yet be explained satisfactorily in all respects, but there are three stages generally identified[33]: an induction period during which crevices are not formed and usually associated with the time required for developing the concentration gradients by diffusion; an initiation period in which crevices start to form; finally, a propagation period corresponding with fully-developed crevices growing rapidly.

Recommendations to minimise[34] this form of corrosion include the use of molybdenum-chromium-nickel alloys, the use of welded joints, the removal of deposits from steel surfaces and the application of water-repellent sealant compounds in flanged joints.

3.3.3. Pitting Corrosion

This is an extremely localised attack resulting in holes in the metal. This type of corrosion is very dangerous since the steel may quickly be perforated or, on the other hand, pits may serve as initial points of development for other forms of corrosion, e.g. intergranular corrosion, crevice corrosion, stress-corrosion-cracking or corrosion fatigue; a complete piece of equipment may be rendered unserviceable without suffering any general attack merely because of a single highly localised area of damage. Pitting corrosion usually occurs in media that contain halogen ions or halogen-containing anions, specifically Cl^-, Br^- and ClO^-. Fluoride and iodide ions show less tendency to cause pitting. The E-i curve of steels in these media are usually characterised by a marked contraction of the passive

range, showing then a reduction of the range of potentials in which the material can be safely used. The phenomenon and mechanism are difficult to elucidate on, and are not yet fully understood. Since it is the subject of the present dissertation this type of corrosion will be reviewed extensively in the next chapter.

3.3.4. Stress-Corrosion-Cracking

This form of corrosion is the result of the conjoint action of mechanical stresses and aggressive environments upon the material and is manifest in the development of cracks leading to fracture and failure. Sensitised steels suffer intergranular cracking enhanced by the mechanical load but in unsensitiséd steels the cracking is usually intragranular or transgranular[35]. The stress may be either externally applied or the result of residual internal stresses introduced by fabrication. The media in which it is produced vary, but the more severe cases are found in solutions containing chloride ions and caustic solutions. The phenomenon is usually described in terms of three stages[36]; an induction period which accounts for most of the time to fracture (t_f); the initiation of cracks and, finally, propagation of these cracks until complete failure occurs or the stresses responsible for the cracking are relieved. Even though the electrochemical nature of the phenomenon is without question, there is no general agreement on the mechanisms and the topic forms the subject of extensive current researches.

4. THE PASSIVATION MECHANISMS AND BREAKDOWN OF PASSIVITY

4.1 THE PASSIVATION MECHANISMS

The electrochemical behaviour of metal electrodes is well illustrated by the current voltage curves. The occurrence of three distinct stages, i.e., active, passive and transpassive regions, is the result of different processes taking place at the metal-solution interface which according to the electrochemical conditions will be more or less favoured.

The active region is commonly associated with the free dissolution of the metal. Metal ions go into the solution where they are stabilised by hydration or solvation. The kinetics of the reaction follows a Butler-Volmer relationship and the overall process is expressed by:

$$M \rightarrow M^{n+} + ne \qquad (16)$$

This is, of course, a simplified expression of the reaction since studies on anodic dissolution of pure metals have shown that the reaction mechanism is a more complex matter. In the case of iron, for instance, Banhoeffer and Heusler[37-39] found that dissolution rate was slower in acids than in relatively alkaline solutions and also that the value of Tafel slope is 30 mV per decade. They explained these facts with a catalytic mechanism as follows:

$$Fe + H_2O \rightleftharpoons Fe\,H_2O_{ads}$$

$$Fe\,H_2O_{ads} \rightleftharpoons Fe\,OH^-_{ads} + H^+$$

$$Fe\,OH^-_{ads} \rightleftharpoons Fe\,OH_{ads} + e \qquad (17)$$

$$Fe + Fe\,OH_{ads} \rightleftharpoons Fe\,(Fe\,OH)_{ads}$$

$$Fe\,(Fe\,OH)_{ads} + OH^- \xrightarrow{rds^*} Fe\,OH_{ads} + Fe\,OH^+ + 2e$$

$$Fe\,OH^+ + H^+ \rightarrow Fe^{2+} + H_2O$$

Bockris, Despic and Drazic[40, 41] confirmed the dependence of the dissolution rate on the hydroxyl ion concentration, reporting a reaction order of unity for $[OH^-]$ and the same value for ferrous ion concentration. They found a different value for the Tafel slope, i.e., 40 mV per decade, and they proposed the following reaction mechanism:

$$Fe + H_2O \rightleftharpoons Fe\,OH_{ads} + H^+ + e$$

$$Fe\,OH_{ads} \xrightarrow{rds} Fe\,OH^+ + e \qquad (18)$$

$$Fe\,OH^+ + H^+ \rightleftharpoons Fe^{2+} + H_2O$$

In this case there is not the troublesome step of the earlier mechanism which requires the simultaneous transfer of two electrons, an unlikely event rather than a probable one.

The mechanism for dissolution of iron has received more attention[42] to elucidate these discrepancies but it is not our intention to go through the details of these particular discussions. The relevant point is that the different values of Tafel slope from

* rds = rate determining step.

which result any proposed mechanism have been ascribed to differences in the preparation of the material (iron) under study[43]; in other words, the treatment of the material prior to its study might influence the results from kinetic studies and hence the mechanistic interpretation given to them. This is one of the reasons for the existence of very few reported studies on the kinetics and mechanism of the anodic dissolution of stainless steels other than descriptions of the overall reactions, because the complexity of the system introduces too many variables to be controlled, i.e., composition, structure, surface condition and the nature of the electrolyte.

In any case, reaction mechanisms which explain the dissolution in the active region are based on kinetics which would predict a monotonous increase in current density as the overpotential is increased indefinitely. The onset of passivity shows phenomenologically that this is not true and that there must exist other reaction paths which eventually change the overall kinetics of the processes taking place on the metal electrode. The elucidation of the passivation mechanism has been the subject of a long discussion which has not achieved full agreement among different authorities in the field. There have been two main hypotheses which can explain the active-passive transition as determined using current-voltage curves; they are conceptually different though some authors[44,45] argue that their differences are rather semantic in the sense that both theories make the same description of the phenomenon but using different words. It is important to outline the basic principles involved in these two theories because of the influence they have had on our view of localised corrosion problems, pitting in particular.

4.1.1 The Adsorption Theory

This theory has been developed by Uhlig[46-49] and Kolotyrkin[22,50,51] among others. They described passivity as the result of specific adsorption of anions or molecules on the metal surface. Anions or highly polarisable molecules e.g., water, reaching the metal form chemical bonds by sharing their electrons with the surface metal atoms, using the unfilled or uncoupled atomic orbitals (chemisorption). As a primary consequence, there is a diminution in the exchange current density of the dissolution reaction which is manifest by a displacement of the potential towards more positive values; there is also an obstruction to the dissolution at the sites where chemisorption has occurred, resulting in a reduced effective area for dissolution and therefore a further decrease in the measured current density. Passivity is established when the active sites of the surface are subject to this adsorption or when the whole area is covered by adsorbed anions or molecules, in which case a monolayer of the adsorbed complex protects the metal. This is a dynamic state with a continuous exchange of adsorption and desorption i.e., competition between the passivity and dissolution processes. According to Kolotyrkin[22] the process at the metal surface can be represented by:

$$Me + m\,H_2O \rightarrow Me\,(H_2O)_m \begin{cases} \xrightarrow{a} Me\,(H_2O)^{n+} + ne \\ \xrightarrow{b} Me\,[O^{2-}\ H^{+}\ H^{+}] \end{cases} \qquad (19)$$

The passivating reaction b will begin at an appreciable rate only on reaching the passivation potential which presumably might be equal or more positive than the potential of zero charge for the interface, making the adsorption a more favoured process than the dissolution mechanism a. The kinetics of the passivation process is as follows[50]; the dissolution rate of metal is given by:

$$i = K\, C^1 \exp \{ (\alpha_1\, F/RT)\, \Delta\phi \} \qquad (20)$$

where C^1 is the number of atoms per cm^2. In the absence of specific adsorption this quantity may be considered constant (C_o^1); with the superimposition of adsorption, however, this quantity must change with the potential, and can be represented as an exponential relation:

$$C^1 = C_o^1 \exp \{ (-\alpha_2\, F/RT)\, \Delta\phi \} \qquad (21)$$

The dependence of the steady dissolution rate (I_s) on the potential may be expressed then by:

$$I_s = K\, C_o \exp \{ (\alpha_1 - \alpha_2)\, F/RT\, \Delta\phi \} \qquad (22)$$

Providing that in the first stage of the passivation process at $E_{pp} < \Delta\phi < E_F$ $\alpha_2 >> \alpha_1$ and in the second stage, at $\Delta\phi > E_F$ $\alpha_2 = \alpha_1$; this equation can reproduce the experimentally observed drop of the current density with potential and its independence of potential in the passive region, i.e., the phenomenology of E-i curves.

The formation of the adsorbed layer is subject to other energetic considerations as has been indicated by Uhlig[46,48] who suggested that one of the factors determining passivity is the ratio of the work function (WF) to the enthalpy of sublimation (ΔH_s) of the metal; if this ratio is less than unity, conditions are favourable to passivation via chemisorption because electrons would escape more readily than the atoms. If it is greater than unity atoms would tend to diffuse to the solution more easily and passivity, if established , is due to a different mechanism, e.g., the formation of a diffusion barrier layer due to oxide films. It has been found[46] that metals like Cr, Ni, Fe with unfilled or uncoupled d electron bands with ratio ($WF/\Delta H_s$) less than or equal to unity are prone to the former behaviour while metals like Cu, Pb, Zn with no d electron bands to spare show higher values of the ratio and do not exhibit passivity as thin film layers (chemisorbed monolayer). This illustrates the importance of the electronic structure of metals in relation to the passivity phenomenon on alloys, an aspect which has sometimes been regarded as a theory on its own[52]. In Uhlig's view[47,49], vacancies in the d band structure of a transition metal determine the passivating behaviour of an alloy of a transition metal with a non-transition metal or a metal with filled d band. These vacancies can be filled or coupled with electrons from the non-transition metal; as the number of vacancies depends on the composition, there exist critical concentrations at which all of the vacancies are coupled and the alloys begin to behave like the non-transition metal. This is exemplified by Cu-Ni alloys which experimentally show a transition at 35-40% Ni; above this concentration the alloy behaves like nickel. In considering

alloys of transition metals such as Fe-Cr, the d band is not filled by alloying but these are specific compositions at which d electron coupling is optimum. Assuming that the uncoupled d electrons of the more easily passivable component of a binary alloy (Cr in the example given above) are coupled primarily with d electrons donated by the less passivable component, it is possible to calculate this critical specific composition; Uhlig[49] has reported a calculated value of 13.6 for the critical atomic percentage of chromium in Fe-Cr alloys which is in good agreement with the observed value of 12.7 at % Cr for the "stainless" character.

The principle criticism of this theory is that in most of the instances in which passivity has been observed, the passive state is associated with a film with a thickness greater than a monolayer[53].

4.1.2 The Film Theory

The film theory was initially suggested by Faraday (1840) and has become the most widely accepted theory of passivity, particularly since the experimental work of Evans[54]. Passivity is explained in terms of a very thin film, commonly an oxide, which acts as a barrier between the solution and the metal obstructing in this way its dissolution.

Metal electrodes under anodic polarisation undergo dissolution but by raising the potential a condition is reached where the reaction of oxide formation is thermodynamically

favoured[44]; as the oxide film is being formed the effective area for dissolution decreases and passivity is established when the whole surface is covered by the film. The oxide film dissolves chemically at a very low rate controlling the dissolution of the metal; in other words, the processes in the passive region are film formation and film dissolution or degradation. The behaviour of the electrode in the passive region depends on the properties of the film[55]. Thus, if the film is a good electron conductor then it can sustain electron transfer processes on its surface and the field across it cannot rise to values high enough for significant ionic transport, resulting in a very low rate of growth and the film tends to remain very thin, e.g., for chromium, iron and nickel. On the other hand, if the electron conductivity is very poor, high fields across the film are readily obtainable favouring ionic transport and growth of the film as for aluminium. Hoar[55] has suggested the following general characteristics of an oxide for good passivation of the metal:

Very low ionic conductivity.

Appreciable electron conductivity.

Very low chemical solubility and dissolution rate.

A wide range of potential in which it is thermodynamically stable.

High compressional strength and good adhesion to the metal surface.

The experimental evidence in support of the existence of tangible oxide films on metal surfaces in passive conditions is so strong that it is regarded as a well-established fact. Evans[54], as long as fifty years ago, could isolate the "invisible" film

formed on passivated iron; later Vernon, Wormwell and Nurse[56] stripped off the film formed on an austenitic stainless steel using similar techniques.

Unfortunately, the thickness of passive films, range 1-10 nm as determined from ellipsometry and coulometry data[57,58], and the conditions in which they are formed make an assessment of their properties very difficult. In consequence, there is a diversity of opinions and hypotheses about the meaning of passivation potential, passivation mechanism and structure and composition of oxide films. The case of iron has been extensively studied and serves to illustrate briefly this problem. According to Evans[59], the passive film on iron is essentially Fe_2O_3 and the passivation potential corresponds to the equilibrium potential of the following reaction:

$$Fe_2O_3 + 6H^+ + 2e \rightleftharpoons 2\ Fe^{2+} + 3H_2O \quad E^\theta = 0.73\ V \qquad (23)$$

This reaction explains the destruction of the passive state by reductive dissolution[60,61] of the film formed on iron in air when immersed in acid solutions unless there is a strong oxidising chemical in the solution or the potential is kept at high values artificially with an imposed cathodic reaction.

Vetter[62], Nagayama and Cohen[63,64] have found more probable a duplex structure for the passive film, Fe_3O_4-Fe_2O_3, with the magnetite close to the iron surface and the hematite at the outside. The cathodic reduction of passive films on iron exhibits two waves indicating the presence of two distinct oxides[63]. The

passivation potential is found to be in agreement with thermodynamic data for the reaction[62,64]:

$$3\ Fe_2O_3 + 2H^+ + 2e^- = 2\ Fe_3O_4 + H_2O \qquad (24)$$

Finally, Brusic and Bockris[65] proposed a prepassive film of $Fe(OH)_2$ which in the passivation process becomes Fe_2O_3. At the initial stages of the polarisation there is a competition between dissolution of the metal and hydroxide formation; on reaching the passivation potential the metal surface is mainly covered by the hydroxide which starts to transform to oxide; passivity is established when the transformation has been accomplished. There are other opinions about passivity on iron and other metals but in any case the basic causative problem of passivity is not by any means clear, though our understanding of the phenomenon has greatly improved by the introduction of sophisticated and refined techniques.

There is, of course, no general agreement in the interpretation of the kinetics and mechanism which reproduce the experimental active-passive transition. Schwabe, Ebersbach and Ritter[66] have proposed a model which has the value of being the first theoretical calculation of the transition in terms of this theory. According to them, the reaction of film formation (i_{ff}) and dissolution of the metal (i_{diss}) share an intial step as follows:

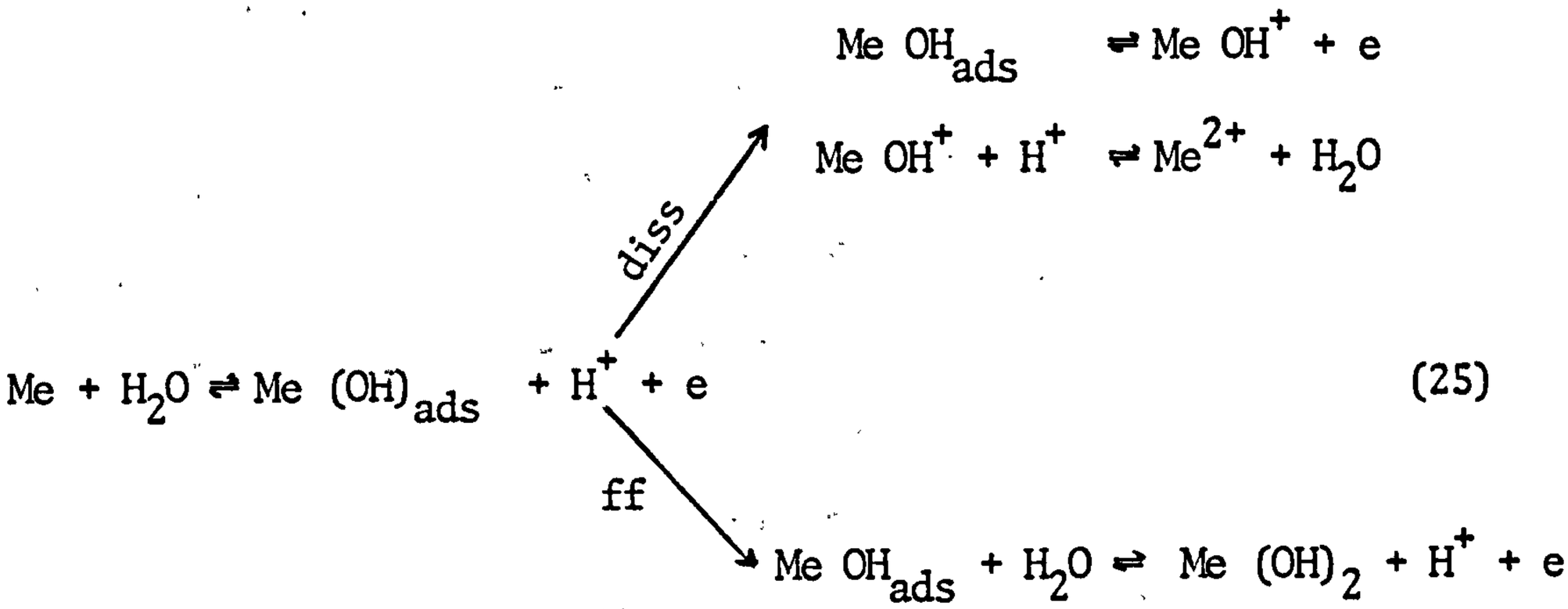

The current density will be given by:

$$i = (i_{ff} + i_{dis})\ (1 - \theta) \qquad (26)$$

where θ, the surface coverage, is a function of time according to:

$$\frac{d\theta}{dt} = C\ i_{ff}\ (1 - \theta) \qquad (27)$$

assuming no degradation of the film and where C is a constant.

In these conditions it follows that:

$$i = (i_{ff} + i_{dis})\ \exp\{- C\ i_{ff}\ t\} \qquad (28)$$

which shows a rapid diminution in current density as the film is being formed because i_{ff} occurs in the negative exponent of the expression The passivation potential might correspond to a particular situation of the system but this is not elaborated in Schwabe's work. It does not correspond with the equilibrium potential for the reaction M → Oxide which is the value introduced in the explicit expression of i_{ff}.

Passivity on alloys is essentially of the same nature as for pure metal but the phenomenon is more complex due to the increased number of variables in the system. It has been observed for a long time[67] that a more noble or more easily passivable metal will transfer its passivating characteristics to the alloy when combined with a more active metal; the effect being marked from a certain critical composition which has been interpreted as the minimum composition required for an oxide film formed mainly from the more noble metal. For example, Rhodin and Nielsen[68] have chemically analysed passive films stripped from the surface of passivated iron-chromium alloys and shown Cr-enrichment, this effect becoming important at about 12% Cr content after metal. These same authors also found nickel and molybdenum enrichment in films stripped from type 304 and type 316 stainless steels respectively. More recent investigations with improved techniques have produced somewhat contradictory results. Thus Kruger and McBee[69] studying a series of iron-chromium alloys by transmission electron microscopy have confirmed the Cr-enrichment of the oxide film, they also reported structural changes with composition going from spinel for 5% Cr to amorphous or polycrystalline structures at 25% Cr. These authors have suggested that the "stainless" character lies in the amorphous degree of the film. Okamoto[25,70] using several techniques in the study of type 304 austenitic stainless steel has also found evidence that suggest an amorphous film, confirming the previous observations. Furthermore the composition of the film is potential dependent; at low potentials the film is mainly chromium oxide or hydroxide with a high water content (about 30%); at high potential there is a diminution of water content and an

enrichment of nickel and iron in the film. This is illustrated in Fig. 8. The well known beneficial effect of molybdenum additions on the corrosion resistance of stainless steels appears to be associated with some different effect from the supposed enrichment of the oxide film, as has been revealed by Staehle et al [71,72] after studying several austenitic and ferritic steels with different Mo-contents. This illustrates the complexity of the phenomenon in the case of multi-component systems.

This theory is not exempt from criticism. The most common argument against it is the fact that the passivation potential is usually much higher than the equilibrium potential for the reaction metal → oxide, e.g., E_{pp} (Fe)> $E^{\theta}(Fe_2O_3/Fe)$, $E_{pp}(Ni)$> $E^{\theta}(NiO/Ni)$ and $E_{pp}(Cr)$> $E^{\theta}(Cr_2O_3/Cr)$ by 0.62 V, 0.24 V and 0.54 V respectively[73].

The concept of adsorption implies a specific interaction in which a particle, ion or molecule makes contact with the metal surface. Depending on the electrochemical conditions and intrinsic properties of the molecules and the metal atoms there may be:
a) desorption after a period of time without any chemical transformation being produced except heat transfer; b) electron transfer between the atoms in contact; c) chemical transformation between atoms in contact involving electron sharing but not electron transfer, i.e., chemical bond formation; and d) desorption or not of this product. It is possible to think of a surface wholly covered by a chemisorbed "complex" which would hinder metal dissolution but from there on the concept of adsorption is of very little value unless it is argued that the phenomenon is due to successively adsorbed layers; this argument would be based on the not always explicit assumption that the first

monolayer constitutes a distinct phase which in some degree would condition the adsorption process if any. This is conceptually what is implied in the oxide film theory. One consideration is how the new phase develops and a quite separate issue is what the characteristics of this new phase are. Therefore it is not possible to explain both aspects with just one concept. This is precisely what had happened to a certain extent in the earlier views of the passivity phenomenon leading to these two theories which sometimes have run parallel, complementary or in conflict with each other. To accommodate these differences there are two possibilities: to look at the problem with a different approach or to synthesise the two existing theories. Modern passivation theory has taken the last option[44,74,75]; the primary act of passivation is the formation of a tightly-held layer of monomolecular dimensions, containing oxide or hydroxide anions and metal cations. The process involves the formation of a new phase, an oxide, in steps that include adsorption as an important intermediate stage. The current-voltage behaviour is a function of the simultaneous processes of film formation, its dissolution and metal dissolution. The critical passivation potential does not necessarily correspond with the equilibrium potential of the metal-oxide system. In the active region dissolution is hindered by a decrease of free electrode area and in the passive region dissolution depends entirely on the properties of the passivating film.

4.2. BREAKDOWN OF PASSIVITY

It is widely accepted that the rupture of the passive state is an important aspect of any localised corrosion manifestation. In this sense, pitting is an example par excellence where it occurs in its simple form without the intervention of other factors which lead to the other manifestations, e.g., crevice corrosion.

4.2.1. Phenomenology of Pitting Corrosion

This form of localised attack which is not exclusive to stainless steels is morphologically characterised by the presence of small holes (pits) randomly distributed on the metal surface and larger unattacked areas. By small holes is meant that the width of the attacked area is equal or less than the depth[76]. It seems convenient to complement it by stating that the dimensions change preferentially in depth and volume rather than in the apparent surface area. It has been generally recognised that this type of attack occurs when halogen ions, chlorides in particular, are present in the solution; in this sense the phenomenon can be regarded as a specific action of these anions. Because stainless steels are usually in a passive state this type of corrosion is associated with local depassivation or offsetting of that state by the action of the aggressive anions. This is better appreciated by the marked change produced on the E-i curve for the material when determined in a solution containing the damaging anion as compared with the curve obtained without it.

This is illustrated in Fig. 11, the curve ABCDE represents the typical electrochemical behaviour of an austenitic stainless steel in H_2SO_4 at 25°C while the curve ABCGH represents its behaviour when the solution is a mixture of H_2SO_4 and NaCl. The current density in the branch GH of the curve is due mainly to pitting corrosion as can be easily revealed by examination of the metal surface. The main effect is then a contraction of the passive range. It is common practice to characterise the phenomenon by the potential at which it is initially manifest; this is denoted the breakdown potential (E_b), the critical pitting potential (E_c) or the rupture potential. At potentials more negative than E_b the metal is in the passive state and above E_b pitting corrosion occurs, i.e., passive and active states coexist on the surface of the metal. Another peculiarity of this phenomenon is its time dependence; this is manifest when a specimen of material is held at its breakdown potential and is suddenly exposed to the aggressive solution. In these circumstances the conditions required for pitting corrosion to occur are fulfilled almost instantaneously, but a certain period of time has to elapse, called the induction time (τ), before any manifestation of the attack can be recorded[77]. This fact results in a degree of uncertainty with regard to the determination of the breakdown potential in addition to the experimental error assigned to equipment, i.e., the value of the breakdown potential depends on the experimental procedure; therefore it cannot be regarded as a precise parameter. However, it has been identified as a useful means to estimate the tendency for pitting of metals and alloys under various conditions[78, 79].

The manifestation of pitting corrosion depends on numerous factors besides the necessary requirements of high redox potential of the solution to produce passivation and the presence of halogen ions to destroy it. These factors are commonly grouped into metallurgical and environmental ones[80].

> Metallurgical factors: are those which derive from the characterisation of the physical state of the material. They are nature and composition, structure, mechanical and thermal treatments.
>
> Environmental factors: are those which derive from the characterisation of the solution in which the corrosion reaction takes place. They are nature and concentration of aggressive anions, nature and concentration of non-aggressive anions, pH and temperature.

4.2.1.1. Metallurgical factors

a) Nature and composition of metal

The occurrence of pitting corrosion on metals is as widespread as the passivity phenomenon; pure metals exhibit different degrees of passivity hence different susceptibilities towards pitting can be expected. In effect, metals yield different values of breakdown potential when determined in the same conditions, as illustrated in Table II. Unfortunately, there is not a direct correspondence with the degree of passivity as determined by Tomashov[27]; aluminium which has a high degree of passivity exhibits a low value of E_b which would mean that it is highly susceptible to undergo pitting corrosion. On the other hand, chromium which also

has a high degree of passivity exhibits a high pitting resistance, i.e., its E_b value is high. These examples illustrate the strong dependence of the corrosion reaction on the nature of the metal; certainly the chemistry of chromium is largely conditioned by the d-band electrons which are not available in the case of aluminium. A better correspondence is found when comparing transition metals such as Cr, Ni, Fe. The susceptibility to pitting corrosion increases as the degree of passivity decreases. It must be emphasised that iron is not only difficult to passivate, but also the passivation process is hindered in the presence of chloride ions; the minimum concentration of chloride ions to produce pitting on iron has been found to be 3×10^{-4}M, while the values of E_b reported in the Table II are determined in 0.1M NaCl. This would make it very difficult to passivate iron in such conditions and that is why there is no reported value of E_b for iron in the table. This fact has been observed by Uhlig[81] when studying a series of Cr-Fe alloys at 25°C and 0.1M NaCl solution; alloys with Cr contents below 12% exhibit no passivity and hence no localised breakdown of passivity leading to pitting.

The nature of stainless steels is commonly expressed by their composition and a general assessment of their pitting susceptibilities is made by considering the effect of the alloying elements on the value of the breakdown potential for a given condition of temperature and chloride ion concentration. Thus the system Cr-Fe has been studied in neutral[81] and in acid solutions (pH=3)[78] of 0.1M NaCl at 25°C. It has been found that above 12% Cr content there is a shift of the breakdown potential towards more noble values, an effect which occurs abruptly in the

range of 25-40% Cr. Above 57.8% Cr no pitting was observed and the breakdown of passivity observed corresponded with that of the transpassive region[78, 81]. Nickel also produces a beneficial effect on the pitting resistance of iron although it is not as important as that of chromium[81]. Additions of nickel to Cr-Fe alloys result in shifting the E_b value of the alloy in the noble direction[81]. A more significant effect occurs with small additions of molybdenum[81, 85]; 2.5% Mo yields a shift of 500mV according to Uhlig[81], and 900 mV when the Mo content is raised to 4.6%. Tomashov et al[85] have studied the effect of a series of elements such as: Mo, Si, V, Re, Ce, Ti, Nb and Ta, which were introduced as minor elements in a basic alloy of 18% Cr - -14%Ni austenitic stainless steel. Mo, Si, V and Re manifested a significant beneficial effect measured by the shift on the value of E_b in the noble direction or the number of pits formed. The other elements (Ce, Nb, Ti, Ta) exhibited a deleterious effect on the corrosion resistance of the alloy.

The effect of interstitial solutes are more difficult to assess. It is generally accepted that carbon has a detrimental effect[78]; nitrogen on the other hand has been found[86] to improve the pitting resistance of stainless steels.

b) <u>Structure of the metal</u>

The structural differences between austenitic, ferritic and martensitic stainless steels certainly result in differences in

their corrosion behaviour. Austenitic steels are distinctly more resistant to pitting corrosion than ferritic steels[78] but this difference in behaviour cannot be accounted for only by their structure because they are different in nature, i.e., there is an important addition of nickel in austenitic steels; therefore consideration of the structural aspects of pitting corrosion have to be confined to a given type of stainless steel.

The relatively successful explanation of intergranular corrosion in terms of a relevant structural feature, i.e., carbide precipitation, has incidentally induced researchers to look for a feature which would explain the 'localisation' of pitting corrosion. Streicher[87] studying a series of 18-8 austenitic stainless steels has found that pits develop preferentially at the grain boundaries though they can be produced on the grain surface if the conditions of the test are more severe. Tomashov et al[85, 88] have also found this preference. They studied the effect of the grain size on the susceptibility of chromium-nickel steels to pitting corrosion; it was found that the breakdown potential shifted towards more positive values when the grain size was increased from 0.005mm to 0.07mm; above this value, E_b was constant and the number of pits decreased.

Inclusions are widely recognised as potential sites for pitting corrosion. Electron microprobe analysis of inclusions in a single crystal of 16% Cr-Fe alloy and several commercial stainless steels[89-91] have revealed that pits nucleate

predominantly at sulphide inclusions which are preferred sites compared with oxide inclusions. It was also reported that only 60% of the pits on the single crystal exhibited sulphur traces. Wranglen[92, 93] considers sulphide inclusions, iron sulphide in particular, as the main cause of pitting corrosion in carbon steels and stainless steels. The high electron conductivity of FeS favours the formation of microgalvanic cells which could lead to localised attack: in carbon steels these inclusions act as cathodes in relation to the base metal but they are anodes in stainless steels because of the oxide film.

Finally, dislocations are another structural feature which have received consideration since it is well-known that they are subject to preferential dissolution leading to regularly shaped pits, i.e., etch pits. Schwenk[77] has observed the formation of hexagonal pits on stainless steel when it is held at a potential near E_b ; the regular shape of the pits is due to crystallographic control of the dissolution process. He found that the bounding walls correspond to planes of (111) orientation which are the closest packed planes in austenite. This crystallographic effect is lost when the conditions of pit formation are more severe, e.g., a higher potential than E_b, in which case hemispherically shaped pits are found. The dissolution process inside pits is more likely to resemble those of an electro brightening process[77, 94]. Although it is well-known that etch pits are mainly associated with dislocation or impurities located at them, a similar relationship for pitting corrosion manifest as crystallographic dissolution has still to be proved. The experimental evidence obtained by electron transmission microscopy has not produced conclusive results on this

issue[95, 96]. Frankenthal and Pickering studying an iron-chromium alloy (24% Cr) using this technique have found that low indexed crystal planes are preferentially attacked and that the pits are not associated with emergent dislocations.

c) Mechanical treatments

The variations in energy content of metallic materials subjected to severe cold work are equivalent to a few milivolts in their electrochemical potential; however, it is generally accepted that mechanical treatments affect the manifestation of corrosion phenomena[97]. Thus, Uhlig has observed that hot-rolled sheets of a stainless steel exhibit preferential edge pitting[80]; it is assumed that this effect is observed in most wrought stainless steel products[78]. Cold work has very little effect on the breakdown potential of austenitic stainless steels but the intensity of the pitting phenomenon appears to be greatly influenced, i.e., the number of pits is higher for these conditions[82, 98]. Mechanically polished surfaces are more resistant to pitting corrosion, but when it occurs, pits tends to be fewer, larger and deeper[78, 80].

d) Thermical treatments

This metallurgical factor certainly has an effect on the incidence of pitting corrosion. Austenitic stainless steels heat-treated in the sensitising temperature range show some loss in pitting resistance[78, 80, 85, 87]; this effect initially

thought to be caused by carbide precipitation now appears to be more complex since Uhlig has shown[80] that a very pure 18%Cr - 8% Ni stainless steel with only 0.001%C content corroded in ferric chloride by pitting approximately ten times more than the same alloy quenched from 1100°C; the same effect was observed for a titanium-stabilised 18% Cr - 8% Ni stainless steel. He concluded that carbides per se are not the nuclei of pitting. Heat treatments conducted within suitable ranges of temperatures improve the pitting resistance of stainless steels. This is due to the release of stored energy introduced by cold work, homogenisation of the structure and grain coarsening[78, 80, 85, 87].

4.2.1.2. Environmental factors

a) Nature and concentration of aggressive anions

Pitting corrosion is generally regarded as the result of a specific action of halogen ions on passivated metal-alloys. Chlorides, bromides and hypochlorites are the most aggressive of the halogen-containing anions. Fluorides, iodides and iodine-containing anions are practically without pitting tendencies[99]. Most of the work reported in the literature is concentrated on the effect of chlorides not only because of their aggressiveness, but also because they are the most widespread in nature. It is of interest to note a recent report[100, 101] claiming that this form of localised attack is manifest on stainless steels when treated with organic acid pure methanol mixtures at low temperatures, in the range 0° to -50°C; the organic acids found to produce this effect were: tartaric, malic, lactic and acetic.

Variations in concentration of the aggressive anions produce marked changes in the value of the breakdown potential for the metal-alloys. It is generally recognised that the value of this parameter is shifted towards more negative potentials by increasing the halogen ion concentration with a consequent reduction of the passive range. This effect can lead to total suppression of passivity at very high concentrations of aggressive ions depending on the nature of the metal-alloy. Uhlig[102] studying an 18-8 austenitic stainless steel has found that in neutral solutions a tenfold change in concentration yields a reduction of 0.090mV in the breakdown potential. He also found[80] in earlier experiments a tendency to uniform corrosion at very high concentration which has been confirmed in a more recent investigation by Wilde[103] in types 304 and 430 stainless steels for concentrations of 5 and 10 M LiCl. Some authors[70, 104, 105] have gathered results which suggest that a minimum concentration of the aggressive anion is required to produce pitting; this can be used as a different criterion to assess the pitting susceptibility of different metal alloys. Thus, Stolica[104] studying the effect of chloride ion concentration on the induction time (τ) in a series of Cr-Fe alloys in acid solutions (1N H_2SO_4) has found linear relations of the form:

$$\tau^{-1} = a \ (C_{Cl} - b) \qquad \ldots\ldots\ldots\ldots (30)$$

where τ and C_{Cl} are the induction time and chloride ion concentration respectively. The definition of the minimum concentration corresponds with the condition of τ being infinite ($\tau \rightarrow \infty$) and it can be taken as the term b in the linear expression. This same author has also found a relation of the form:

$$\tau^{-1} = K\ C_{Cl} \qquad \ldots\ldots\ldots (30)$$

for iron in which case there is no clear definition of the minimum concentration of Cl^- for initiation of pitting. Different results have been obtained by Hoar and Jacob[106] when studying an 18-8 austenitic stainless steel; they have found a relation of the form:

$$\log \tau = n \log C_{Cl} \qquad \ldots\ldots\ldots (31)$$

where n varies between 2.5 and 4 depending on other conditions of the experiment, namely the potential at which the specimen is held potentiostatically. These different results can be explained in terms of differences in the experimental procedure but in any case they reveal the fact that characterisation of the phenomenon by a minimum concentration of the aggressive anion is at least as unprecise as the breakdown potential. On the other hand, the shortening of the induction time by increases in Cl^- concentration can be regarded as a well-established feature in the phenomenology of pitting corrosion on stainless steels.

It is important to note that besides inducing pitting halogen ions influence the electrochemical behaviour of metal alloys in other respects. The relation of these other effects to the pitting phenomenon has received little attention although they have been studied to some extent in other contexts, e.g., the effect of chloride ions in stimulating the active dissolution of iron[107, 108]. The E-i curves determined with solution

containing Cl^- usually show higher current densities in all parts of the curve as compared with the current densities of corresponding curves obtained with Cl^-free solutions. According to Greene and Judd[109] pit growth can occur only if the metal dissolution rate increases in the presence of chlorides. If i* is the current density in the presence of Cl^- ions and i the current density in their absence then metals with i*/i = 1 would be completely resistant to pitting. They have found that titanium conforms to this relation while for types 304L and 316 stainless steels the ratio is greater than unity (i*/i>1) at all potentials, even in the passive range in which the comparison could be made. A similar effect has been observed by Wilde and Hodge[110] studying the effect of Cl^- on the anodic dissolution of Cr-Ni alloys in acid solutions. This effect is, however, more typically observed in the active region of the E-i curve which means that there is an increase in the critical current density for passivation by the introduction of the Cl^- ions. Stolica[104] has found that critical current density increases linearly with the Cl^- ion concentration for an 18% Cr - Fe alloy in acid solution.

More interesting in relation to pitting corrosion are the differences in current densities in the passive region, but the small value of the current densities involved introduce experimental problems which are difficult to resolve. Okamoto et al[110] have introduced a noise analysis technique in the study of the passive current of an 18-8 austenitic stainless steel;

they have found that the spectrum, i.e., the r.m.s. values of noise voltage $(\bar{v}^2)^{\frac{1}{2}}$ plotted against frequency, of a passivated specimen in the solution with Cl^- ions has a noticeable peak in the frequency range 15-20 H_2 ; below 5 H_z the pattern of the spectrum changes with time, an effect which is not found in the absence of Cl^- ions.

Finally it must be said that the halogen ion concentration inside fully developed pits appears to differ greatly from that of the bulk solution according to the results of Cl^- ion concentration determinations carried out on solutions taken from artificial pits[111, 112] or the direct measurement of Cl^- ion activity in the neighbourhood of the pits using a suitable electrode [103].

b) Nature and concentration of non-aggressive anions

The intensity of pitting corrosion depends not only on the nature and concentration of the aggressive anions and the oxidising agent if present but also on the presence in the solution of other salts whose anions do not possess aggressive or oxidising action[78, 79]. Generally, the effect observed is a shift of the breakdown potential value in the noble direction by increasing additions of salt, until pitting is completely inhibited, the induction time is also prolonged and the number of pits is lower. Anions found to produce these effects are NO_3^-, SO_4^{2-}, ClO_4^-, CrO_4^{2-}, MoO_4^{2-}, CO_3^{2-} and acetate[79]. According to Uhlig[102] the inhibiting effect can be represented by the minimum anion activity necessary to inhibit pitting in a solution

of given Cl^- ion activity. This is expressed by a relation of the form:

$$\log A_{Cl^-} = A \log A_{Anion} + B$$

where A and B are experimentally determined constants. Equations of this form show that the efficiency of inhibition decreases in the order NO_3^- > Ac^- > SO_4^{2-} > ClO_4^- for an 18-8 austenitic stainless steel[79]. For example, in solutions of unit activity of Cl^- ions which corresponds to 1.5M NaCl solution, the values for the activities of NO_3^-, SO_4^{2-} and ClO_4^- required for completely inhibition are 0.24, 1.15 and 3.4 respectively[102].

c) <u>pH of the solution</u>

The acidity or basicity of aqueous solutions are usually expressed in terms of the pH parameter. It has been found[78, 79, 102] that in the acid range pH has little or no effect on the value of breakdown potentials for stainless steels. It must be emphasised, as stated earlier in section 2.2.2., that the modification of the pH value of a solution induces further modifications to the solution which have to be taken in account. Thus, in the acid range the pH cannot be changed without simultaneously introducing non-aggressive or aggressive anions which can produce an effect of greater importance or significance than the acidity increase per se. Uhlig[102] has found that the slight shift in the breakdown

potential of an 18-8 austenitic stainless steel in the active direction is accounted for by the chloride ions introduced by the acid because he used additions of hydrochloric acid (HCl) to produce changes in the pH of the solution. On the other hand, he used addition of sodium hydroxide (NaOH) to change the pH in the basic range. According to Uhlig[102], hydroxyl ions are the most efficient inhibitor of pitting for this steel, only 0.07 activity of OH^- ions is required to inhibit unit activity of Cl^- ions as calculated from the empirical expression:

$$\log A_{Cl^-} = 1.62 \log A_{OH^-} + 1.84 \quad \text{.....(33)}$$

It must be said that the pH of the solution inside fully developed pits appears to be much lower than the value of the bulk solution according to results obtained from experiments with artificial pits[111, 112].

d) Temperature

Temperature is a common variable to all chemical or electrochemical reactions; the effect is usually an increase in the reaction rate although it is also subject to thermodynamic consideration, i.e., whether the reactions are exothermic or endothermic. In pitting corrosion, a dissminution of the value of breakdown potential has been observed[79] with increasing temperature. Uhlig[102] has found that E_b for an 18-8 stainless steel in 0.1M NaCl at 0°C was above + 0.90V, at 25°C it was +0.35V and in the range 25° - 50°C

it underwent small changes. S-Smialowska[79] has found that E_b values decrease linearly with the temperature in the range 30° - 100°C for types 430 and 304 stainless steels. She has also found that type 316 behaves differently: E_b decreases linearly with the temperature up to 70°C; above this value the breakdown potential changes very little, remaining almost constant. This result has been confirmed by Brigham and Tozer[113, 114] who have suggested the introduction of a critical pitting temperature below which the steel will not pit regardless of the potential and exposure time. It has also been observed[115] that the number of pits increases but their depth change very little as the temperature is increased. The induction time, of course, is also affected by temperature; Hoar and Jacob[106] have observed that a modest rise in temperature from 25° to 40°C lowered the value of τ by two orders of magnitude, suggesting a high apparent activation energy of 250 KJ mol^{-1}. The activation energy of dissolution in pits determined from the temperature dependence of the breakdown potential amounts to 18.8 - 24.2 KJ mol^{-1} as reported by Tousek[116] in his study of Cr steels in the range 5° - 40°C in which he observed that the decrease of breakdown potential is a linear function of the reciprocal value of the absolute temperature, i.e., an Arrhenius-type relation.

4.2.2. Pitting Breakdown Mechanisms

A comprehensive theoretical explanation of the complex phenomenology of pitting corrosion is indeed a difficult task, particularly since the passivity phenomenon is not fully understood as discussed earlier.

It is a common practice among researchers in this field to consider the pitting phenomenon as a two stages process[117]: pit initiation and pit growth or propagation. This distinction has been criticized [118, 119] on the grounds that it is not possible to specify the transition between the two stages, but it is an experimental fact that factors affecting the growth or propagation of a pit are different from those that led to its initiation. For this reason different theoretical approaches are required to account for them. Briefly, the initiation stage is the development of the conditions which lead to the breakdown of the passive state and the propagation stage is the sustained progression of the attack through the metal. The former is considered to be the most important because of its relation to the passivity phenomenon; a better understanding of the processes involved in this stage would facilitate the development of ways to control them. It is preferable to control the initiation process rather than to try to control the propagation process because when the latter stage is reached the damage progresses very quickly.

According to Kruger[120] most of the conditions required for pitting exert their influence in the initiation stage and any model proposed should explain these observations; this author has summarised the main features as follows:

A certain critical potential, E_b (breakdown potential) must be exceeded.

Damaging species, e.g., chloride ions, are needed to initiate and propagate breakdown

There exists an induction time before there is any evidence of pitting attack. This is a manifestation of the time required for condition conducive to permanent breakdown of passivity to develop.

Breakdown occurs at highly localised sites.

The fundamental hypothesis of any theory which pretends to explain these facts are intimately connected with those made in the elaboration of passivity theories and accordingly it is convenient to group the theories of pitting into adsorption and film theories.

4.2.2.1. The adsorption theory of pitting breakdown

This theory, suggested by Kolotyrkin[22, 51] and Uhlig[102] among others, explains pitting as a result of the displacement by aggressive anions of passivating oxygen from the metal surface, a process which implies the destruction of the passive state and the active dissolution of the metal. According to Kolotyrkin[22, 51] the primary and fundamental step of the reaction can be expressed by the following reaction:

$$Me\,O^{2-}_{H+}{}_{H+} + p\,Cl^- \rightleftharpoons Me\,(Cl)^{p-}_{p} + mH_2O \quad \ldots\ldots\ldots(34)$$

The breakdown potential corresponds with the minimum electrode potential at which the aggressive anion becomes capable of displacing the passivating oxygen from the surface. This would mean that a higher affinity of the metal for oxygen than for the

aggressive anion is an important condition for the establishment of the passive state; if the reverse condition is considered then the adsorption of aggressive anions would interfere with the passivating mechanism to such an extent that either passivity cannot be established or at least there is a marked increase in the anodic dissolution in the active region of the E-i curve depending on other factors, e.g., nature of the metal, pH of the solution. Obviously the possibility that this equilibrium (eq. 34) tends towards the right depends not only on the electrode potential but also on the concentration of halogen ions in the vicinity of the metal surface. Taking into consideration the fact that the dissolution of solid metals always takes place non-uniformly and therefore the current is distributed unevenly on the surface the result is that the critical concentration of Cl^- ions is first achieved nearer those areas of the metal surface which dissolve at the higher rate leading to an acceleration of the dissolution process at those areas, i.e., local intensification of the current, and consequently to a much more rapid migration of the activating anion to the active centres. In this form this theory explains the localisation of the attack. Moreover, this sequence of events cannot occur instantaneously to a significant extent implying therefore that they occur over a period of time, i.e., an induction time is required for the establishment of a sustained localised dissolution of the metal. The mechanism of metal dissolution in these conditions is completed by considering the effect of halogen ions on the formation of halide complexes which are assumed to be more liable than

their aqua-counterpart developing a catalytic sequence of reactions which can lead to an autosustained system of metal dissolution in the local area under attack as follows:

$$Me\ O^{2-}_{H^+}{}^{H^+} + p\ C\ell^- \overset{\text{adsorption}}{=} Me\ (C\ell)_p^{p-} + m\ H_2O \quad \text{at the metal surface} \qquad \text{.....(35)}$$

$$Me\ (H_2O)^{n+p} + pC\ell \leftarrow Me(C\ell)_p^{n-p} + ne \quad \text{in the solution}$$

hydrolysis

This mechanism is analogous to that for active dissolution of the metal in the presence of halogen ions for which the following kinetic relation has been suggested[51]:

$$i = KC^{\delta} \exp\left(\frac{\alpha F}{RT}\phi\right) \qquad \text{.....(36)}$$

where C is the concentration of the halogen ions and δ is a constant which depends on the nature of the aggressive anions.

Although this theory explains the four minimum requirements to explain the phenomenology of pitting corrosion and the inhibiting effect of the non-aggressive anions as a competitive adsorption process which depends greatly on the concentration ratio of the different anions, it cannot account for certain observations due to the existence of thin oxide films on the metal surface in the passive state, e.g., the effect of the thickness of the passive film on the induction time[121]. Furthermore, the assumption of the rate determining step for the reaction as chemisorption

appears illogical after a careful examination. The equation which corresponds with the adsorption displacement step does not imply a deterioration of the passive state but a passive state of a different nature; it is the subsequent reaction of the metal atom going into the solution as a complex ion which represents a breakdown of this state, as it is expressed in detail in the reaction scheme 35, in consequence what is important is the ease of this latter step, i.e., chemisorption per se of the aggressive anion does not produce the breakdown of the passive state, it is the desorption of the metal-anion complex with the simultaneous oxidation of the metal atom which results in a destruction of the passive state. Therefore the rate determining step appears more likely to be the desorption and not the chemisorption. The critical potential is assumed to be equal or higher than the potential of zero charge of the metal surface a condition which certainly favours adsorption of anions, but contradicting this view the value has been found[122] to be -0.7 V (SHE) in the important case of iron, a value which is much lower than the passivation potential for the same metal. Kolotyrkin himself supports the idea of adsorption at a much lower potential than E_{pp}[51].

4.2.2.2. Film theories of pitting breakdown

Authors supporting the film theory of passivity have proposed several models to explain pitting corrosion according to their particular or personal views of the nature of the passive film, its structure and properties. Thus, according to Evans[123], passive films always present local imperfections which are suitable

sites for metal dissolution and pit development depending on the conditions. The imperfections originate in various ways. Examples are changes in the nature of the film over outcropping inclusions in the metal and cracks in the passive film formed by the relief of stress in the film imposed by stress in the metal, i.e., the passive film reflects the imperfections of the underlying metal structure. In the absence of aggressive anions these sites are healed by fresh film formation but if aggressive anions are present then metal dissolution can occur. Certainly a period of time has to elapse before any macroscopic manifestation of this process is observed. For a given potential the probability of a pit forming at a point suddenly laid bare will increase with the chloride ion concentration, but it is unlikely that there is a critical chloride ion concentration below which the probability is zero and above which it is finite; similarly at a given chloride ion concentration the probability will rise with potential increases, but it is doubtful whether a potential exists below which the probability becomes zero. The specific effect of Cl^- ions is related to the fact that when sites in the oxide lattice which are normally occupied by O^{2-} ions become occupied by Cl^- ions, the number of vacant cation sites in the neighbourhood must increase if electroneutrality is to be preserved; when once, at the point in question, the concentration of vacant cation sites in the film has become abnormally high, movement of ions through the film becomes much faster than elsewhere, and the pit propagates with increasing velocity.

Sato[124] has suggested that the stability of passive films against breakdown is controlled not only by the electrochemical reactivity of aggressive anions but also by the

mechanical properties of the film itself. If the pressure acting upon the film (film pressure) which is determined by the atmospheric pressure, the interfacial tension and the electrostriction pressure exceeds the critical compressive stress of the film then breakdown results with subsequent metal dissolution or film formation depending on the conditions. In Sato's view this condition can be expressed by:

$$p - p_o = \frac{\varepsilon\,(\varepsilon-1)}{8\pi} E^2 - \frac{\gamma}{L} > \sigma_c \qquad \text{.....(37)}$$

where p is the film pressure, p_o is the atmospheric pressure ε is the dielectric constant of the film, E^2 is the electric field strength, γ is the interfacial tension, L is the thickness of the film and σ_c is the critical compressive stress. From this expression it is clear that conditions for mechanical disruption of the film can be produced by increasing the electric field strength by decreasing the interfacial tension or by increasing the thickness of the film; all these factors are simultaneously affected by the potential and the breakdown potential can be defined as the minimum potential above which the film pressure exceeds the critical compressive stress. It is argued that the effect of Cl^- ions is to diminish the interfacial tension, but this is not by any means clear because this parameter should be considered at the passive film-solution interface which is ignored in Sato's approach.

Okamoto[25, 70] has proposed an interesting reaction mechanism. In his opinion, the passive film is a hydrated oxide

having a gel-like structure which undergoes dehydrogenation by ageing or an anodic polarisation process which can result eventually in an oxide-like structure. There are three types of bridging structures in the passive film H_2O-M-OH_2, HO-M-OH and O-M-O. At low potentials the replacement of Cl^- ions at the bridge position results in the formation of soluble chloride metal complexes by which metal ions are removed from the oxide film. The vacant site created by the removal of metal ions might be filled again by newly produced film as follows:

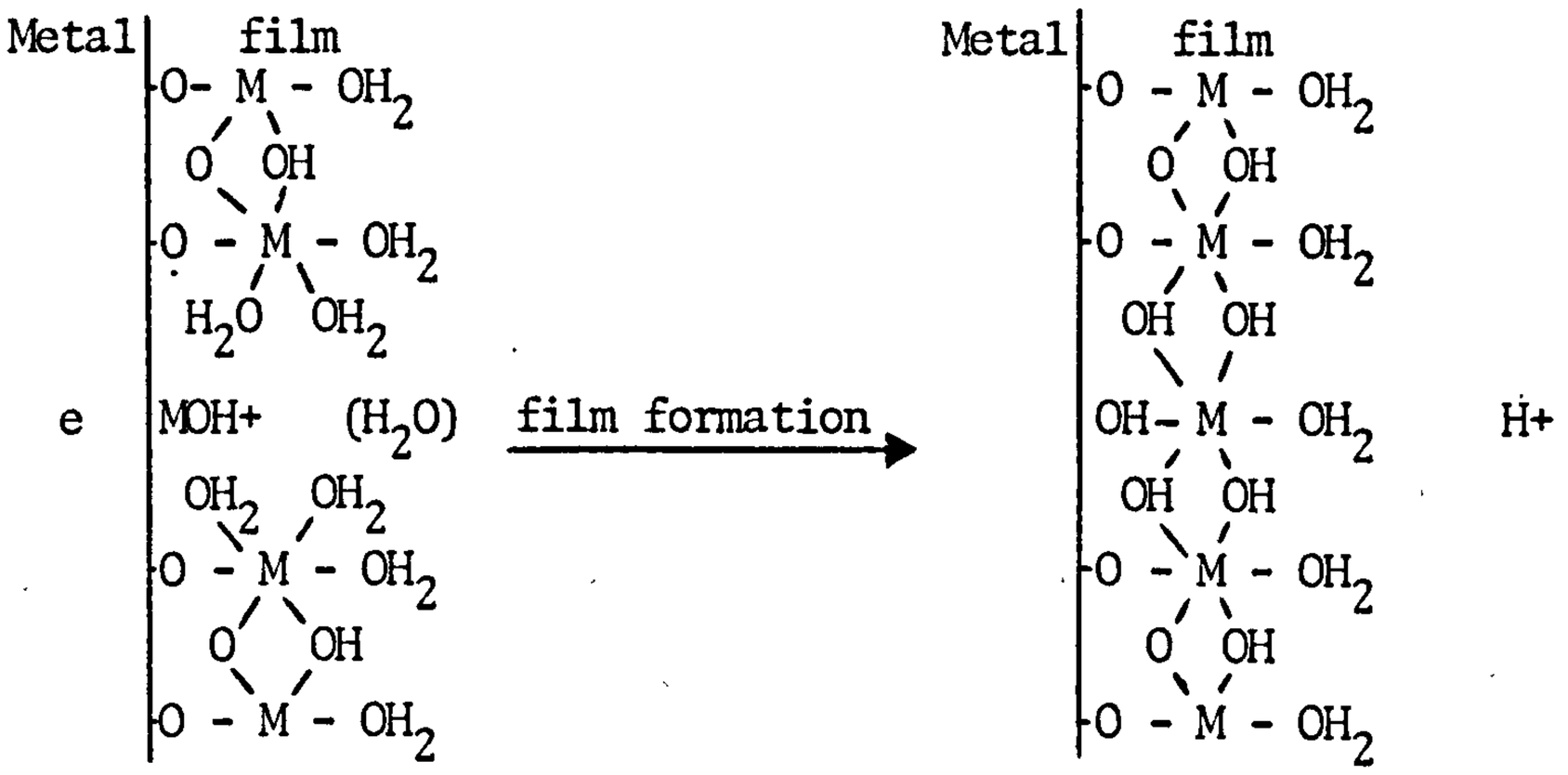

At high potentials, the amount of water is smaller and the fully-formed film can not repair itself as easily as at low potentials; there is a balance of breakdown and film formation which eventually

turns in favour of pit formation when enough Cl^- ions have displaced water molecules from the bridge positions; this is represented as follows:

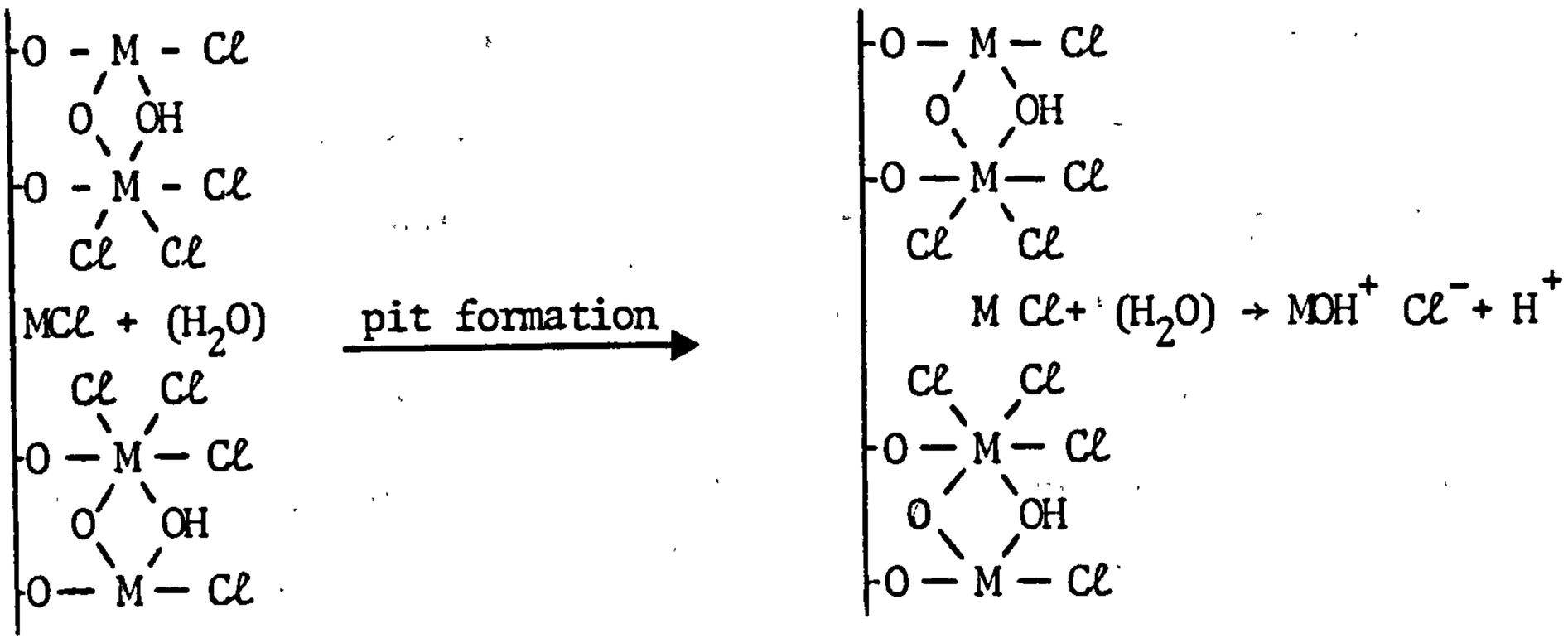

Other authors[125-128] consider that the breakdown of the passive film is occasioned by adsorption of the aggressive anions on the oxide film followed by migration through the film. The breakdown potential is related to the preferential adsorption of the damaging anions and the induction time to the period of time which has to elapse for the anions to migrate from the oxide surface to the metal surface. These theories are usually described as penetration models[120].

Although there is general agreement that the dynamic breakdown and repair processes are critical in determining the development of localised corrosion[129]; the degree of uncertainty still present on the structure and properties of the passive film, as well as the lack of quantitative data for adequate description of the phenomenon make these theories

incomplete. The kinetics of the process are therefore, an unknown aspect of breakdown as yet.

Finally, it must be emphasised that the pit propagation stage has been studied less extensively than the pit nucleation stage. All theories assume that the conditions inside fully developed pits are different from those prevailing on the metal surface and the bulk solution, e.g., the Cl^- ion concentration is shifted, making them subject to an autosustained active dissolution process in which Cl^- ions act as catalyst. Hoar[129] has suggested that these conditions inside pits resemble those of an electrobrightening process, but again these aspects are by no means clear.

4.2.3. The Problem in Studying Pitting

Corrosion mechanisms are difficult to identify even when the main features of the phenomena are appreciated and empirical solutions to related practical problems have been found. From the introduction it is apparent that the purpose of developing corrosion science is to provide a framework for understanding corrosion processes which can be used eventually to devise improved solutions to practical corrosion problems. To accomplish this purpose, philosophical as well as technical difficulties must be confronted in the design of research programmes concerned with the processes of metal deterioration, i.e., the nature of a given problem must be assessed.

From earlier discussions, it is apparent that pitting corrosion can be considered only in the context of the passive state

yet unlike the passive state pitting is a manifestation of the natural tendency of the metal/solution system to evolve towards its ultimate equilibrium; if the passive state did not exist dissolution would occur by general corrosion so that there could be no pitting phenomenon. It is this intimate relation which lies at the heart of the problem of understanding pitting corrosion; a passive state must first be established if pitting is to be perceived. Passivity can be studied without reference to pitting, but pitting cannot be studied without reference to the passive state. In this sense pitting studies can be considered as tests for our concepts of the passive state.

The complex phenomenology of pitting corrosion presents two aspects which merit reflections because they are the source of most of the difficulties in approaching the problem.

Firstly, the intervention of halogen ions in the manifestation of pitting is usually referred to as 'specific action', but this is really only a euphemism for suggesting that there is an unknown electrochemical reaction scheme between the metal or the passive film and the damaging anion. The identification of the reactants and intermediaries which actually participate in such a reaction scheme is in itself a difficult electrochemical aspect of the pitting problem which has not yet been satisfactorily resolved. This introduces the intrinsic difficulty that the application of the main theoretical tool, the Butler-Volmer equation,

is open to question for the following reasons. The equation is developed from the exchange current density at equilibrium for a singly-activated reaction on a plane surface, but the pitting reaction is fundamentally a localised reaction depending on complex interactions between the metal, the passive film and the environment so that it is uncertain whether an equilibrium condition, as required by the Butler-Volmer equation actually exists. To remove this inconsistency, recognising the usefulness of the Butler-Volmer equation the task is to reconcile the equation with the new situation, in other words, to assume a new equilibrium in which the passive film plays an important part, i.e., to consider the complex equilibrium of the system metal/metal-passive film interface/passive film/passive film-solution interface/solution. Certainly alternative approaches can be considered, e.g., to assume that the reaction is the same as occurs in the active region at low potentials, but to a different degree; in any case the problem of elucidation of the reaction scheme remains as subject for further investigation.

Secondly, pitting corrosion occurs locally at points on the metal surface. It is widely recognised that this bcalisation of the attack not only responds to the existence of the passive state, but also in a somewhat obscure manner to the metal structure. In this sense, it is a metallurgical problem or more precisely a metallurgical aspect of pitting corrosion. Investigations of this aspect seem to have been conducted with a

deterministic approach, i.e., trying to identify one particular feature which is wholly responsible for the localisation of the attack; the results are not conclusive in this respect and it is now generally accepted that the attack occurs randomly; pits can be produced on the grain surface, at grain boundaries, dislocations, inclusions and inhomogeneities of the metal structure, depending on the conditions of the metal, the value of the applied potential and the concentration of damaging anions, etc. Moreover, most of the information is based on photographic records, i.e., qualitative information, but there is very little quantitative data in this respect; although it is widely recognised for example that more important than the nominal sulphur content is the size and distribution of sulphide inclusions, its distribution in relation to other features of the metal structure, etc. Finally, pits observed under severe pitting corrosion are far bigger than any microscopic feature of the metal surface, the explanation given is that when once a suitable site undergoes attack interacting factors come into play which sustain the dissolution process, e.g., galvanic cells are set up with the active pits as anodes and the passivated surface as the cathode. This explanation does not make explicit any mechanism of the process and what is more important it ignores the metal structure leaving this aspect more obscure.

It is in this context of ideas that further research appears necessary. The purpose of the present work was to examine the pitting process with particular reference to the role of the metal structure as a contribution to the so-called metallurgical problem of pitting corrosion, i.e., localisation of the attack.

5. EXPERIMENTAL

5.1 EXPERIMENTAL APPROACH

From earlier discussions it can be appreciated that pitting corrosion is influenced by numerous factors. All of them have been studied earlier in a more or less systematic way on many materials; the results have been found very useful in defining the conditions in which the phenomenon is manifest and in developing better materials from a corrosion point of view. However they have been less successful in explaining the phenomenon itself, particularly as has already been pointed out, the reaction mechanism and the development of pits. In respect of the latter aspect, which is our major concern, it means that a suitable description of the phenomenon has not yet been obtained or proposed. How localised holes are produced in a metal structure is still unexplained and this may be considered as a structural problem in itself; factors which affect the manifestation of the structural feature concerned, i.e., pits, do not alter the fact that they are still being produced, i.e., these factors are not the essential variables on which the stability of the pits ultimately depend. An adequate description therefore requires definition of the variables which rationally account for the evolution of the system under study so that the experimentation should be directed towards the search for these variables. In this sense it is convenient first to observe how the phenomenon is produced without taking any a priori position in regard to the metal structure, to proceed to define the parameters or variables which permit a

characterisation, then to test the variables thus introduced and finally to describe the phenomenon in terms of these variables.

Advantage can be taken of E-i curves which illustrate quite clearly how the electrochemical behaviour of a given system evolves and indicate the onset of pitting. However information from experiments of this kind does not reveal the fundamental characteristic of the phenomenon, namely the localisation of the attack. The measured current intensity results from a population of pits evolving simultaneously whose areas are changing with time. To observe what is happening on the metal surface the specimen under test must be examined while the E-i curve is being produced. Ideally this would require equipment for observation in situ which is not only difficult to set up but may also be very expensive. The common practice to overcome this difficulty is to examine by stages under the following assumption:

i. All specimens used are equally representative of the material.

ii. All the environmental factors are kept constant.

Provided these assumptions are valid a set of specimens withdrawn at different stages during anodic polarisation would represent the evolution of the process as represented by a single E-i curve determined over the whole potential range for one specimen. This approach would condition other experimental aspects to some extent because the assumption made must be strictly observed. It must be noted that it is also tacitly assumed that the dissolution current of the metal can be related to damage on the surface and

that this damage is observable. This hypothesis could be right, naive or wrong but in any case it has to be established through experience.

Certainly a possible alternative approach is to take a single representative specimen, to interrupt the polarisation at a selected stage of interest, to examine it and to resume the experiment from the previous condition and to continue to a further stage. This is not the preferred approach because of the intrinsic difficulty that it is implied that a continuous evolution of the system is independent of the history of the material, i.e., previous treatments, hypothesis which is most likely wrong because it is well known that a specimen subjected to cyclic polarisation manifests hysteresis.

5.2 SPECIMEN PREPARATION

Although stainless steels are very complex metallic systems they are the most suitable and interesting material for pitting corrosion investigation. Their passivating characteristics and their industrial importance have made them the object par excellence of localised corrosion researchers. For the present work austenitic stainless steel AISI 316 type was selected on the further assumption that its high corrosion resistance would favour an easier observation of the pitting process. This steel was supplied by British Steel Corporation Special Steels Division in Sheffield, as

rod taken from their normal production line, of 1.25 cm diameter and chemical analysis as follows:

	Cr	Ni	Mo	C	Si	Mn	P	S	Fe
%	16.86	12.65	2.25	0.05	0.45	1.65	0.016	0.030	balance

Some of these rods were cut into pieces 12 cm long and heat treated at 1100°C in a muffle furnace controlled to ± 5°C. This solution treatment was of 2 hours duration after which the rods were water-quenched. This procedure was selected because it results in a fully austenitic structure without precipitated carbides and a minimal amount of possible strain energy stored in the fabrication process. Specimens were prepared from these heat-treated rods through the different phases of this work as follows:

a) To validate anodic polarisation characteristics determined using a special technique designed to facilitate the microscopic examination, a series of cylindrical specimens of different areas given in Table III to provide a suitable reference. Apart from this correlation no other use was made of cylindrical specimens.

b) To examine the pitting process and the effect of chloride ion concentration disc-shaped specimens 4 mm thick and 12.5 mm diameter were prepared.

c) To examine the effect of cold work disc-shaped specimens were deformed with a forging hammer. Dimension changes and deformation percentages are given in Table IV.

5.3 DETERMINATION OF ANODIC POLARISATION CURVES

Current voltage curves of metal electrodes can be determined either by measuring the steady potential reached by the metal electrode when a given current intensity is applied or by measuring the steady current intensity when a given potential (over potential) is applied. Both procedures are theoretically equivalent but in practice the latter is the most widespread since the introduction of the potentiostat in the early 1950's[130]. The basic principle involved in both techniques is the separation of a natural corrosion process comprising simultaneous anodic and cathodic reactions on the metal surface into an anodic process on the metal surface and a complementary cathodic process on another suitable electrode, i.e., construction of an electrochemical cell. In the potentiostatic technique a third electrode is introduced into the circuit to monitor the potential of the metal-anode and the depolarisation current flowing from the cathode is measured with an ammeter or recorder. Selection of the technique depends on the interest of the researcher as well as the facilities available and costs involved. The present work was performed with a Wenking 70TS1 potentiostat coupled with a Wenking SMP69 stepping motor generator which permits potentiodynamic determination of E-i curves; these were recorded using a Servoscribe potentiometer recorder. Technical descriptions of this equipment are given in Appendix I.

It must be emphasised that despite the advances in electronics which have led to the development of reliable, accurate

and precise equipment, E-i curve determinations depend also on other experimental factors which may outweigh these benefits resulting in inaccuracy and imprecision, particularly for the recorded values of current intensity as evident from the conclusions given in a report of the American Society for Testing and Materials (ASTM) in this respect[131]. They have recommended a standard experimental procedure which minimises the effect of possible sources of error, e.g., crevice corrosion, measurement of specimen potential, interfering cathodic reactions, the influence of surface condition and potential sweep rate. The main feature of this standard procedure are as follows:

1. Surface finish: wet grind with 240 grit SiC paper, then wet polish with 600 grit SiC paper until previous coarse scratches are removed. Samples should be prepared just prior to experiment (maximum delay time 1 hour).

2. Standard test solution: 900 cm^3 1.0N H_2SO_4 prepared from reagent grade acid and distilled water.

3. Solution temperature: 30 ± 1°C

4. Purging atmosphere: H_2 saturated at 150 cm^3/min. Begin purge 0.5 hour before specimen immersion.

5. Auxiliary electrode: platinised platinum.

6. Reference electrode: saturated calomel electrode (SCE). A salt-bridge/probe combination containing test solution should separate SCE reference from the solution in the test cell. Locate probe tip approximately 2 mm from specimen electrode.

7. Specimen mounting: Teflon compression gasket assembly as described by Stern and Makrides[132].

8. Specimen cleaning: just prior to immersion, degrease for 5 minutes in boiling benzene and then rinse with distilled water.

9. Pre-polarisation: open circuit specimen immersion time 1 hour.

10. Scan direction: active to noble.

11. Potentiostatic potential step rate: 50 mV each 5 minutes (current recorded after 5 minutes at potential).

12. Potentiodynamic potential sweep rate: 0.6 V/h. (Current recorded continuously as potential varies).

For the purposes of the present work some departures from this procedure were made although the essential recommendations were kept to obviate the above mentioned errors. The following modifications were made:

1. The surface finishing procedure recommended by ASTM was replaced by the polishing procedure used as standard practice in metallography laboratories, i.e., wet grinding successively with grades 180, 240, 400, 600 silicon carbide papers and then polishing with 6 μm and 1 μm diamond paste. The finishing was checked under the optical microscope at 100x. This finishing permits a clearer resolution of the metallic surface structure.

2. The temperature of the solution was changed to 25 ± 0.5°C to accord with standard practice in electrochemical laboratories.

3. Purging atmosphere: white spot oxygen-free nitrogen provided by British Oxygen Company (B.O.C.) was used instead because it is a less expensive and safer way to eliminate oxygen dissolved in the test solution used; it also provides an inert atmosphere.

4. Specimen mounting: the recommended Teflon compression gasket assembly is suitable only for cylindrical specimens which are susceptible to edge effects on pit distribution; such specimens also present curved surfaces unsuitable for metallographic work where flat surfaces obviously are preferred. A new holder electrode assembly was made to suit this purpose taking elements from the design proposed by France[133]. It consists of two plastic components, a teflon rod which provides support for the assembly when immersed in the solution, and a polycarbonate body which contains the specimen. This body is demountable into its parts which permits easy introduction and withdrawal of specimens. Basically it is a piece of plastic with a tapped core closed by a screw cap made of the same material and with an orifice of 0.5 cm^2. Disc shaped specimens 12.5 mm diameter can be introduced into this cap leaving an area equal to that of the orifice exposed to the test solution. Electrical contact is made by a metallic spring which compresses the specimen against a rubber gasket making a leak-proof seal, and completed with metallic rods through the other parts of the assembly. The whole assembly is illustrated in the diagram given in Fig. 12 and the photographs given in Fig. 13, 14.

5. Specimen cleaning: methanol was used instead of benzene because it is less expensive and less hazardous to work with. No rinse with distilled water was used.

6. The potential step rate was 10 mV per minute because the recommended value of 50 mV per minute is not available in the Wenking equipment. In any case this value corresponds with the transverse rate of 0.6 V/h recommended for the potentio-dynamic sweep rate.

7. Test solution: 1000 cm^3 of solution were prepared from reagent grade chemicals in every test; 200 cm^3 for the salt-bridge/probe combination and 800 cm^3 for the test cell. The chemicals used were supplied as follows:

<u>NaCl</u> Analar (Analytical reagent),

FW = 58.44, Assay ≥ 99.9 NaCl

B.D.H. Chemicals Ltd.

$\underline{H_2SO_4}$ Analar (Analytical reagent)

FW = 98.07 Assay > 98%

B.D.H. Chemicals Ltd.

H_2O Distilled or bidistilled de-ionised with conductivity $3.4 \times 10^{-6}\ \Omega^{-1}\ mol^{-1}$.

The complete experimental assembly used in E-i curve determination is shown in Fig. 15. It must be added that the small exposed area yielded only a small current intensity requiring the introduction of an electronic filter to reduce noise level in the potentiometric recorder; this was done in accordance with the potentiostat manufacturer's specifications.

It was very time consuming to develop the equipment and procedures needed to introduce these modifications and to master the techniques to the point where the results were reliable and there was confidence in the assumptions made in the experimental approach. The problems of detail encountered may be illustrated by the following two examples:

i. Immersion of the new electrode holder assembly in the test solution trapped air bubbles between the exposed metallic surface and the plastic cap. This problem was overcome by dropping test solution on the exposed specimen surface to fill the gap before immersion in the solution.

ii. The rubber gasket which is introduced between the specimen and the inner wall of the plastic cap could be used only once to avoid contamination of other specimens, i.e., a new gasket was required every time a test was performed. Rubber gaskets were punched from a rubber sheet with a suitable cutting tool made for the purpose.

A standard specimen holder of the Stern-Makrides type was used to determine anodic polarisation curves of cylindrical specimens with different areas so that a comparison of performance of the standard holder with the new holder could be made.

5.3.1 Observation of Pitted Surfaces Produced by Anodic Polarisation

To examine the initiation and growth of pits several samples were submitted to the experimental procedure already described. In a preliminary experiment three specimens were tested in a solution of 0.05 M H_2SO_4 and another three were tested in a solution of 0.1 M NaCl and 0.05 M H_2SO_4 to compare the effects of acid and acid chloride media. The anodic polarisation was not continued throughout the potential range of interest but stopped at different stages for every sample to represent frozen stages of the polarisation process. The stages chosen in this preliminary experiment were the maximum activity on reaching the passivation potential, the middle of the passive range and a point in the transpassive or pitting range where the current intensity was approximately equal to that at the maximum activity (i_{CRI}). These specimens were used to gather qualitative information.

For quantitative evaluation of the information a more extensive programme of tests was conducted in which new batches each of eight specimens were prepared. In this case the solutions were made with bidistilled de-ionised water. The anodic polarisation was interrupted at:

The passivation potential.

The initiation of the passive range.

The middle of the passive range.

The end of the passive range.

A point in the transpassive or pitting range where the current intensity was less or equal to that at the maximum activity (i_{CRI}).

A point in the transpassive or pitting range where the current intensity was twice the i_{CRI} value.

A point in the transpassive or pitting range where the current intensity was about 100 μA.

A point in the transpassive or pitting range where the current intensity was about 200 μA.

5.3.2 Effect of Chloride Ion Concentration

Anodic polarisation curves were determined for solutions of 0.05 M H_2SO_4 in distilled water containing chloride ion concentrations of 0.5 M and 1.0 M besides those already obtained for 0.1 M. Two further tests in all these Cl^- concentrations were conducted, interrupting the polarisation at the point of maximum activity on reaching the passivation potential (E_{pp}).

5.3.3 Effect of Cold Work

Anodic polarisation curves of cold-worked specimens were determined in 0.05 M H_2SO_4 and in 0.05 M H_2SO_4 + 0.1 M NaCl solutions. A new electrode holder assembly was required for them because the changes in dimensions on making the specimen made them unsuitable for the original holder. The new holder was made on the same pattern as the original but leaving space to accommodate specimens of various diameter, in the range 12mm to 20mm.

5.4 OPTICAL AND ELECTRON-OPTICAL MICROSCOPY

Examination of specimens was carried out with a Leitz optical microscope and Cambridge stereoscan S400 and S600 scanning electron microscopes. Electrolytic etching in 1% oxalic acid solution or 0.05 M H_2SO_4 solution at 2.0 V for 60 seconds was used when required.

5.5 MEASUREMENT OF PIT-SITE DENSITY (N_A)

Quantitative evaluation of the pitting process is usually expressed by the number of pits per unit area (pit density) or by dimensional changes of pits as a function of time. In the context of the present experimental approach and the results obtained through experimentation an estimate of the number of sites seemed to provide a valuable means of quantifying the information. Certainly this was not accomplished without facing problems of site definition, selection of the parameters to be measured and selection of a suitable criterion for measurement.

The term site was assigned to any pit-like irregularity observed on the metal surface. This is a departure from the common view of regarding a site as any imperfect on of the metal structure. This definition was found to be more in accordance with the observation made and the phenomenon under study; it is also more workable from an experimental point of view taking into consideration the fact that imperfections of a metal structure which might stimulate pitting can be of different character, e.g., atomic, microscopic and macroscopic defects which are difficult

to evaluate. Sites as microscopical features on a metal surface can be represented by a model of particles on a homogeneous phase and hence they can be treated mathematically and experimentally with the techniques and procedures within the framework of stereology. A site population is characterised by two parameters; the number of sites per unit area (site density) and the size distribution of the sites. The site density which was the only parameter estimated in the present work is determined simply by counting the number of sites in a given area of the specimen. Although counting is a simple means of quantification it presents experimental difficulties particularly when performed visually. Ideally the conditions for precise counting are; clean binary field e.g., black particles in a white phase, features of equal size and uniform distribution through the phase. In practice, actual features on a metal structure deviate more or less from these requirements resulting in low accuracy and loss of precision which are intrinsic in the counting procedure. The use of modern quantimeters has partially overcome these problems but for the present work this kind of facility was not available and the alternative chosen was the time consuming visual procedure. Estimation of representative values of site density were performed by visual counting on micrographs taken with the aid of a Stereoscan S600 electron microscope. Advantage was taken of this technique to set the criterion of counting because sites appear as small black spots surrounded by a white circle; the smallest sites do not necessarily exhibit the black spot and they appear as white spots recognisable in the grey background of the surface. All of these features were included in the total counts. From every specimen a sample of 30 photographs corresponding to 30 fields

chosen randomly was prepared and simple statistics were applied to obtain a representative value of the site density. This counting technique was also applied to estimate dislocation density by counting etch-pits which develop when a specimen is etched electrolytically in a 0.05M H_2SO_4 solution.

6. RESULTS

6.1. ANODIC POLARISATION CHARACTERISTICS

Anodic polarisation curves determined through different phases of the present work are shown in figures 16 to 63. The usual simple pattern of E-i curve for this stainless steel type was found, i.e., an active range followed by a passive range and the reoccurrence of activity in the transpassive or pitting range depending on the nature of the test solution. To characterise these curves, values of open-circuit potential* (E_R), passivation potential (E_{pp}), critical current density (i_{CRI}), passive current density (i_p) and breakdown potential (E_b) or transpassive potential (E_T) were measured or calculated. This information is presented in Table V, where the significant experimental conditions are also recorded, i.e., test solution composition, pH, recorder sensitivity. Two values are recorded for breakdown or transpassive potentials; E_b or E_T represents the value at which the polarisation curve initially departs from the passive line as evidenced from the recorder chart; E_b* or E_T^* corresponds with the value calculated from the intersection of the tangent to the passive line with the tangent to the transpassive or pitting line where there is an apparent indication of sustained current increments. All these values are referred to the standard saturated calomel electrode (SCE). It is evident from the figures that a linear scale was used in recording current intensities; the small dissolution current of this material and the small area exposed to the solution permitted the equipment to be used in a linear response range.

*Also known as rest potential

The effect of the surface area of specimens on the anodic polarisation curves is shown by figures 16 to 25. The curve in Fig. 21 exhibits a discontinuity in the early stages of the passive range due to a change for experimental convenience in the recording scale, i.e., the sensitivity of the potentiometric recorder, from the 500 mV to 200mV scale. This is not true of Fig. 23, where a sudden rupture of the passive line was produced at an overpotential of +790mV followed by repassivation and an indication of the occurrence of an interfering cathodic reaction. Since the prescribed experimental procedure was strictly followed this curve appears to be abnormal. The characteristics of these curves are tabulated in Table V where an apparent effect of the recording sensitivity on the values of breakdown potential can be appreciated; this effect is represented in Fig. 64, which shows that E_b values tend to be lower at high recorder sensitivity.

Leaking and crevice effects were the major experimental problems confronted in setting up the new electrode holder assembly, as illustrated in Fig. 26, 27. These sources of error were minimised by the introduction of rubber gaskets which resulted in a reproducible and satisfactory passive current density in well-defined curves, Fig. 27c, 27d.

Anodic polarisation curves which were interrupted at some prescribed value of overpotential are shown in Figures 28 to 49. The (E, i) co ordinates where polarisation runs were interrupted are summarised in Fig. 65, 66. The numbers assigned to these points are the numbers of the figures which give the corresponding polarisation curves and they are linked by an imaginary complete anodic polarisation curve.

Increasing the chloride ion concentration resulted as expected in decreasing the value of the breakdown potential; a tenfold change in concentration corresponds to 84mV shift in the active direction. It is also found that values of critical current densities (i_{CRI}) were higher than those from curves in which chloride ions were absent. These effects are represented in Fig. 67, 68.

Finally, anodic polarisation curves of cold-worked specimens are given in Figures 55 to 63. Breakdown potentials determined from these curves are plotted against the degree of deformation in Fig. 69. The value corresponding to the curve in Fig. 61 is abnormal because it was produced when other equipment in the laboratory was switched on introducing interference extraneous to the system under study.

6.2. OPTICAL AND ELECTRON-OPTICAL MICROSCOPY

Micrographs of the structure of the stainless steel after heat-treatment are given in Fig. 70, 71. The structure is a fully austenitic matrix with some non-metallic inclusions as expected; dislocations, associated with etch-pits, and twins exhibited are typical defects of wrought stainless steels.

Specimens tested in 0.05M H_2SO_4 and 0.05M H_2SO_4 + 0.1M NaCl solutions did not exhibit noticeable differences under the optical and electron-optical microscopes, even though they corresponded with different stages of polarisation and different solutions, as is evident from the

micrographs in Figures 72 to 97. The attack of the solution appears to be concentrated on certain areas giving the appearance of dark spots uniformly distributed over the exposed metal surface when examined at low magnification under the optical microscope. Closer examination of these features revealed preferential attack on these areas generating pit-like features, as evident when examined under oblique illumination. There was also evidence of a passive film present at these particular points. Confirmation of this morphology, i.e., pit-like structure, is provided by scanning electron-optical micrographs as given in Fig. 95, 100. The better depth resolution of this technique revealed smaller points of attack which could not be resolved by the optical microscope. Basically pit-like structures appear as black spots surrounded by whitish areas. It is interesting to observe that polished specimens certainly did not exhibit these features, as illustrated in Fig. 98; on the other hand specimens which have been held in contact with the solution and without an imposed anodic or cathodic polarisation showed the same type of features as exemplified in Fig. 99 to 101. No evidence of crevice corrosion was found on any of the specimens tested to produce the curve in Fig. 66, except for the last point in the pitting range where the current density is about 400 $\mu A\ cm^{-2}$. At this high current density, specimens tested in 0.05 M H_2SO_4 solution started to exhibit overall dissolution leading to etching patterns as illustrated in Fig. 104. On the other hand changing the nature of the solution to 0.05 M H_2SO_4 + 0.1 M NaCl resulted in damage to the surface mainly due to crevice corrosion attack although pitting is also produced as illustrated in Figs. 105 to 110.

Finally, micrographs given in Figs 111 to 114 correspond with the cold-worked specimen which produced the anodic polarisation curve shown in Fig. 61; they illustrate the intensity of the attack and the complexity of the dissolution process inside pits.

6.3. MEASURE OF SITE DENSITY (N_A)

The collection of data used in the determination of site densities is given in Table VI, where the values of number of sites counted (N), magnification (Mag.), area of the micrograph (A_{OBS}), true area of the field examined (A_t) and site density (N_A) for every micrograph are included. These data are grouped in sets and every set constitutes one data sample. Each sample-set is characterised by the nature of the solution in which the corresponding specimen was tested and the (E, i) coordinates of the point at which the anodic polarisation curve was interrupted. Mean values of site densities (N_A) and standard deviations (S) for every sample are summarised in Table VII. The average of relative error of site density determinations was 14% over a 9 to 18% range. This error is 4.5 times the average of the standard error of the mean site densities determined taking account of the size sample. These data are given in Table VII where estimated values of site densities per cm^2 together with their standard deviations are also included. These latter values are plotted in Fig. 115.

It was found that most of the sites formed even before anodic polarisation of the specimen, i.e., at the rest potential, E_R; and that their number expressed as site density, remained constant over a wide range of overpotentials. It was only at high current densities in the transpassive or pitting range that an increase in site density could

be appreciated as illustrated in Fig. 115.

Changing the nature of the test solution by increasing the chloride ion concentration resulted in an increase of the site density initially formed on the specimen. This effect is represented in Fig. 116, where values of site density at the overpotential corresponding with the maximum active current are plotted against the chloride ion concentration; a tenfold increase in concentration resulted in a 26% increase of the site density. Finally, the breakdown potential (E_b) represented as a function of the site density determined at low overpotential and at different chloride ion concentrations exhibits the same pattern of variation as that given by E_b vs. $C_{c\ell}$, as evident in Fig. 117. E_b shifts towards the active direction as the value of N_A increases.

6.3.1. Variance Analysis

Due to the high relative error on the site density determinations a simple variance analysis was conducted to assess whether the different values obtained were significant in view of statistical variations. For this purpose the Null hypothesis "All samples analysed come from the same site population" was tested at 5% significance level against the alternative hypothesis "not all the samples analysed come from the same site population". The calculation consisted of an estimation of the variance between samples and the variance within samples. The variance ratio (F) was compared with the significance point of the F-distribution for the corresponding degrees of freedom at the fixed significance level, chosen to be 5% ($F_{0.05}$), and the Null hypothesis was rejected when $F>F_{0.05}$.

This calculation was done initially for all the samples corresponding to specimens treated in the same solution but whose anodic polarisation curves were interrupted at different stages, and then successively with a reduced number of samples until the Null hypothesis could not be rejected. The results of the statistical analysis are summarised in Table VIII, where n_T and $\bar{N}_T$ represent the site sample and mean site density totals for the set of samples.

For specimens tested in 0.05 M H_2SO_4 solution three samples corresponding with the transpassive range had to be withdrawn from the calculation to conform with the Null hypothesis. For specimens tested in 0.05M H_2SO_4 + 0.1M NaCl solution the condition of no rejection of the Null hypothesis was obtained in two instances; first by withdrawing five samples, three corresponding with the pitting range, one corresponding with the point of maximum activity and one corresponding with the initiation of the passive range; secondly by withdrawing just four samples, two corresponding with the pitting range, one corresponding with the point of maximum activity and one corresponding with the initiation of the passive range.

6.3.2. t - Student Test

To compare site density values corresponding with specimens tested in solutions which differ in nature the well-known t-student test was applied. The Null hypothesis "site density values represent the same site population" was tested at different significance levels against the alternative hypothesis "site density values represent different site

population". Samples which resulted in no rejection of the Null hypothesis in the variance analysis were used for the comparison of the site density of specimens tested in 0.05M H_2SO_4 solution with the site density of specimens tested in 0.05 M H_2SO_4 + 0.1M NaCl solution. The latter was compared with the site densities of specimens tested in 0.05M H_2SO_4 + 0.5M NaCl and 0.05M H_2SO_4 + 1M NaCl solutions. The results are given in Table IX. The Null hypothesis could be rejected in all the cases examined at the 5% significance level, i.e. $t > t_{0.05}$.

6.3.3. Test of Normality

To validate the results given in the earlier sections the normality of the site density values distribution was verified by examining the proportions of observations in intervals surrounding the mean[134]. This consisted of counting the values outside the intervals $(\bar{N}_A - S, \bar{N}_A + S)$, $(\bar{N}_A - 2S, \bar{N}_A + 2S)$ and $\bar{N}_A - 3S, \bar{N}_A + 3S)$ and comparing their frequencies with the theoretical probabilities for a normal distribution, i.e., 1/3, 1/20, 1/300. The following statistical relation was applied:

$$Z = |\hat{P} - P| / \sqrt{P\frac{(1-P)}{n}} \qquad \text{.....(38)}$$

where n is the size sample, $\hat{P}$ and P are the observed and theoretical frequencies respectively in the interval considered. The condition $Z > 3$ would indicate lack of normality[134]. This test was applied to the samples which resulted in no rejection of the Null hypothesis in the variance analysis and to the sample corresponding with the

specimen tested in 1.0M NaCl + 0.05M H_2SO_4 solution. The results are given in Table X; all the samples resulted in distributions which can be well represented by a normal distribution, as illustrated by histograms given in Fig. 118.

7. DISCUSSION

The experimental approach followed in the present investigation of pitting corrosion of an austenitic stainless steel and its results are critically examined in the following sections. As a preliminary the initial assumptions are discussed because they are fundamental prerequisites which must be fulfilled to validate the results. Then the experimental technique is discussed because of the particular conditions in which it was applied; finally a separate discussion of the different phases of the experimental design is presented, i.e., observation of metal surfaces throughout different stages of the anodic polarisation curve, measurement of site density (N_A) as a means of quantifying the microscopical information, testing of the site density as an important variable on the pitting phenomenology and interpretation of the phenomenon in terms of this variable.

7.1 VALIDITY OF THE ASSUMPTION

The present investigation involved examination of successive specimens whose anodic polarisation were interrupted at pre-selected values of (E, i) coordinates under the assumption that using representative specimens of the metallic material and keeping the environmental factors constant they would represent "frozen" stages of an anodic polarisation curve as determined with only one representative specimen of the material over the complete range of overpotential of interest. Although the experimental procedure was designed to fulfill these two conditions, they could not be taken for granted so that some elements of control were introduced to check them. Certainly it must be said that

experiments in general are considered controlled experiences which permit the identification or measurement of properties or their relationships or to perceive how a phenomenon is manifest and how it is affected by controlled change in prescribed factors. It is in this context that results have a significance. Extrapolation of the validity of results to other situations which are uncontrolled and where presumably the same phenomenon is being produced following the same relations, is a philosophical aspect, i.e., the philosphical problem of induction, which is beyond the scope of the present dissertation. Since the two assumptions made are independent from each other, the elements of control are different and are discussed separately in the next two sections.

7.1.1 Representativeness of Specimens

Theoretically a representative specimen of a material is a small amount of it which contains proportionally all the characteristics and properties of the bulk with the exception, of course, of those properties which are independent of the amount of material, i.e., intensive properties. If this is true, the specimens are suitable for laboratory tests and results using them can be extrapolated to the bulk material and from these considerations derives the importance assigned to this aspect in any research.

Following common practice in corrosion studies of wrought austenitic stainless steels, specimens were prepared from rods which had been previously prepared, i.e., annealed at 1100^{o}C for two hours and water quenched. This treatment of

the material resulted in a fully austenitic structure without precipitated carbides, as is evident from the micrographs given in Figs. 70,71, which correspond with the description given in the ASTM Atlas of Microstructure[135] for the microstructure of this stainless steel in these conditions. Apart from small side effects such as stress produced by the rapid cooling and the machining used for specimen preparation, whose importance and quantification are difficult to assess and to control, specimens prepared from these rods can be considered as representative of the bulk from a metallurgical view point. However, two factors must be considered in respect of the representativeness of specimens. First, corrosion reactions are processes which occur on the metal surface or more precisely at the metal-solution interface, a fact which requires a consideration of representative surfaces of the specimens instead of specimens themselves and this can only be conceived in statistical terms due to the impossibility of preparing two identical metal surfaces. Secondly, the representativeness of specimens depends fundamentally on the nature of the test or experiment to be performed and can only be judged in terms of the reproducibility of the experiment. In consequence, the question of whether all of the specimens prepared are equally representative of the material has to be examined in terms of their electrochemical behaviour in the conditions of interest, i.e., the pitting condition. For this purpose, the potentiodynamic technique of determining anodic polarisation curves provides a suitable mechanism by which to represent the electrochemical behaviour of the specimens and the elements of control required. In this sense, from the data in TABLE V for the anodic polarisation characteristics of cylindrical specimens which differ in surface area determined in 0.05M H_2SO_4 + 0.1M NaCl

solutions, it can be appreciated that the values of rest-potential (E_R), passivation potential (E_{pp}), critical current density (i_{CRI}) and passive current density (i_p) are all fairly constant as expected, taking account of the fact that all of them are intensive parameters. The critical current intensity (I_{CRI}) and passive current intensity (I_p) which are extensive parameters are of course different exhibiting a linear function of the surface area of specimens. It must be emphasised that experimental values of current intensities or densities are subject to considerable variation as has already been pointed out, e.g., specimens whose areas are 8.40 and 8.12 cm^2 exhibited I_{CRI} of 62 and 105 μA respectively. Values of breakdown potential (E_b) are also fairly constant provided the instrumental factors remain constant, e.g., the actual value is influenced by the recorder sensitivity used; thus the mean value of E_b determined using the 1V recording scale of the potentiometer recorder is 533 mV and using the 0.2V scale is 435 mV, a difference of 100 mV which cannot be assigned to statistical fluctuations; this effect is illustrated in Fig. 64. In the light of these results it can be concluded that the specimens exhibited the same electrochemical behaviour and due to this reproducibility the required condition of representativeness can be considered satisfied.

7.1.2 Constancy of the Environmental Factors

This assumption is easier to validate because environmental factors can be reproduced with a high precision, i.e., they are subject to much less variation than metal surface preparation. The nature of the solution is the factor of most concern because of the marked influence it can produce on the electrochemical behaviour of

the metal-electrode as represented by anodic polarisation curves. All solutions prepared were intended to have the same acidity by fixing the concentration of the sulphuric acid at 0.05M; this was controlled by measuring the pH before every test; it can be appreciated from data given in TABLE V that the pH was reasonably constant throughout the different solutions, within the range 1.10 - 1.50 and with a mean value of 1.3 ± 0.1. The chloride ion concentration was not controlled by measuring its activity but this is a factor which is likely to change very little taking into consideration the fact that the chloride ions were introduced as weighed amounts of Analytical Reagent grade sodium chloride. Other external factors were kept constant in accordance with a standard experimental procedure, e.g., the temperature was kept constant at 25.0 ± 0.5^{o}C with the use of a thermostated water bath; and hence it can be concluded that the requirement of constancy on the environmental factor was satisfied.

7.2 APPRAISAL OF THE EXPERIMENTAL ELECTRO-CHEMICAL TECHNIQUE

The usual purpose of the potentiodynamic technique is the determination of anodic polarisation characteristics which yield comparative information for various metal/environments systems. In the present work it has been used for a different purpose, i.e., to provide a basis on which to standardise the polarisation of specimens of the same steel in the same environment to preselected values of (E,i) coordinates. Standardisation is , of course , essential because the precise mode of polarisation may condition the subsequent phenomena observed. In addition, the introduction of modifications to the standard procedure to suit the experimental

approach adopted, in particular the new-style of electrode holder, requires examination for the following reasons. First, departures from an established standard procedure can be accepted only on the grounds that the major features of the curves determined are not substantially altered though there may be room for variations in the values of parameters measured justified by the modifications themselves. Secondly, as a result of the introduction of the new holder the specimen surface area exposed to the solution is only 0.5 cm^2; this scaling down of the specimen size may introduce difficulties in satisfying the reproducibility of the parameters measured and hence doubts could arise about the representativeness of specimens vis a vis the technique.

The results of anodic polarisation characteristics determined in 0.05M H_2SO_4 + 01M NaCl solution using the standard, i.e., ASTM procedure[131], procedure with the recorder set to the 0.2V scale can be compared with the corresponding results determined using the modified procedure. It is apparent from TABLE V, that the agreements on values of rest potential (E_R), passivation potential (E_{pp}) and passive current densities (i_p) is fairly good within the experimental error given by the standard deviation for each set of results; taking into consideration that crevice corrosion is usually manifest in E-i curves by values of passive current density which are higher than when this form of corrosion is absent[136]; the good agreement on the values of i_p indicates that this usual source of error was avoided or minimised to an acceptable level. The only exception was the curve for which the polarisation was interrupted at (792 mV, 400 μA cm^{-2}) which exhibited an i_p value of 5μA cm^{-2} and incidentally this particular specimen exhibited a

crevice corrosion effect as illustrated in Fig. 105. On the other hand, values of critical current densities (i_{CRI}) are higher for curves determined using the modified procedure than for those determined using the standard procedure. This discrepancy may be due to the different surface finishing procedures. Surfaces polished to a 1μ diamond paste finish may have a higher energy content than those only ground with silicon carbide papers because of the greater amount of mechanical work imposed on the surface, giving rise to an initially higher reactivity as measured by the i_{CRI} value. Finally, values of breakdown potential (E_b) determined using the modified procedure are lower and with higher variability than those from curves determined using the standard procedure. This would suggest that polished specimens are more susceptible to pitting corrosion than ground specimens in disagreement with currently accepted views. However, the apparent E_b^* (as defined in section 6.1) values which correspond with the point of sustained pitting corrosion and can be associated with pit growth stage, are higher for the curves determined using the modified procedure than for those determined using the standard procedure, and hence the opposite conclusion may be drawn, i.e., ground specimens reach more easily the conditions of sustained pitting corrosion and hence are less resistant than well-polished specimens. Actually the low values of E_b determined using the modified procedure can be explained by geometrical factors and instrumental factors, e.g., recorder sensitivity. It is widely recognised that E-i curves are influenced by the electrochemical cell design, i.e., geometrical factors, which affects mass transport rates or diffusion fluxes by altering the hydrodynamic conditions where they are produced. In this respect, it must be noted that in the new electrode holder assembly the specimen is encapsulated in such a way that the solution in contact with it is

less perturbed by agitation than in the standard holder where the specimen is freely exposed to the solution. As the specimen is anodically polarised the Cl^- ion concentration of the solution near the metal electrode is enriched [103], an effect which if imperturbed would produce a lower value of E_b than if perturbed. On the other hand it is apparent from the results given in TABLE V that the recording scale of 0.05V, 0.1V and 0.2V were used in determining the E-i curves when the modified procedure was applied; it has already been pointed out that there is a tendency to estimate lower values of E_b at higher recorder sensitivity; values of E_b plotted against recorder sensitivity are represented in Fig. 64.

The modified procedure of E-i curve determination was also applied to examine the effects of Cl^- ion concentration and cold work. the widely - observed [79] shift of breakdown potential in the active direction by increasing the Cl^- in concentration was reproduced when E-i curves were determined with 0.05MH_2SO_4 + 0.5MNaCl and 0.05MH_2SO_4 + 1.0MNaCl solutions. Although only a few results were available they illustrate the general trend of the variation as given in Fig. 67; a tenfold change in Cl^- ion concentration resulted in a negative shift of 84 mV on the value of E_b. It is interesting to observe that there is little or no difference between E_b and E_b^* when determined at 0.5M and 1.0M Cl^- ion concentrations, a fact which contrasts with the large difference observed at 0.1M Cl^- ion concentration, i.e., 376 mV. Taking into consideration the fact that E_b corresponds with the point of rupture of the passive line and E_b^* with that of sustained dissolution, i.e., E_b may be associated with pit initiation stage and E_b^* with pit growth stage, these results would suggest that at high Cl^- ion concentration the conditions for pit growth and passivity breakdown are simultaneously satisfied which reveals the weakness of separating the phenomenon.

On the other hand, the active dissolution of the metal electrode is enhanced by increases in Cl^- ion concentration, as it can be appreciated from Fig. 68. The critical current densities vary linearly with the Cl^- ion concentration in the small range considered in accord with previous observations for other steels[104].

Finally, E_b values of cold-worked specimens exhibit a complex dependence on the degree of deformation, as illustrated in Fig. 69. It must be said that the preparation of cold-worked specimens by forge-hammering involved several mechanical factors whose assessment and control are very difficult to elucidate, e.g., blows of the hammer cannot be guaranteed constant and specimens received different number of blows to produce the different degrees of deformation. In consequence, to give a significance or correct interpretation of the variation of E_b with the degree of deformation is too speculative because they may be just due to the uncontrolled variability introduced in the specimen preparation, A study of variability at every degree of deformation must be performed before attempting to assess an effect on E_b. In electrochemical respects, this experiment can be considered incomplete, to say the least but the features revealed in subsequent surface examinations discussed later are highly significant and suggest that this approach should be continued in more refined form.

7.3 METAL SURFACE EXAMINATION

The initial phase proposed in the experimental approach was to observe the changes produced in the metal surface at different stages of its anodic dissolution. Specimens whose anodic polarisations

were interrupted at different values of (E,i) co-ordinates correspond well with different stages of the electrochemical behaviour of the material, i.e., active,passive and transpassive or pitting ranges, as represented in Fig. 65. Microscopical examinations of their surfaces revealed that there were no differences between the features observed on them, as evident throughout the micrographs given in Figs. 72 to 97. All of these surfaces exhibited preferential dissolution resulting in pit-like features, even though the change of electrolyte composition from 0.05M H_2SO_4 to 0.05M H_2SO_4 + 0.1M NaClwas accompanied as expected by a contraction of the passive range on the E-i curve, as in Fig. 65. Moreover, the same pattern of features was found on specimens which were neither anodically nor cathodically polarised, they were subjected to the preparatory experimental procedure and withdrawn from the solution after reaching the open-circuit potential (E_R). Micrographs of these specimens are given in Figs. 99, 100, 101. In consequence, the metal surfaces prepared were indistinguishable when examined under the optical or electron optical microscope and no correlation could be found between the observed features and the (E,i) co-ordinates at which polarisations were interrupted within the range of overpotentials considered, i.e., the technique used for metal surface examination cannot resolve what is manifest on the E-i curve in the range considered. However, the features revealed by the microscopical examinations are very important in regard to our views of passivity and pitting corrosion on this material and will be discussed later. Certainly no major differences were anticipated between specimens corresponding with the active and passive ranges but only between active or passive specimens and those corresponding with the transpassive and pitting ranges. Here the lack of resolution of distinctive features is due to the low current density values reached at

the moment of interruption of the test. To produce morphological differences the dissolution rate has to be increased or to be maintained constant for a longer time. Pit-like features found in specimens tested in 0.05M H_2SO_4 solution were not due to chloride ion contaminated water used for the solution preparation taking into account the fact that these observations were confirmed for the further specimens represented in Fig.66, whose E-i curves were determined using solutions prepared with bidistilled de-ionised water. The only exceptions were found for the specimens whose co-ordinates are (1000 mV, 400μA cm^{-2}) and (790 mV, 400μA cm^{-2}) in the transpassive and pitting range respectively in Fig. 66. At these points differences of the metal dissolution processes could be eventually perceived by microscopy; the specimen tested in 0.05 M H_2SO_4 solution exhibited an initial formation of etch patterns which are usually associated with overall dissolution of the metal surface, as illustrated in Fig. 104. The specimen tested in 0.05M H_2SO_4 + 01M NaCl solution exhibited well-developed pits and crevices which are manifestations of localised dissolution on the metal surface, as shown in the micrographs given in Figs. 105 to 110. These exceptions illustrate limitations of the technique adopted and the difficulties of studying pitting phenomenon. Morphological evidence of metal dissolution are produced at stages subsequent to the initiation of the phenomenon and what is perceived is the result of a catastrophic behaviour which corresponds with the growth stage, e.g., from a comparison of point 54 (780 mV, 172 μA cm^{-2}) with point 55 (790 mV, 400 μA cm^{-2}) given in Fig. 66, it can be appreciated that both points lie in the pitting range; however microscopical examination of their surfaces reveals that for the first point there is no indication of metal dissolution in contrast with what was observed for the latter point.

It is convenient to discuss separately the implications of all of this evidence on the three different aspects of pitting, namely, passivity, pit initiation and pit growth.

7.3.1 The Nature of Passivity

In regard to passivity it appears that the very first act of contact of the metal with the solution has an important bearing on subsequent processes which occur by anodic polarisation. This initial metal - solution interaction results in metal dissolution which transforms the flat, even polished surface into a surface with pit-like irregularities; actually they are morphologically pits as is evident by comparing Fig. 98 which shows a polished surface with Figs. 99, 100, 101, which correspond with specimens withdrawn at the rest-potential (E_R). On the other hand the initial metal-solution interaction seems to lead to an equilibrium state characterised by the rest-potential where there is no indication of net dissolution although the thermodynamic conditions for its further dissolution are still present. Therefore the metal is in a passive state, i.e. the immersion of 316 austenitic stainless steel in 0.05M H_2SO_4 or 0.05 M H_2SO_4 + 0.1M NaCl solutions produces the same phenomenon as when immersing iron in fuming nitric acid. This comparison may be regarded as a phenomenological proof of the passivity of the 316 stainless steel in these conditions. This assertion has an important implication for if, having reached the rest potential, the specimen is anodically polarized there will be metal dissolution until a maximum value of current density (i_{CRI}) is reached after which there is again a manifestation of the passivity phenomenon, as evident in an E-i curve. There is therefore a

transition from one passive state (at E_R) to another passive state (at E_F). Let us call the first the initial passive state and the second the anodic passive state. It must be noted that the initial passive state does not correspond with what Frankenthal[137] called primary passivation. This author studying passivity of a 24% Cr Fe alloy in 0.05M H_2SO_4 solutions applied the concept of primary passivation to the process which occurs after the point (E_{pp}, i_{CRI}) in an E-i curve, near or at the Flade potential, E_F, and which certainly leads to the anodic passive state. The manifestation of the initial passive state will depend on the nature of the metal, its treatment before immersion in the solution and the nature of the solution. A precise assessment of this phenomenon is obviously beyond the context of the present dissertation but it is noteworthy that failure in realising this presentation of the passivity phenomenon may be at the base of the contradictory opinions in respect to passivity in stainless steels.

The transition from one passive state to another may involve the partial or total destruction of the initial passive state or the transformation of the initial passive state to the anodic passive state depending on numerous factors, e.g., electro-chemical conditions; what is certain is that the anodic passive state when fully established is characterised by a film covering the metal surface. In this respect, the micrographs given in Figs. 76, 77 obtained in normal and oblique illuminations are conclusive; it can be appreciated how the film has been

unfolded by localized attack underneath. This evidence is completely in agreement with the previous observations of Evans[54] in his famous experiment. The immediate conclusion is that the passive film is not a perfect layer uniformly deposited over a flat surface, it is a film with holes at the areas where the irregularities, namely pits, are. That the inner surfaces of the pits are equally passivated by a film of the same nature is a matter open to speculation; the specific conditions inside the pits may be so different from those prevailing in the unattacked areas that if there is any film it may be rather different in structure and hence in properties. The cognitive consequence of these facts, i.e. an imperfect film, is important for if an experiment is made to study the film growth by interferometry, e.g. thickness as a function of the overpotential, it will produce results which are strictly valid for the flat surfaces but not necessarily for the inner surfaces of the pits.

7.3.2. Pitting Initiation

It is obvious that the initial irregularities formed on the metal surface which correspond with the morphological definition of pits are suitable sites for later preferential dissolution whose evolution will depend on the electrochemical conditions. Before going further it must be said that these pits do not correspond with the pitting phenomenon from a corrosion science view point because pitting has to be regarded as a process rather than a morphological feature in itself. When the specimen is anodically polarised in 0.05M H_2SO_4 solution, these sites may act as points of initiation for the metal dissolution although this process is not restricted to them; the micrograph given in Fig. 104 is illustrative of this process. When the

nature of the solution is changed to 0.05M H_2SO_4 + 0.1M NaCl, the pitting phenomenon occurs; in this respect the best sites for the initiation process are precisely the initial pits formed at low overpotentials. It is what occurs inside these sites that leads to the conditions for developing a system undergoing sustained dissolution with a catastrophic effect. The breakdown of the passive state or passivity is a phenomenon intimately related to such a process and cannot be associated with the morphological disruption of the flat metal surface, as is usually proposed, i,e., breakdown of passivity does not mean breakdown of the external metal surface. Due to the intrinsic difficulties in perceiving what occurs inside these sites the process must be inferred and will be discussed in a later section.

7,3,3 Pit Growth

Pits observed on the specimen which was severely attacked were of two morphological types;; a crystallographic type as shown in Fig. 110, and a hemispherical type, as shown in Fig. 109. They correspond well with similar pit types observed by Frankenthal and Pickering[138] for 304 stainless steel, 20% Cr-Fe and 18% Cr-6% Ni-Fe alloys. The polished hemispherical type and the pit-type associated with inclusions usually described in the literature[138-140] were not observed. This is presumably due to the fact that the metal dissolution was concentrated at the surface area underneath the gasket, an effect usually associated with crevice corrosion. However, close examination of this area revealed three distinctive features, as shown in Fig. 106. Feature A, corresponds with localised dissolution initiated at the zone in which the free metal surface merges with the covered metal surface and propagated inside the

steel underneath the surface forming a crevice. A detailed view of this feature, given in Fig. 107, shows that the inner surface was preferentially dissolved leading to a rough appearance though hemispherical and crystallographic pits can be distinguished. Feature B, corresponds with localised dissolution on the covered surface. A detailed view of this feature, given in Fig. 108, reveals that the dissolution resulted in pits whose inner surfaces were preferentially dissolved, i.e., pitted; the surface area surrounding the major pits exhibits general and localised dissolution resulting in hemispherical and crystallographic minor pits. Finally, feature C corresponds with general dissolution on the covered surface, in large areas spreading from pits found somewhere within them. Taking into account the fact that specimens tested in 0.05M H_2SO_4 solutions did not exhibit any crevice corrosion at any value of current density it is clear that the localised dissolution of the metal underneath the gasket is a pitting corrosion process which degenerates to crevice corrosion because of the specific conditions in which it is manifest. This is the reason why crevice and pitting corrosion are manifest simultaneously and with the same phenomenology in most of the situations in which stainless steels are tested in Cl^- ion media. On the other hand, preferential dissolution inside pits and crevices which is in agreement with previous observations in mild steel[141], iron and stainless steels[138,140] would suggest that the metal dictates the path of its dissolution, i,e., pit propagation is determined to a great extent by the state of the metal and its structure and not only by the solution composition inside the pits as is currently assumed[138,142]. These two aspects are intimately related and are not physically separable, However, the fact that there are two distinctive morphologies, i.e., crystallographic pits and polished hemispherical pits, suggests that according to

circumstances one aspect can prevail over the other and each may be considered as manifestations of extreme examples of the complex metal dissolution process, i.e. a metal dissolution process determined or controlled by the metal and a metal dissolution process determined or controlled by the solution. Certainly the polished pit has been observed so often and the crystallographic pit so rarely that this separation seems highly speculative. In this respect additional evidence must be considered. The cold worked specimen whose E-i curve is given in Fig. 61, determined in 0.05M H_2SO_4 + 0.1M NaCl solution exhibited a severely attacked surface, i.e. pitted, as evident from micrographs given in Figs 111, 112, which show both polished and non-polished hemispherical pits. Close examinations of the non-polished pits revealed that in most of the cases their inner walls exhibited striations and in a very few cases highly crystallographic dissolution, as illustrated in Figs 113, 114. These features are conclusive evidence for propagation mechanisms mainly determined by the state and structure of the metal. Dissipation of stresses accumulated in the metal as a result of the cold work, i.e. deformation, is mainly responsible for a feature type propagation as found commonly in stress-corrosion-cracking tests; and a highly activated dislocation notch is responsible for the crystallographic propagation observed.

7.4. MEASUREMENT OF SITE DENSITY (N_A)

The quantitative evaluation of the pitting phenomenon based on the microscopical examination of specimens anodically polarised to preselected (E,i) values was the second stage of the experimental approach. This is a troublesome aspect because qualitative observations showed that the development of pit morphology is not a progressive

It was found that changes in the site density throughout the E-i curve were small in the range considered, as is apparent in Fig. 115 where site density estimates for specimens tested in 0.05M H_2SO_4 and 0.05M H_2SO_4 + 0.1M NaCl solutions are represented as functions of the potential. All the site density values were an order of magnitude smaller than the etch-pit density produced by electrolytic metallographic etching and estimated using the same visual counting procedure. It must be said that etch-pits are associated with dislocations but their measurement underestimates the real value of dislocation density which is actually several orders of magnitude higher; however, etch-pit counts can be taken as a measure of that fraction of the dislocations which in appropriate electrochemical conditions would act as points for preferential dissolution. The small variations observed cannot be taken as significant unless the variability of N_A between specimens is assessed; it can be appreciated that the relative error in N_A determinations, given in TABLE VII, although in agreement with the magnitude of error normal for the procedure chosen[145], forfeits the use of sample size as a means to increase precision in the N_A determination, i.e. the standard error in $\bar{N}_A$ is roughly 4.5 times smaller than the error of the method used in N_A determinations. Certainly, it would have been preferable to test several specimens for every (E,i) co-ordinate to determine the value of N_A with greater precision because the variability of N_A between specimens for every (E,i) co-ordinate is thus introduced in the evaluation of the final value, i.e. an assessment of the representativeness of specimens vis a vis the measurement[146]. To elucidate this matter with the data available a simple variance analysis was conducted with the Null Hypothesis, "All samples analysed come from the same site population" which means

that all specimens were considered as equally representative of the material and that the site density is not affected by the anodic polarisation. This hypothesis was tested at a 5% significance level against the alternative hypothesis, "Not all the samples analysed come from the same site population". The results of this calculation, given in TABLE VIII, show that the site densities of three of the specimens tested in 0.05M H_2SO_4 solution are not representative of the same site population which means that there is some cause of variability other than the statistical fluctuation. Taking into consideration the fact that these three specimens correspond with the transpassive region of the E-i curve, their variation can be assigned to the specific conditions in which they were tested, i.e. the higher site density is due to the anodic current developed on the specimens which results in a production of additional sites. On the other hand, the results of the calculation show also that the site densities of four of the specimens tested in 0.05M H_2SO_4 + 0.1M NaCl are not representative of the same site population. In this case, it is possible to assign the cause of variation to the anodic current for the specimens which correspond with the pitting range but not for the specimens which correspond with the maximum activity and initial stages of the passive range. Taking into consideration the fact that this variation was not detected in the specimens tested in 0.05M H_2SO_4 solution it can be concluded that the surfaces of these specimens are not representative of the material vis a vis the measurement, i.e. N_A determination.

It is now possible to answer the question whether there is any difference between specimens tested in 0.05M H_2SO_4 and 0.05M H_2SO_4 +

0.1M NaCl solutions in regard to the features presented in their surfaces. For this purpose the t-student test was applied to the results for the specimens which were statistically equally representative of the same site population, i.e. results for specimens which conform to the Null Hypothesis in one solution were compared with corresponding results for the other solution. The null hypothesis, "site density values represent the same site population" was tested against the alternative hypothesis, "site density values represent different site populations". The results of the calculation, given in TABLE IX, show that the null hypothesis can be rejected at a 5% significance level and hence it can be concluded that the addition of Cl^- ions in the solution increases the site population. This conclusion will be confirmed in the next section.

To summarise, as a result of the quantitative evaluation of the microscopical information available it can be concluded that for the 316 austenitic stainless steel sites for possible initiation of the pitting process are formed not at the breakdown potential (E_b); they are the result of the first metal-solution interaction at a much lower potential, namely the rest potential, E_R.

7.5 TESTING SITE DENSITY (N_A)

The fact that the initial metal-solution interaction resulted in preferential dissolution which is a consequence of the anisotropic behaviour of metallic materials would suggest that the site density parameter used in its evaluation is somehow related to the state of the metal and may be taken as one of the fundamental

variables which condition the manifestation of the pitting phenomenon in this material, i.e., 316 austenitic stainless steel. However, to consider this parameter as an independent variable would require an assessment of changes produced in the manifestation of the phenomenon by controlled changes of N_A. This introduces the intrinsic difficulty that because N_A is neither a variable of the metal nor a variable of the solution but a parameter chosen to evaluate the metal-solution interaction, i.e., it is a variable of the metal dissolution process, it can be changed only by altering the process itself which can be done either by changing the state of the metal or changing the nature of the solution. This assessment can be done empirically by preparing specimens which correspond with different metal states and testing them in a given solution selected as a means of revealing N_A, after which a correlation with the pitting process can be made. Alternatively, specimens could be selected which correspond with a given metal state and tested in different solution compositions. These two options were considered, the former by preparing specimens with different degrees of deformation under the assumption that cold work produces changes in the metal state and the latter by testing specimens in 0,05M H_2SO_4 + 0.5M NaCl and 0.05M H_2SO_4 + 1.0M NaCl solutions and interrupting their anodic polarisation at the (E_{pp}, i_{CRI}) coordinates. It has already been pointed out that E-i curves of cold-worked specimens produced results whose interpretation is open to question. Therefore only the results obtained in the second option are available and were used in the testing of N_A.

It was found that increases in Cl^- ion concentration resulted in small increases in the site population as measured by N_A and illustrated in Fig. 116. These small variations in N_A

values were not due to statistical fluctuations; they were found to be different at a 5% significance level when applying a t-student test, as given in TABLE IX. On the other hand, breakdown potential (E_b) values determined for the different solution compositions and plotted against N_A, exhibit a similar form of variation as that for E_b vs C_{Cl} in the same concentration range. It seems then that the pitting process, characterised by E_b, is determined to a certain extent by the amount of sites initially formed at a potential far below E_b, i.e., the higher the initial site population the lower the breakdown potential value. On the other hand chloride ions introduced in the solution not only result in an increase in the dissolution rate of the metal as measured by i_{CRI} but also in an increase in the site population. It may be concluded that for the small range of concentration tested the site density (N_A) appears to be a variable upon which the phenomenon can be represented. Certainly further experiments have to be done in the future to define more precisely the role of N_A as a variable though the limited data available so far is encouraging.

7.6 INTERPRETATION OF THE PITTING PHENOMENON

The interpretation of the pitting corrosion phenomenon in a 316 austenitic stainless steel, in terms of the variable used in its evaluation, was the last phase envisaged in the experimental approach. This rationalisation process has to provide an explanation of the localisation of the pitting process, the catastrophic behaviour of the metal-solution system in chloride ion solutions and the decrease in breakdown potential values by increases of chloride ion concentration which were the main features

observed in the experimental work. It must be said that because of the nature of the approach selected and the parameter measured, i.e., site density, the rationalisation will result in a clarification and initial understanding of the role of the metal at the expense of leaving obscure the electro-chemical aspect of the metal dissolution. Moreover these two aspects have to be treated at different levels; the former at the microscopical level and the latter at the atomic level; in this sense the former is a manifestation of the latter. It is not the purpose of the present work to subject this aspect to detailed analysis.

As in any rationalisation process, some hypotheses have to be put forward as a preliminary because they provide the framework on which the interpretation is given; these hypotheses will not necessarily correspond with the actual reality of the phenomenon but are reasonable approximations which do not have to be proved. Certainly if the hypotheses are badly formulated the resulting interpretation will be incorrect in the sense that it cannot match the experimental results which are the measure of the appropriateness of the interpretation. It is convenient to discuss separately the hypotheses, the interpretation of the localisation of the attack, the catastrophic behaviour and the breakdown potential and the influence of the Cl^- in concentration upon it.

7.6.1 Hypotheses

Two hypotheses have to be considered, one relates to the metal structure and another to the dissolution process.

The first hypothesis: It is apparent from earlier discussions that pit-sites formed on the metal surface as a result of the initial metal-solution interaction are somehow related to the metal structure, It is a fact that the metal is dissolved at those points which afterwards appear as pit-sites though their ultimate nature is not known; it is conceivable that pit-sites may arise from inclusions washed away by chemical or electrochemical dissolution, dislocations resulting in etch-pits, triple points of crystal grains with different orientations, etc. As long as no discrimination is made in the pit-site counting it is possible to assume that the metal contains a number of susceptible sites disseminated throughout its structure. Only those at the surface will be subjected to dissolution when in contact with the solution but not all of the surface sites react as a result of the metal-solution interaction; that depends upon the electrochemical conditions, e.g., the nature of the solution as shown by the evidence that a different number of pit-sites were counted for the different solution compositions used. It will be assumed then that the metal is formed by planes, any of which contains the same site distribution. To avoid confusion the words "site" will be reserved for these particular points in the metal matrix and pit-site for those at the surface which have undergone interaction with the solution.

The second hypothesis: Microscopical metal surface examinations revealed that the metal always tends to dissolve anisotropically; even pits exhibit preferential dissolution in their inner surface as shown in Figs 108, 114. On the other hand, Brusic[147], Novakovsky[148] and Lickhachev[149] have found

that the passive current density measured on passivated iron in neutral solutions corresponds with a metal dissolution process which is more vigorous than that required for film formation in regenerating the chemically dissolved film or that required for film growth. Therefore it will be assumed that sites are preferred points for dissolution compared with the metal matrix and that in the passive range the passive current density is concentrated mainly at the pit-sites because,as irregularities, they are areas of dissolution preferred over the flat surface which is covered by the passive film.

7.6.2 Localisation of the Attack

Among the previous theories of pitting corrosion (discussed in section 4.2.2.2) only Evans' view assumes the existence of irregularities in the passive film suitable for preferential dissolution and pit generation depending on the electrochemical conditions. Other theories assigned the localisation to preferred sites in the passive film which under the high overpotential and the specific effect of Cl^- ions undergo dissolution which, on reaching the metal, is autosustained by the effect of a cell comprising a pit anode and a passive film cathode. However, in the particular instance treated in the present work, i.e., 316 austenitic stainless steel, evidence has been produced to show that although there are irregularities suitable for the preferential dissolution of the metal they are formed at a potential far below the breakdown potential and their number is much higher than the number of pits observed in a severely damaged surface, e.g., the pit-site density in 0.05M H_2SO_4 + 0.1M NaCl is 3.0×10^5 cm^{-2} which would correspond with a site population of

1.5×10^5 in a surface area of 0.5 cm^2 and this population contrasts with the number of well-developed pits in a severely damaged surface as apparent from Fig. 111. This evidence reveals quite clearly the localisation problem of pitting corrosion and suggests that pit formation is not only dependent on the existence of a pit-site per se but it is conditioned by other factors and only a small fraction of a pit-site population will meet the conditions for pit formation.

The structural factor which is our major concern will determine to a large extent this population behaviour. From a structural point of view, it is apparent that a pit-site which is near to a site of the metal structure will evolve more rapidly towards pit-formation than one which is not near to such a site, i.e., as the metal dissolves at the pit-sites those which encounter a site of the metal structure will dissolve more rapidly. To express this idea more precisely, values of pit-site density (N_A) determined at low overpotentials can be used to calculate the probabilities for these events. It must be said that stereological parameters are interpreted as geometrical probabilities[150]. Considering a small hemispherical pit-site of radius 0.5μm which is a reasonable assumption for the mean size of pit-sites observed as apparent from micrographs given in Figs. 102, 103; the probabilities of finding 0, 1, 2, ..., n sites in the area thus defined, i.e., $2\pi r^2$, can be given by the terms of a Poisson distribution with parameter $2\pi r^2 N_A$, as follows,

$$P_n(2\pi r^2) = e^{-2\pi r^2 N_A} \quad \frac{(2\pi r^2 N_A)^n}{n!} \qquad (39)$$

with n = 0, 1, 2, ..., n

A calculation of these probabilities for n = 0,1,2, given in TABLE XI for any of the N_A values determined at different solution compositions, shows that the highest probability is for the non-occurrence of the event, i.e., P =o, and the probabilities of the event "encountering a site inside the pit-site", i.e., P_n=1, are very small and even smaller for the event "encountering two sites inside the pit-site", i.e., P_n=2. These results were rather expected because having introduced a Poisson distribution it would mean that the events for n = 1 and n = 2 are considered as unlikely events. However, the P_n= 1 and P_n = 2 probabilities, even if small, are not negligible because taking into account the fact that there is a high population of pit-sites formed initially the result is that there is a non-negligible number of pit-sites for which the event "encountering a site inside the pit-site" will probably occur although it corresponds with only a small fraction of the site population. For example, from TABLE XI, the total pit-site population of the specimen tested in 0,05M H_2SO_4 solution is $1,25 \times 10^5$ but only 500 of them, corresponding with 0.4% of the population, will probably meet the condition. These probabilities increase with the chloride ion concentration because of the higher values for site population found at these concentrations. It seems then that P_n = 1 is an expression of the structural factor which conditions pit formation and explains why there will be only a few pits in the growth stage compared with the initial pit-site population. Certainly the size of the pit-site is another important structural factor which affects the probability P_n= 1. The calculation of P_n= 1 for different values of r, i.e., different pit-site areas at a selected N_A value, given in TABLE XII, shows that an increase of r from 0.5μm to 1μm and from 0.5μm to 2μm result

respectively in increases of 200 and 1500% in the P_n=1 probability. These calculations would suggest that once a new site is encountered in a pit-site because of the metal dissolution it will increase its inner surface which if represented by a new radius value will produce the result that this pit-site in particular will have an even higher probability of encountering a new site and the pit-site in question will be preferred over other pit-sites for metal dissolution. This process would explain the fact that in the passive range the current intensity is constant; not all the sites maintain the same dissolution rate. Those favoured probabilistically would sustain a higher value and because it is a fact that the total value of dissolution rate is constant it must be concluded that a larger proportion of pit-sites will maintain an even smaller value of dissolution rate, i.e., pit-sites in which the event of $P_n = 1$ does occur are more favoured for further preferential dissolution at the expense of making the population for which P_n=0 even greater. This dynamic process will result in a highly localised dissolution area in the metal structure and it is clear that pit formation is a logical consequence of the existence of a passive film covering most of the metal surface and the existence of discretely distributed sites within the metal, i.e., the process of pit formation cannot be confined only to the metal surface.

7.6.3 The Catastrophic Behaviour of Pitting Corrosion

The evolution of pit-sites into growing pits is indeed also determined by the electrochemical reactions taking place inside the pit-sites. Although these processes are unknown it is plausible to assume that the interaction of the solution with a site

revealed in the inner surface of a pit-site results in an outburst of metal dissolution because sites may be considered energetically more active than the metal matrix and may react with the solution independently of its particular composition, e.g., H_2SO_4 or H_2SO_4 + NaCl. After the interaction, the further evolution of the pit-site depends on the electrochemical conditions although it has now a higher probability for encountering a new site and a higher dissolution rate. It is possible to conceive that when the dissolution current intensity reaches such a value that there is a high probability that the new inner surface revealed contains a new site then the pit-site will be able to sustain a dissolution process with extremely high intensity, i.e., there is a high probability for the event "encountering a new site" per unit of time. It is apparent that a pit-site in these conditions will evolve rather explosively and it is possible to associate these conditions with a catastrophic point in the evolution of the pit-site. This condition can be expressed mathematically by:

$$\left(\frac{dr}{dt}\right)_{\substack{\text{catastrophic}\\ \text{point}}} = \lambda = \frac{1}{2} \left(N_A\right)^{-\frac{1}{2}} \qquad (40)$$

where r is the changing radius of the pit-site and λ is the average distance between sites in a population characterised by N_A [151]. It can be appreciated that the catastrophic point does not necessarily correspond with a critical pit-site size but rather with its dynamic growth process, namely the pitting process, leading to pit formation, i.e., if a big pit-site does not reach the condition above given for any particular circumstances it will not be able to develop into a pit by a pitting corrosion

process; on the other hand if in a small pit-site this condition is reached, then the pitting corrosion process leading to a pit will probably occur. It seems that the catastrophic condition, as expressed by equation 40, is a necessary requirement to be fulfilled if pitting corrosion is to occur but obviously it is not sufficient, particularly because this condition which relates to the dissolution process with the metal structure has a statistical meaning, i.e., there is a high probability per unit of time for the event "encountering a new site" and hence it is indeterminate. If $(dr/dt) < \lambda$, it would be very unlikely to produce pitting in a catastrophic manner but if $(dr/dt) > \lambda$ it would probably occur. This indeterministic nature of the catastrophic condition is the reason why the characterisation of the pitting corrosion process by a particular value of potential, i.e., breakdown potential (E_b), or a particular value of time, i.e., induction time (τ), are uncertain and why they depend strongly on the experimental procedures used in their determination and cannot be taken as a precise assessment of the phenomenon at least within the meaning and significance given to them in current pitting corrosion theories discussed earlier, section 4.2.2. Certainly the catastrophic point is time-dependent because the process is evolutive and potential-dependent because of the electrochemical nature of the metal dissolution. It is possible to associate the induction time with the period of time required to reach the catastrophic condition which implies that the induction time has also to be interpreted in a probabilistic context. Unfortunately the relation of pit-site size with time which would correspond with the other parameter needed for the rigorous description of the site population is not available and hence an explicit expression of

$\tau = f(\lambda)$ or $\tau = f(N_A)$ cannot be given. Similarly, it is possible to associate the breakdown potential with the catastrophic condition and this is the subject of the following section within the limitations imposed by the nature of the present work. Finally it must be said that the catastrophic behaviour of the pitting corrosion process is of course limited to what has been the manifestation of the phenomenon in a laboratory where conditions affecting the phenomenon can be artificially changed at will. Outside of these situations it is arguable whether pitting is always manifest catastrophically although the pitting process as described in the present work cannot be dissociated from the catastropnic condition, i.e., the pitting process either occurs in a catastrophic manner or it does not occur at all.

7.6.4 The Breakdown Potential

It has already been assumed that the metal dissolution of the passivated metal is concentrated mainly at the pit-sites initially formed at much lower potential than the breakdown potential; it is now clear that some of them will grow but it is a requirement for the pitting process to occur that the catastrophic condition be reached. This process demands an increment of the metal dissolution rate at the pit-sites which obviously can be produced by increasing the potential at which the metal surface is held. Therefore it is possible to associate the particular value of potential for which the dissolution current satisfies the catastrophic condition, namely "the catastrophic overpotential or overpotential at the catastrophic point, η_{cp}," with what is usually called "the breakdown potential, E_b". To provide an explicit relationship, let us consider a hemispherical pit-site of radius r. At any time, the volume thus defined

corresponds with an amount of material which has gone into solution by electrochemical transfer of a charge Q(t). The current intensity can be immediately given approximately by:

$$I(t) = \frac{Z\rho F}{M} \; 2\pi \; r^2 \; (\frac{dr}{dt}) \qquad (41)$$

where F is the Faraday constant, ρ is the density of the material, Z the number of electron transferred in an overall reaction and M the molecular mass of the metallic material. Introducing the catastrophic condition, using equation 40, and assuming that the dissolution process can be approximated by a Tafel relation which is what is called the high field approximation of the Butler-Volmer equation e.g., 13,, then the catastrophic condition may be expressed as:

$$(\frac{dr}{dt})_{cp} = \frac{M}{Z\rho F} \; i_o \; e^{\frac{\alpha F}{RT}\eta_{cp}} = \frac{1}{Z} \; N_A^{-\frac{1}{2}} \qquad (42)$$

This expression not only makes explicit the relation between the electrochemical parameters which describe the metal dissolution and the metal structure but also emphasises the indeterminate character of the catastrophic overpotential and hence the breakdown potential. By raising the overpotential, the probability for the occurrence of the event "encountering a new site" is increased exponentially and when the event does occur in a given pit-site it renders this pit-site even more favoured for localised dissolution , a process which may be catastrophic only for $\eta > \eta_{cp}$ where thereis such a dissolution rate that the event "encountering a new site per unit time" is highly probable. If the overpotential is artificially set at η_{cp}, there is not necessarily an immediate

occurrence of the pitting process in its catastrophic form but there is a high probability for its occurrence. At $\eta > \eta_{cp}$, it can occur more easily and at$\eta < \eta_{cp}$ it is an event unlikely to occur. It can be appreciated that this indeterminancy is intrinsic in the phenomenon itself, a fact which lies at the root of the uncertainty in determining the breakdown potential E_b. On the other hand, it must be said that for $\eta < \eta_{cp}$ the process of localised dissolution occurs as an event more favoured probabilistically than general dissolution because of the passive film. This dissolution, even though it is not manifest in a catastrophic manner, may lead to serious localised corrosion problems in real situations in contrast with laboratory experiences.

Using equation 42, it is possible to estimate the catastrophic overpotential, η_{cp}, from the structural data N_A determined at low overpotentials and the electrochemical data provided by the active range of E-i curves for the system studied although the values obtained are open to question because of the nature of the technique, i.e., the potentio-dynamic technique, and the small range of overpotentials at which the metal under investigation is in the active state. It must be said that assuming a Tafel expression as an approximation for the relation between the overpotential and the dissolution rate occurring at the pit-sites is a consequence of the second hypothesis formulated earlier in section 7.6.1, besides that it is in line with the evidence found by Wilde[103] and Rosenfeld, Danilov, Oranskaya[152] who suggested that the dissolution rate in the pitting range follows the same relation with the overpotential as in the active range. These additional results are

given in TABLE XIII. It is interesting to note that the value of the breakdown potential calculated for the 0.05M H_2SO_4 solution from the corresponding catastrophic overpotential (η_{cp}) is 1.09V. This value is so high that it is well within the actual transpassive range of the metal-solution system considered, where the basic condition for localised dissolution, i.e., a passive film covering most of the metal surface, is no longer applicable and hence a pitting corrosion process cannot be developed on the metal surface. On the other hand, the calculated breakdown potential, E_b(cal), decreases as the Cl^- ion concentration increases although the calculated values are in disagreement with the experimental ones. It is noteworthy however that the disagreement is markedly reduced as the Cl^- ion concentration is increased, a fact which suggests that the disagreement is the result of oversimplifying the calculation, i.e., the calculation is based on the bulk Cl^- ion concentration instead of the real concentration near or inside the pit-sites. Moreover, the effect of these real concentrations upon N_A has not been introduced in the calculation.

To summarise, the structure of the material plays an important role in determining the manifestation of the localised dissolution of the metallic material. The localisation itself is not the result of the existence per se of an irregularity in the passive film or the underlying metal but the result of a population behaviour under a dynamic interaction with the solution better understood in terms of the probabilities of occurrence of the event "encountering a new site inside a pit-site". This dynamic process tends to develop a highly localised area of dissolution which is manifest catastrophically. The breakdown

potential is related to the catastrophic condition and hence its determination is intrinsically uncertain because of its statistical nature. The interpretation of the phenomenon in terms of N_A though not elaborated in detail can be considered satisfactory thus accomplishing the purpose of the present work.

8. CONCLUSIONS AND SUGGESTIONS FOR FURTHER WORKS

Pitting corrosion on a 316 austenitic stainless steel has been examined from a phenomenological point of view with the intention of clarifying the role of the metal in the dissolution process. Certainly it would have been ambitious to expect to accomplish this purpose in a detailed way, because of the complexities of the metal under investigation and the process itself. However, some important progress has been made in our views and understanding of the phenomenon for this particular material which merits further work to extend it more generally to other materials.

8.1. CONCLUSIONS

1. The anodic passive state of AISI 316 stainless steel in acid media is characterised by a metal surface exhibiting a large number of pit-like irregularities and hence the passive film is a discontinuous structure.

2. The pitting process is related to metal dissolution at these pit-like irregularities formed at potentials far below the breakdown potential and to the presence of a passive film covering most of the metal surface.

3. The localisation of the pitting process depends strongly on the metal structure. Contrary to current opinion this localisation is not the result of the existence per se of imperfections in the passive film or in the underlying metal but the result of imperfections discretely distributed throughout the whole metal. In consequence this aspect of

the phenomenon is better understood in statistical terms.

4. The pitting process is manifest catastrophically and hence it is wrong to consider a division of the phenomenon into an initiation stage and a growing stage.

5. The breakdown potential corresponds neither with a disruption of the passive film nor with the onset of a new electrochemical reaction different from that which may occur at lower overpotentials. It corresponds with the potential at which the dissolution current intensity satisfies the catastrophic condition, and hence it is intrinsically indeterminate, i.e., the breakdown potential has no fundamental significance except in the context of the catastrophic condition.

6. The role of Cl^- ions in pitting is not to introduce any fundamental changes in the nature of the metal dissolution beyond that normally observed at low overpotentials in the active region. The effect is to facilitate the development of the catastrophic condition by enhancing metal dissolution, particularly at the pit-sites. This effect is also manifest in the increased population of pit-like irregularities developed at low overpotentials and in increased values for i_{CRI}.

8.2. SUGGESTIONS FOR FURTHER WORK

1. As a necessary complement of this phenomenological investigation an evaluation of the pit-site size distribution and its changes in time or potential is required for a better description of the pitting phenomenon on AISI 316 stainless steel from a structural point of view.

The use of a quantimeter or image analyser may be of great help in carrying out these studies because these instruments reduce the time needed to provide the data as well as increasing the precision of the measurements.

2. Obviously the present investigation has to be extended to other metallic materials, particularly other stainless steels, to explore the generalisation of the presented phenomenological description of the pitting process. In this sense the present investigation provides the guidelines in the experimental approach and procedures which can be improved by the introduction of the metallographic techniques already mentioned.

3. The electrochemical aspect of the pitting process has to be considered in detail in the future because the present work has shown that the structural conditions for the occurrence of the pitting process are also available in solutions with no Cl^- ions although the pitting process was not actually realised. This future study has to include the effect of overpotential on the movability, diffusion and activity of Cl^- ions in the neighbourhood of pit-sites. The effect of higher Cl^- ion concentrations on N_A has to be investigated as well as the reaction mechanism for metal dissolution in the presence of Cl^- ions.

4. It would be important from a practical point of view to study the nature of sites and its relation to pit-sites. It is in this context that the nature and distribution of sulphide inclusions have to be examined though it is recommended that this work should be extended to include dislocations, grain boundaries, triple points, phase distribution, etc.

5. It would be worthwhile applying this phenomenological presentation to other forms of localised corrosion, in particular stress-corrosion-cracking, corrosion fatigue and crevice corrosion.

APPENDIX I

THE POTENTIOSTAT-PRINCIPLE AND APPLICATION TO CORROSION STUDIES

The metal/solution interface at which a natural aqueous corrosion process is proceeding adopts a rest potential, $E_{R\ 1}$ of such a value that the vector sum of the currents flowing from all of the contributing electrochemical reactions is zero. If the potential is artificially displaced from E_R , the magnitude of the net current flowing at the interface yields information on the corrosion characteristics of the system. The function of a potentiostat is to impose a controlled potential of the required constant value, or to follow any pre-determined potential programme scan and to record the resultant external current. This is accomplished as follows:

A sample of the metal (the working electrodes) is exposed to the selected environment in a suitable cell, its potential relative to the solution is measured by a capillary probe (luggin probe) close to it and connected via a salt bridge to a vessel containing a reference electrode (e.g., a saturated calomel electrode). The potentiostat compares the actual potential with a pre-set control potential of opposite sign and applies the difference (the error signal) to the input of a DC power amplifier which supplies a correcting current between the working electrode and a third electrode in the cell (a counter electrode) of such a direction and magnitude as to eliminate the error signal. The current supplied is the required external current and is recorded by a chart recorder.

The applied potential can be programmed by superimposing the output of a motor driven potentiometer on the constant control of the potentiostat. If the potentiometer potential is scanned continuously with time the technique is termed "potentiodynamic" and if varied in regular discreet steps it is termed "potentiostatic".

The features of a good potentiostat instrument which determine its performance are:

(i) rapid response

(ii) electrical stability, especially during periods when the external circuit exhibits the unstable electrical characteristic of decreasing current with increasing potential.

(iii) sufficient output power

(iv) high impedance at the reference electrode input.

The potentiostat used for the experiments in the present work was a Wenking Type 70 TS1 having the following characteristics:

Response Time	< 10μs
Output Power	25W, ± 25V at ± 1A
Input Impedance	> 10 w
Output current characteristics	0-200 μA linear
	200 μA - 1mA transition range
	> 1mA logarithmic

OPERATING PRINCIPLE OF THE SCANNING POTENTIOMETER

The essential unit of the Scanning Potentiometer SMP 69 which controls the output is a stepping motor working directly on the shaft of a ten turn potentiometer. The position of the potentiometer slider is indicated by a 1000 division dial. The precision potentiometer is fed by selectable voltages which can be changed-over in 4 ranges from 1 to 10 Volt. 100 steps of the motor correspond exactly to one full turn and 1000 steps cover the full range of the 10-turn potentiometer. Each step of the motor changes the dial indication by one division so that the output voltage varies stepwise in 0.1% steps of the complete range in use, i.e., in steps of 1 mV in the 1 V up to 10 mV in the 10 V range. The magnitude of the output voltage in mV equals the reading at the dial multiplied by the selected factor of the "Multiplier" switch of 1, 2, 5 or 10. This factor corresponds to the complete range of the potentiometer in Volts.

The "Stepping Rate" of the motor is variable in 9 calibrated course positions of a change-over switch in the range from 300 steps/min to 0.03 steps/min with an overlapping fine adjustment, so that the variation ratio is about 1 : 30 000. The stepping rate variation is caused by changing-over precision resistors and controlling the voltage drop at these resistors by a potentiometric voltage divider for fine adjustment. The resulting current through these resistors is either charging or discharging a fixed high insulation capacitor in the feedback circuit of an operational amplifier. Each change-over from charging to discharging and vice versa initiates a motor step. If the "fine" potentiometer is posed to its final

position marked "cal" the stepping rate if calibrated and corresponds to the number of steps/min indicated at the switch "Stepping Rate". The change rate of the output voltage in mV/min then equals the selected stepping rate multiplied by the factor of the "Multiplier" switch. It is variable in a ratio 1 : 300 000.

The potentiometer "Upper Level" is limiting the output voltage rise at a level setting in the range from 0 to 1000 divisions of the potentiometer dial. In position "single ramp" of the operating selector switch the motor stops there, in position "periodic triangle" it reverses. The green signal lamp "rise" indicates rising output voltage and the red lamp "fall" lights on when the output voltage changes to decrease or remains constant when the motor stops. An intermediate position of the operating selector switch "manual preset" opens the possibility of slightly moving the potentiometer dial by hand to preset or reset the output voltage. A relais controls the reverse or stop of the motor. It can be operated also by pressing the non-lighting push button "rise" or "fall".

In the normal operation the motor drives the potentiometer dial indication and the corresponding output voltage from zero to the selected "Upper Level" setting and stops or reverses there. At the upper end of the potentiometer range (1000 divisions on the dial) a micro-switch initiates the same operation. In position "periodic triangle" the motor reverses again when reaching zero thus cycling between zero and the upper level setting.

When the "external stop" terminals on the front panel are short circuited the motor stops and the scan of the output voltage can be interrupted for a certain time interval. The output voltage remains constant during this time interval and starts scanning again when the external contact is opened. This additional programming possibility can be applied when enlarged potential variations (i.e., 10 steps of the motor during a relative short period of contact brake) should be programmed after rather long time intervals (of contact make). This external programming contact may be operated by laboratory clocks or other timing units.

The SMP has a floating output if the link plug bridging the black output terminal to ground has been removed. The polarity of the green output terminal to the black one below can be reversed, it is indicated at the "polarity" switch. The output impendance is max. 20 KOhm in parallel with 10 uF. Strip chart recorders directly connected to the output terminals of the SMP should have an input impendance of at least 20 MOhm if the indication of the output voltage by the potentiometer dial has to remain accurate.

REFERENCES

1. Shreir L.L., "Corrosion" Vol.1, p.1,6, 2nd Ed. Newnes-Butterworth (1976).
2. Bockris J.O'M. and Reddy A.K.N., "Modern Electrochemistry" Vol.2, p.1255, Plenum Press (1970).
3. Ibid p.16.
4. Pourbaix M., "Atlas of Electrochemical Equilibria in Aqueous Solutions", Pergamon Press, Oxford. (1966)
5. Durrant P.J., and Durrant B., "Intr.to Ad. Inorg. Chem" p.1064, 2nd Edition Longman (1970).
6. Bockris J.O'M. and Reddy A.K.N., "Modern Electrochemistry" Vol.2, chapter 7, Plenum Press (1970).
7. Butler J.A.V., Proc. Roy. Soc. (london), (1936), A157, 423.
8. Colombier L., and Hochmann J., "Stainless and Heat Resistant Steels", Introduction, English Transl. Edward Arnold (Publishers) Ltd., (1967) London.
9. Pickering F.B., "Physical Metallurgy and The Design of Steels" p.164, Applied Science Publishers Ltd. (1978).
10. Metal Handbook 8th Edition, Vol.8, p.291. American Society for Metals (1972).
11. Baerlerken E., Fischer W.A., and Lorentz K., Stahl Eisen. (1961), 81, 768.
12. Cook A.J., and Jones F.W., J. Iron Steel Inst. (London), (1943), 148, 217.
13. Colombier L., and Hochmann J., "Stainless and Heat Resistant Steels", p.10, English Transl. Edward Arnold (Publishers) Ltd. (1967) London.

14. Bungart E., Kunze E., and Horne, Arch. Eisenhüttenweisen, (1950), 29, 193.

15. Owens E.A., and Liu Y.H., J. Iron Steel Inst. (London) (1949), 163. 132.

16. Monypenny J.H.G., "Stainless Iron and Steel" Vol.I, p.61, 3rd Ed. rev. Chapman and Hall, London (1951).

17. Peckner D., and Bernstein J.M., "Handbook of Stainless Steels" p.14-1, McGraw-Hill (1977).

18. Ibid, p.4-15.

19. Pickering F.B., Inter. Metals Rev. (1976), 21, 227.

20. Hoar T.P., "Corrosion" VI, p.1-114, Shreir L.L., Ed., 2nd Edition, (1976), Newnes-Butterworths (London).

21. Bonhoeffer K.F., and Gerischer H.Z., Elektrochem. (1948), 52, 149.

22. Kolotyrkin Y.M., Proc. 1st Inter. Symp. Corrosion (1961), p.10.

23. Shreir L.L., "Corrosion" Vol. I, p1-103, Shreir L.L., Ed., 2nd Edition, Newnes-Butterworths (1976).

24. West J.M., "Electrodeposition and Corrosion Processes", p.87, 2nd Edition Van Nostrand Co. Ltd., (1971).

25. Okamoto G., Corros. Sci., (1973), 13, 471.

26. Oliver R., CITCE 6, Poitiers (1954), Butterworth, London (1955), p.314.

27. Tomashov N.D., "Theory of Corrosion and Protection of Metals", p.330, The McMillan Company, (1966).

28. Peckner D., and Bernstein J.M., "Handbook of Stainless Steels", p.16-4, McGraw-Hill, (1977).

29. Rockel M.B., Corrosion, (1973), 29, 393.

30. Bain E.C., Aborn R.H., and Rutherford J.B., Trans. Amer. Soc. Steel Treating, (1933), 21, 481.

31. Osozawa K., Bohnenkamp K., and Engell H.J., Corros. Sci. (1966), 6, 421.

32. Peckner D., and Bernstein J.M., "Handbook of Stainless Steels" McGraw-Hill (1977).

33. Shreir L.L., "Corrosion" V.I, p.1-145, Shrier L.L. Ed., 2nd Edition (1976), Newnes-Butterworths (London).

34. Peckner D., and Bernstein J.M., "Handbook of Stainless Steels", McGraw-Hill (1977).

35. Edeleanu C., and Snowden P.P., J. Iron St. Inst., (1957), 186, 406.

36. J.G. Hines, "Corrosion" vol. I, p.8-54, Shreir L.L., Ed., 2nd Edition, Newnes-Butterworths (1976).

37. Bonhoeffer K.F., and Heusler K.E., Z. Electrochem (1957), 61, 122.

38. Heusler K.E., Z. Electrochem, (1958), 62, 582.

39. Ibid, (1962), 66, 177.

40. Bockris J.O'M., Drazic D., and Despic A.R., Electrochim Acta, (1961), 4, 325.

41. Ibid, (1962), 66, 293.

42. Kelly E.J., J. Electrochem. Soc., (1965), 112, 124.

43. Brusic V., "Oxide and Oxide Films", Vol. I, p.13., Diggle J.W., Ed., Marcel Dekker Inc., New York (1972).

44. Hoar T.P., Corros. Sci., (1967), 7, 341.

45. Brusic V., "Oxide and Oxide Films", Vol. I, p.9., Diggle J.W., Ed., Marcel Dekker Inc. N.Y.,(1972).

46. Uhlig H.H., and Mears R.B., "Corrosion Handbook", p.26., Uhlig H.H., Ed. Wiley, N.Y., (1948).

47. Uhlig H.H., Z. Elektrochem, (1958), 62, 700.

48. Uhlig H.H., Proc. Passivity and its Breakdown on Iron and Iron Base Alloys, USA- JAPAN Seminar., p.19, NACE (1976).

49. Ibid., p.21.

50. Kolotyrkin Y.M., Z. Electrochem., (1958), 62, 619.

51. Kolotyrkin Y.M., J. Electrochem. Soc., (1961), 108, 209.

52. Tomashov N.D., "Theory of Corrosion and Protection of Metals", p.339., McMillan (1966).

53. Brusic V., "Oxides and Oxide Films", Vol.I, p.17., Diggle J.W., Ed., Marcel Dekker Inc. N.Y., (1972).

54. Evans U.R., J. Chem. Soc., (1927), 1024.

55. Hoar T.P., "Corrosion", Vol. I, p.1-222., Shrier L.L., Ed., 2nd Edition, Newnes-Butterworth (1976).

56. Vernon W., Wormwell F., and Nurse, J. Iron St. Inst. (1944), 150, 81.

57. Bockris J.O'M., Reddy A.K.N., and Rao B., J. Electrochem.Soc., (1960), 113, 1133.

58. Vetter K.J., "Electrochemical Kinetics Theoretical and Experimental Aspects" (Trans. Sy. Scripta Technica), Academic Press, N.Y., (1967).

59. Evans U.R., J.Chem. Soc. (1930), 480.

60. Pryor M.J., and Evans U.R., J. Chem. Soc., (1949), 3330.

61. Pryor M.J., and Evans U.R., J. Chem. Soc., (1950), 1259.

62. Vetter K.J. Z. Elektrochem., (1958), 62, 642.

63. Nagayama M., and Cohen M., J. Electrochem. Soc., (1962), 109, 781.

64. Ibid., (1963), 110, 670.

65. Brunsic V., Bockris J.O'M., and Genshaw, Symposia Faraday Soc., (1970), 4, 177.

66. Schwabe K., Ebersbach U., and Ritter K., Electrochim. Acta, (1967), 12, 927.

67. Tamman G., Metallurgy. Moscow: United Scientific and Technical Publishing House, (1935).

68. Rhodin T.N., and Nielsen A., Z. Elektrochem., (1958), 62, 707.

69. Kruger J., and McBee C.L., Electrochim. Acta., (1972), 17,1337.

70. Okamoto G., Proc. 5th Int. Cong. on "Metallic Corrosion". plenary lecture, TOKYO-JAPAN, Corros. NACE (1972).

71. Staehle R.W., and Lumsden J.R., Scripta Met., (1972), 6, 1205.

72. Staehle R.W., Yaniv A.E., and Lumsden J.R., Proc. Passivity and its Breakdown on Iron and Iron Base Alloys, USA-JAPAN- Seminar, p.72 NACE (1976).

73. West J.M., "Electrodeposition and Corrosion Processes" p.90, 2nd Edition, Van Nostrand Reinhold Co. Ltd., (1971).

74. Sato N., Proc. Passivity and Its Breakdown on Iron and Iron Base Alloys, USA-JAPAN Seminar, p.1, NACE (1976).

75. Brusic V., "Oxides and Oxide Films". Vol. I, p.61, Diggle J.W., Ed., Marcel Dekker. NY. (1972)

76. Champion F.A., J. Inst. Metals (London), (1943), 69, 47.

77. Schwenk W., Corrosion, (1964), 20, 129t.

78. Kolotyrkin Y.M., Corrosion, (1963), 19, 261t.

79. Szklarska - Smialowska Z., Corrosion, (1971), 27, 223.

80. Uhlig H.H., "Corrosion Handbook", p.165, Uhlig H.H., Ed., John Wiley & Son N.Y. (1948).

81. Uhlig H.H., and Horvath J.J., Electrochem. Soc. (1968), 115, 791.

82. Engell H.J., and Forchhammer P., Werkst U., Korr., (1969), 20, 1.

83. Bond A.P., and Lizlovs E.A., J. Electrochem. Soc., (1968), 115, 1130.

84. Ibid., (1973), 120, 603.

85. Tomashov N.D., Chernova O.P., and Markova N., Corrosion (1970), 20, 166t.

86. Osozawa K., and Okato N., Proc. Passivity and Its Breakdown on Iron and Iron Base Alloys, USA-JAPAN Seminar, p.135, NACE (1976).

87. Streicher M.A., J. Electrochem. Soc. (1956), 103, 375.

88. Tomashov N.D., Chernova O.P. and Markova N., Zashetita Metallov., (1970), 6, 21.

89. Szummer H.,Szklarska-Smialowska Z, and Janik-Czachor M., Corros. Sci., (1968), 8, 833.

90. Ibid., (1969), 9, 423.

91. Szklarska-Smialowska Z., Szummer A. and Janik-Czachor M., Bri. Corr. J., (1970), 5, 159.

92. Wranglen G., Corros. Sci., (1969), 9, 582.

93. Ibid, (1974), 14, 331.

94. Hoar T.P., Mears D.C. and Rothwell G.P., Corros. Sci., (1965), 5, 279.

95. Frankenthal R.P. and Pickering H.W., J. Electrochem. Soc., (1965), 112, 761.

96. Edeleanu C. and Gibson J.G., Phil. Mag., (1960), 5, 709.

97. Procter R.P.M., "Corrosion", Vol. I, p.1-34, Shreir L.L. Ed., 2nd Edition, Newnes-Butterworths (1976).

98. Randak A. and Trantes F.W., Werkst. u. Korr., (1970), 21, 97.

99. Shreir L. L., "Corrosion", Vol. I, p.1-154, Shreir L.L. Ed., 2nd Edition, Newnes-Butterworths (1976).

100. Tajima S., Komatsu S. and Momose T., Proc. Passivity and Its Breakdown on Iron and Iron Base Alloys, U.S.A.-Japan Seminar, p.140, NACE (1976).

101. Tajima S. , Komatsu S, and Momose T., Corros. Sci., (1976), 16, 191.

102. Uhlig H.H. and Leckie H.P., J. Electrochem. Soc., (1966), 113, 1262.

103. Wilde B.E., Proc. Passivity and Its Breakdown on Iron and Iron Base Alloys, U.S.A.-Japan Seminar, p.129, NACE (1976).

104. Stolica N., Corros. Sci., (1969), 9, 205.

105. Ibid., p.455.

106. Hoar T.P. and Jacob W.R., Nature, (1967), 216, 1299.

107. McCafferty E. and Hackerman N., J. Electrochem. Soc. (1972), 119, 999.

108. Chin R.J. and Nobe K., J. Electrochem. Soc., (1972), 119, 1457.

109. Greene N.D. and Judd G., Corrosion (1965), 21, 15.

110. Okamoto G. Tachibana K., Nishiyama S., and Sugita T., Proc. Passivity and Its Breakdown on Iron and Iron Base Alloys, U.S.A.-JAPAN Seminar, p.106, NACE (1976).

111. Suziki T., Yamake M. and Kitamura Y., Corrosion (1973), 29, 18.

112. Suziki T., Proc. Passivity and Its Breakdown on Iron and Iron Base Alloys, U.S.A.-JAPAN Seminar, p.126, NACE (1976).

113. Brigham R.J., Corrosion (1972), 28, 177.

114. Brigham R.J. and Tozer E.W., Corrosion, (1973), 29, 33.

115. Rozenfeld I.L., and Danilov I.S., Corros. Sci., (1967), 7, 129.

116. Tousek J., Kovol Mater., (1978), 16, 476; Metals Abstract (1979), 35-0278.

117, Aziz P.M. and Goddard H.P., Ind. Eng. Chem., (1952), 44, 1791.

118. Greene N.D. and Fontana M.G., Corrosion (1959), 15, 25 t.

119. Greene N.D., J. Electrochem. Soc., (1957), 104, 393.

120. Kruger J., Proc. Passivity and Its Breakdown on Iron and Iron Base Alloys, U.S.A.-JAPAN Seminar, p.91, NACE (1976).

121. Kruger J. and McBee C.L., Localized Corrosion, p.252, Staehle, Brown and Kruger Ed., NACE (1974).

122. Rybalka L.E., Leikis D.I. and Zelinski A.G., Elektrokimiya (1976), 12, (8), 1340; Metals Abstracts (1977), 34-0226.

123. Evans U.R., "The Corrosion and Oxidation of Metals", 2nd Supplementary Volume, p.70, Edward Arnold (Publishers) Ltd. (1976).

124. Sato N., Electrochimica Acta., (1971), 16, 1683.

125. Heine M.A., Keir D.S. and Pryor M.S., J. Electrochem. Soc., (1965), 112, 29.

126. Pryor M.J., "Localized Corrosion", p.2, Staehle, Brown, Kruger and Agrawal, Ed, NACE (1974).

127. McBee C.L. and Kruger J., "Localized Corrosion", p.252, Staehle, Brown, Kruger and Agrawal, Ed, NACE (1974).

128. Ambrose J.R. and Kruger J., Proc. 4th Int. Cong. Met. Corros., p.698, NACE (1972).

129. Sato N., Proc. Passivity and Its Breakdown on Iron and Iron Base Alloys, U.S.A.-JAPAN Seminar, p.142, NACE (1976).

130. Roberts M.H., J. Appl. Phys., (1954), 5, 351.

131. ASTM Recommended Procedure, Committee G-1 (1967).

132. Stern M. and Makrides A.C., J. Electrochem. Soc., (1960), 107, 782.

133. France W.D. (Jr)., J. Electrochem. Soc., (1967), 114, 818.

134. Bhattacharya G.K. and Johnson R.A., "Statistical Concepts and Methods", p.221, John Wiley and Sons (1977).

135. Metals Handbook, Vol. 7, p.139, 8th Edition, American Society of Metals (1972).

136. Greene N.D., France W.D. and Wilde B.E., Corrosion, (1965), 21, 275.

137. Frankenthal R.P., J. Electrochem. Soc., (1967), 114, 542.

138. Frankenthal R.P., and Pickering H.W., J. Electrochem. Soc., (1972), 119, 1304.

139. Wilde B.E. and Armijo I.S., Corrosion, (1967), 23, 208.

140. Wagner G.H., Desestret A., Corin H. and Grall L., Compt. Rend., 270, Serie C, 1093.

141. Ashworth V., Boden P.J., Leach J.S. and Nehru A.Y., Corros. Sci, (1970), 10, 481.

142. Hoar T.P., "Corrosion", Vol I, p. 1-127, Shreir L.L. Ed., 2nd Edition, Newnes-Butterworths (1976).

143. Janik-Czachor M., Bri. Corros. J., (1971), 6, 57.

144. Kita H., Enyo M. and Bockris J. O'M., Can. J. Chem., (1961), 39, 1670.

145. Pickering F.B., "The Basis of Quantitative Metallography", p.13, Inst. Metallurgical Technicians (1976).

146. Moore G.A., Proc. Applications of Modern Metallographic Techniques, Symposium, p.3, ASTM (1970).

147. Brusic V., "Oxides and Oxide Films", Vol. I, p.60, Diggle J.W. Ed., Marcel Dekker Inc. N.Y. (1972).

148. Novakovsky V.M., Electrochim. Acta, (1965), 10, 353.

149. Novakovsky V.M. and Likhachev M.A., Electrochim. Acta., (1967), 12, 267.

150. De Hoff R.T., "Quantitative Microscopy", p.11, Rhines F.N. and De Hoff R.T. Ed., McGraw-Hill N,Y. (1968).

151. Gurland J., "Quantitative Microscopy" , p.283, Rhines F.N. and De Hoff R.T. Ed., McGraw-Hill N.Y. (1968).

TABLE I

NOMINAL VALUES FOR THE CRITICAL PASSIVATING CURRENT DENSITIES AND FLADE POTENTIALS FOR ETCHED Fe-Cr ALLOYS IN 10% SULPHURIC ACID (*)

Composition %(wt.) Cr	i_{crit} (mA/cm2)	E_F (V,NHE)
0	1000	+0.58
2.8	360	0.58
6.7	340	0.35
9.5	27	0.15
12	27	0.01
14	19	-0.03
16	12	-0.02
18	11	+0.10
18Cr-8Ni	2	(-0.10)

TABLE II

CRITICAL PITTING POTENTIALS FOR VARIOUS METALS IN 0.1N NaCl,25°C (**)

Metal	Critical potential, V
Al	-0.45
Ni	0.28
18-8	0.26
Zr	0.46
Cr	1.0
Ti	1.0

(*) Data taken from ref. 26
(**) Data taken from ref. 81

TABLE III

DIMENSIONS OF CYLINDRICAL SPECIMEN PREPARED FOR E-i CURVES DETERMINATION USING THE ASTM STANDARD PROCEDURE[131].

1.- Specimens tested using 1V recording scale.

Length (cm)	Diameter (cm)	Area (cm^2)
2.090	1.127	8.39
1.540	1.125	6.43
1.010	1.135	4.61
1.025	0.836	3.24

2.- Specimens tested using 0.20 V recording scale.

Length(cm)	Diameter (cm)	Area (cm^2)
2.085	1.096	8.12
1.542	1.101	6.28
1.008	1.110	4.48
1.027	0.790	3.04
0.725	0.708	2.00

TABLE IV

THICKNESS CHANGE OF SPECIMENS WHEN SUBJECTED TO THE ACTION OF A FORGING HAMMER.

Initial Thickness (mm)	Final Thickness (mm)	%Deformation
4.53	4.02	11
4.51	4.00	11
3.96	3.36	15
4.34	3.64	16
5.04	4.09	19
5.02	4.08	19
4.72	3.62	23
6.05	4.19	31
6.04	4.18	31

* $\%\ \text{Deformation} = \dfrac{|\ \Delta\ \text{thickness}\ |}{\text{Initial thickness}} \times 100$

TABLE V

ANODIC POLARIZTION CHARACTERISTICS FOR AISA 316 AUSTENITICS STAINLESS STEEL FROM POTENTIODYNAMICALLY DETERMINED CURVES .

1.- Following the standard procedure with recording scale 1 V and in 0.05 M H_2SO_4 + 0.1 M NaCl

PH	E_R(mV)	E_{pp}(mV)	I_{CRI}(μA)	i_{CRI}(μA/cm^2)	I_p(μA)	i_p(μA/cm^2)	E_b(mV)	E_b^*(mV)	Remarks
1.30	-350	-310	62	7.4	12.5	1.48	550	728	Specimen area = 8.39 cm^2 Curve given in Fig. 16
1.30	-358	-278	102	15.9	10	1.55	565	702	Specimen area = 6.43 cm^2 Curve given in Fig. 17
1.30	-382	-322	82	17.8	7.5	1.62	591	728	Specimen area = 4.61 Curve given in Fig. 18
1.40	-366	-306	42	13.0	5.0	1.54	522	663	Specimen area = 3.24 Curve given in Fig. 19
1.40	-354	-294	25	10.3	2.5	1.03	438	756	Specimen area = 2.42 Curve given in Fig. 20
Mean	- 363	-302		14.25		1.44	533	715	
Standard Deviation	12.6	16.7		3.29		0.24	58.7	34.9	
% Error	3.5	5.5		23		16	11	4.8	

TABLE V (Cont.)

2.- Following the **standard** procedure with recording scale 0.2 V and in 0.05 M H_2SO_4 + 0.1 M NaCl .

PH	E_R(mV)	E_{pp}(mV)	I_{CRI}(μA)	i_{CRI}(μA/cm^2)	I_p(μA)	i_p(μA/cm^2)	E_b(mV)	E_b^*(mV)	Remarks
1.25	-364	-316	105	12.9	7.0	0.9	426	636	Specimen area = 8.12 cm^2 Curve given in Fig.21
1.25	-366	-307	90	14.4	5.0	0.8	434	614	Specimen area = 6.28 cm^2 Curve given in Fig. 22
1.30	-366	-318	48	10.8	4.5	1.0	424	-	Specimen area = 4.48 cm^2 Curve given in Fig. 23
1.30	-364	-305	44	14.5	3.0	1.0	446	676	Specimen area = 3.04 cm^2 Curve given in Fig. 24
1.30	-351	-304	21	10.5	3.5	1.8	448	688	Specimen area = 2.00 cm^2 Curve given in Fig. 25
Mean	-362	-310		12.62		1.1	435	653	
Standard Deviation	6.0	6.5		2.0		0.4	11	34	
% Error	1.6	2.1		15		36	2.5	5.2	

3.- Introducing the modified procedure with disk-shaped specimens and in 0.05M H_2SO_4+0.1M NaCl solutions .

PH	Recorder Scale(V)	E_R(mV)	E_{pp}(mV)	I_{CRI}(μA)	i_{CRI}(μA/cm^2)	I_p(μA)	i_p(μA/cm^2)	E_b	Remarks
1.30	0.1	-346	-	30	60.0	-	-	-	No passivation was obtained Curve given in Fig. 26 a
1.30	0.1	-356	-286	17	34	-	-	-	No passivation was obtained Curve given in Fig. 26 b
1.20	0.1	-342	-292	7.5	15	1.5	3.0	498	Expected E-i pattern obtained Curve given in Fig. 26 c

TABLE V (Cont.)

1.20	0.05	-356	-286	13.5	27	2.5	5.0	-	Passivation no well set Crevice effect. Fig.27 a
1.20	0.05	-374	-294	18.75	37.5	2.0	4.0	-	Passivation no well set Crevice effect. Fig.27 b
1.20	0.05	-356	-296	4.0	8.0	0.75	1.5	314	Expected E-i pattern obtained when rubber washers are used. Curve given in Fig.27 c
1.20	0.1	-370	-290	10	20	0.75	1.5	330	Expected E-i pattern obtained when the above run was repeted. Curve given in Fig. 27 d

4.- Preparing specimens which correspond with different stages of the E-i curve for metal surface examinations.

Solution Composition	PH	Recorder Scale	E_R	E_{pp}	I_{CRI}	i_{CRI}	I_p	i_p	E_b	E_b^*	E_T	E_T^*	Remarks
$0.05M H_2SO_4$	1.30	0.1	-360	-300	6.5	13	-	-	-	-	-	-	Interrupted at (-290,13) (*) Curve given in Fig. 28
"	1.20	0.1	-360	-300	6.0	12	0.75	1.5	--	-	-	-	Interrupted at (230,1.5) Curve given in Fig. 29
"	1.30	0.1	-360	-310	7.0	14	0.75	1.5	-	-	740	839	Interrupted at (860,15) Curve given in Fig.30
$0.05M H_2SO_4$ + 0.01M NaCl	1.10	0.1	-364	-294	8.5	17	-	-	-	-	-	-	Interrupted at (-284,17) Curve given in Fig. 31
"	1.20	0.1	-380	-310	13.5	27	0.75	1.5	-	-	-	-	Interrupted at (100,1.5) Curve given in Fig. 32
"	1.20	0.1	-372	-302	12.5	25	0.75	1.5	448	748	-	-	Interrupted at (768,12) Curve given in Fig. 33

(*) (E,i) coordenates are given in ($mV, \mu A/cm^2$)

TABLE V (Cont.)

5.- Preparing specimens which correspond with different stages of the E-i curve for Pit-Site Density estimation .

Solution Composition	PH	Recorder Scale	E_R	E_{pp}	I_{CRI}	i_{CRI}	I_p	i_p	E_b	E_b^*	E_T	E_T	Remarks
$0.05MH_2SO_4$	1.40	0.1	-350	-300	3.5	7.0	-	-	-	-	-	-	Interrupted at (-280,7.0) Curve given in Fig. 34
"	1.20	0.05	-360	-310	6.5	13	-	-	-	-	-	-	Interuupted at (-160,1.0) Curve given in Fig. 35
"	1.50	0.1	-370	-310	8.0	16	0.75	1.5	-	-	-	-	Interrupted at (220,1.5) Curve given in Fig. 36
"	1.20	0.05	-356	-290	6.0	12	0.5	1.0	-	-	-	-	Interrupted at (644,3.0) Curve given in Fig. 37
"	1.50	0.1	-342	-282	3.5	7	0.5	1.0	-	-	730	-	Interrupted at (858,7.0) Curve given in Fig. 38
"	1.30	0.2	-342	-282	4.5	9	0.5	1.0	-	-	739	858	Interrupted at (898,44) Curve given in Fig. 39
"	1.30	0.2	-356	-296	6.5	13	1.0	2.0	-	-	684	866	Interrupted at (974,220) Curve given in Fig. 40
"	1.40	0.5	-370	-310	12.5	25	2.5	5.0	-	-	840	896	Interrupted at (1000,400) Curve given in Fig. 41
$0.05MH_2SO_4$+ 0.1M NaCl	1.20	0.1	-370	-310	9.0	18	-	-	-	-	-	-	Interuupted at (-310,18) Curve given in Fig. 42
"	1.30	0.05	-374	-310	9.2	18	-	-	-	-	-	-	Interuupted at (-174,4.0) Curve given in Fig. 43
"	1.20	0.1	-378	-308	12.5	25	1.0	2.0	-	-	-	-	Interrupted at (22,2) Curve given in Fig. 44
"	1.30	0.05	-386	-326	15.5	31	0.75	1.5	-	-	-	-	Interrupted at (314,3.0) Curve given in Fig. 45
"	1.20	0.1	-382	-326	14.0	28	1.0	2.0	318	-	-	-	Interrupted at (478,9) Curve given in Fig. 46

TABLE V (Cont.)

$0.05M H_2SO_4$ + 0.1M NaCl	1.30	0.2	-366	-306	7.5	15	0.5	1.0	364	655	-	-	Interrupted at (734,44) Curve given in Fig. 47
"	1.20	0.2	-360	-290	7.0	14	1.0	2.0	370	700	-	-	Interrupted at (780,172) Curve given in Fig. 48
"	1.40	0.5	-378	-318	20.0	40	2.5	5.0	382	714	-	-	Interrupted at (790,400) Curve given in Fig. 49

6.- Illustrating the effect of Cl^- ion concentration .

Solution Composition	PH	Recorder Scale	E_R	E_{pp}	I_{CRI}	i_{CRI}	I_p	i_p	E_b	E_b^*	Remarks
$0.05M H_2SO_4$ + 0.5M NaCl	1.20	0.1	-396	-316	15	30	0.75	1.5	224	224	Curve given in Fig. 50
"	1.20	0.1	-400	-320	18.5	37	-	-	-	-	Interrupted at (-320,37) Curve given in Fig. 51
$0.05M H_2SO_4$ + 1.0M NaCl	1.10	0.1	-394	-314	23	46	1.0	2.0	231	251	Curve given in Fig. 52
"	1.10	0.1	-392	-312	20.5	41	1.0	2.0	228	228	Second run at this concentration with different specimen. Curve given in Fig. 53
"	1.10	0.1	-394	-314	25.0	50	-	-	-	-	Interrupted at (-314, 50) Curve given in Fig. 54

7.- Illustrating the effect of cold work .

Solution Composition	PH	Recerder Scale	E_R	E_{pp}	I_{CRI}	i_{CRI}	I_p	i_p	E_b	E_b^*	E_T	E_T^*	Remarks
0.05M H_2SO_4	1.40	0.05	-344	-284	2.5	5	0.75	1.5	-	-	566	828	% Deformation = 11 Curve given in Fig. 55
"	1.40	0.2	-368	-308	6.5	13	1.0	2.0	-	-	602	852	% Deformation = 15 Curve given in Fig. 56
"	1.50	0.05	-344	-284	2.5	5	0.75	1.5	-	-	636	837	% Deformation = 19 Curve given in Fig. 57
"	1.50	0.05	-336	-276	1.5	3	0.75	1.5	-	-	624	835	% Deformation = 31 Curve given in Fig. 58
0.05M H_2SO_4+ 0.1M NaCl	1.30	0.2	-376	-316	9.0	18	1.0	2.0	84	-	-	-	Interrupted at (234,54) % Deformation = 9 Curve given in Fig. 61
"	1.30	0.2	-380	-310	11	22	1.0	2.0	280	-	-	-	% Deformation = 10 Curve given in Fig. 60
"	1.40	0.05	-364	-304	5.0	10	0.75	1.5	336	501	-	-	% Deformation = 11 Curve given in Fig. 59
"	1.40	0.05	-378	-318	9.0	18	0.75	1.5	192	434	-	-	% Deformation = 19 Curve given in Fig. 62
"	1.40	0.05	-372	-312	9.0	18	0.75	1.5	338	630	-	-	% Deformation = 31 Curve given in Fig. 63

TABLE VI

EXPERIMENTAL DATA FOR PIT-SITE DENSITY ESTIMATION.*

1.- For specimen tested in 0.05 M H_2SO_4 , $(E,i) = (E_R , i_o)$

N	Mag	A_{OBS} (mm^2)	A_t (mm^2)	N_A (mm^{-2})
56	700	10773	0.0219	2557
62	"	"	"	2831
46	"	"	"	2100
52	"	"	"	2374
54	"	"	"	2465
51	"	"	"	2328
50	"	"	"	2283
40	"	"	"	1826
47	"	"	"	2146
44	"	"	"	2009

* The data includes the following parameters:

N, number of sites counted; Mag, Magnification used; A_{OBS}, Surface area of the photograph; A_t, True surface area of the field; N_A, site density.

TABLE VI (cont.)

2.- For specimen tested in 0.05 M H_2SO_4 , (E,i)** = (-280, 7.0)

N	Mag	A_{OBS} (mm^2)	A_t (mm^2)	N_A (mm^{-2})
54	675	10562.75	0.0231	2337
50	"	"	"	2164
47	"	"	"	2034
45	700	"	0.0215	2093
51	675	"	0.0231	2207
46	700	"	0.0215	2139
49	700	"	0.0215	2279
58	675	"	0.0231	2510
43	700	"	0.0215	2000
50	"	"	"	2325
76	"	"	"	3534
56	"	"	"	2604
52	"	"	"	2418
55	"	"	"	2558
64	675	"	0.0231	2770
73	"	"	"	3160
61	"	"	"	2640
57	"	"	"	2467
45	"	"	"	1948
41	"	"	"	1774
46	"	"	"	1991
62	"	"	"	2683
39	700	"	0.0215	1813
36	"	"	"	1674
41	"	"	"	1906
37	"	"	"	1720
58	"	"	"	2697
57	"	"	"	2651
56	"	"	"	2604
62	"	"	"	2883

** (E,i) are given in (mV, μAcm^{-2})

TABLE VI (cont.)

3.- For specimen tested in 0.05 M H_2SO_4 , (E,i) = (-160; 1.0)

N	Mag	A_{OBS} (mm^2)	A_t (mm^2)	N_A (mm^{-2})
61	650	10250	0.0242	2520
64	"	"	"	2644
69	"	"	"	2851
62	"	"	"	2561
47	"	"	"	1942
57	"	"	"	2355
48	"	"	"	1983
59	"	"	"	2438
61	"	"	"	2520
57	"	"	"	2355
73	"	"	"	3016
61	"	"	"	2520
55	"	"	"	2272
57	"	"	"	2355
63	"	"	"	2603
60	"	"	"	2479
58	"	"	"	2396
53	"	"	"	2190
65	"	"	"	2685
66	"	"	"	2727
69	"	"	"	2851
44	"	"	"	1818
49	"	"	"	2024
71	"	"	"	2933
43	"	"	"	1776
48	"	"	"	1983
56	"	"	"	2314
58	"	"	"	2396
35	"	"	"	1446
45	"	"	"	1859

TABLE VI (cont.)

4.- For specimen tested in 0.05 M H_2SO_4, (E,i) = (220, 2.0)

N	Mag	A_{OBS} (mm^2)	A_t (mm^2)	N_A (mm^{-2})
44	725	10562	0.0200	2200
56	"	"	"	2800
44	"	"	"	2200
37	"	"	"	1850
42	"	"	"	2100
41	"	"	"	2050
54	"	"	"	2700
51	"	"	"	2550
56	"	"	"	2800
45	"	"	"	2250
53	"	"	"	2650
47	675	"	0.0231	2034
52	675	"	"	2251
55	700	"	0.0215	2558
50	"	"	"	2325
51	"	"	"	2372
54	"	"	"	2511
53	"	"	"	2465
56	"	"	"	2604
57	"	"	"	2651
60	"	"	"	2790
50	"	"	"	2325
64	"	"	"	2976
56	"	"	"	2604
50	"	"	"	2325
64	"	"	"	2976
59	"	"	"	2744
42	"	"	"	1953
49	"	"	"	2279
46	"	"	"	2139
41	"	"	"	1906

TABLE VI (cont.)

5.- For specimen tested in 0.05 M H_2SO_4, (E,i) =(644, 3.0)

N	Mag	A_{OBS} (mm^2)	A_t (mm^2)	N_A (mm^{-2})
71	625	10250	0.0262	2709
40	"	"	"	1526
60	650	"	0.0242	2479
73	650	"	"	3016
54	625	"	0.0262	2061
78	"	"	"	2977
80	"	"	"	3053
83	"	"	"	3167
72	"	"	"	2748
65	"	"	"	2480
72	"	"	"	2748
82	"	"	"	3129
74	"	"	"	2824
91	"	"	"	3473
76	"	"	"	2900
75	"	"	"	2862
74	"	"	"	2824
86	"	"	"	3282
83	"	"	"	3167
85	"	"	"	3244
73	"	"	"	2786
79	"	"	"	3015
76	"	"	"	2900
75	"	"	"	2862
69	"	"	"	2633
82	"	"	"	3129
67	"	"	"	2557
73	"	"	"	2786
81	"	"	"	3091
77	"	"	"	2938
82	"	"	"	3129

TABLE VI (cont.)

6.- For specimen tested in 0.05 M H_2SO_4, (E,i) =(858,7.0)

N	Mag	A_{OBS} (mm^2)	A_t (mm^2)	N_A (mm^{-2})
50	700	10562	0.0215	2325
61	"	"	"	2837
62	"	"	"	2883
60	"	"	"	2790
58	"	"	"	2697
70	687	"	0.0223	3139
55	675	"	0.0231	2380
73	"	"	"	3160
67	"	"	"	2900
66	"	"	"	2857
60	687	"	0.0223	2690
64	"	"	"	2869
56	"	"	"	2511
55	675	"	0.0231	2380
74	700	"	0.0215	3441
50	"	"	"	2325
43	"	"	"	2000
58	"	"	"	2697
72	687	"	0.0223	3228
62	700	"	0.0215	2883
44	"	"	"	2046
77	"	"	"	3581
55	"	"	"	2558
74	"	"	"	3441
65	"	"	"	3023
64	"	"	"	2976
45	"	"	"	2093
63	675	"	0.0231	2727
53	"	"	"	2294
49	700	"	0.0215	2279

TABLE VI (cont.)

7.- For specimen tested in 0.05 M H_2SO_4, (E,i) = (898, 44.0)

N	Mag	A_{OBS} (mm^2)	A_t (mm^2)	N_A (mm^{-2})
73	650	10374	0.0245	2979
82	625	"	0.0265	3094
74	"	"	"	2792
87	"	"	"	3283
78	"	"	"	2943
75	"	"	"	2830
73	637	"	0.0255	2862
77	"	"	"	3019
81	"	"	"	3176
86	"	"	"	3372
69	"	"	"	2705
82	"	"	"	3215
68	"	"	"	2666
73	"	"	"	2862
63	"	"	"	2470
74	"	"	"	2901
64	"	"	"	2509
85	"	"	"	3333
91	"	"	"	3568
84	625	"	0.0265	3169
86	"	"	"	3245
90	"	"	"	3396
76	"	"	"	2867
92	"	"	"	3471
73	"	"	"	2754
83	"	"	"	3132
82	"	"	"	3094
77	637	"	0.0255	3019
76	"	"	"	2980
75	"	"	"	2941

TABLE VI (cont.)

8.- For specimen tested in 0.05 M H_2SO_4, (E,i) = (974, 200)

N	Mag	A_{OBS} (mm^2)	A_t (mm^2)	N_A (mm^{-2})
53	650	10435	0.0246	2154
52	"	"	"	2113
74	"	"	"	3008
84	675	"	0.0229	3668
64	"	"	"	2794
80	650	"	0.0246	3252
54	"	"	"	2195
72	"	"	"	2926
70	"	"	"	2845
61	"	"	"	2479
58	"	"	"	2357
59	"	"	"	2398
79	"	"	"	3211
83	"	"	"	3373
71	675	"	0.0229	3100
66	650	"	0.0246	2682
72	675	"	0.0229	3144
64	650	"	0.0246	2601
65	"	"	"	2642
57	"	"	"	2317
71	"	"	"	2886
79	"	"	"	3211
73	"	"	"	2967
87	675	"	0.0229	3799
77	"	"	"	3362
86	"	"	"	3755
74	"	"	"	3231
68	"	"	"	2969
62	"	"	"	2707
71	"	"	"	3100
75	"	"	"	3275
76	"	"	"	3318
67	"	"	"	2925

TABLE VI (cont.)

9.- For specimen tested in 0.05 M H_2SO_4, (E,i) = (1000, 400)

N	Mag	A_{OBS} (mm^2)	A_t (mm^2)	N_A (mm^{-2})
67	675	10004	0.0219	3059
82	"	"	"	3744
84	"	"	"	3853
87	"	"	"	3972
90	"	"	"	4109
98	"	"	"	4474
110	"	"	"	5022
83	"	"	"	3789
86	"	"	"	3926
78	"	"	"	3561
92	"	"	"	4200
91	"	"	"	4155
86	"	"	"	3926
82	"	"	"	3744
80	"	"	"	3652

TABLE VI (cont.)

10.- For specimen tested in 0.05 M H_2SO_4 + 0.1 M NaCl, (E,i) = (E_R, i_o)

N	Mag	A_{OBS} (mm^2)	A_t (mm^2)	N_A (mm^{-2})
62	700	10773	0.0219	2831
54	"	"	"	2465
57	"	"	"	2602
50	"	"	"	2283
72	"	"	"	3287
78	"	"	"	3561
74	"	"	"	3378
58	"	"	"	2648
70	"	"	"	3196
60	"	"	"	2793

TABLE VI (cont.)

11.- For specimen tested in 0.05 M H_2SO_4 + 0.1 M NaCl, (E,i) = (-300, 19)

N	Mag	A_{OBS} (mm^2)	A_t (mm^2)	N_A (mm^{-2})
53	675	10793	0.0236	2245
73	"	"	"	3093
50	"	"	"	2118
65	"	"	"	2754
53	"	"	"	2245
55	"	"	"	2330
52	"	"	"	2203
56	"	"	"	2372
53	"	"	"	2245
59	"	"	"	2500
54	"	"	"	2288
51	"	"	"	2161
40	"	"	"	1694
37	"	"	"	1567
52	"	"	"	2203
33	"	"	"	1398
48	"	"	"	2033
62	"	"	"	2627
49	"	"	"	2076
42	"	"	"	1779
41	"	"	"	1737
47	"	"	"	1991
70	"	"	"	2966
67	"	"	"	2838
50	"	"	"	2118
52	"	"	"	2203
46	"	"	"	1949
54	"	"	"	2288
45	"	"	"	1906
51	"	"	"	2161
42	"	"	"	1779

TABLE VI (cont.)

12.- For specimen tested in 0.05 M H_2SO_4 + 0.1 M NaCl, (E,i) = (-174, 4)

N	Mag	A_{OBS} (mm^2)	A_t (mm^2)	N_A (mm^{-2})
40	687	10562	0.0223	1793
36	"	"	"	1614
41	675	"	0.0231	1774
44	"	"	"	1904
55	"	"	"	2380
52	"	"	"	2251
38	650	"	0.0249	1526
54	675	"	0.0231	2337
57	"	"	"	2467
61	"	"	"	2640
43	687	"	0.0223	1928
41	"	"	"	1838
60	"	"	"	2690
65	"	"	"	2914
52	675	"	0.0231	2251
50	"	"	"	2164
55	"	"	"	2380
51	"	"	"	2207
48	687	"	0.0223	2152
59	"	"	"	2645
69	675	"	0.0231	2987
76	"	"	"	3290
55	"	"	"	2380
46	"	"	"	1991
61	687	"	0.0223	2735
41	"	"	"	1838
52	700	"	0.0215	2418
50	725	"	0.0200	2500
55	687	"	0.0223	2466
52	700	"	0.0215	2418

TABLE VI (cont.)

13.- For specimen tested in 0.05 M H_2SO_4 + 0.1 M NaCl, (E,i) = (22, 2)

N	Mag	A_{OBS} (mm^2)	A_t (mm^2)	N_A (mm^{-2})
69	675	10793	0.0236	2923
76	"	"	"	3220
81	"	"	"	3432
67	"	"	"	2838
77	"	"	"	3262
80	"	"	"	3389
61	"	"	"	2584
67	"	"	"	2838
68	"	"	"	2881
83	"	"	"	3516
54	"	"	"	2288
72	"	"	"	3050
82	"	"	"	3474
78	"	"	"	3305
91	"	"	"	3855
75	"	"	"	3177
58	"	"	"	2457
72	"	"	"	3050
71	"	"	"	3008
94	"	"	"	3983
73	"	"	"	3093
84	"	"	"	3559
71	"	"	"	3008
65	"	"	"	2754
56	"	"	"	2372
68	"	"	"	2881
58	"	"	"	2457
60	"	"	"	2542
57	"	"	"	2415
72	"	"	"	3050
65	"	"	"	2754
76	"	"	"	3220

TABLE VI (cont.)

14.- For specimen tested in 0.05 M H_2SO_4 + 0.1 M NaCl, (E,i) = (314, 3)

N	Mag	A_{OBS} (mm^2)	A_t (mm^2)	N_A (mm^{-2})
77	675	10416	0.0228	3377
66	"	"	"	2894
75	"	"	"	3289
61	"	10458	0.0229	2663
59	"	"	"	2576
78	662	"	0.0238	3277
72	"	"	"	3025
62	"	"	"	2605
76	650	"	0.0247	3076
54	"	"	"	2186
66	"	"	"	2672
57	"	"	"	2307
65	"	"	"	2631
82	637	"	0.0257	3190
84	"	"	"	3268
58	625	"	0.0267	2172
64	700	"	0.0213	3004
52	"	"	"	2441
55	"	"	"	2582
79	"	"	"	3708
63	"	"	"	2957
73	"	"	"	3427
53	"	"	"	2488
62	"	"	"	2910
78	687	"	0.0221	3529
67	"	"	"	3031
70	700	"	0.0213	3286
64	"	"	"	3004
67	"	"	"	3145
62	712	"	0.0206	3009
80	"	"	"	3883

TABLE VI (cont.)

15.- For specimen tested in 0.05 M H_2SO_4 + 0.1 M NaCl, (E,i) = (478, 9)

N	Mag	A_{OBS} (mm^2)	A_t (mm^2)	N_A (mm^{-2})
76	675	10793	0.0236	3220
63	"	"	"	2669
67	"	"	"	2838
83	"	"	"	3516
85	"	"	"	3601
68	"	"	"	2881
75	"	"	"	3177
71	"	"	"	3008
74	"	"	"	3135
74	"	"	"	3135
65	"	"	"	2754
82	"	"	"	3474
70	"	"	"	2966
62	"	"	"	2627
76	"	"	"	3220
59	"	"	"	2500
65	"	"	"	2754
53	"	"	"	2245
69	"	"	"	2923
72	"	"	"	3050
63	"	"	"	2669
69	"	"	"	2923
68	"	"	"	2831
67	"	"	"	2838
75	"	"	"	3177
77	"	"	"	3262
81	"	"	"	3432
75	"	"	"	3177
81	"	"	"	3432
65	"	"	"	2754
62	"	"	"	2627
76	"	"	"	3220
64	"	"	"	2711

TABLE VI (cont.)

16.- For specimen tested in 0.05 M H_2SO_4 + 0.1 M NaCl, (E,i) = (734, 44)

N	Mag	A_{OBS} (mm^2)	A_t (mm^2)	N_A (mm^{-2})
79	712	10458	0.0206	3834
64	700	"	0.0213	3004
58	"	"	"	2723
75	675	"	0.0229	3275
70	"	"	"	3056
72	"	"	"	3144
78	"	"	"	3406
80	662	"	0.0238	3361
68	650	"	0.0247	2753
90	"	"	"	3643
84	"	"	"	3400
65	637	"	0.0257	2529
98	675	"	0.0229	4279
68	"	"	"	2969
83	687	"	0.0221	3755
76	"	"	"	3438
81	"	"	"	3665
71	700	"	0.0213	3333
76	"	"	"	3568
79	"	"	"	3708
67	687	"	0.0221	3031
73	700	"	0.0213	3427
64	"	"	"	3004
63	"	"	"	2957
55	"	"	"	2582
60	"	"	"	2816
75	687	"	0.0221	3393
77	662	"	0.0238	3235
96	650	"	0.0247	3886
59	687	"	0.0221	2669

TABLE VI (cont.)

17.- For specimen tested in 0.05 M H_2SO_4 + 0.1 M NaCl, (E,i) = (780, 172)

N	Mag	A_{OBS} (mm^2)	A_t (mm^2)	N_A (mm^{-2})
102	712	10458	0.0206	4951
92	"	"	"	4466
85	"	"	"	4126
93	700	"	0.0213	4366
78	"	"	"	3631
86	687	"	0.0221	3891
98	675	"	0.0229	4279
83	"	"	"	3624
84	"	"	"	3668
89	662	"	0.0238	3739
76	"	"	"	3193
93	650	"	0.0247	3765
94	"	"	"	3805
95	"	"	"	3846
80	675	"	0.0229	3493
73	"	"	"	3187
77	"	"	"	3362
95	687	"	0.0221	4298
75	"	"	"	3393
88	675	"	0.0229	3842
74	687	"	0.0221	3348
90	"	"	"	4072
84	700	"	0.0213	3943
70	687	"	0.0221	3167
88	700	"	0.0213	4131
76	"	"	"	3568
81	"	"	"	3802
76	687	"	0.0221	3438
75	712	"	0.0206	3640
82	687	"	0.0221	3710
63	675	"	0.0229	2751

TABLE VI (cont.)

18.- For specimen tested in 0.05 M H_2SO_4 + 0.1 M NaCl, (E,i) = (790, 400)

N	Mag	A_{OBS} (mm^2)	A_t (mm^2)	N_A (mm^{-2})
100	675	10004	0.0219	4566
93	"	"	"	4246
105	650	"	0.0236	4449
85	"	"	"	3601
102	"	"	"	4322
89	"	"	"	3771
94	"	"	"	3983
84	"	"	"	3559
86	"	"	"	3641
80	"	"	"	3389
79	"	"	"	3347
98	"	"	"	4152
82	"	"	"	3474
73	"	"	"	3093
93	"	"	"	3940

TABLE VI (cont.)

19.- For specimen tested in 0.05 M H_2SO_4 + 0.5 M NaCl, (E,i) = (-320, 37)

N	Mag	A_{OBS} (mm^2)	A_t (mm^2)	N_A (mm^{-2})
88	675	10540	0.0231	3809
82	"	"	"	3549
87	"	"	"	3766
85	"	"	"	3679
71	"	"	"	3073
94	"	"	"	4069
65	"	"	"	2813
66	"	"	"	2857
81	"	"	"	3506
93	"	"	"	4025
102	"	"	"	4415
79	"	"	"	3419
74	"	"	"	3203
97	"	"	"	4199
85	"	"	"	3679

TABLE VI (cont.)

20.- For specimen tested in 0.05 M H_2SO_4 + 1.0 M NaCl, (E,i) = (-314, 50)

N	Mag	A_{OBS} (mm^2)	A_t (mm^2)	N_A (mm^{-2})
96	675	10540	0.0231	4155
71	"	"	"	3073
70	"	"	"	3030
95	"	"	"	4112
92	"	"	"	3982
78	"	"	"	3376
89	"	"	"	3852
87	"	"	"	3766
81	"	"	"	3506
84	"	"	"	3636
86	"	"	"	3722
90	"	"	"	3896
108	"	"	"	4675
97	"	"	"	4199
99	"	"	"	4285

TABLE VI (cont.)

21.- Etch-pits for specimen electrolytically etched in 0.05 M H_2SO_4 at 2.0 V for 60 sec.

N	Mag	A_{OBS} (mm^2)	A_t (mm^2)	N_A (mm^{-2})
294	675	10458	0.0229	12838
305	"	"	"	13318
270	"	"	"	11790
279	"	"	"	12183
217	700	"	0.0213	10187
250	675	"	0.0229	10917
253	675	"	0.0229	11048
209	700	"	0.0213	9812
245	700	"	"	11502
289	"	"	"	13568
249	"	"	"	11690
271	"	"	"	12723
251	675	"	0.0229	10960
244	"	"	"	10655
262	"	"	"	11441
286	"	"	"	12489
269	"	"	"	11746
236	"	"	"	10305
255	"	"	"	11135
277	"	"	"	12096
219	"	"	"	9563
225	"	"	"	9825
282	"	"	"	12314
236	"	"	"	10305
266	"	"	"	11615

TABLE VII

MEAN VALUES OF PIT-SITE DENSITY (N_A), STANDARD DEVIATION (S), VARIATION COEFFICIENT (S/N_A), STANDARD ERROR OF THE MEAN (SE), AND FINAL VALUES OF N_A CALCULATED FROM DATA GIVEN IN TABLE VI .

(E,i) Coordenate	size sample (n)	$N_A(mm^{-2})$	$S(mm^{-2})$	S/N_A	SE	$N_A x10^5(cm^2)$
1.- For specimens tested in 0.05 M H_2SO_4 solutions .						
(E_R , i_o)	10	2292	289	0.13	0.04	2.3 ± 0.3
(-280,7.0)	30	2352	435	0.18	0.03	2.3 ± 0.4
(-160,1.0)	30	2360	375	0.16	0.03	2.4 ± 0.4
(220,2.0)	31	2417	312	0.13	0.02	2.4 ± 0.3
(644,3.0)	31	2854	373	0.13	0.02	2.8 ± 0.4
(858,7.0)	30	2733	418	0.15	0.03	2.7 ± 0.4
(898,44.0)	30	3021	271	0.09	0.02	3.0 ± 0.3
(974,200)	33	2931	448	0.15	0.03	2.9 ± 0.4
(1000,400)	15	3944	440	0.11	0.03	3.9 ± 0.4
2.- For specimens tested in 0.05 M H_2SO_4 + 0.1 M NaCl solutions .						
(E_R ,i_o)	10	2899	428	0.15	0.05	2.9 ± 0.4
(-300,19)	31	2189	389	0.18	0.03	2.2 ± 0.4
(-174,4.0)	30	2295	416	0.18	0.03	2.3 ± 0.4
(22,2.0)	32	3019	423	0.14	0.02	3.0 ± 0.4
(314,3.0)	31	2955	427	0.14	0.03	2.9 ± 0.4
(478,9.0)	33	2993	318	0.11	0.02	3.0 ± 0.3
(734,44)	30	3261	425	0.13	0.02	3.3 ± 0.4
(780,172)	31	3758	448	0.12	0.02	3.7 ± 0.4
(790,400)	15	3855	442	0.12	0.03	3.8 ± 0.4
3.- For the specimen tested in 0.05M H_2SO_4+ 0.5M NaCl solution .						
(-320,37)	15	3604	474	0.13	0.03	3.6 ± 0.5
4.- For the specimen tested in 0.05M H_2SO_4+ 1.0M NaCl solution .						
(-314,50)	15	3817	450	0.13	0.03	3.8 ± 0.5
5.- For etch-pit counting						
	25	11441	1101	0.10	0.02	11 ± 1

TABLE VIII

VARIANCE ANALYSIS

i) For specimens tested in 0.05M H_2SO_4

n_r	$\bar{N}_r$	Source of Variation	Degree of freedom	Variance Estimate	F	$F_{0.05}$	Remarks*
240	2734	between specimens	8	4976941	3.85	1.94	Calculation including all the data available.
		within specimens	231	1292313			
225	2653	between specimens	7	2342741	2.13	2.00	Calculation excluding data of specimen with (E,i) = (1000, 400).
		within specimens	217	1098713			
192	2605	between specimens	6	2233600	2.48	2.09	Calculation excluding data of specimens with (1000, 400) and (946,218) coordenades.
		within specimens	185	898009			
162	2527	between specimens	5	1454129	1.76	2.21	Calculation excluding data of specimens with (1000, 400) , (946,218) and (888,44) coordenades.
		within specimens	156	8245568			

TABLE VIII (cont.)

ii) For specimens tested in 0.05M H_2SO_4 + 0.1M NaCl

n_r	$\bar{N}_r$	Source of Variation	Degree of freedom	Variance Estimate	F	$F_{0.05}$	Remarks
243	2981	between specimens	8	8213694	5.31	1.94	Calculation including all the data available.
		within specimens	234	1546636			
197	2793	between specimens	6	4866748	4.23	2.09	Calculation excluding data of specimens with (792,380) and (780,172) coordenades.
		within specimens	190	1150568			
167	2709	between specimens	5	4299624	4.43	2.21	Calculation excluding data of specimens with (792,380), (780,172), and (724,44) coordenades.
		within specimens	161	969943			
106	2978	between specimens	3	46675	0.072	2.70	Calculation excluding data of specimens with (792,380), (780,172), (724,44), (-310,18) and (-184,5) coordenades.
		within specimens	102	645566			
136	3040	between specimens	4	493756	0.059	2.37	Calculation excluding data of specimens with (792,380), (780, 172), (-310,18) and (-184,5) coordenades.
		within specimens	131	826191			

* (E,i) are expressed in (mV, μA cm^{-2})

TABLE IX

t - STUDENT TEST

Statistic	Degree of freedom	t	$t_{0.05}$	$t_{0.025}$	$t_{0.01}$	Remarks
$t = \frac{\bar{X} - \bar{Y}}{S(1/n_1 + 1/n_2)^{\frac{1}{2}}}$	9	2.06	1.83	2.26	2.81	Comparison of site population of specimens tested in 0.05M H_2SO_4 + 0.1M NaCl solution with site population of specimens tested in 0.05M H_2SO_4 solution.
$t = \frac{X - \bar{X}}{S} n^{\frac{1}{2}}$	4	3.35	2.13	2.776	3.747	Comparison of site density of specimen tested in 0.05M H_2SO_4 + 0.5M NaCl solution with site density of specimens tested in 0.05M H_2SO_4 + 0.1M NaCl solution.
	4	4.47	2.13	2.776	3.747	Comparison of site density of specimen tested in 0.05M H_2SO_4 + 1.0M NaCl with site density of specimens tested in 0.05M H_2SO_4 + 0.1M NaCl solution.

TABLE X

Test of Normality

Interval	n_r	$\bar{N}_a$	s	n_{out}	$\hat{p}$	p	$\frac{(\hat{p} - p)}{\sqrt{\frac{p(1-p)}{n}}}$	Remarks
$(\bar{N} \pm s)$	162	2.5	0.4	51	0.31	0.33	0.27	Data from specimens tested in 0.05M H_2SO_4 solution and whose site densities comform the null hypothesis of the variance analysis.
$(\bar{N} \pm 2s)$	162	2.5	0.4	7	0.04	0.05	0.58	
$(\bar{N} \pm 3s)$	162	2.5	0.4	-	-	0.003	-	
$(\bar{N} \pm s)$	136	3.0	0.4	36	0.26	0.33	1.73	Data from specimens tested in C.05M H_2SO_4 + 0.1M NaCl and whose site densities conform the null hypothesis of the variance analysis.
$(\bar{N} \pm 2s)$	136	3.0	0.4	2	0.015	0.05	1.87	
$(\bar{N} \pm 3s)$	136	3.0	0.4	-	-	0.003	-	
$(\bar{N} \pm s)$	15	3.8	0.4	4	0.26	0.33	0.57	
$(\bar{N} \pm 2s)$	15	3.8	0.4	1	0.06	0.05	0.17	Data from the specimens tested in 0.05M H_2SO_4 + 1.0M NaCl.
$(\bar{N} \pm 3s)$	15	3.8	0.4	-	-	0.003	-	

TABLE XI

Probabilities for the events, "Not encountering a site, $P_{n=0}$", "Encountering a site, $P_{n=1}$", and "Encountering two sites, $P_{n=2}$", in a pit-site of radius, $r = 0.5\,\mu m$, calculated assuming a Poisson distribution, i.e. $P_n = \exp(-2\pi r^2 N_A) \times \frac{(2\pi r^2 N_A)^n}{n!}$.

N_A	Total pit-site* population	$P_{n=0}$	$P_{n=1}$	$P_{n=2}$	Pit-site population for			Fraction of pit-site population for		
					$P_{n=0}$	$P_{n=1}$	$P_{n=2}$	$P_{n=0}$	$P_{n=1}$	$P_{n=2}$
2.5×10^5	1.25×10^5	0.996	0.039	7.6×10^{-6}	1.24×10^5	487	1	0.992	0.004	10^{-5}
3.0×10^5	1.50×10^5	0.995	0.046	1.1×10^{-5}	1.49×10^5	690	2	0.993	0.005	10^{-5}
3.6×10^5	1.80×10^5	0.994	0.056	1.56×10^{-5}	1.79×10^5	1008	3	0.994	0.006	2×10^{-5}
3.8×10^5	1.90×10^5	0.994	0.060	1.79×10^{-5}	1.89×10^5	1140	3	0.994	0.006	2×10^{-5}

* given for a surface area of 0.5 cm^2.

TABLE XII

Effect of the pit-site size on the probability for the event "Encountering a site in a pit-site, $P_{n=1}$", calculated for $N_A = 3.0 \times 10^5$ cm^{-2}.

r (cm)	Area ($2\ r^2$) (cm^2)	P_1	%
5×10^{-5}	1.57×10^{-8}	0,0046	
1×10^{-4}	6.28×10^{-8}	0.019	313
1.5×10^{-4}	1.41×10^{-7}	0.042	813
2.0×10^{-4}	2.5×10^{-7}	0.075	1530

TABLE XIII

Comparison of the experimentally determined breakdown potential E_b(exp) with the breakdown potential E_b(cal) calculated from the estimated catastrophic over-potential η_{cp}.

Solution Composition	N_A (cm^{-2})	λ (cm)	i_{cp} (A cm^{-2})	η_{cp} (V)	E_b(cal)	E_b(exp)
0.05M H_2SO_4	2.5×10^5	0.0032	90.35	1.45	1.09	--
0.05M H_2SO_4 + 0.1M NaCl	3.0×10^5	0.0009	26.02	1.32	0.960	0.330
0.05M H_2SO_4 + 0.5M NaCl	3.6×10^5	0.0008	23.73	1.14	0.780	0.230
0.05M H_2SO_4 + 1.0M NaCl	3.8×10^5	0.0008	23.16	0.747	0.387	0.230

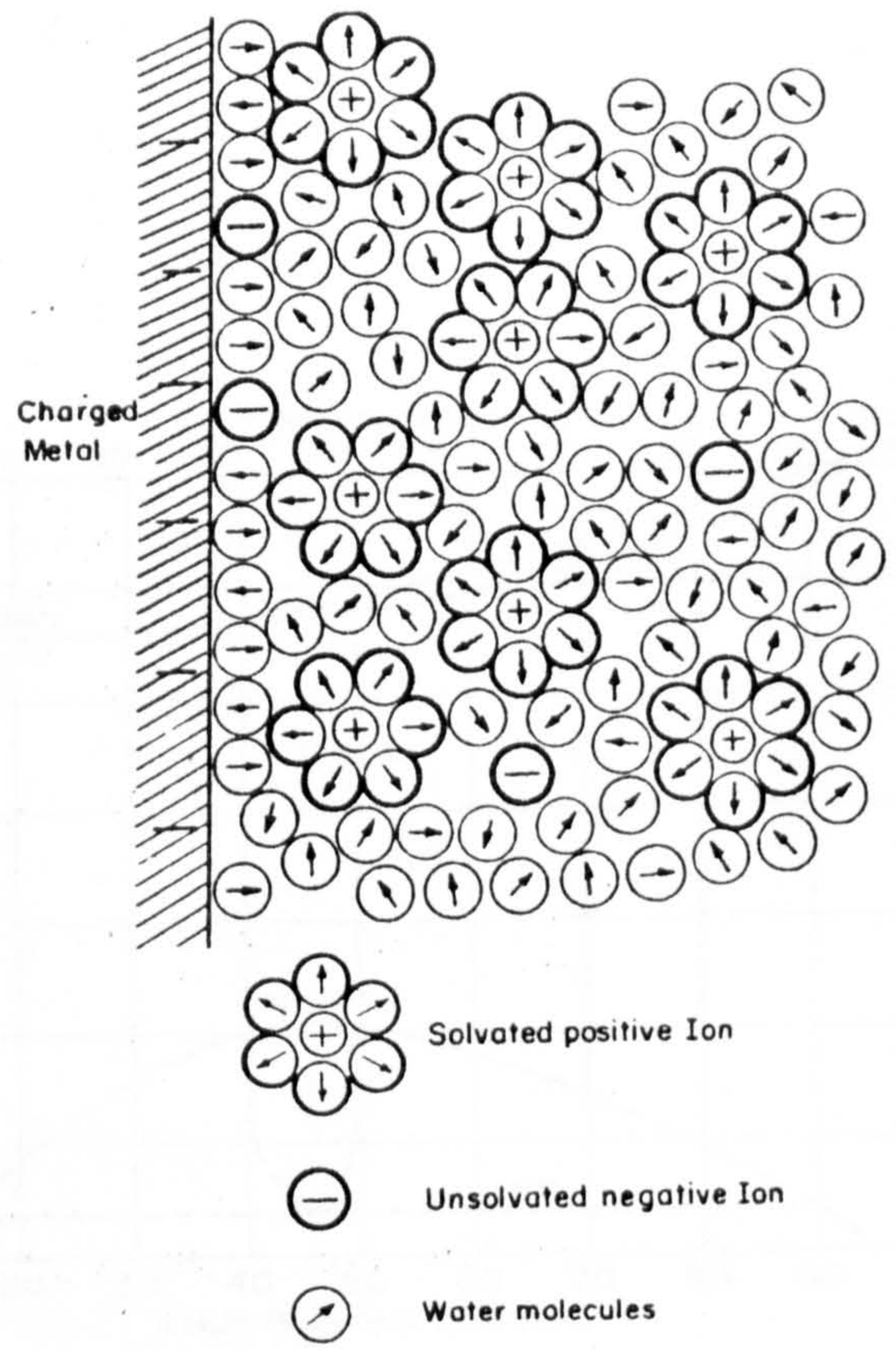

Fig. 1. Schematic Representation of the Structure of an Electrified Interface (Bokris and Reddy[6])

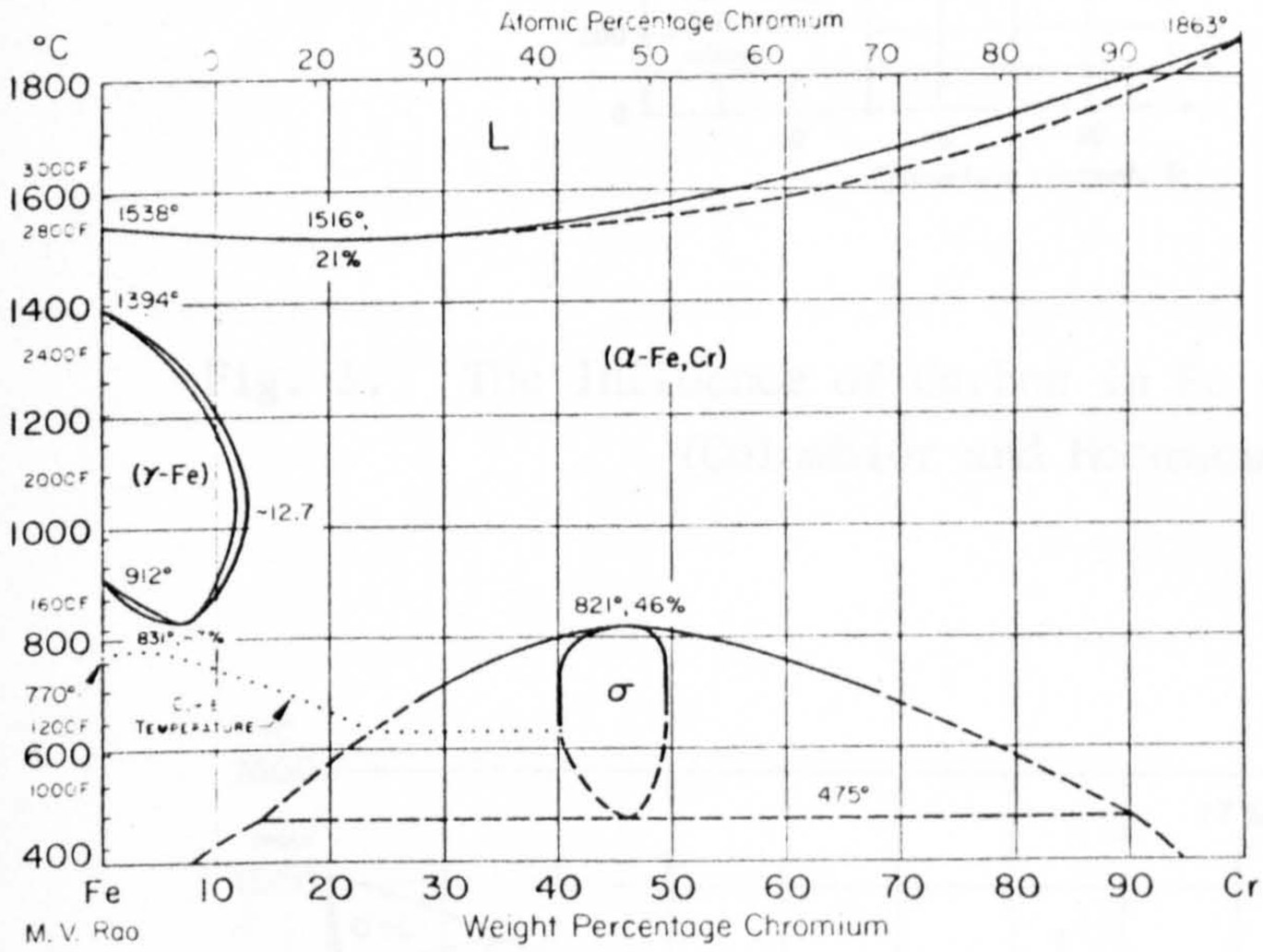

Fig. 2. The Iron-Chromium Binary System[10]
(Metals Handbook, Vol. 8, p.291[10])

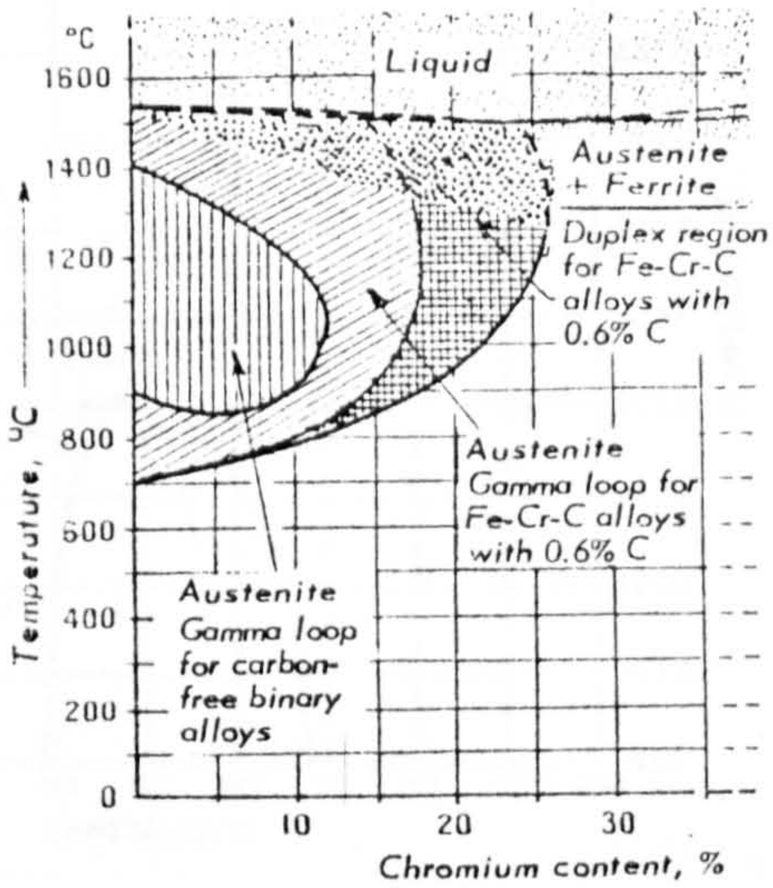

Fig. 3. The Influence of Carbon in Fe - Cr Alloys.
(Columbier and Hochmann[13])

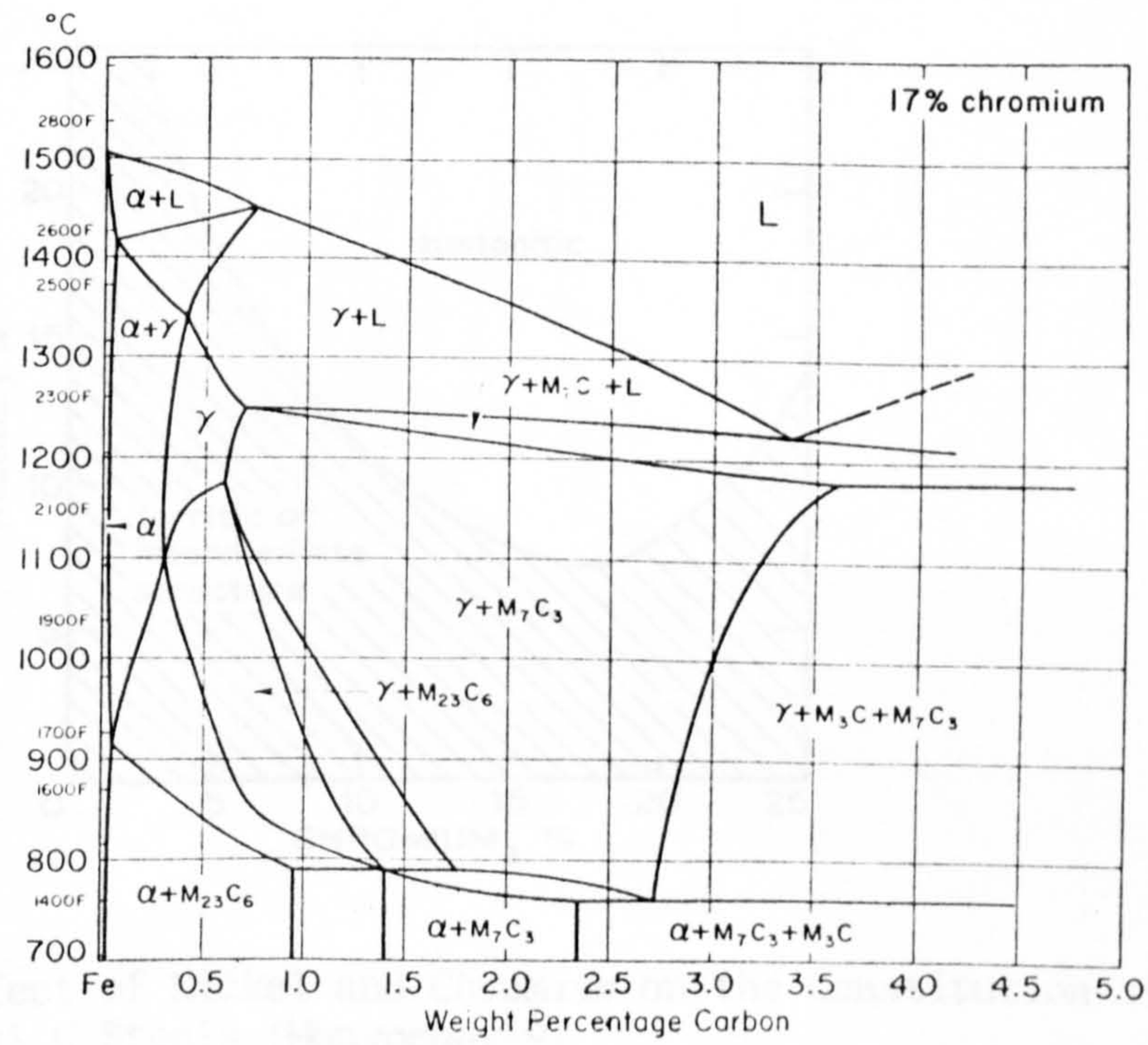

Fig. 4. Section Through Fe - Cr - C Ternary System at 17% Cr.
(Bungart, Kunze and Horne[14])

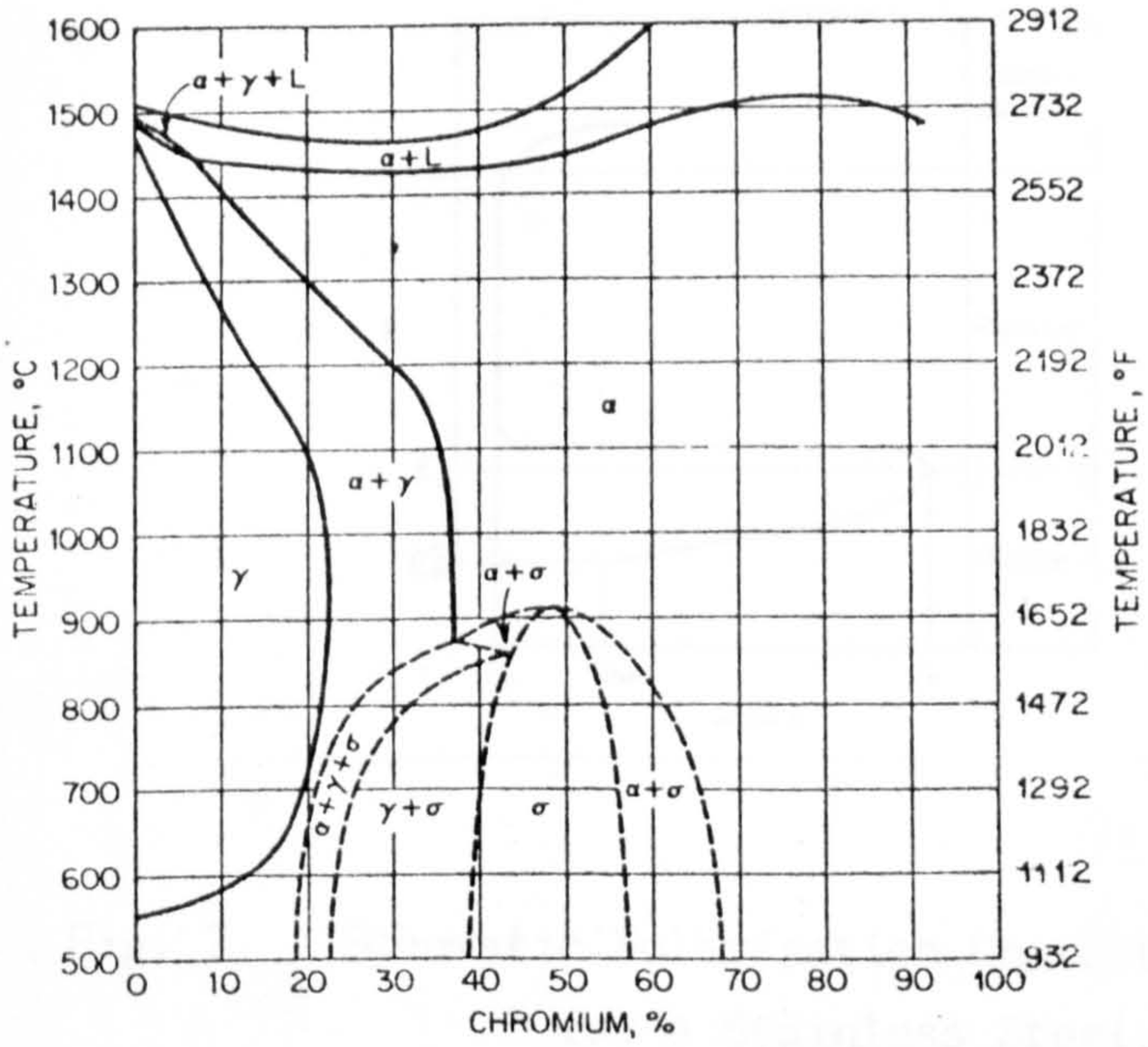

Fig. 5. Section of the Fe-Cr-Ni Ternary System at 8% Ni (Monypenny[16])

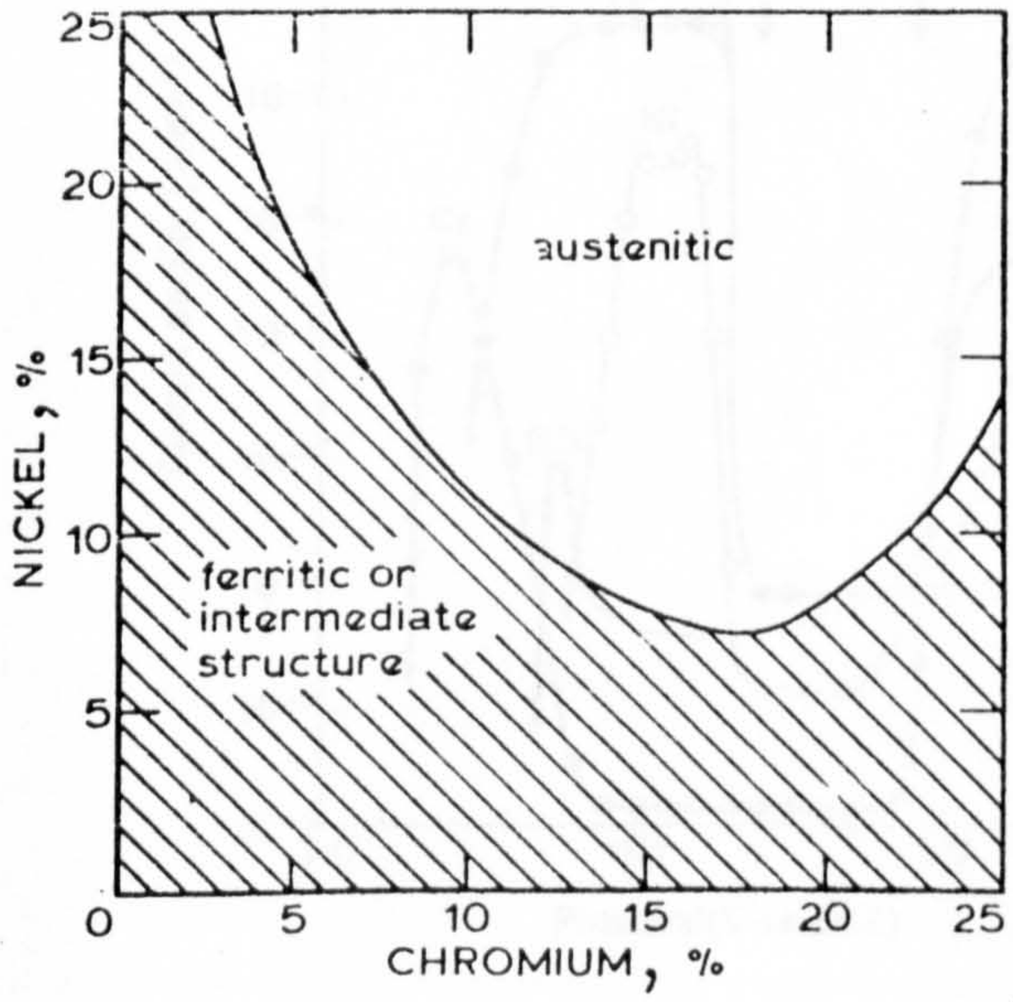

Fig. 6. Effect of Nickel and Chromium on the Constitution of 0.1% C Steels (Monypenny[16])

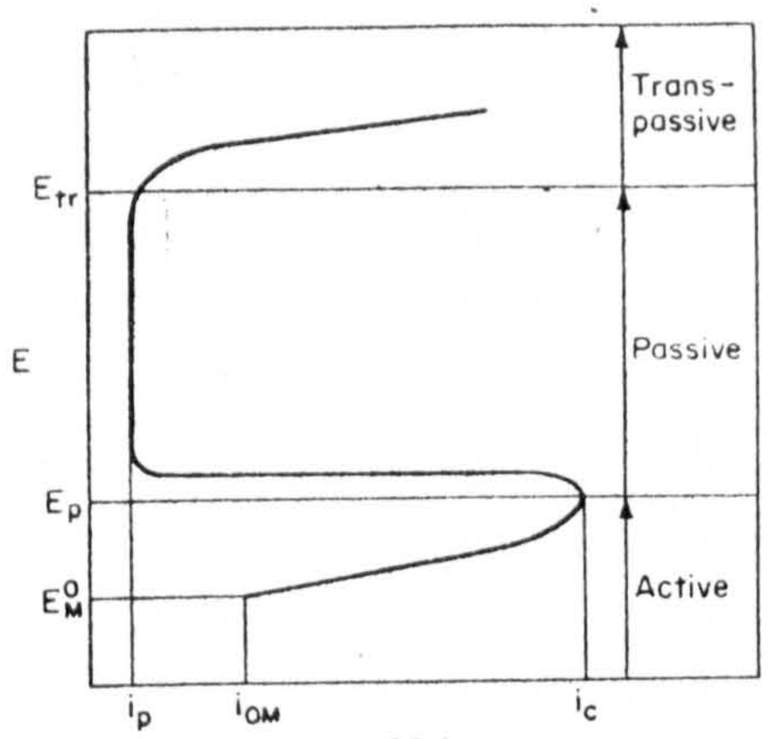

Fig. 7. Schematic Polarisation Characteristics for a Stainless Steel.

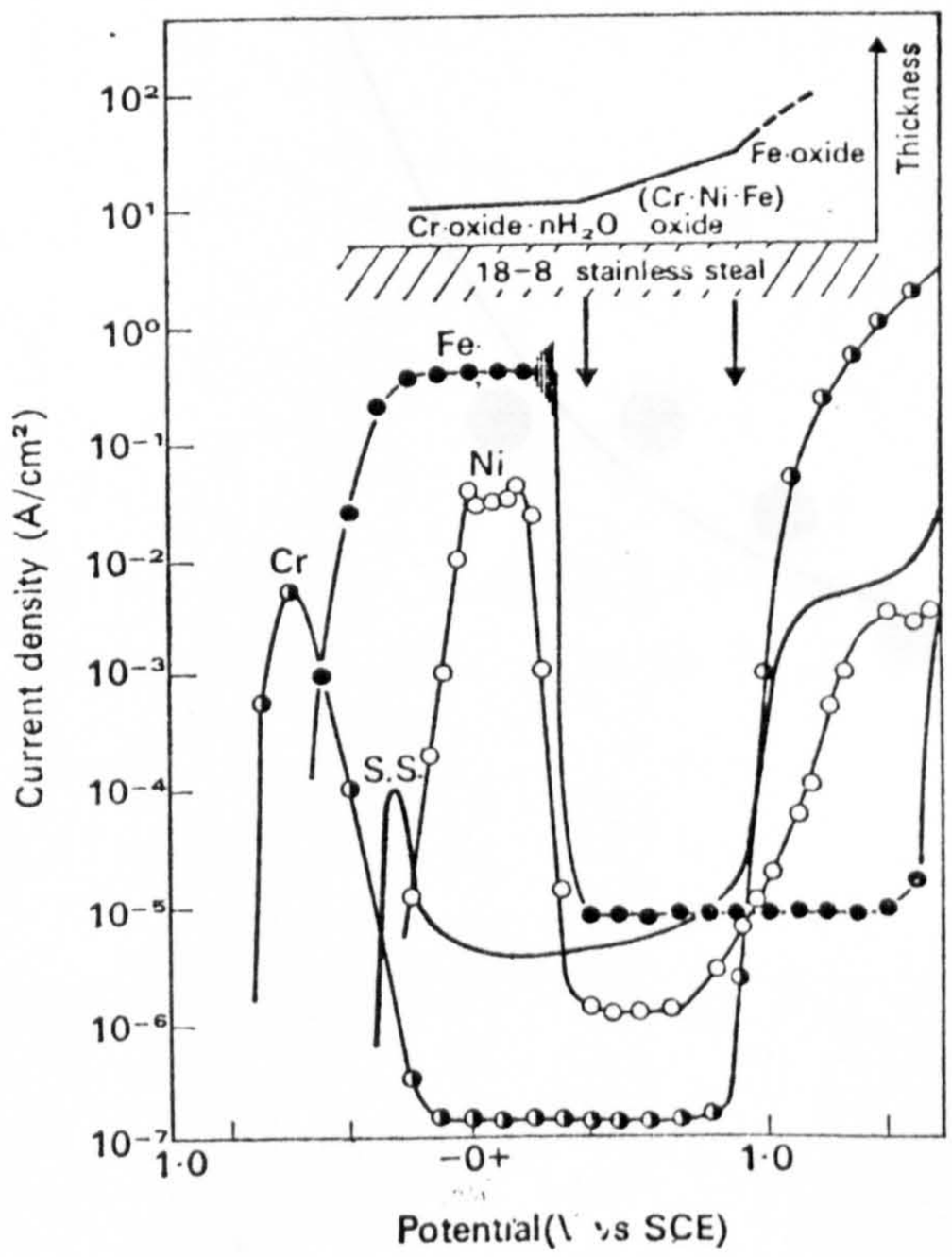

Fig. 8. Comparison of Polarisation Characteristics for Iron, Chromium, Nickel and an 18/8 Stainless Steel. Schematic Sketch at the Top Suggests the Composition and Thickness of the Passive Film on Stainless Steel. (Okamoto[25])

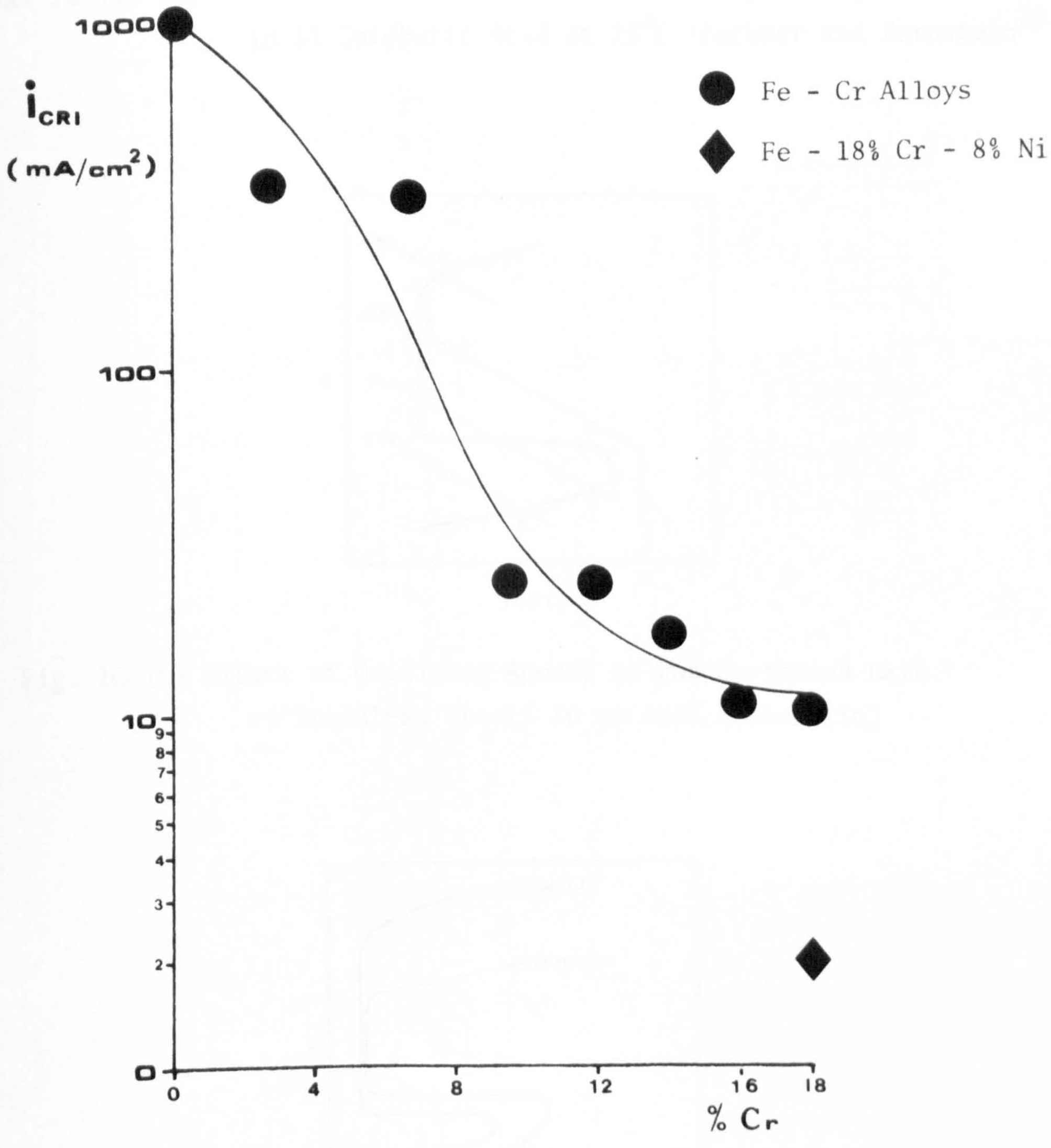

Fig. 9. Effect of Chromium Additions on the Critical Current Density on Iron in Acid Media (Oliver[26])

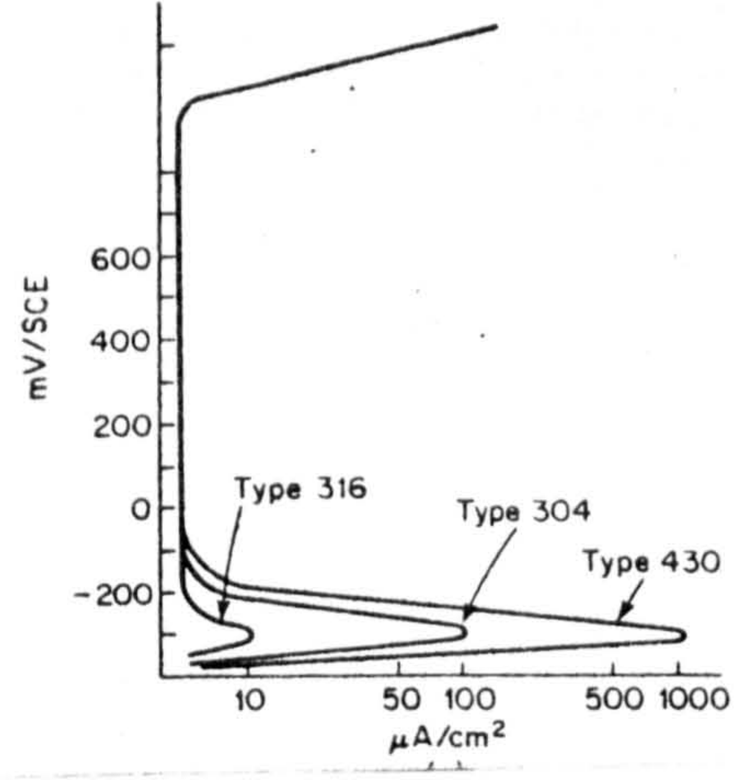

Fig. 10 (a) Polarisation Characteristics of AISI Types 430, 304 and 316 Steels in 5% Sulphuric Acid at 25°C (Peckner and Bernstein[28])

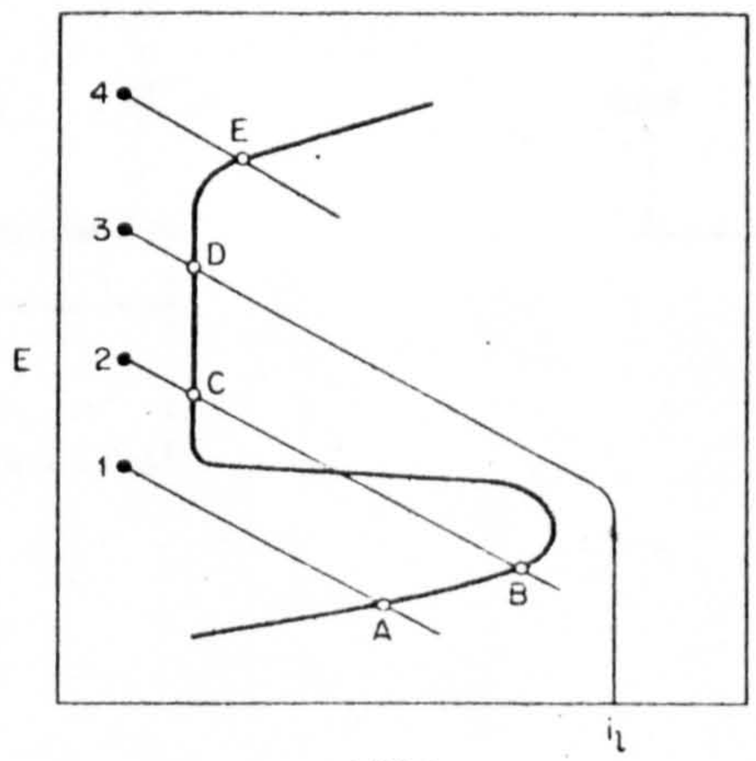

Fig. 10 (b) Effect of Oxidising Agents on the Corrosion Rate of Stainless Steels in an Acid (Schematic)

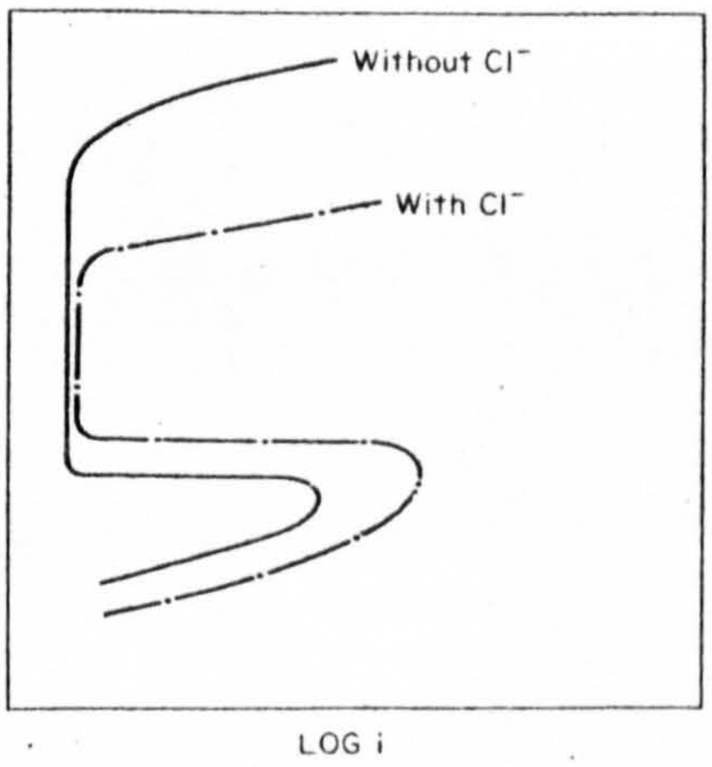

Fig. 11. Effect of Chloride Ions on the Polarisation Characteristics of a Stainless Steel (Schematic).

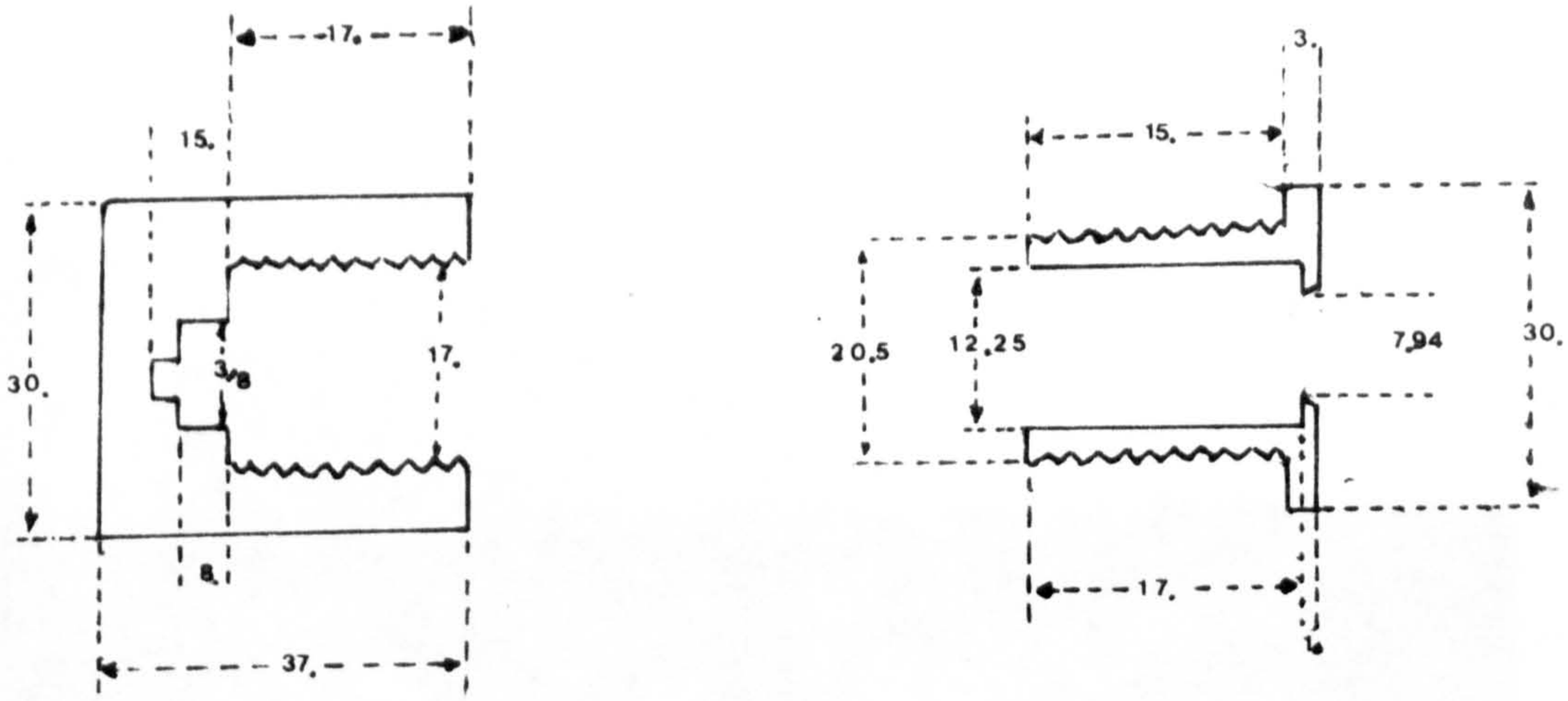

Fig. 12. Electrode Holder for Discs.

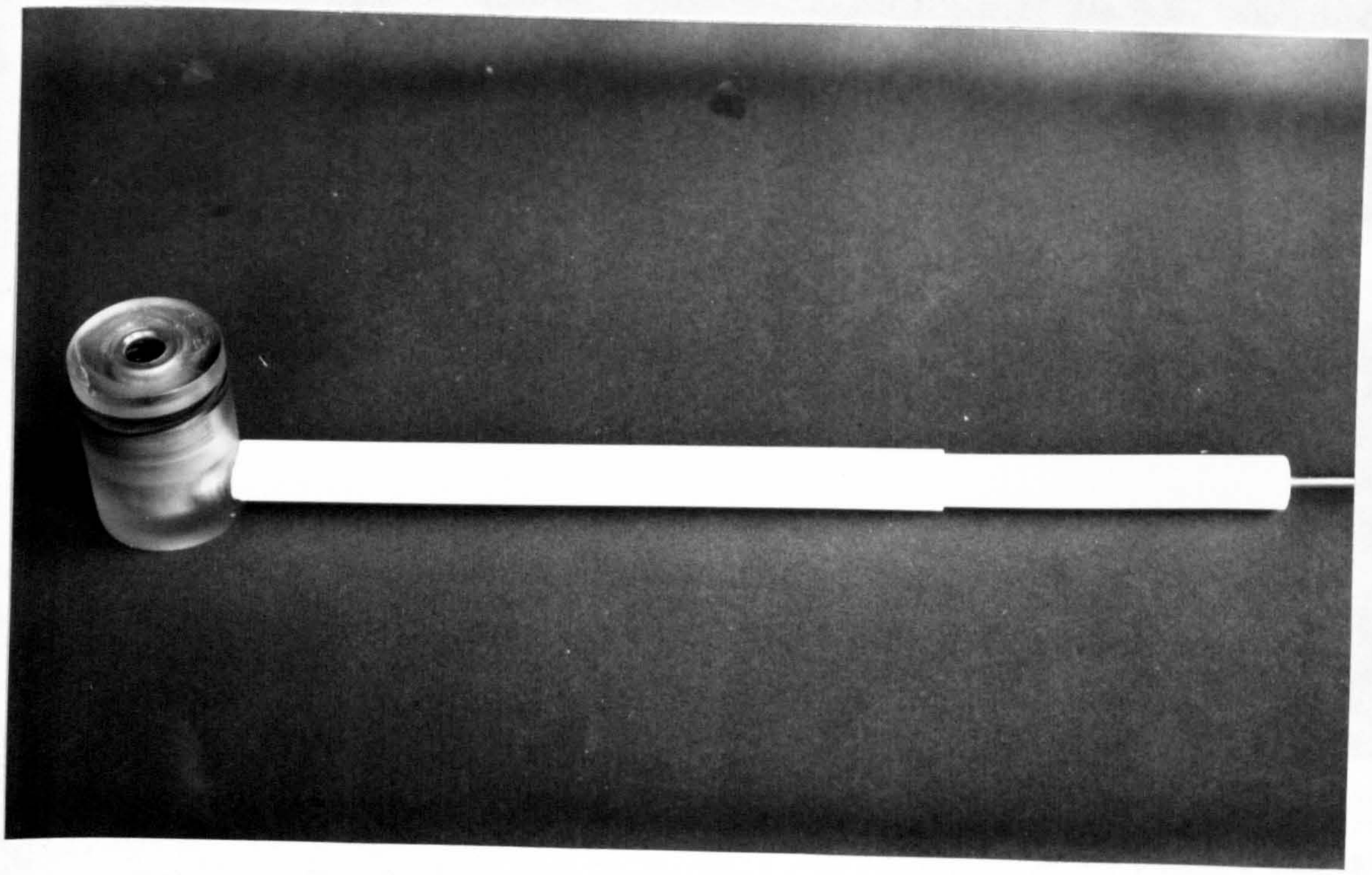

Fig. 13. General View of Electrode Holder for Disc Specimens.

Fig. 14. Dismantled Disc Electrode Holder Showing Component Parts.

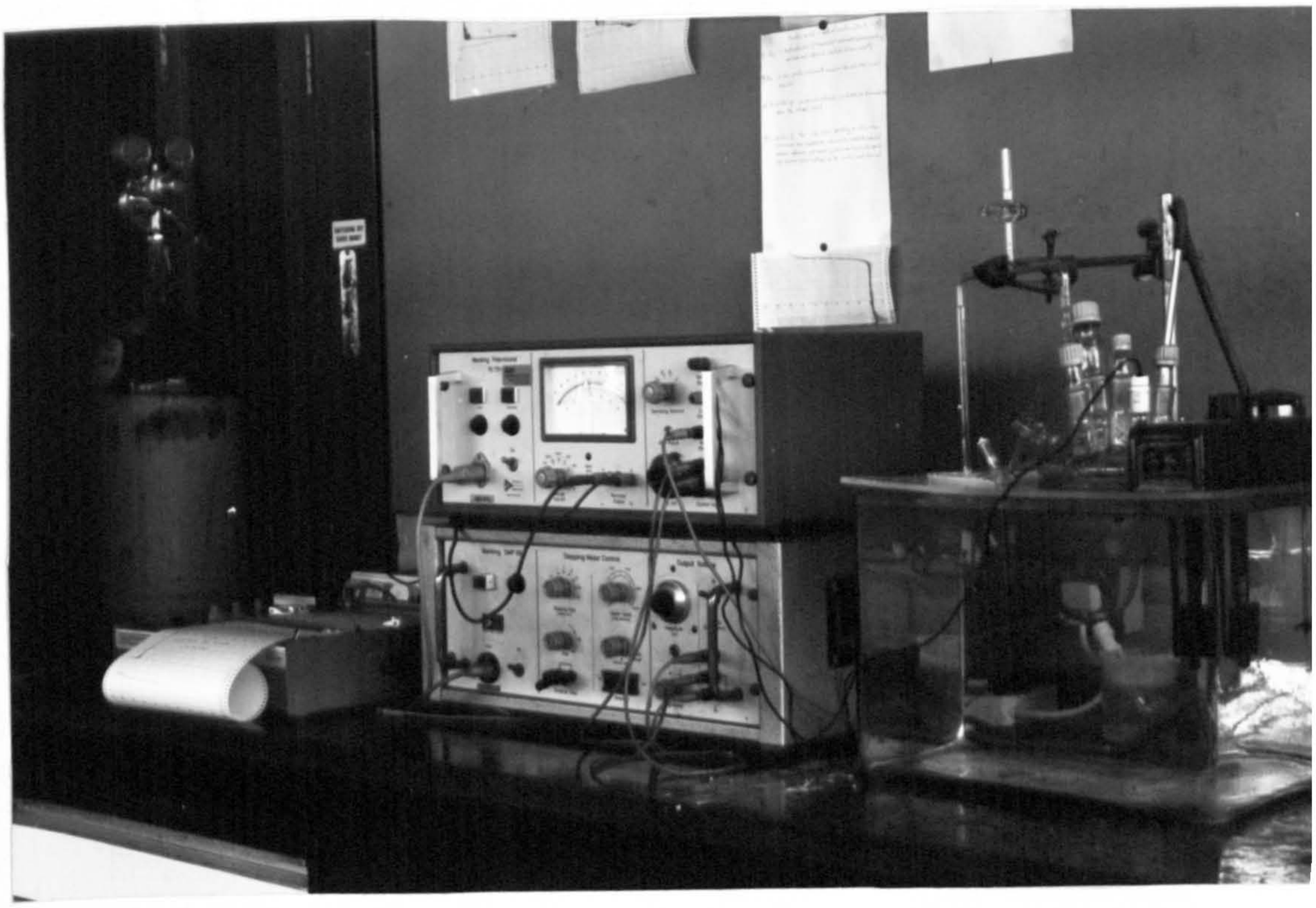

Fig. 15. General View of Equipment, Showing Potentiostat and Polarisation Cell.

ANODIC POLARIZATION CURVES OF AISI 316 AUSTENITIC STAINLESS STEEL. E(V) SCE v i(μA)

1.- Curves determined in 0.05M H_2SO_4 + 0.1M NaCl and following the ASTM standard procedure.

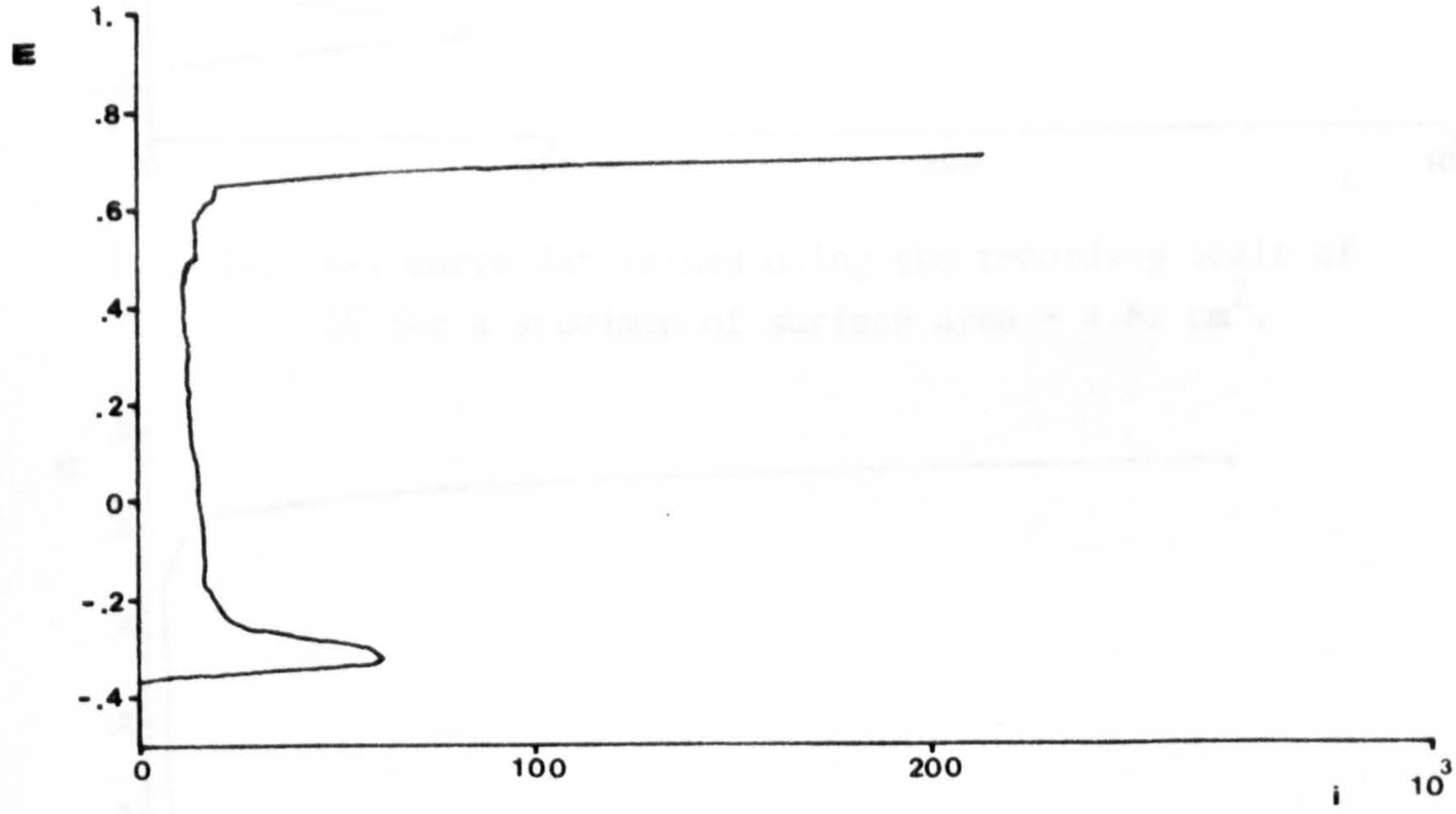

Fig. 16. E-i curve determined using the recording scale of 1V for a specimen of surface area = 8.39 cm^2.

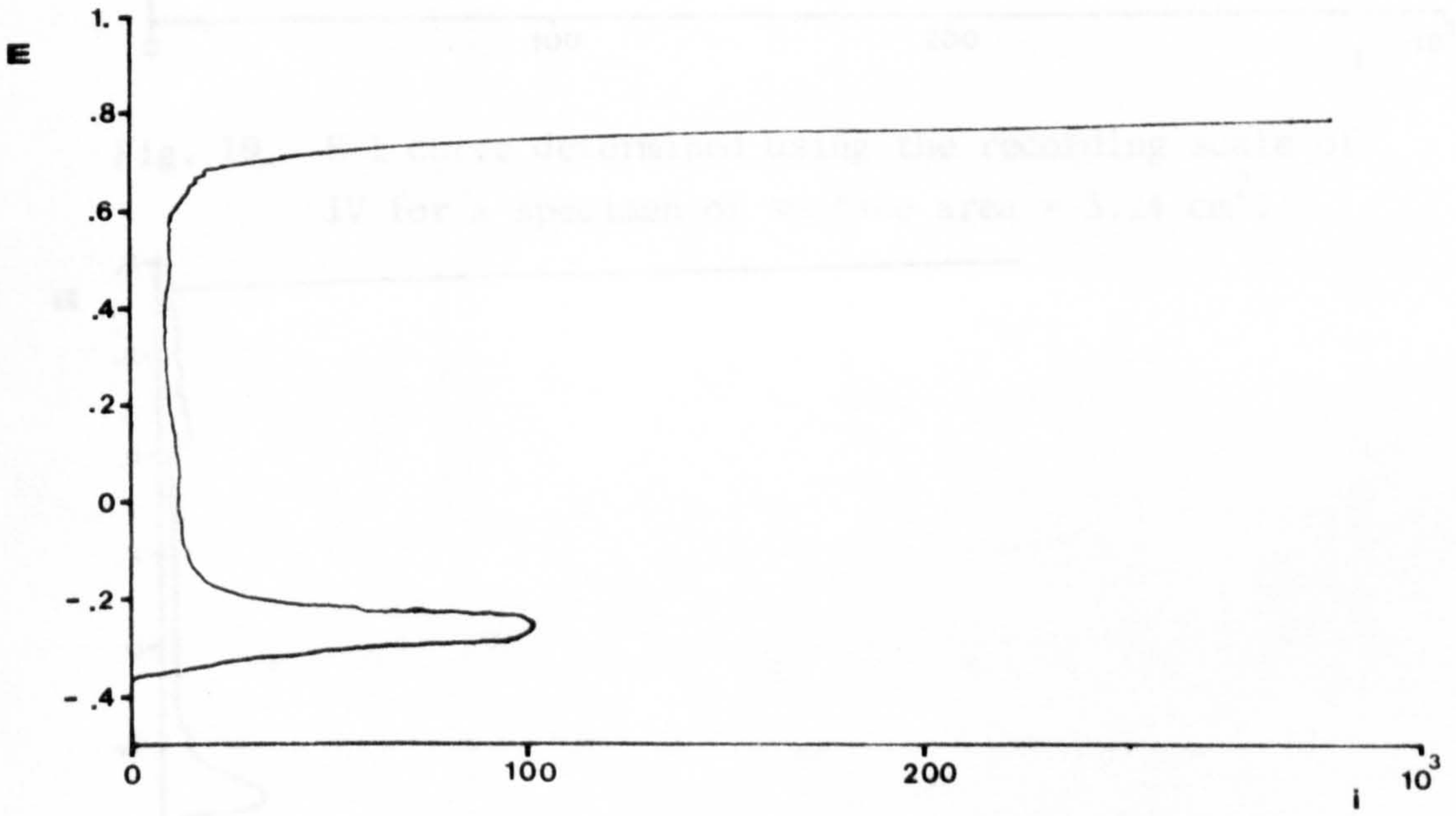

Fig. 17. E-i curve determined using the recording scale of 1V for a specimen of surface area = 6.43 cm^2.

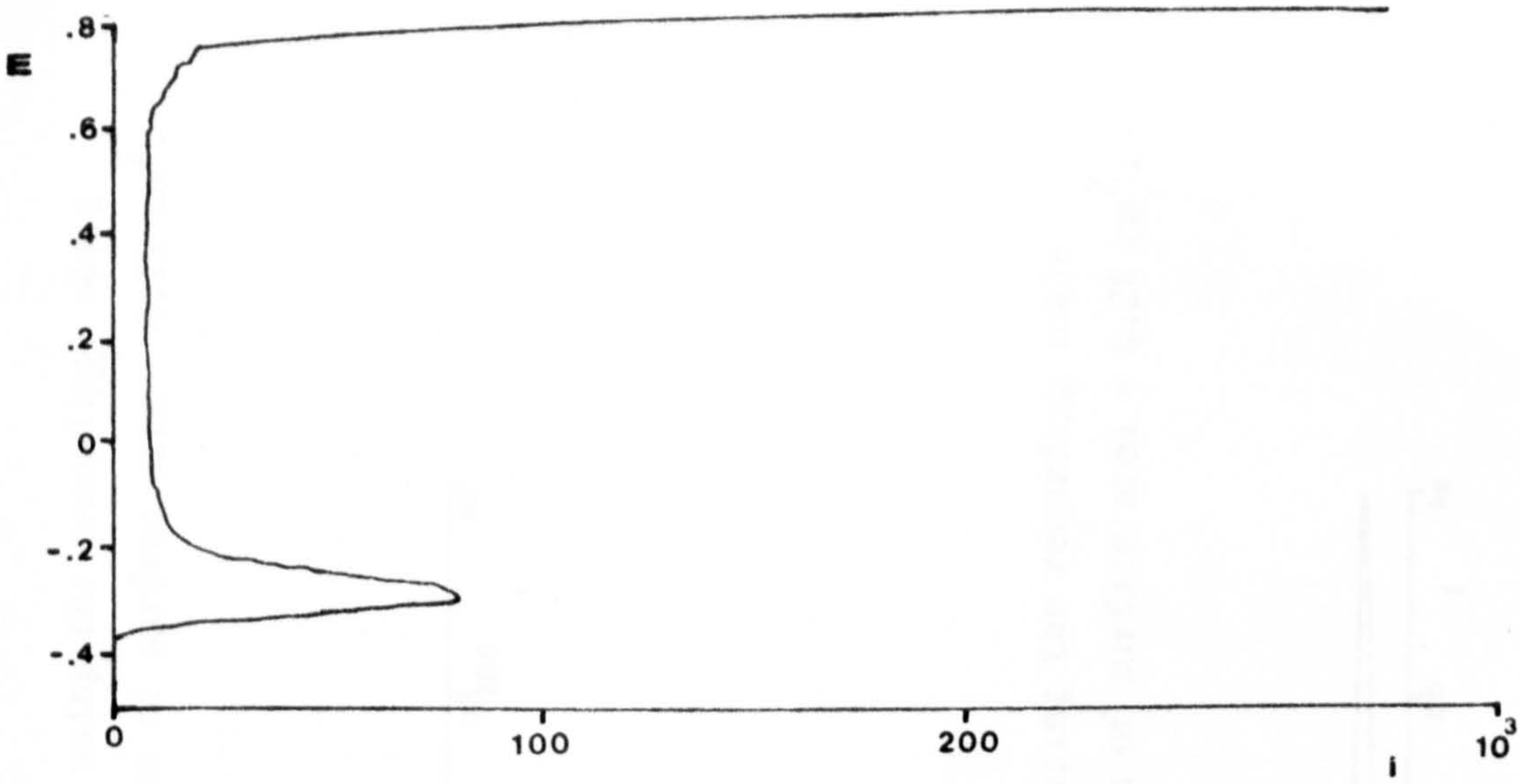

Fig. 18. E-i curve determined using the recording scale of 1V for a specimen of surface area = 4.61 cm^2.

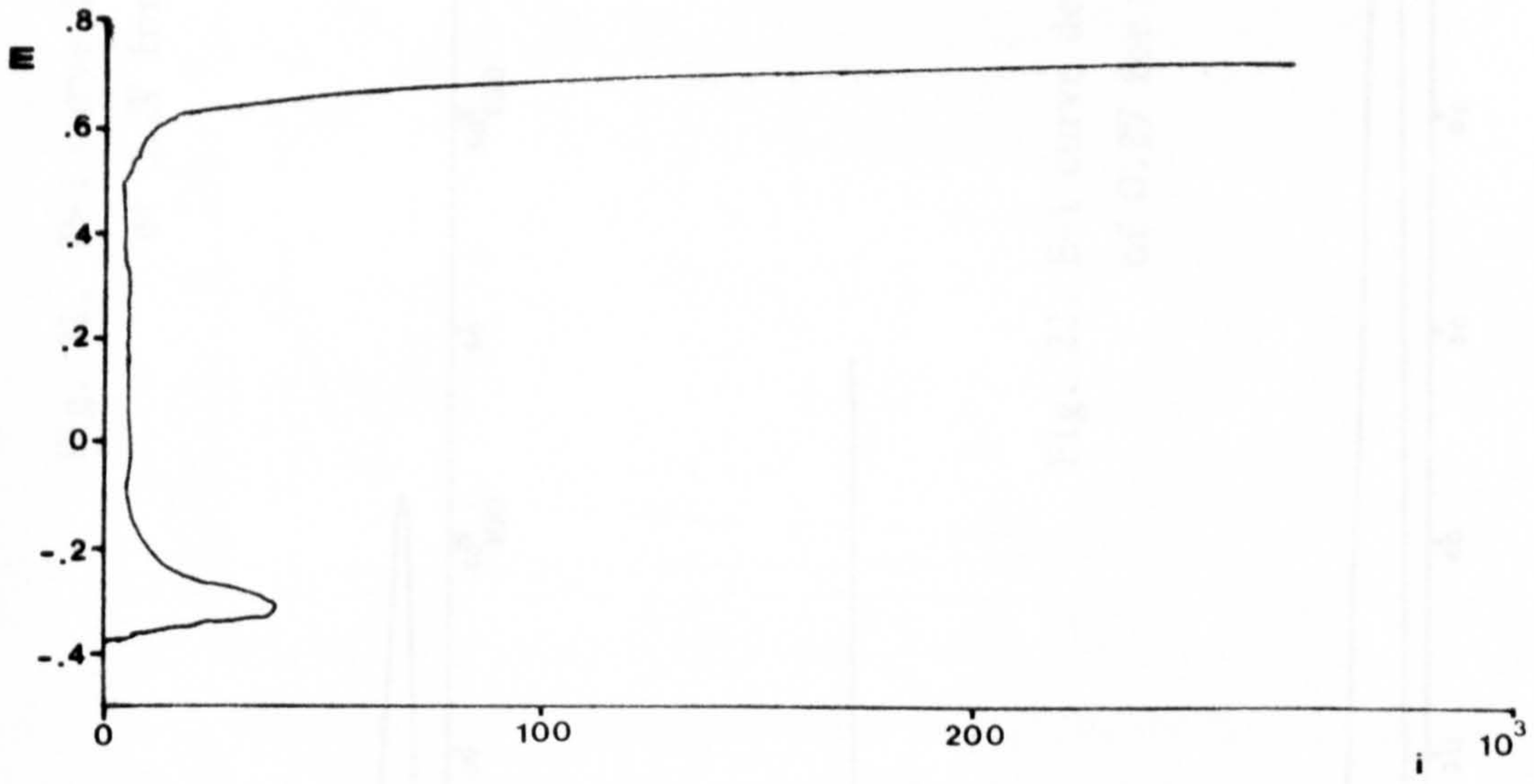

Fig. 19. E-i curve determined using the recording scale of 1V for a specimen of surface area = 3.24 cm^2.

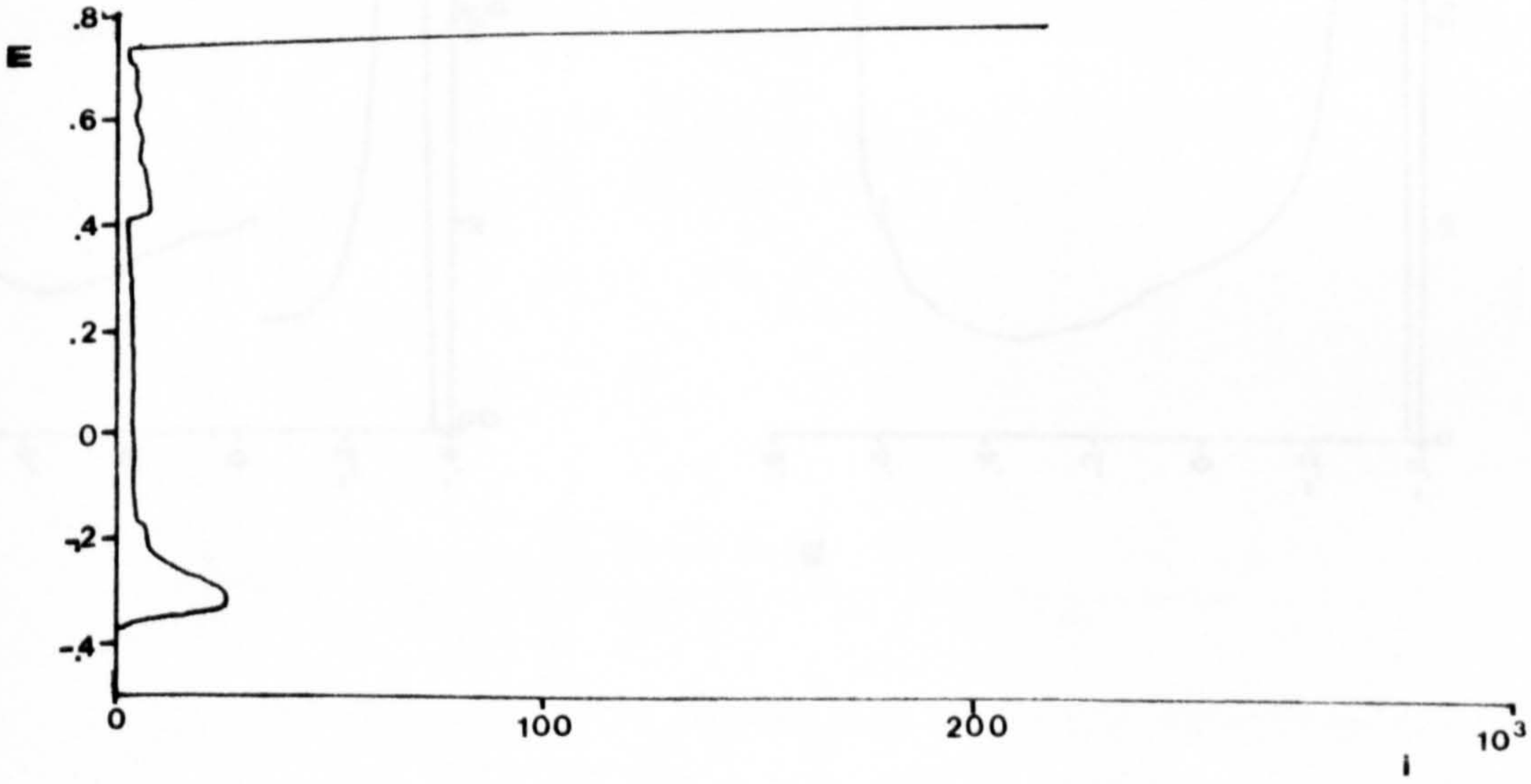

Fig. 20. E-i curve determined using the recording scale of 1V for a specimen of surface area = 2.42 cm^2.

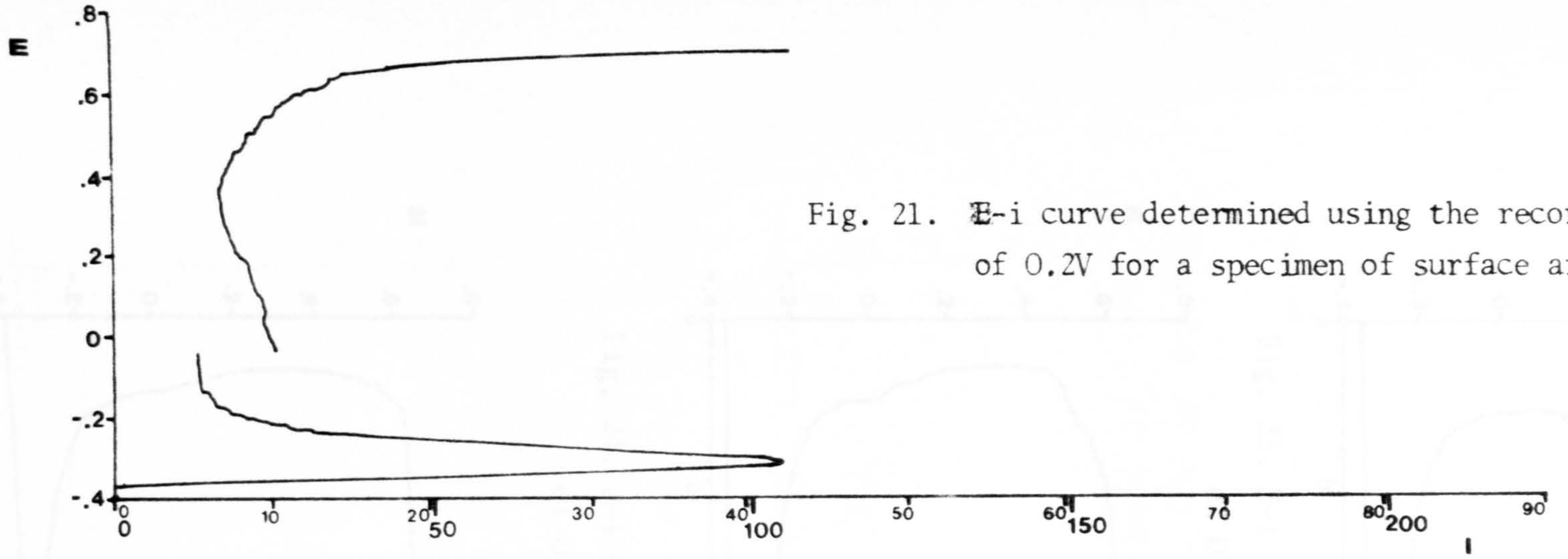

Fig. 21. E-i curve determined using the recording scale of 0.2V for a specimen of surface area = 8.12 cm^2.

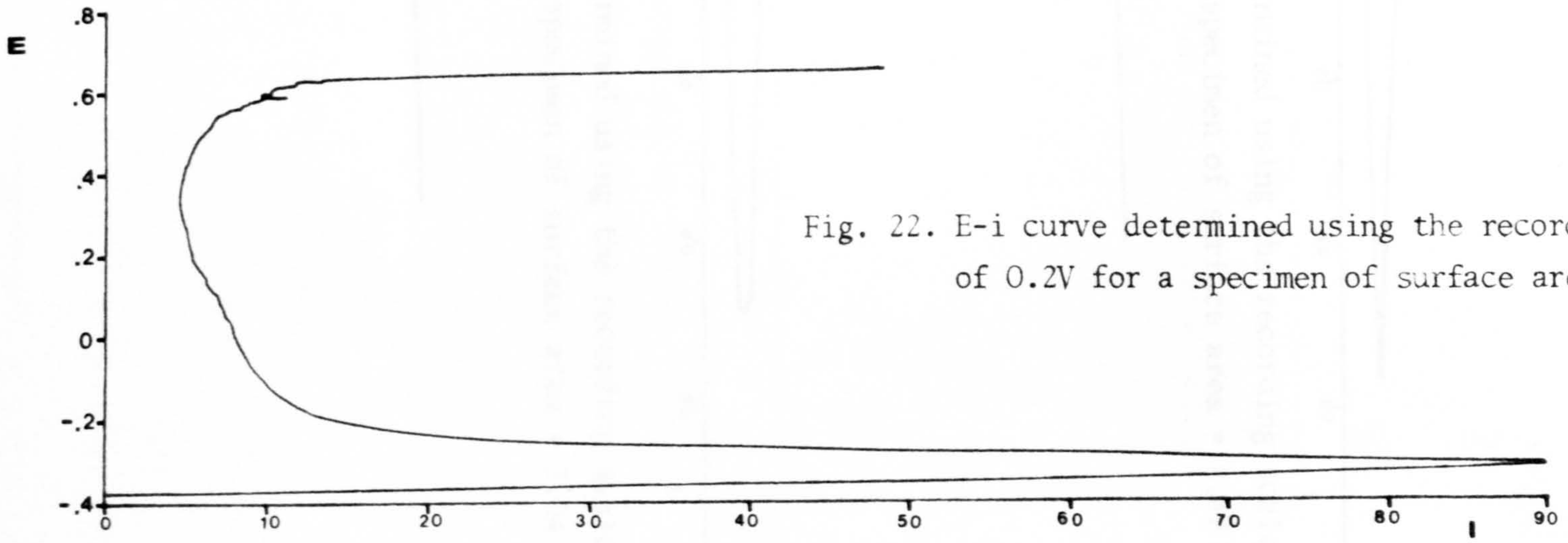

Fig. 22. E-i curve determined using the recording scale of 0.2V for a specimen of surface area = 6.28 cm^2.

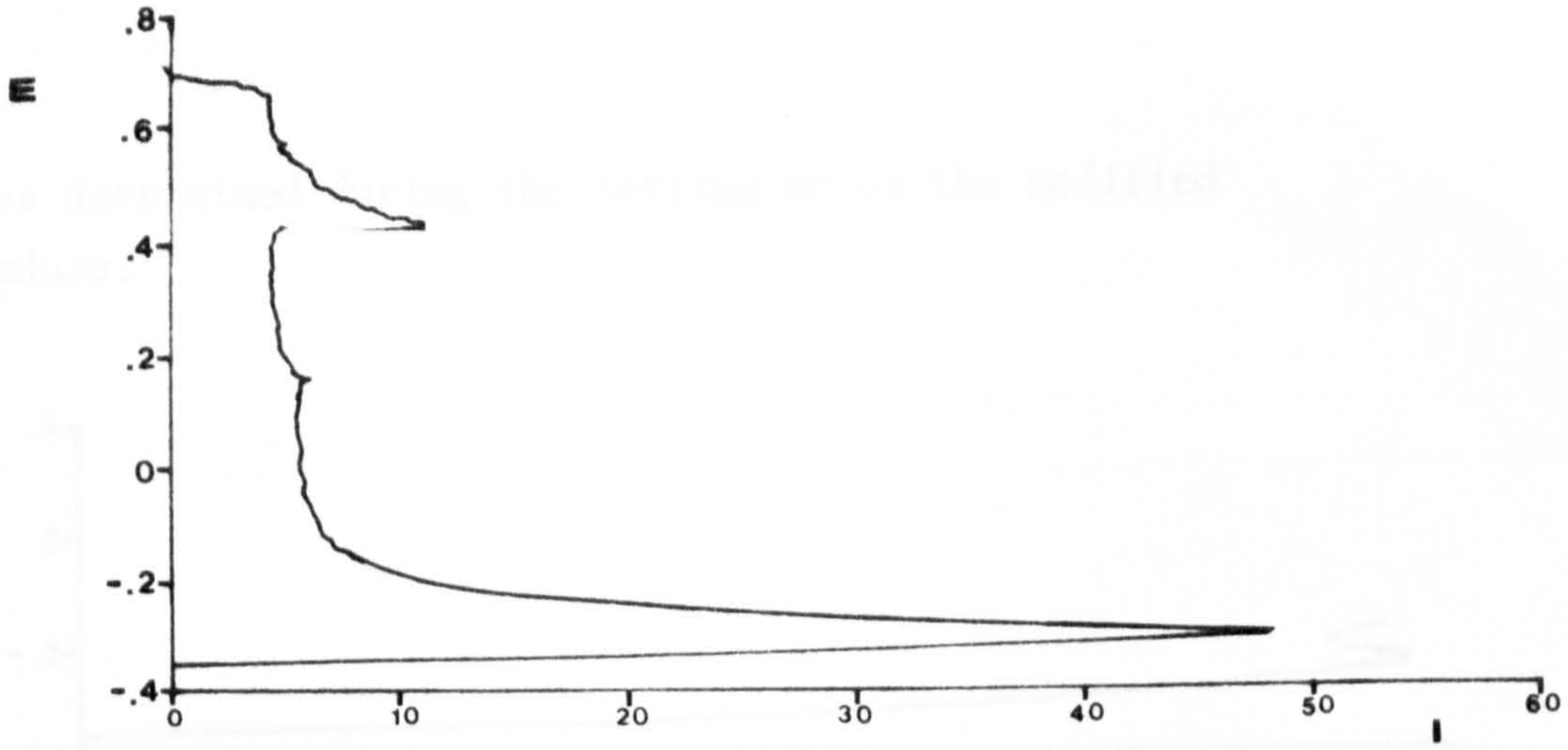

Fig. 23. E-i curve determined using the recording scale of 0.2V for a specimen of surface area = 4.48 cm^2.

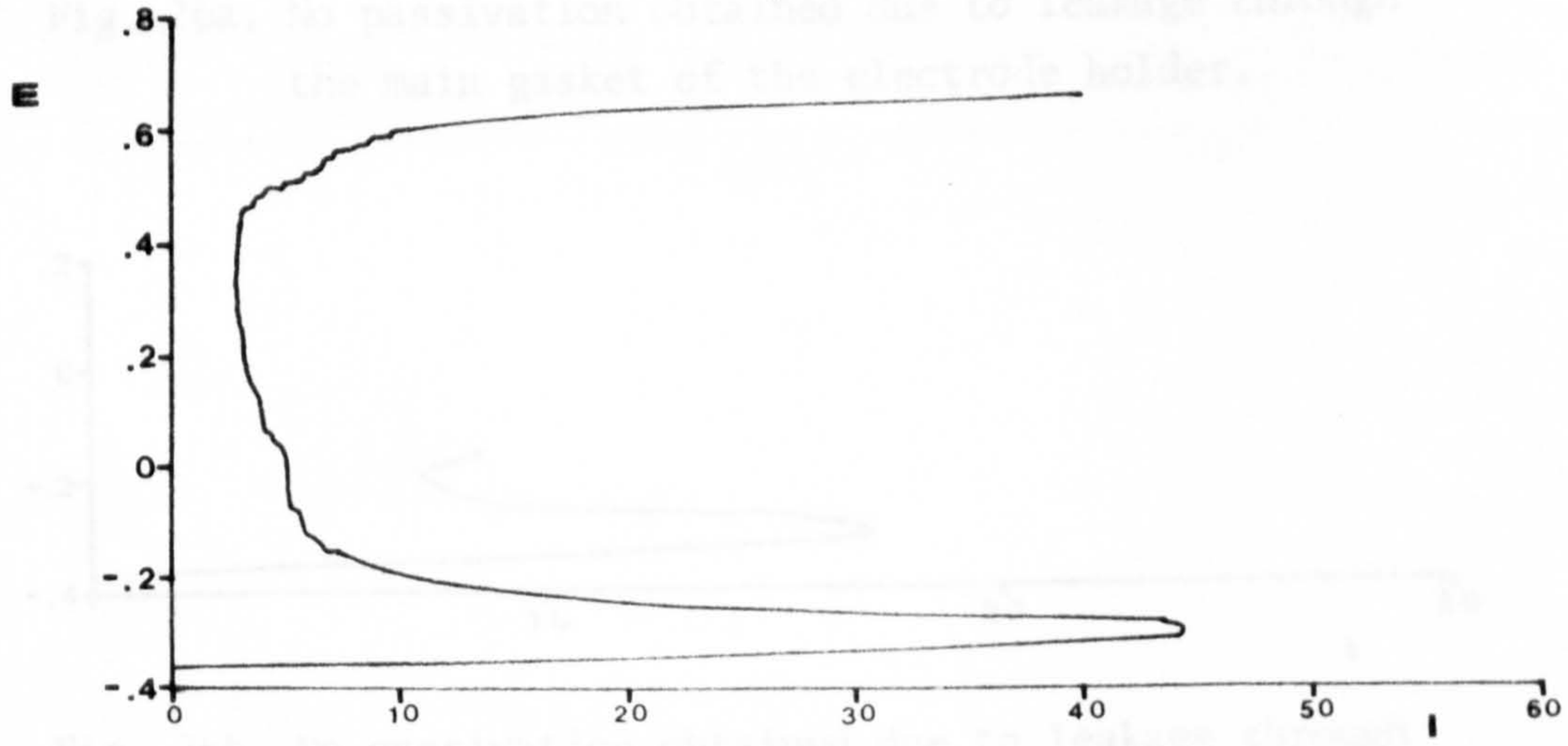

Fig. 24. E-i curve determined using the recording scale of 0.2V for a specimen of surface area = 3.04 cm^2.

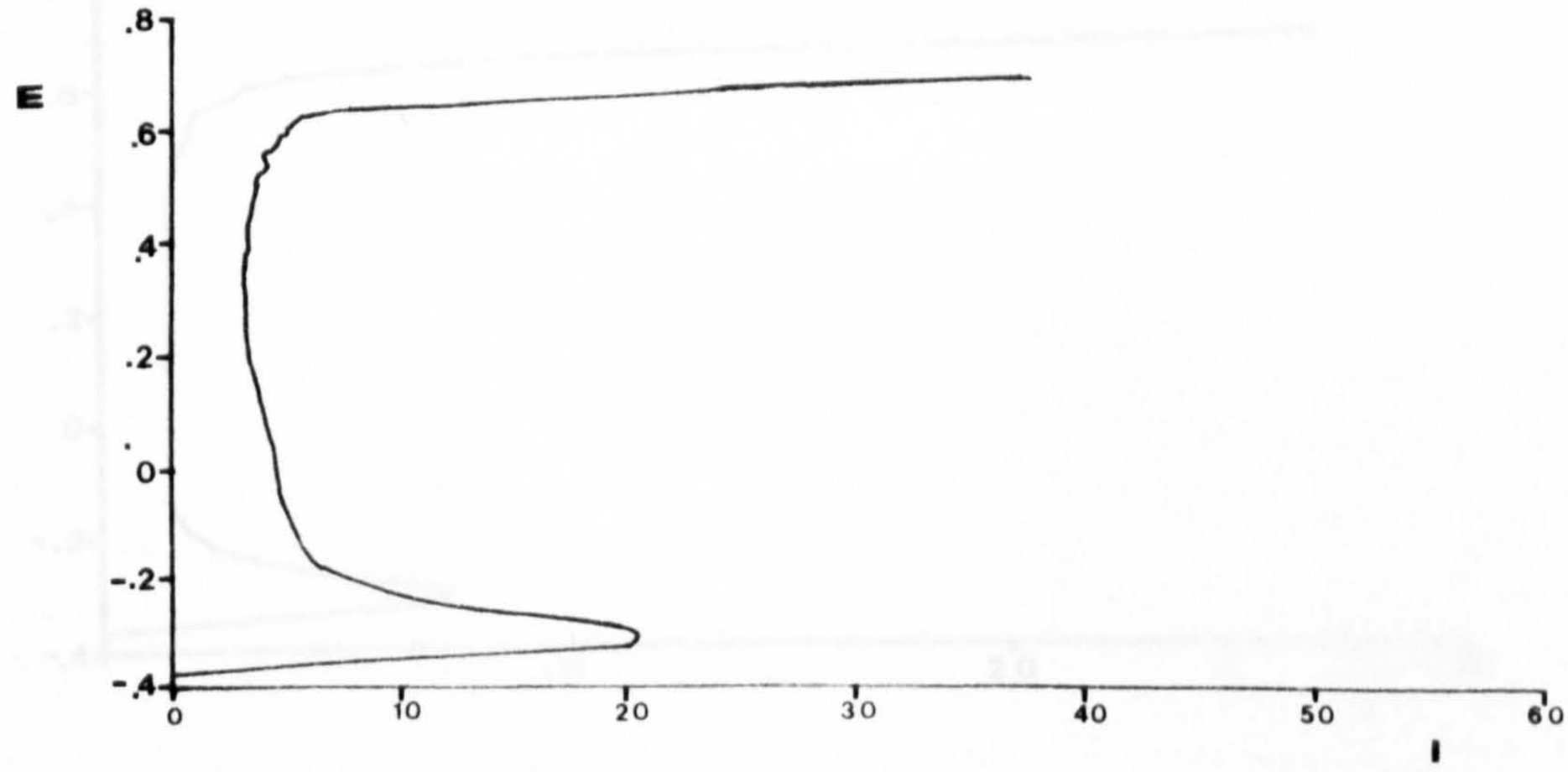

Fig. 25. E-i curve determined using the recording scale of 0,2V for a specimen of surface area = 2.00 cm^2.

2.- Curves determined during the setting up of the modified procedure.

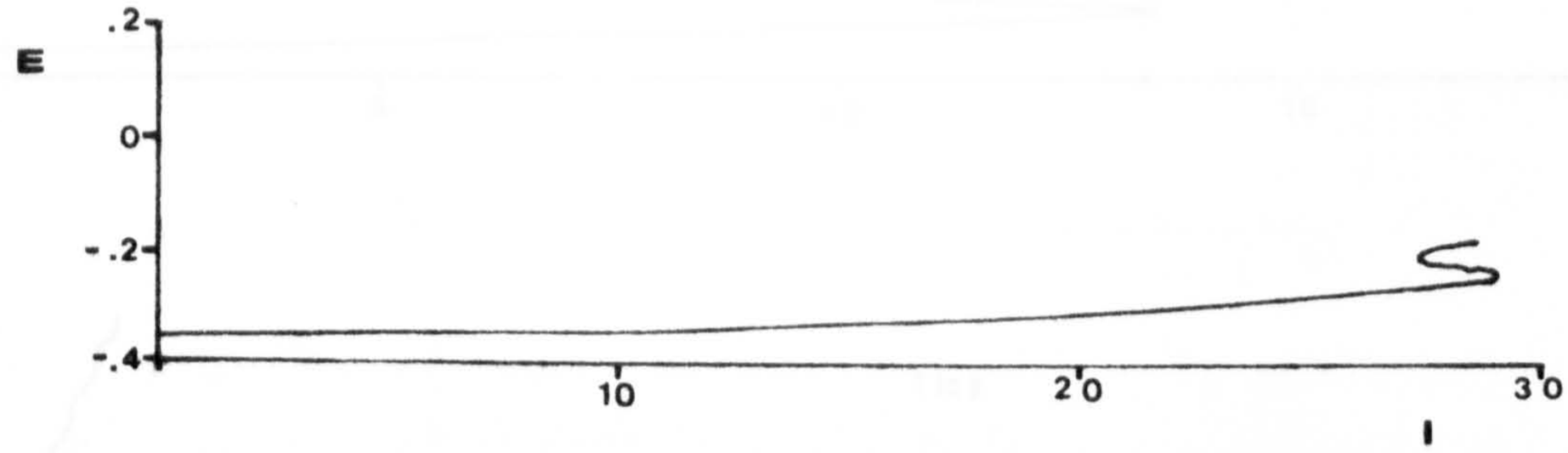

Fig. 26a. No passivation obtained due to leakage through the main gasket of the electrode holder.

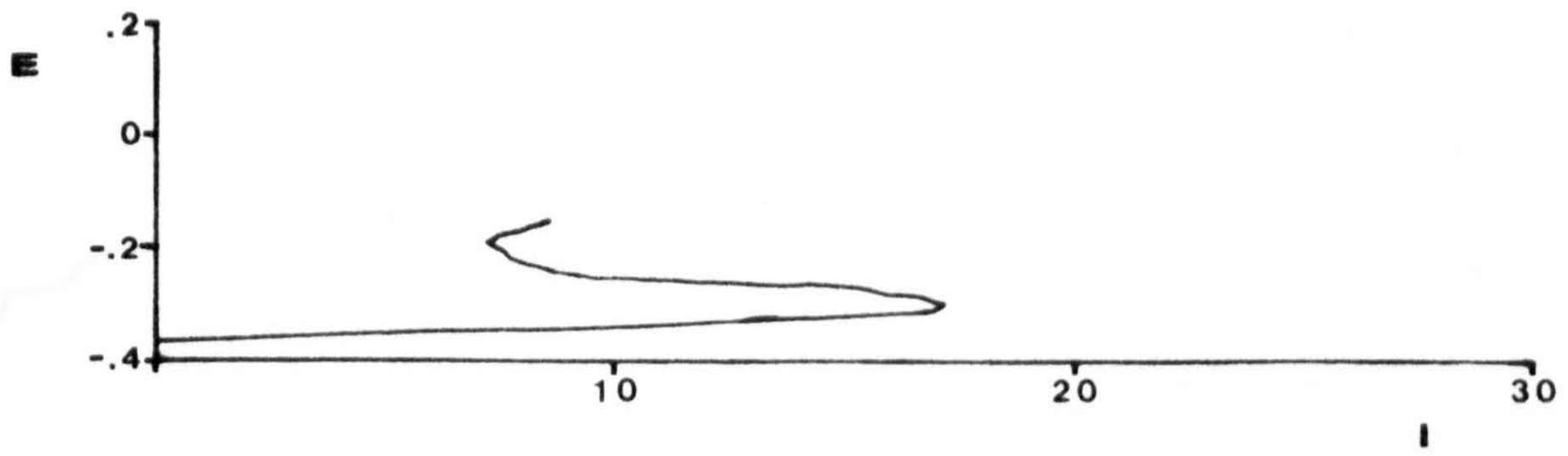

Fig. 26b. No passivation obtained due to leakage through the secondary gasket of the electrode holder.

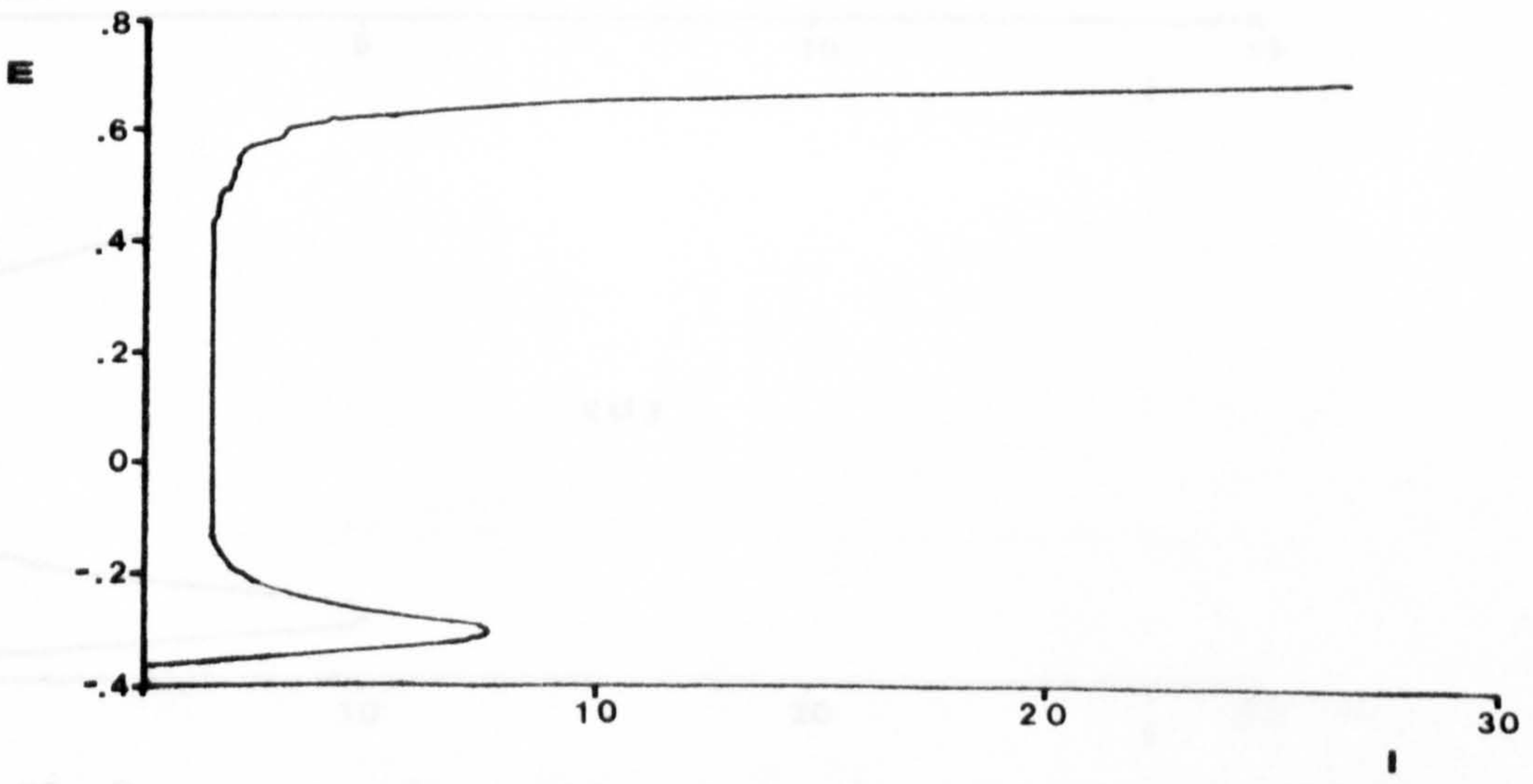

Fig. 26c. Expected E-i pattern obtained.

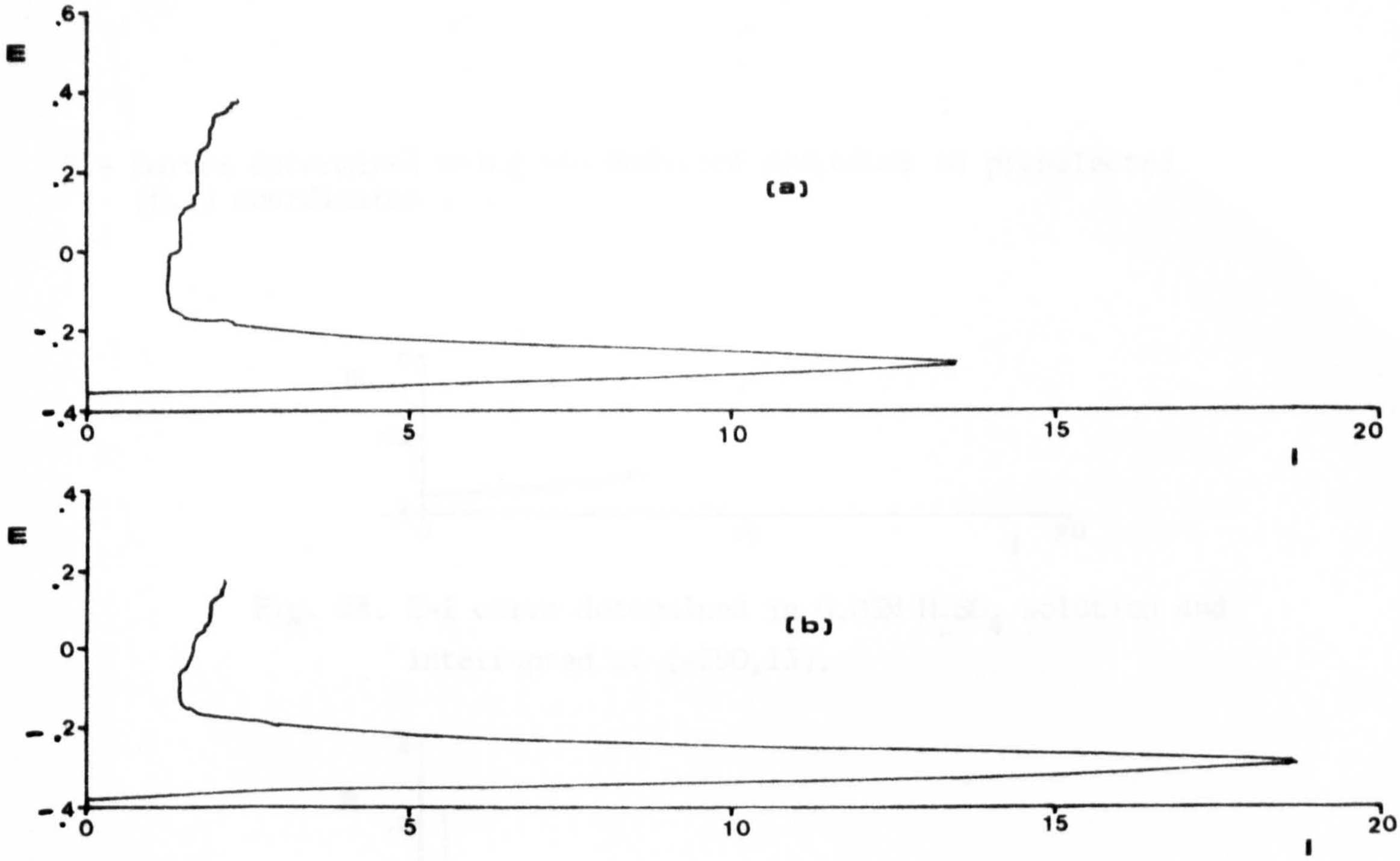

Fig. 27. Recurrence of unstable passivation, (a) and (b), overcome by replacing the PTFE secondary gasket with a rubber one, (c), expected E-i pattern which is reproducible, (c) and (d).

3.- Curves determined using the modified procedure to preselected (E,i) coordinates .

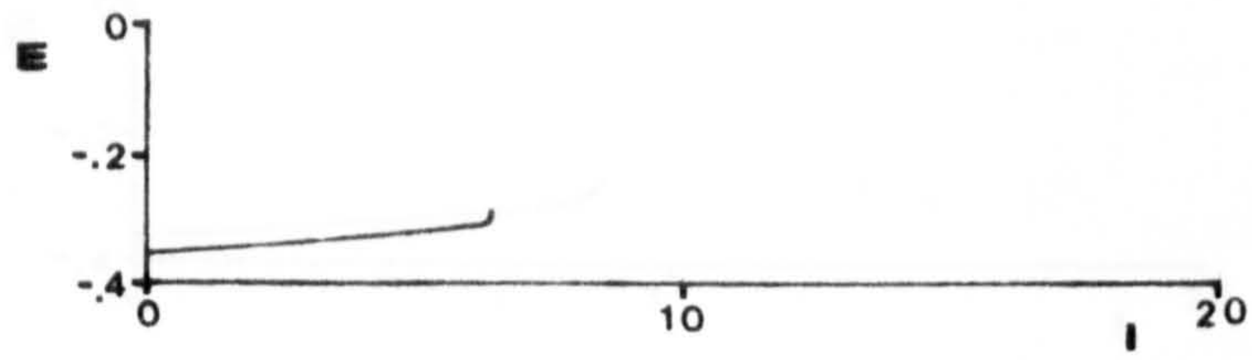

Fig. 28. E-i curve determined in 0.05M H_2SO_4 solution and interrupted at (-290,13).

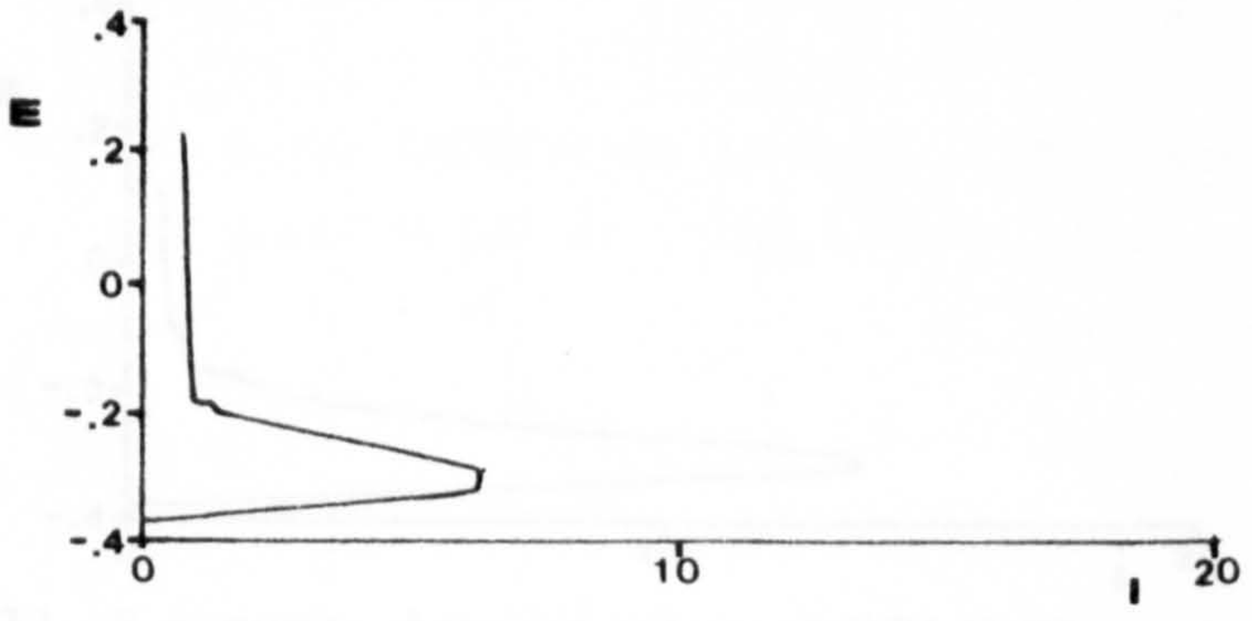

Fig. 29. E-i curve determined in 0.05M H_2SO_4 solution and interrupted at(230,1.5).

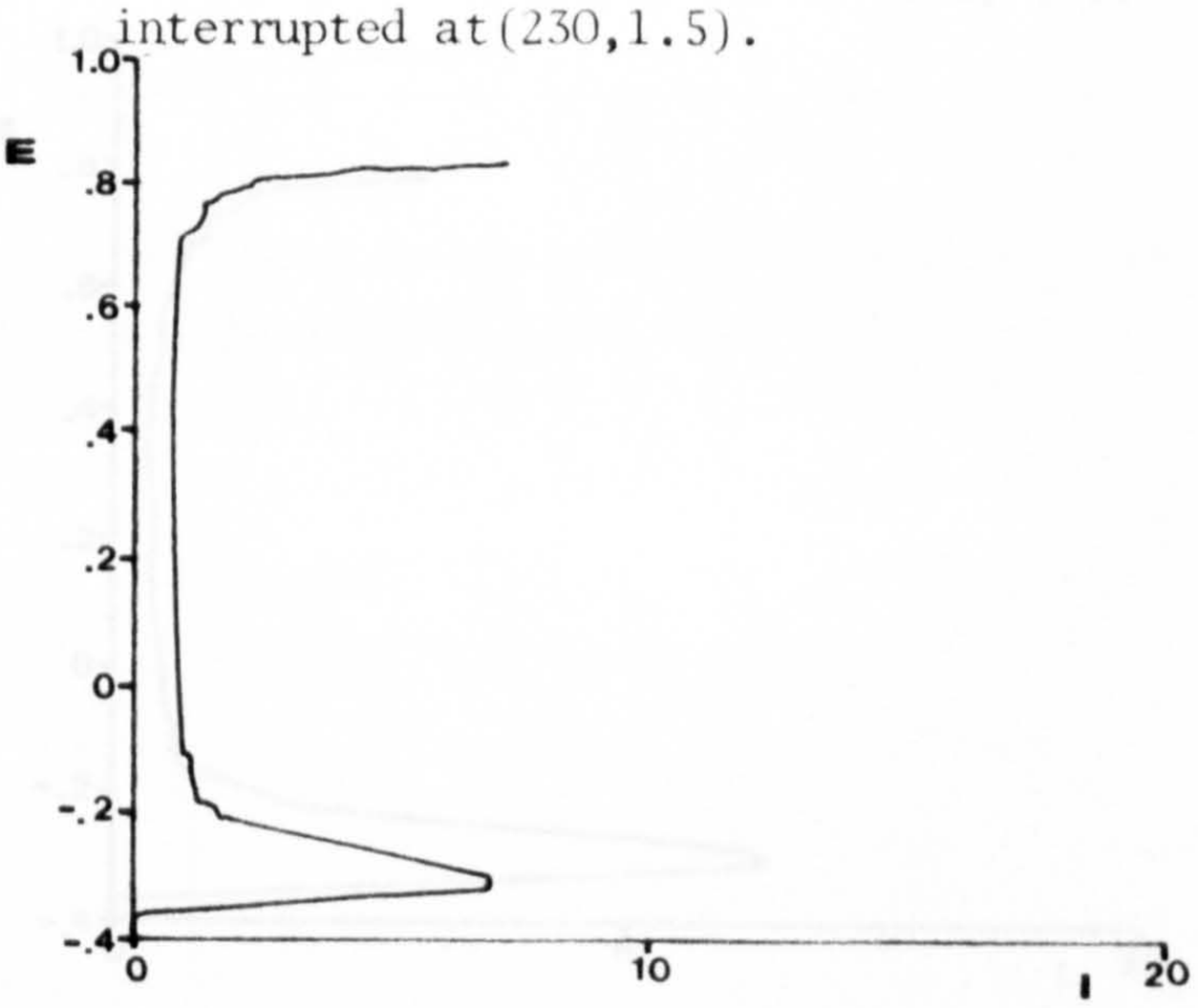

Fig. 30. E-i curve determined in 0.05M H_2SO_4 solution and interrupted at (860,15).

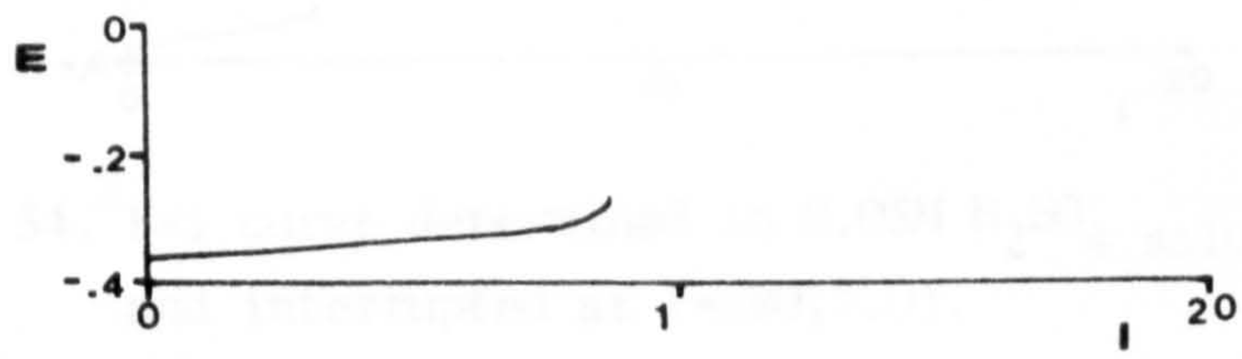

Fig. 31. E-i curve determined in 0.05M H_2SO_4 + 0.01 M NaCl solution and interrupted at (-284,17).

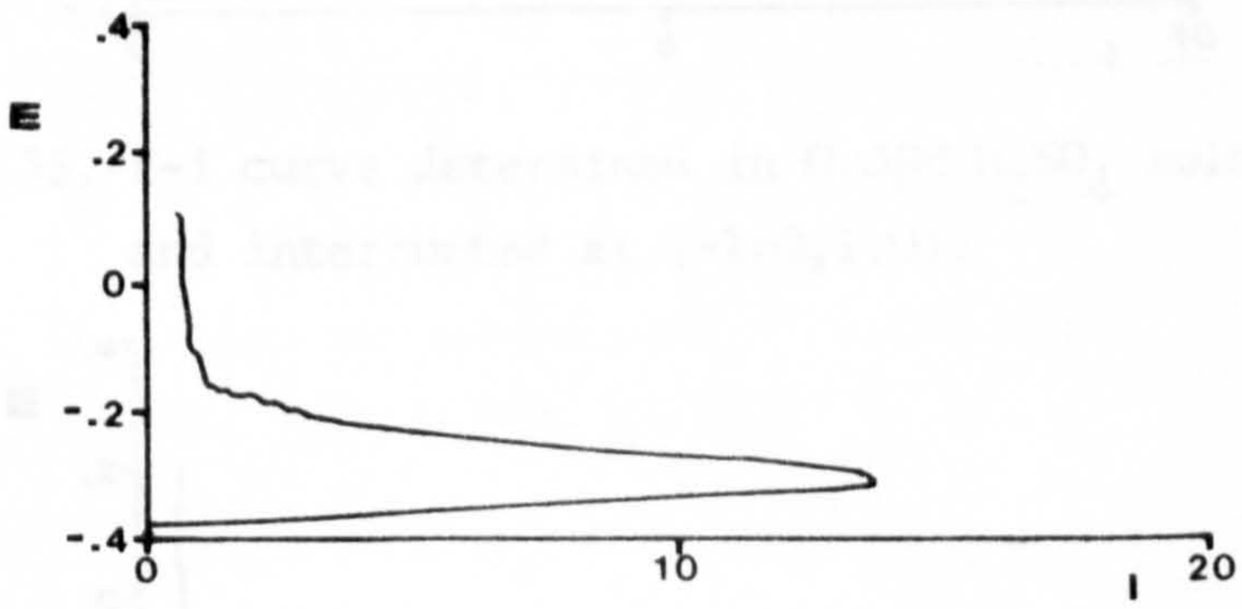

Fig. 32. E-i curve determined in 0.05M H_2SO_4 + 0.01M NaCl solution and interrupted at (100,1.5).

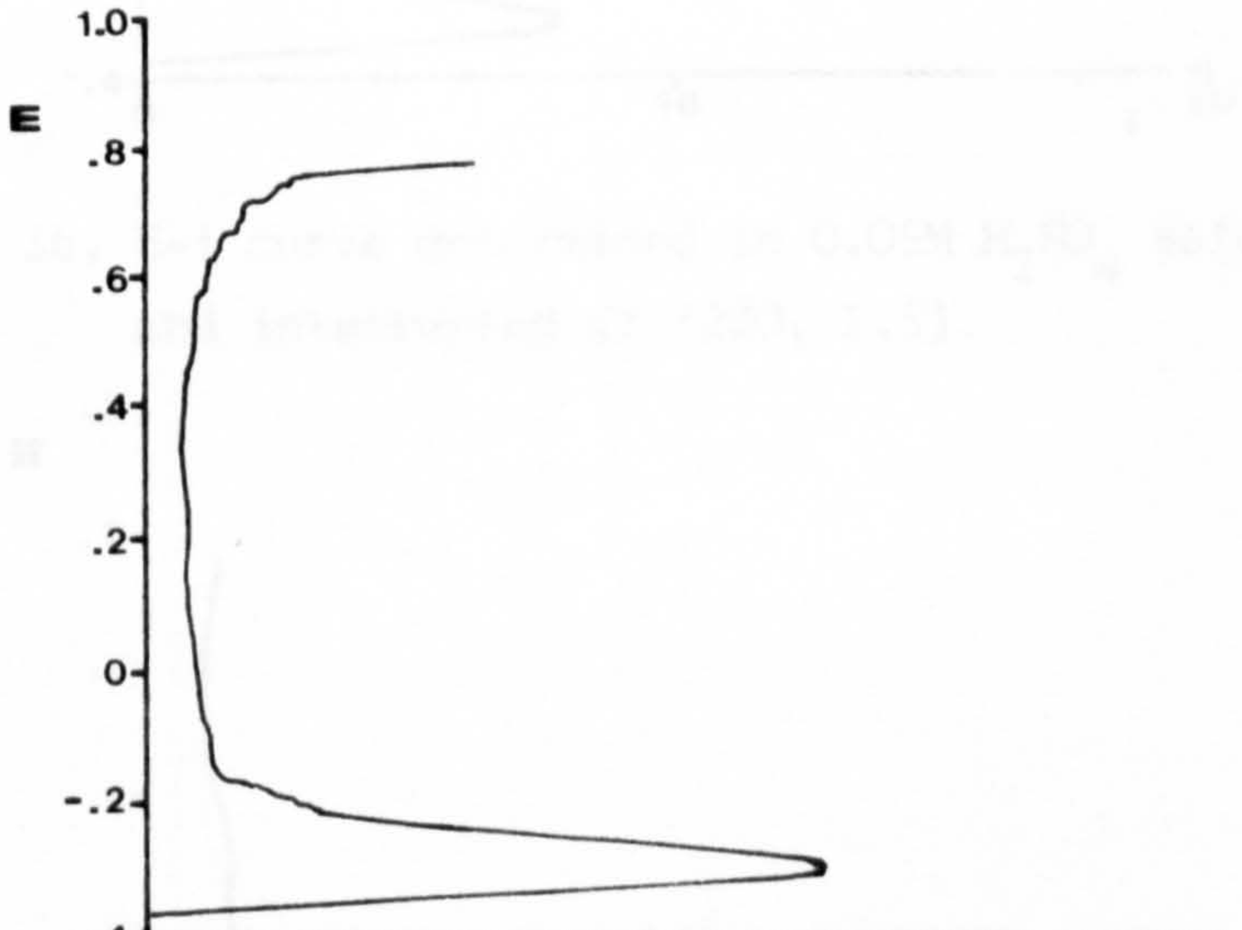

Fig. 33. E-i curve determined in 0.05M H_2SO_4 + 0.01M NaCl solution and interrupted at (768,12).

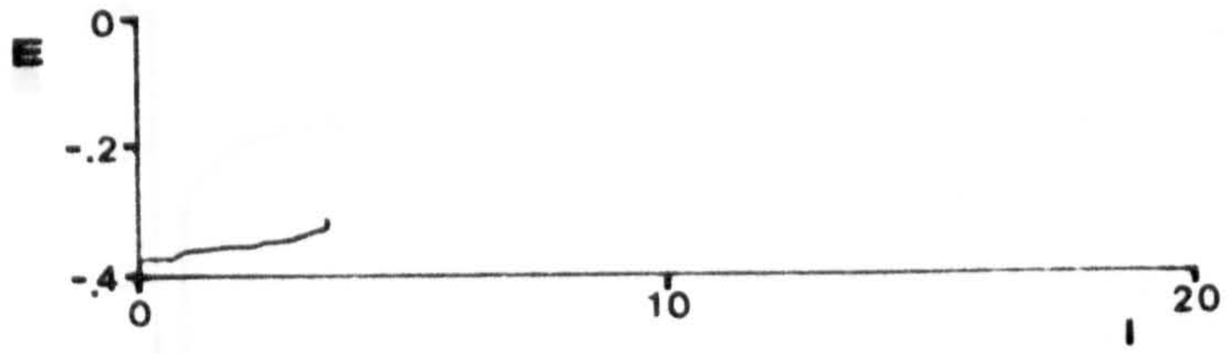

Fig. 34. E-i curve determined in 0.05M H_2SO_4 solution and interrupted at (-280,7.0).

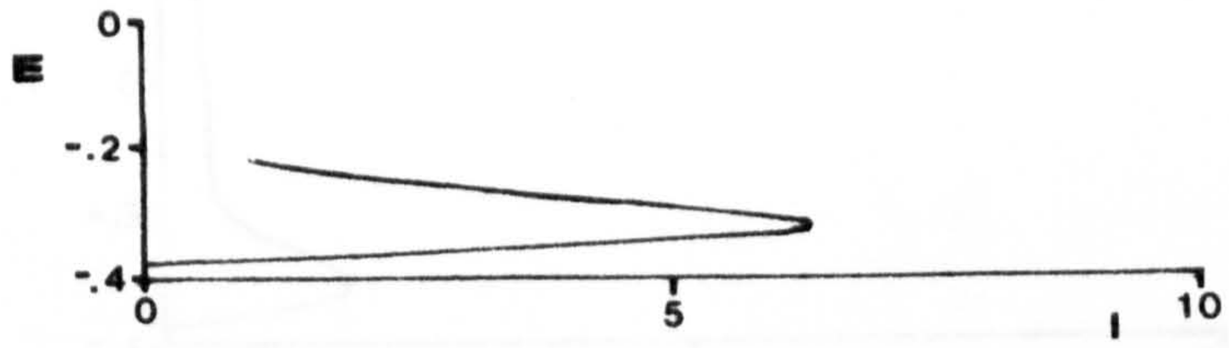

Fig. 35. E-i curve determined in 0.05M H_2SO_4 solution and interrupted at (-160,1.0).

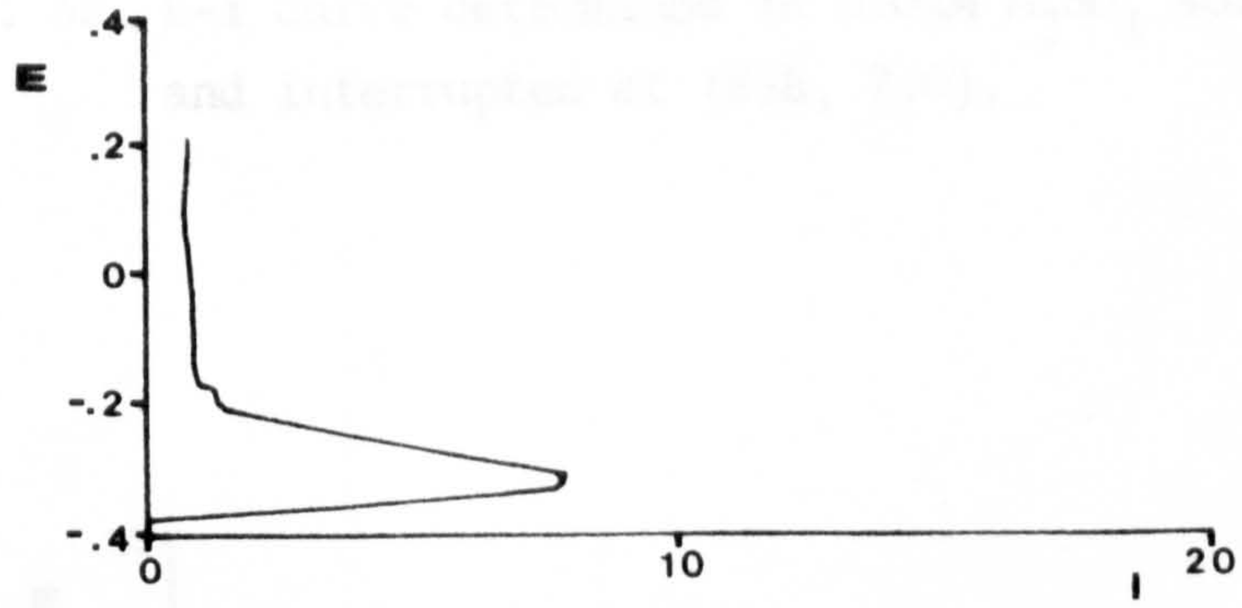

Fig. 36. E-i curve determined in 0.05M H_2SO_4 solution and interrupted at (220, 1.5).

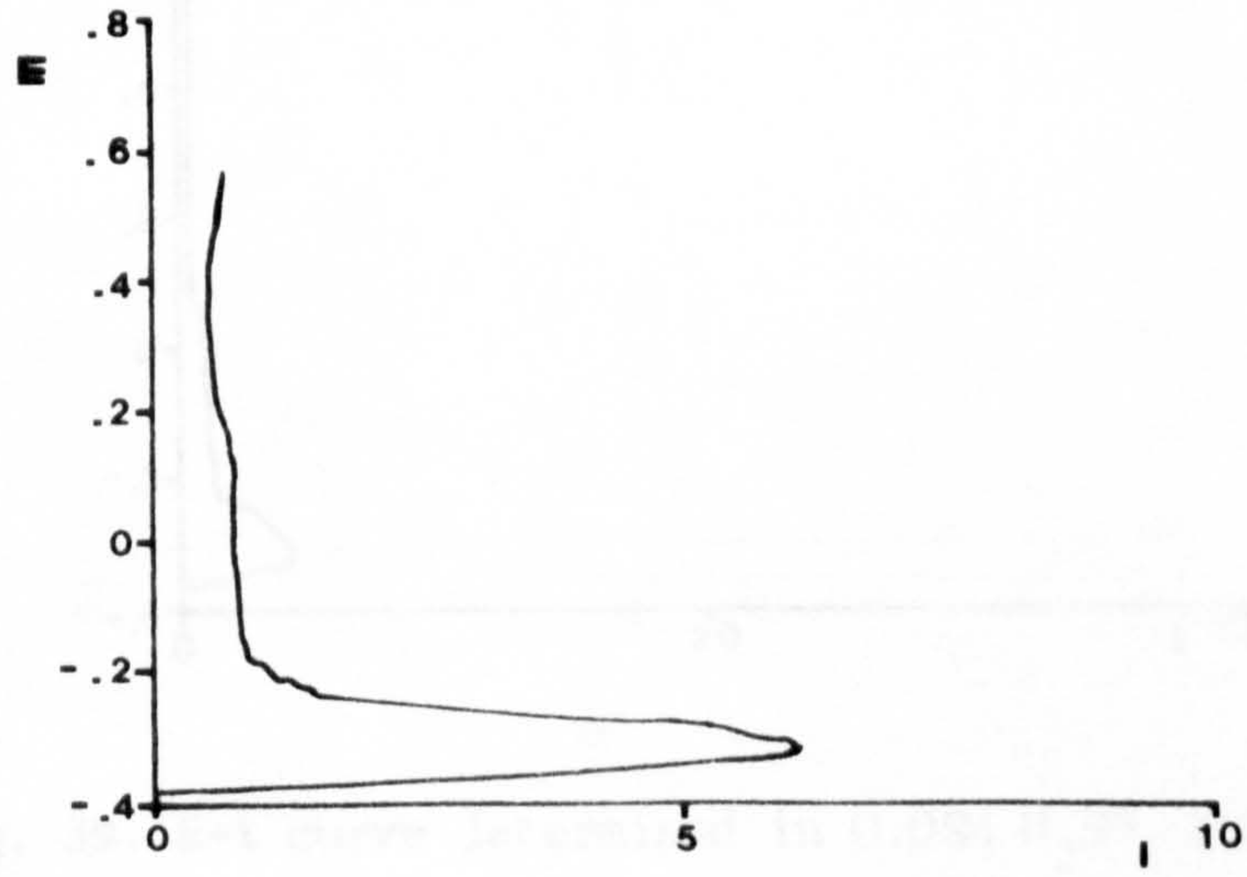

Fig. 37. E-i curve determined in 0.05M H_2SO_4 solution and interrupted at (644,3.0).

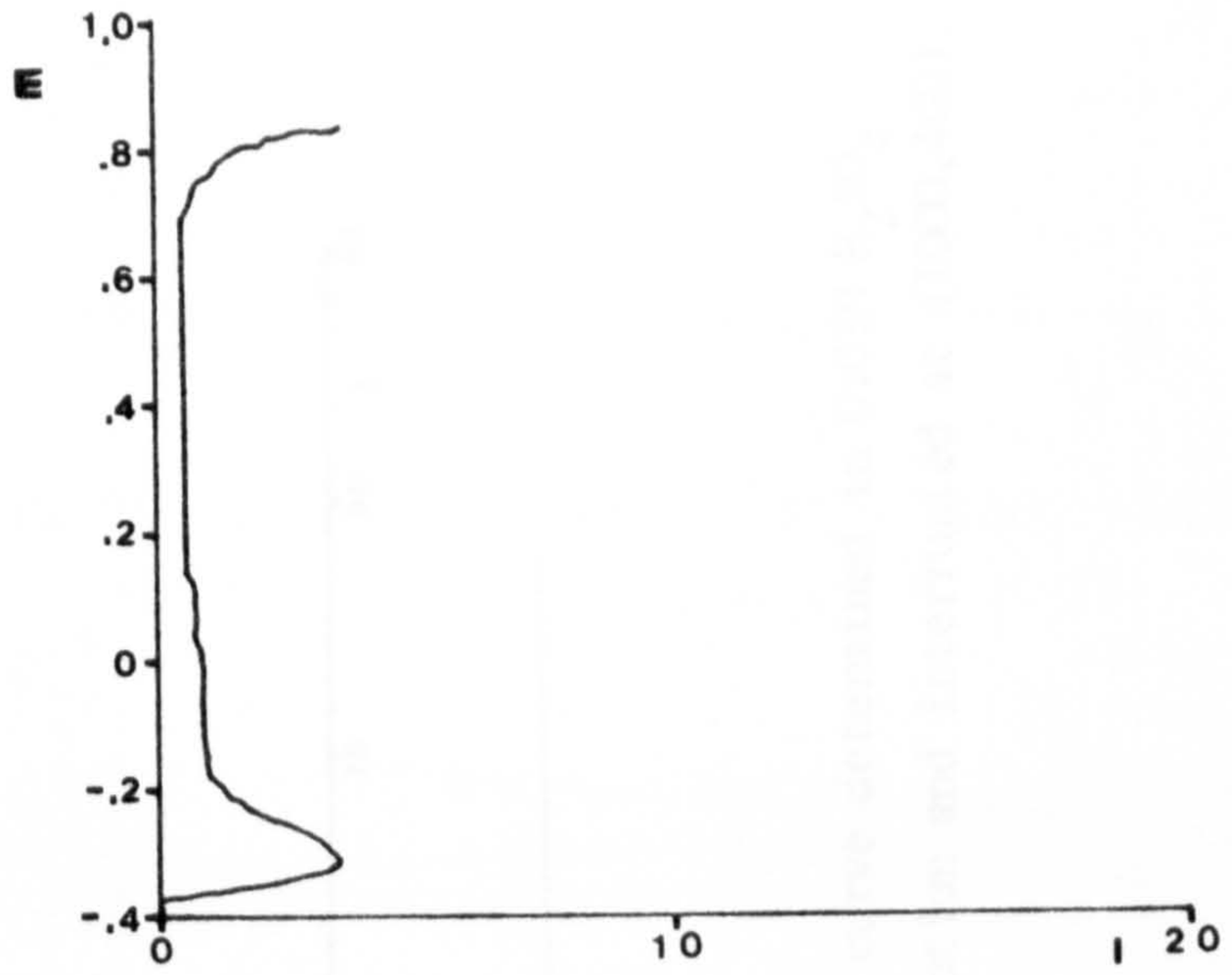

Fig. 38. E-i curve determined in 0.05M H_2SO_4 solution and interrupted at (858, 7.0).

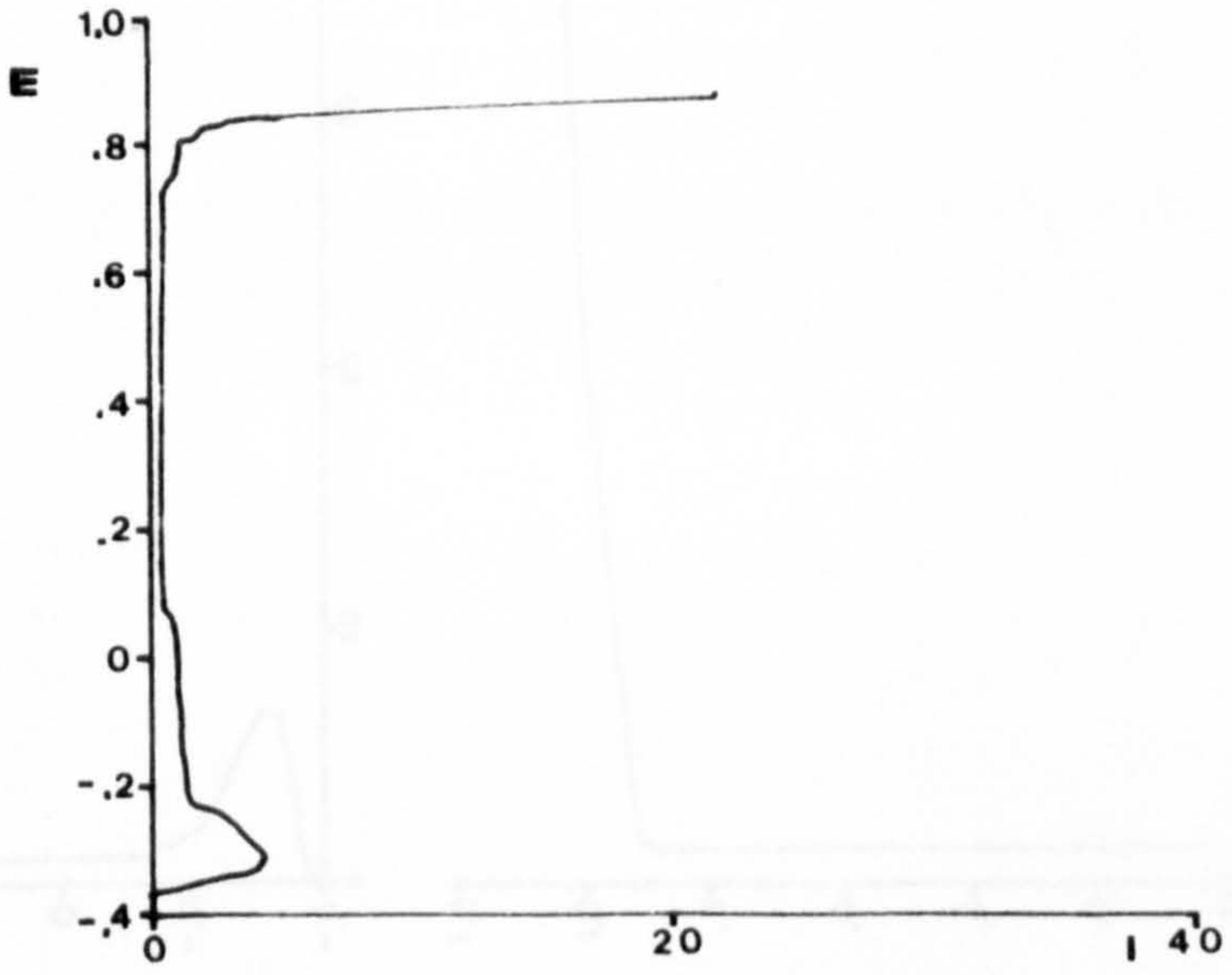

Fig. 39. E-i curve determined in 0.05M H_2SO_4 solution and interrupted at (898,44).

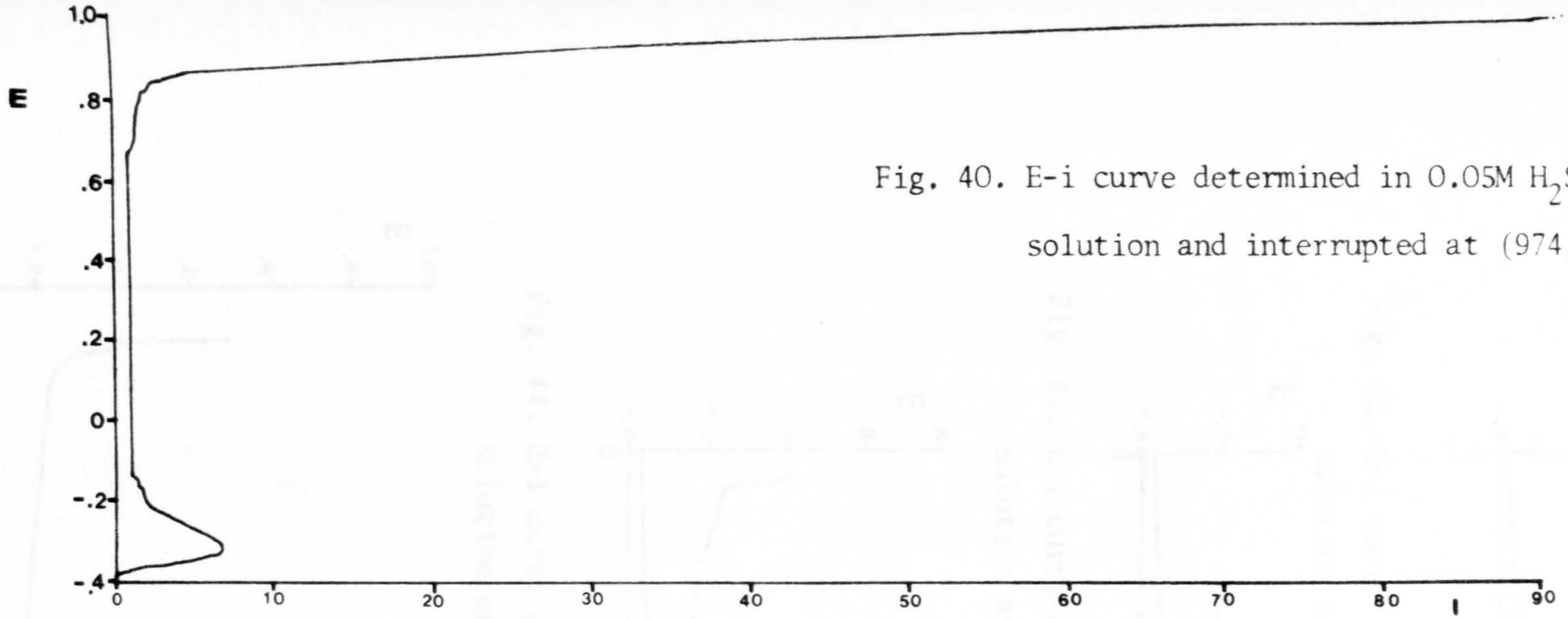

Fig. 40. E-i curve determined in 0.05M H_2SO_4 solution and interrupted at (974,220).

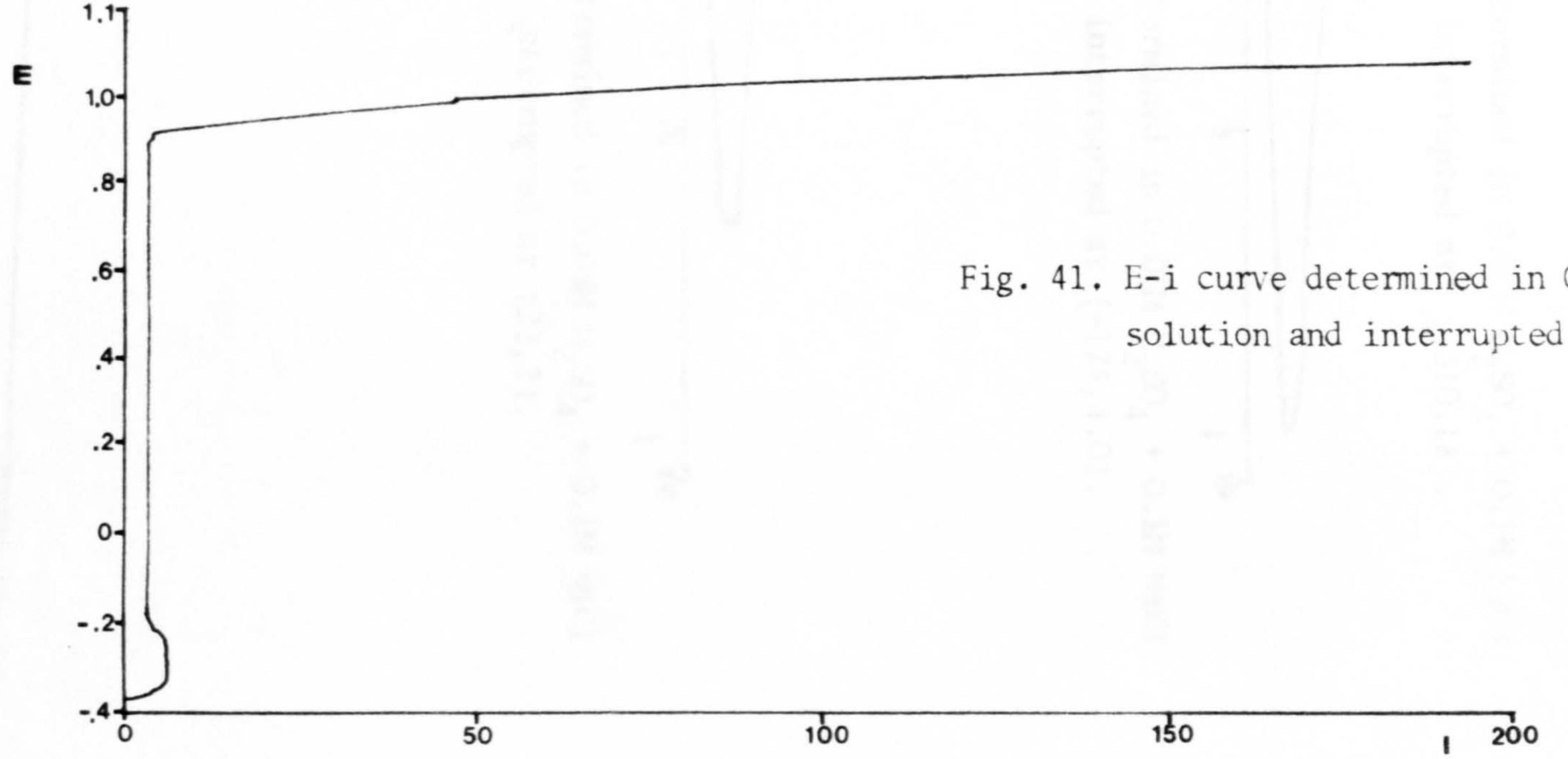

Fig. 41. E-i curve determined in 0.05M H_2SO_4 solution and interrupted at (1000,400).

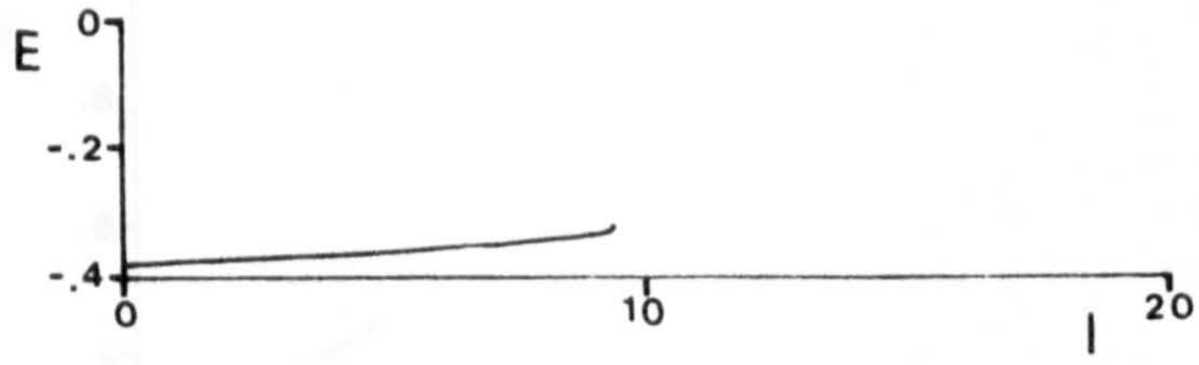

Fig. 42. E-i curve determined in 0.05M H_2SO_4 + 0.1M NaCl solution and interrupted at (-310,18).

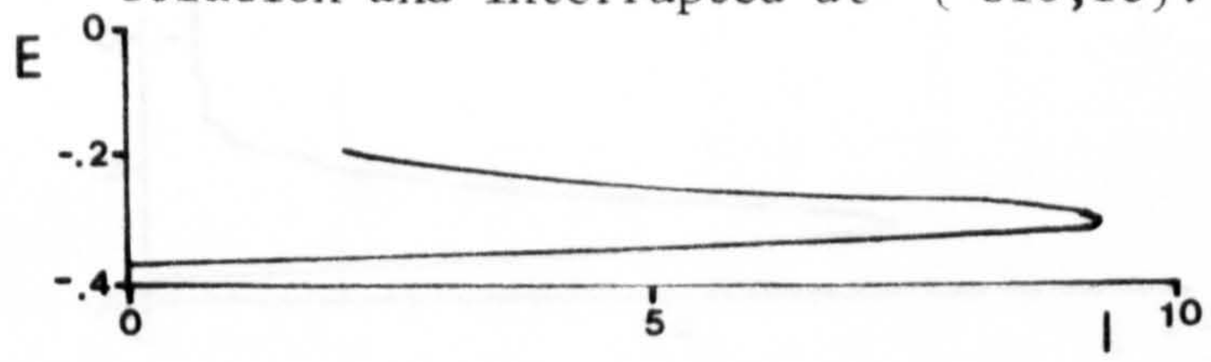

Fig. 43. E-i curve determined in 0.05M H_2SO_4 + 0.1M NaCl solution and interrupted at (-174,4.0).

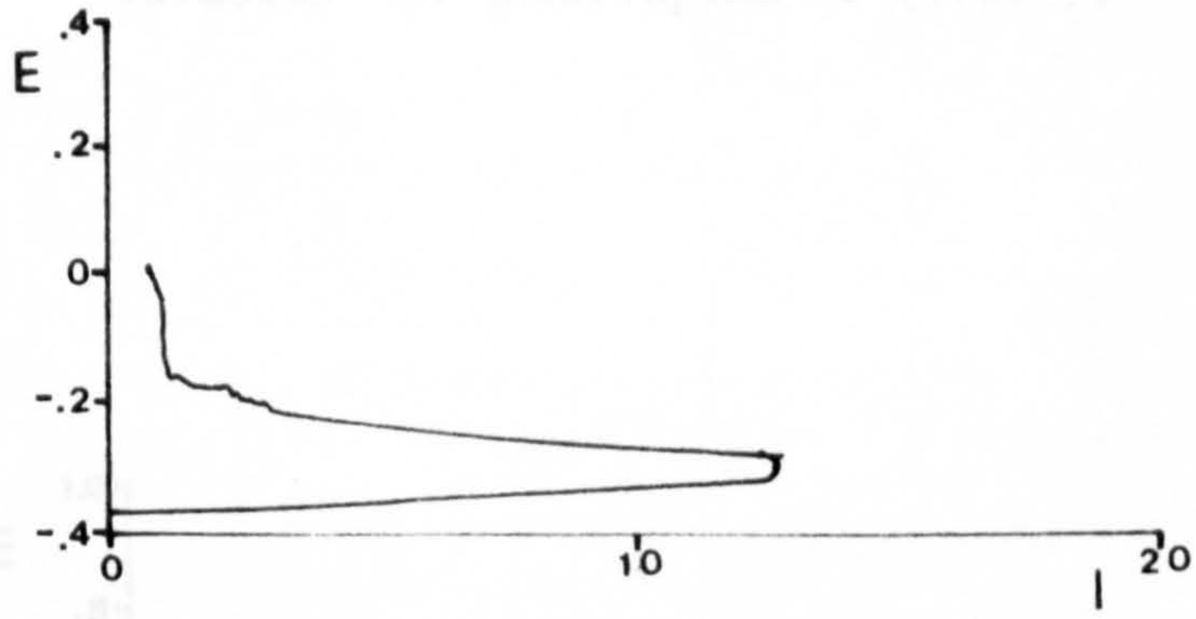

Fig. 44. E-i curve determined in 0.05M H_2SO_4 + 0.1M NaCl solution and interrupted at (22,2).

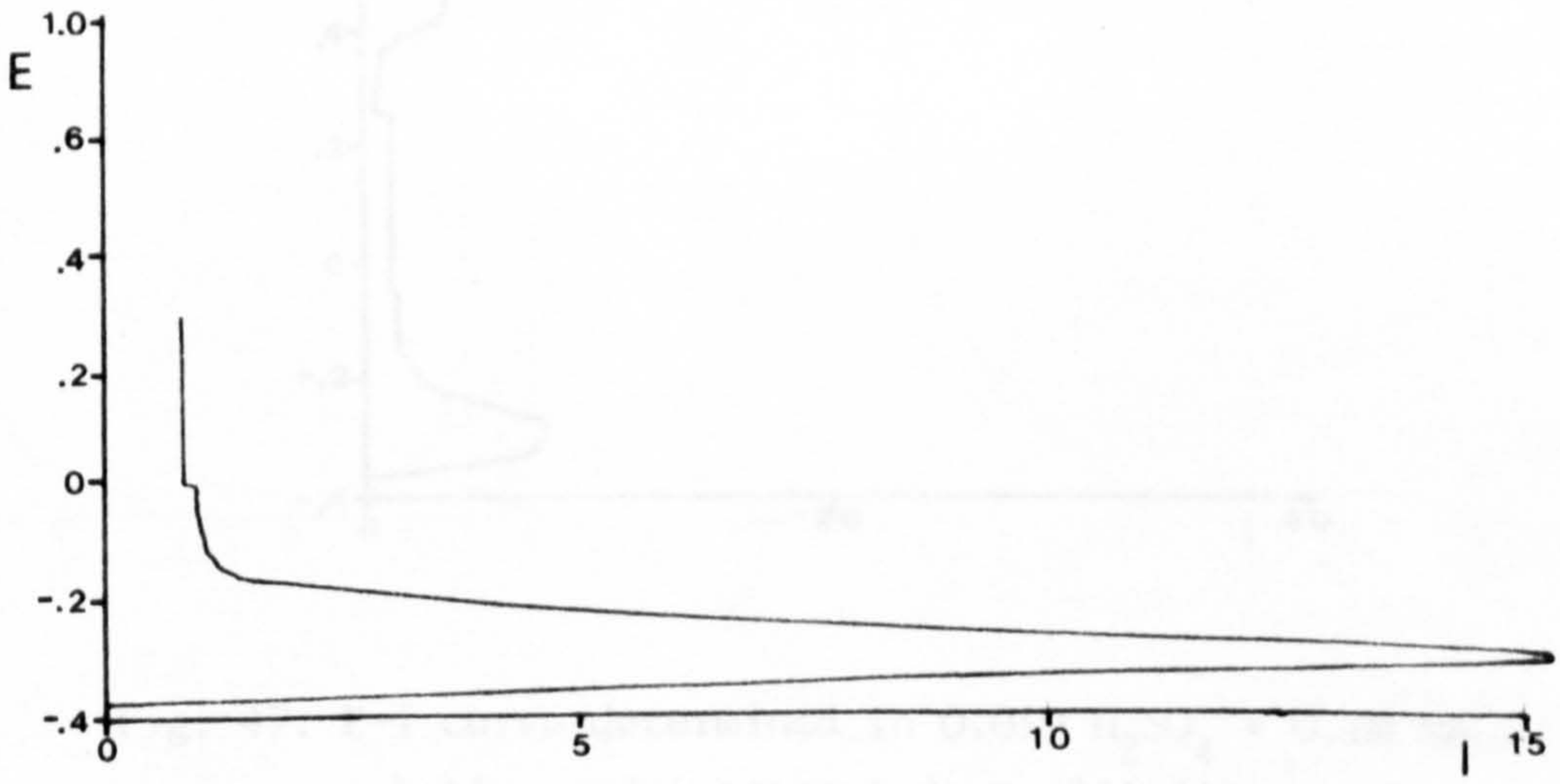

Fig. 45. E-i curve determined in 0.05M H_2SO_4 + 0.1M NaCl solution and interrupted at (314,3.0).

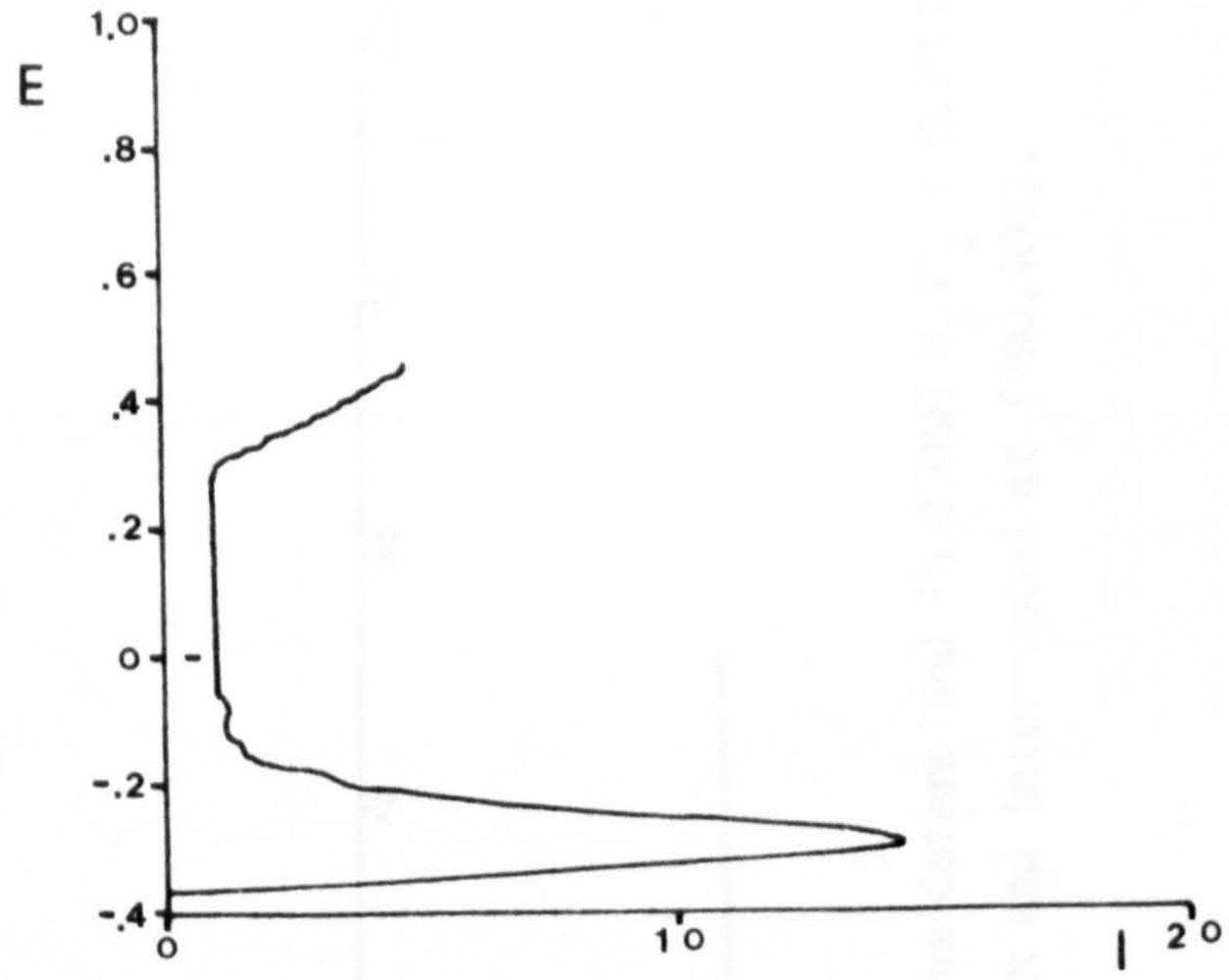

Fig. 46. E-i curve determined in 0.05M H_2SO_4 + 0.1M NaCl solution and interrupted at (478.9).

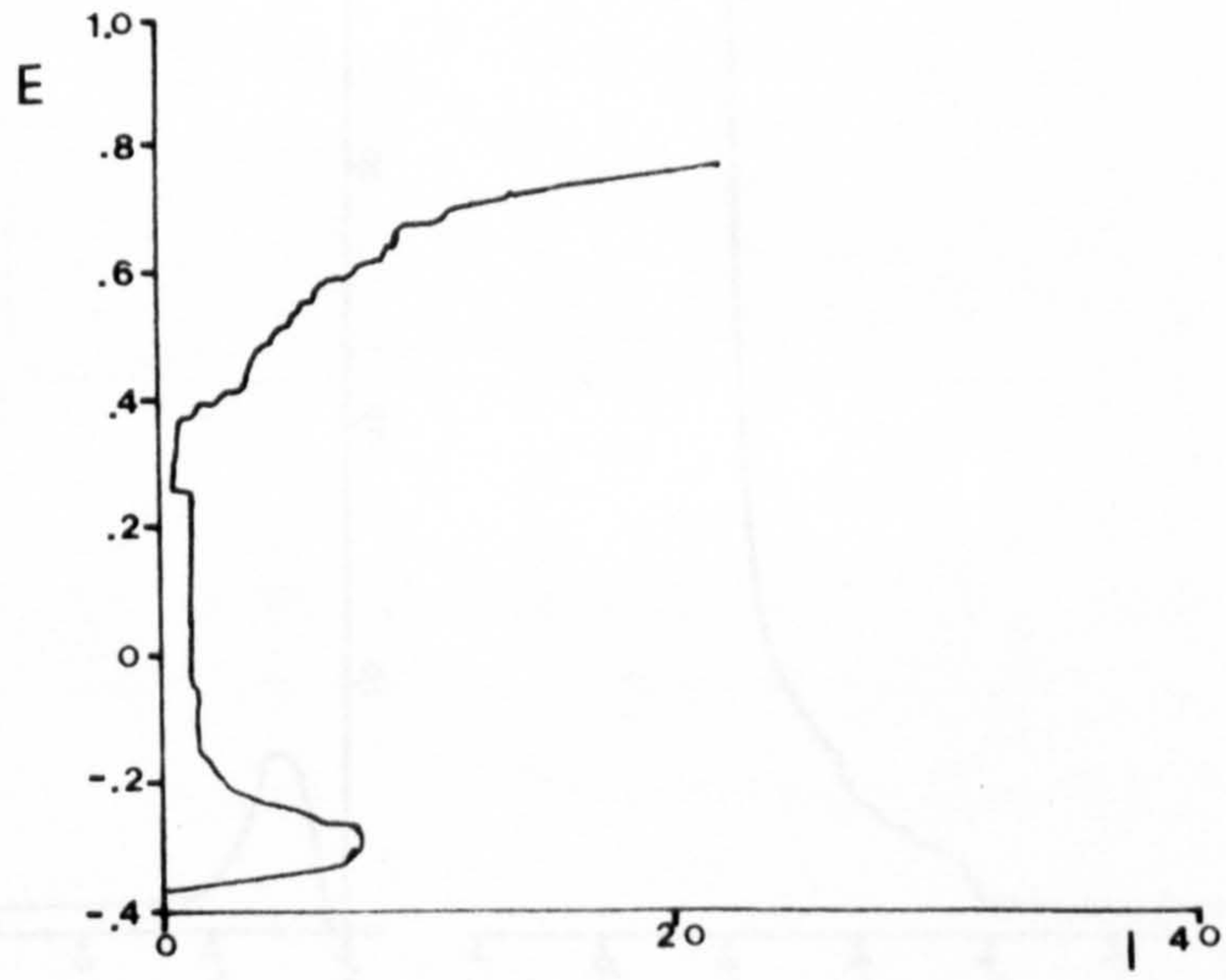

Fig. 47. E-i curve determined in 0.05M H_2SO_4 + 0.1M NaCl solution and interrupted at (734,44),

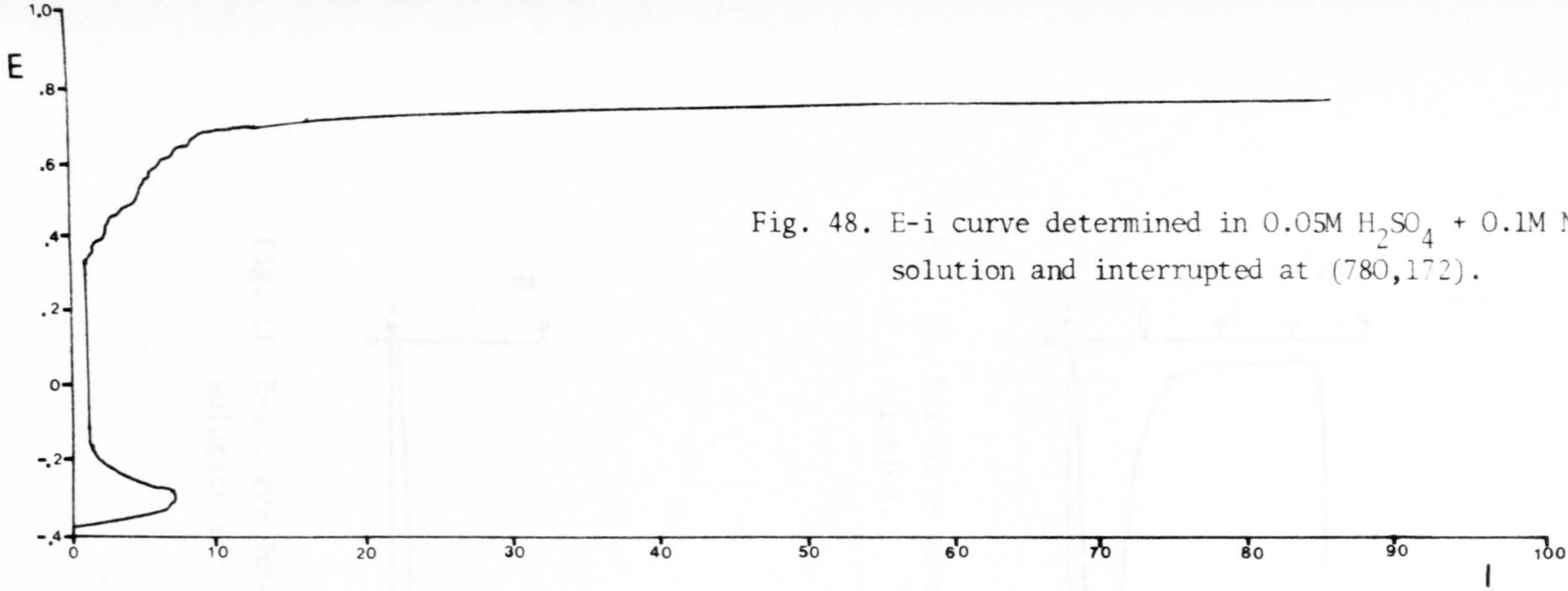

Fig. 48. E-i curve determined in 0.05M H_2SO_4 + 0.1M NaCl solution and interrupted at (780,172).

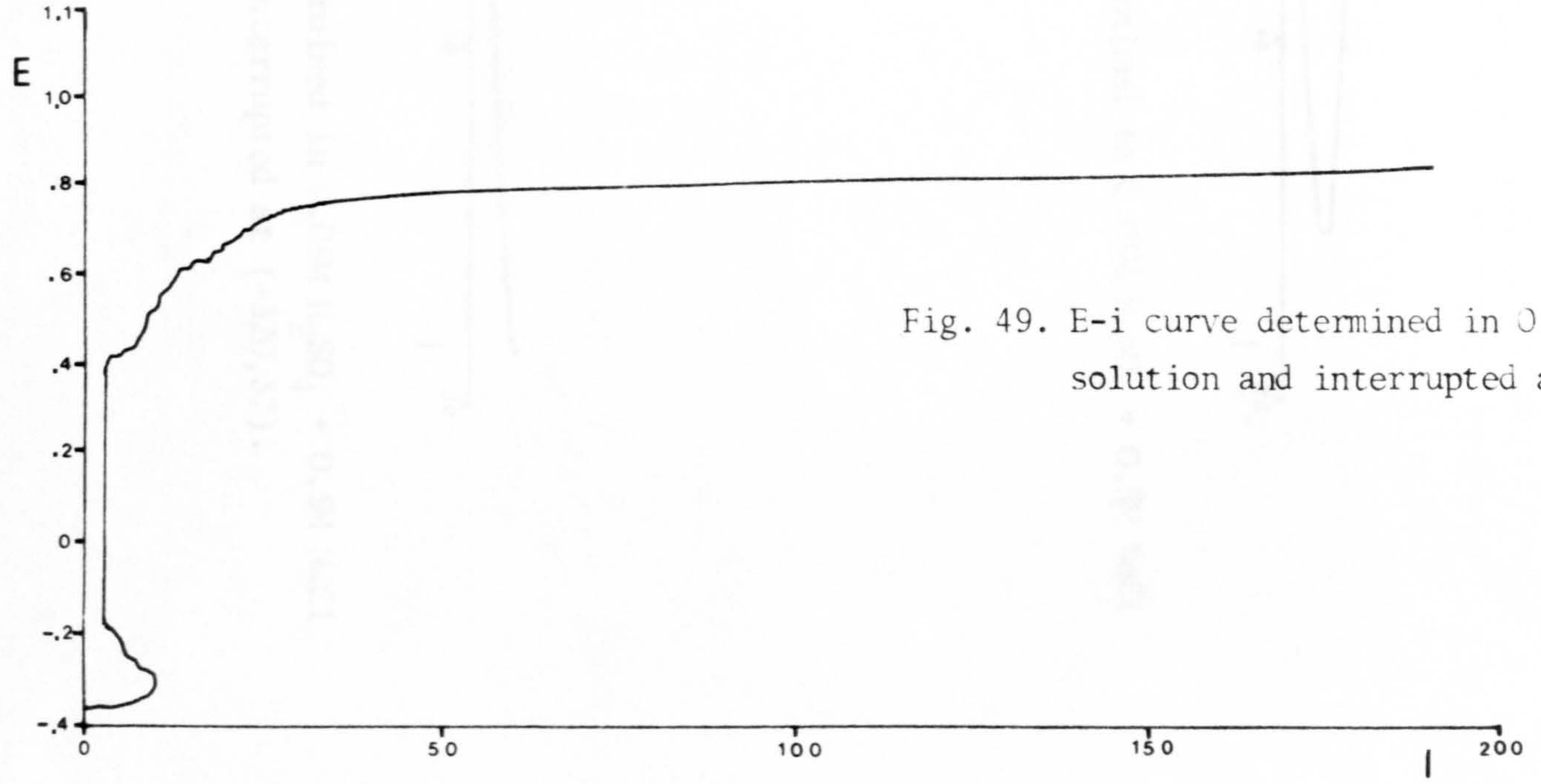

Fig. 49. E-i curve determined in 0.05M H_2SO_4 + 0.1M NaCl solution and interrupted at (790,400).

4.- Curves determined in higher Cl^- ion concentration.

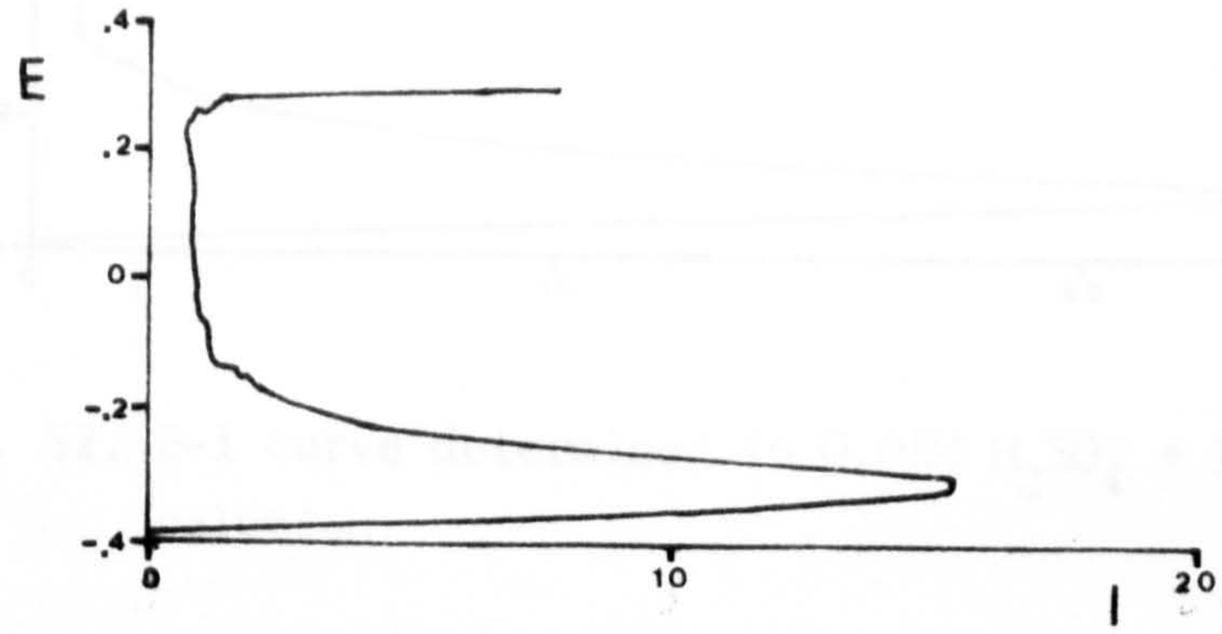

Fig. 50. E-i curve determined in 0.05M H_2SO_4 + 0.5M NaCl solution.

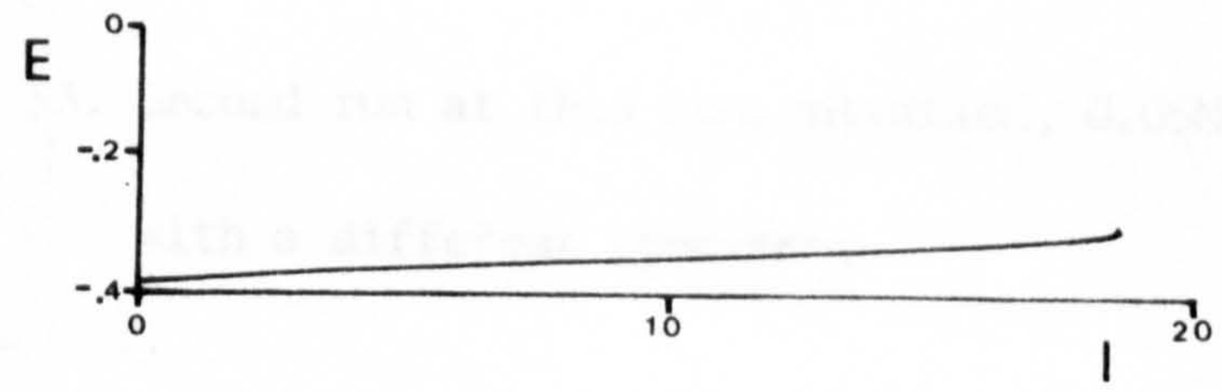

Fig. 51. E-i curve determined in 0.05M H_2SO_4 + 0.5M NaCl solution and interrupted at (-320,37).

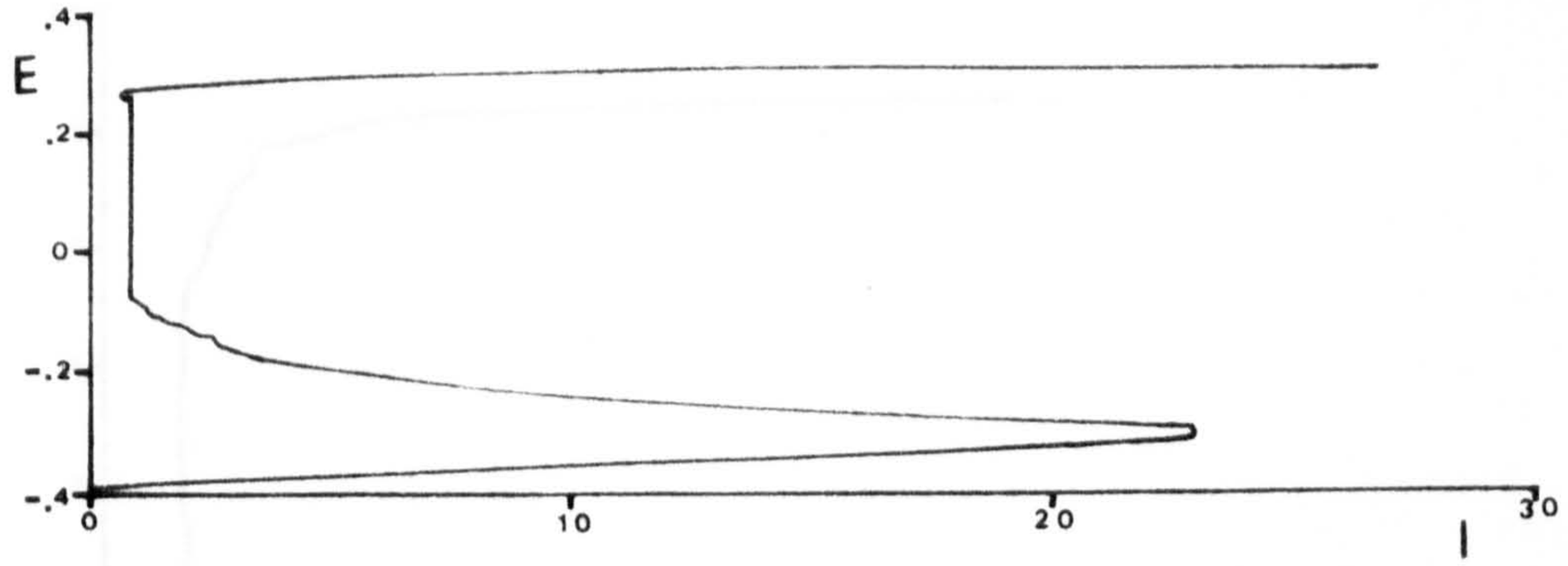

Fig. 52. E-i curve determined in 0.05M H_2SO_4 + 1.0M NaCl solution.

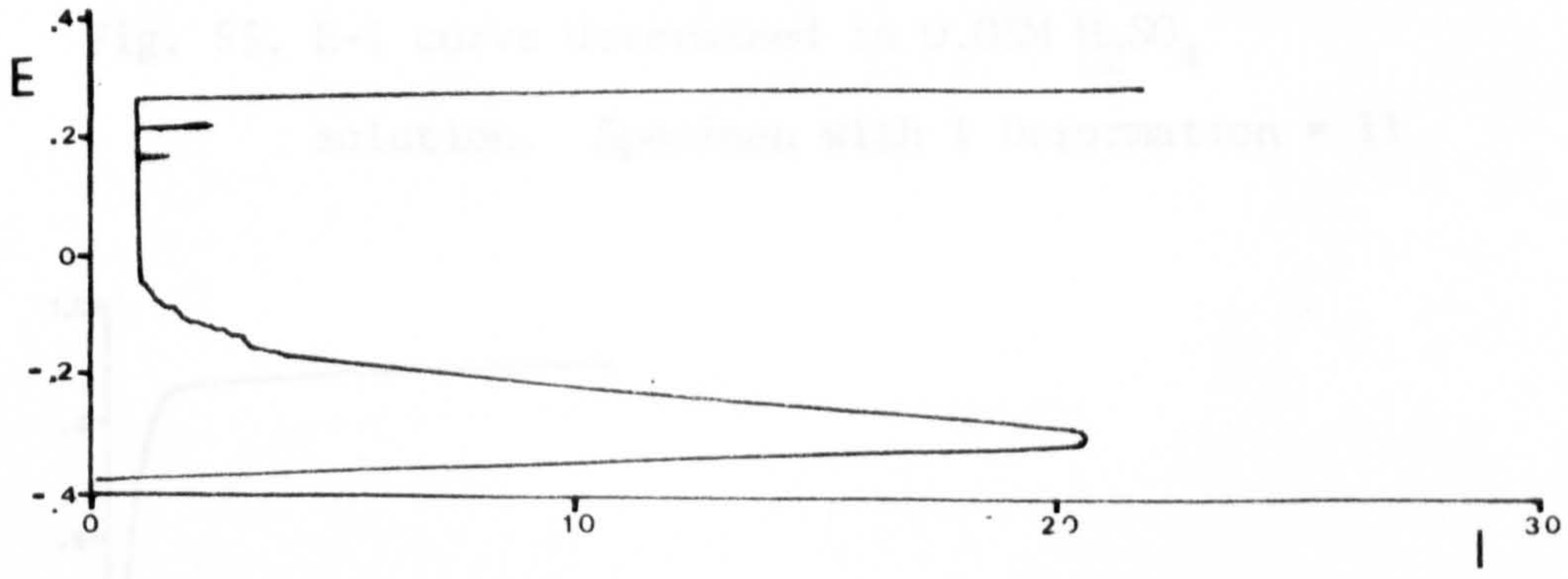

Fig. 53. Second run at this concentration, 0.05M H_2SO_4 + 1.0M NaCl, with a different specimen.

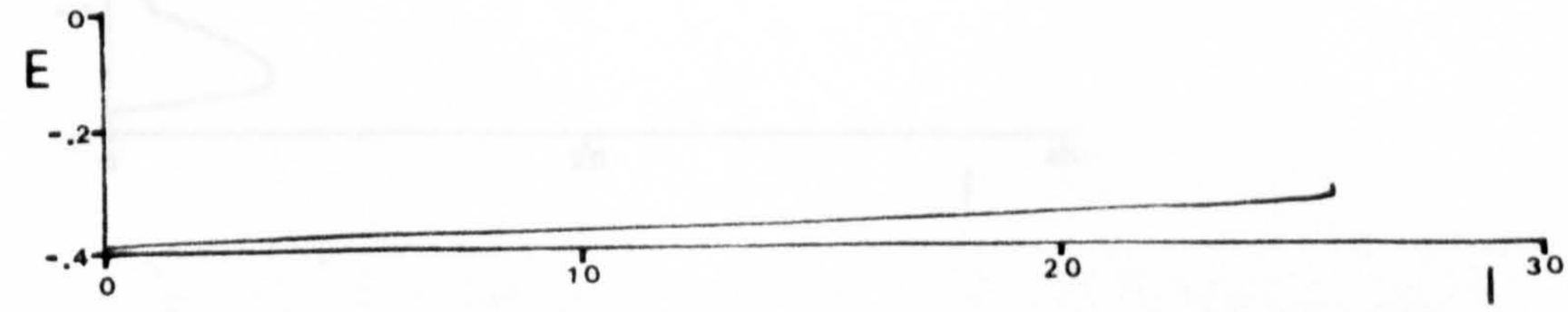

Fig. 54. E-i curve determined in 0.05M H_2SO_4 + 1.0M NaCl solution and interrupted at (-314,50).

5.- Curves determined with cold-worked specimens.

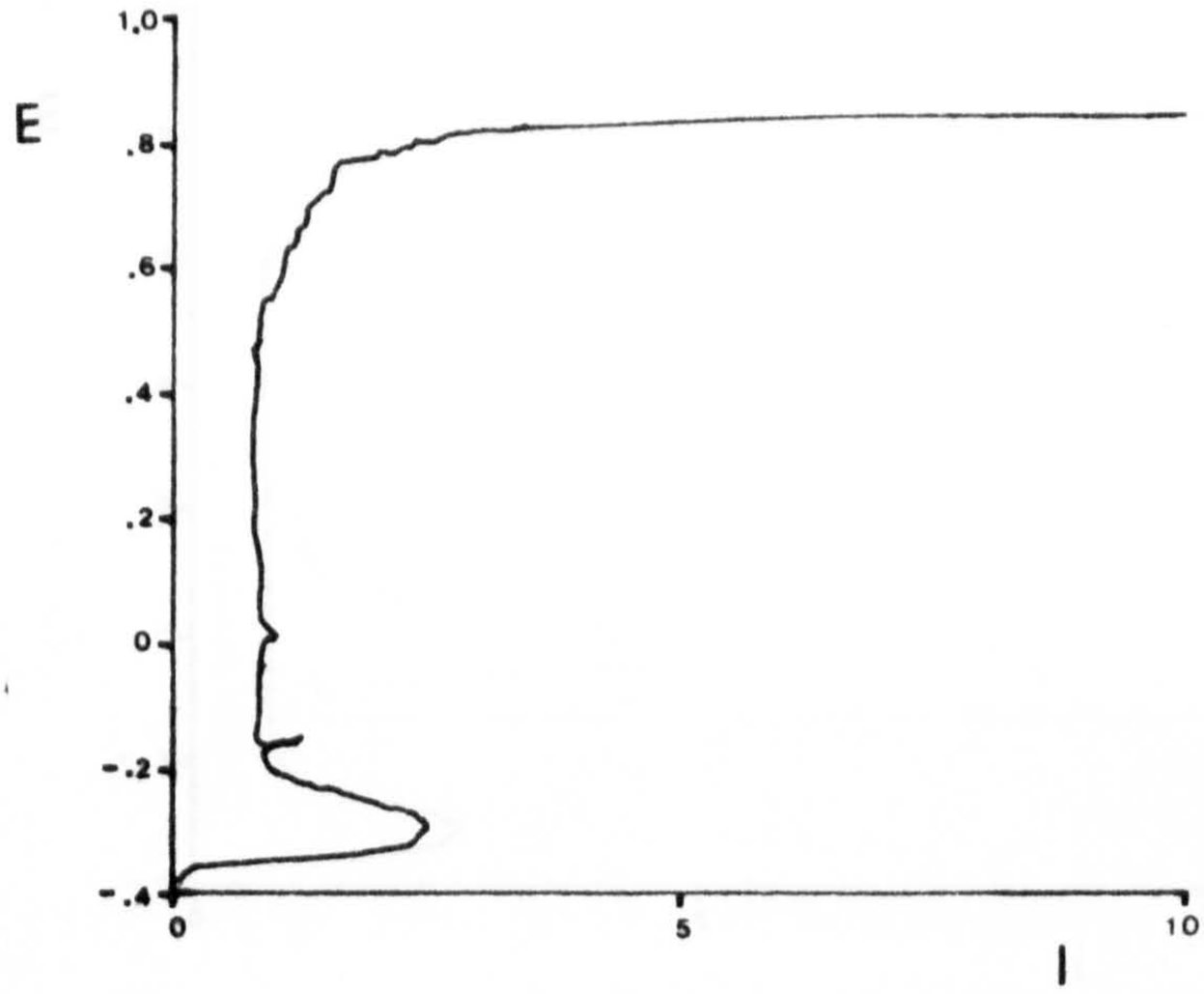

Fig. 55. E-i curve determined in 0.05M H_2SO_4 solution. Specimen with % Deformation = 11.

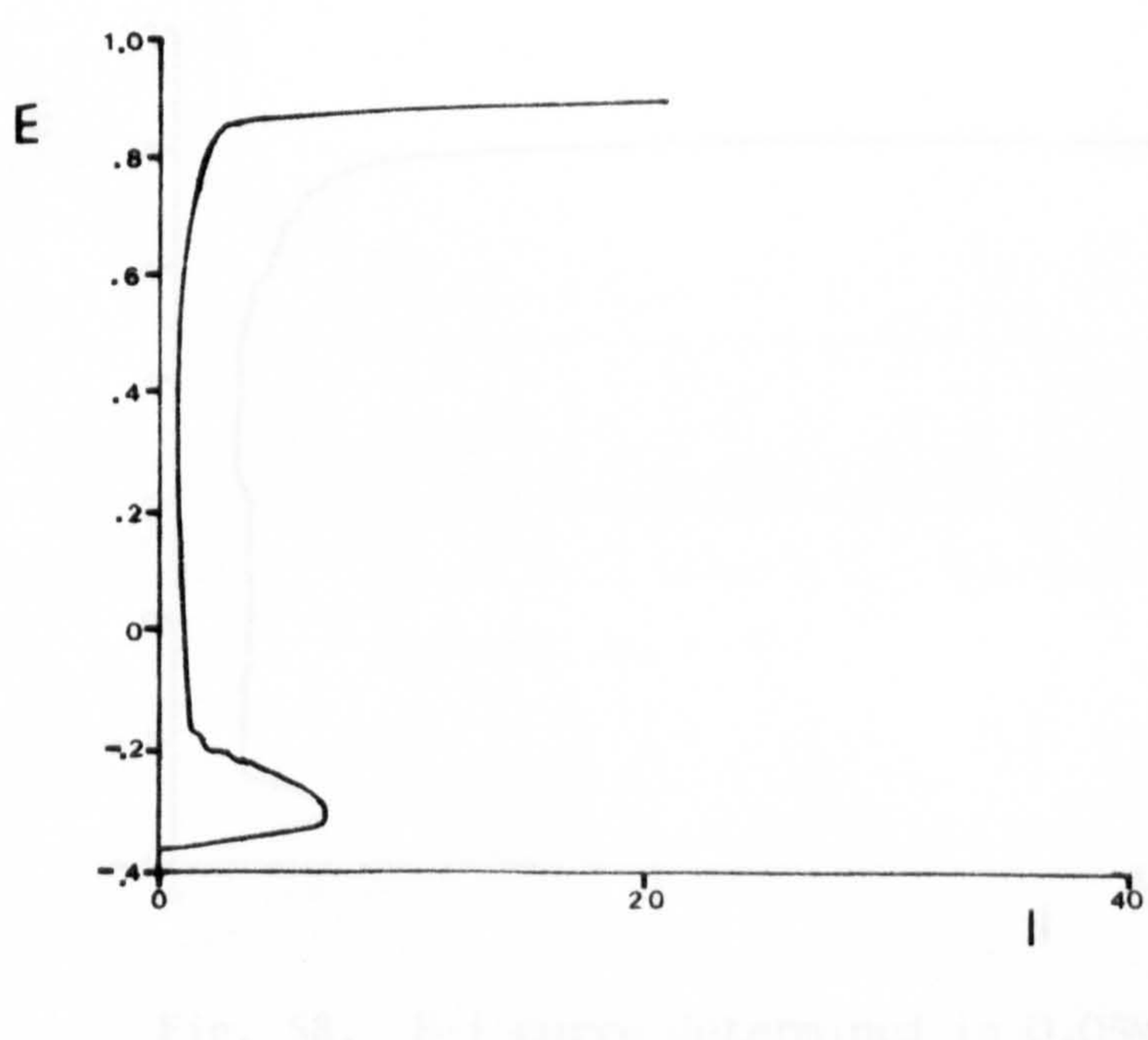

Fig. 56. E-i curve determined in 0.05M H_2SO_4 solution. Specimen with % Deformation = 15.

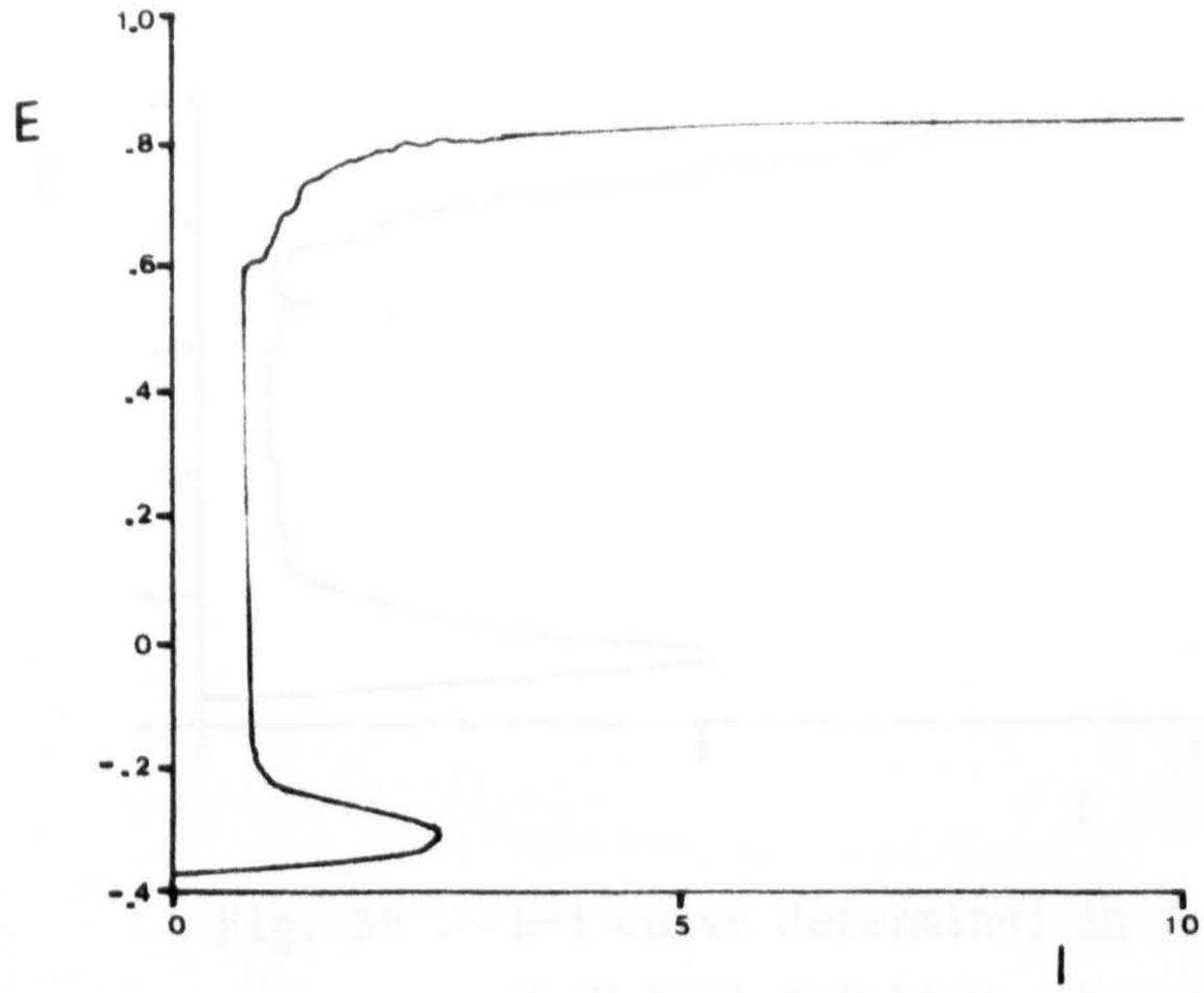

Fig.57. E-i curve determined in 0.05M H_2SO_4 solution.
Specimen with % Deformation = 19.

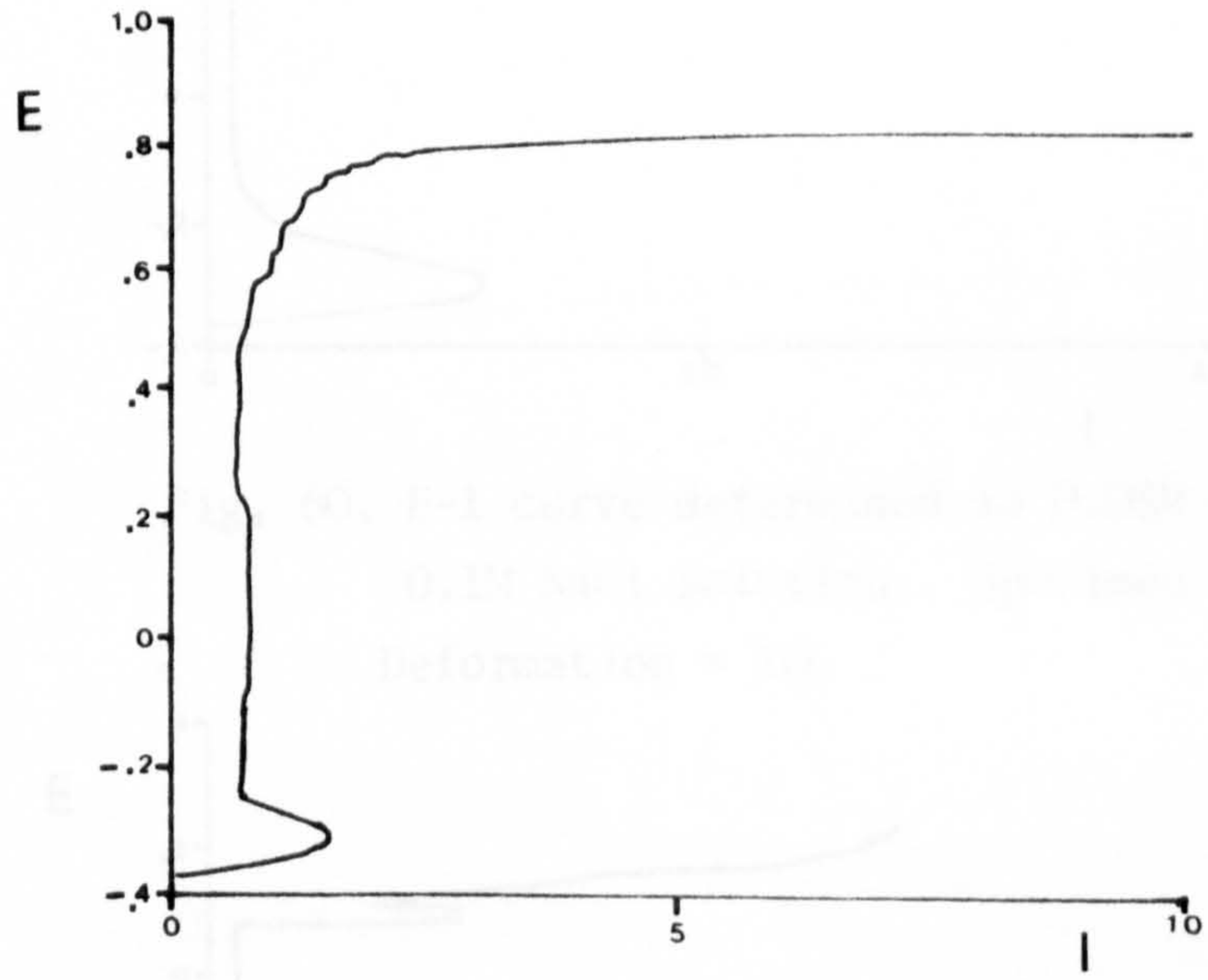

Fig. 58. E-i curve determined in 0.05M H_2SO_4 solution.
Specimen with % Deformation = 31.

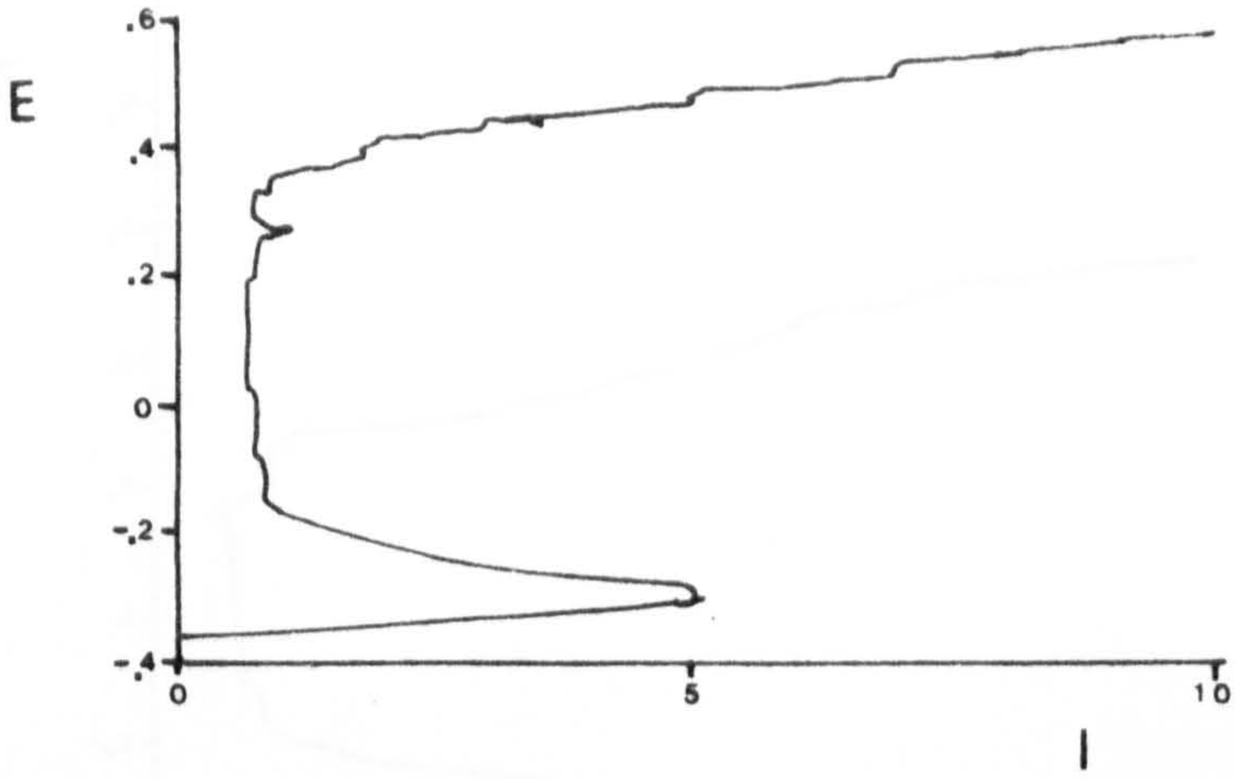

Fig. 59 . E-i curve determined in 0.05M H_2SO_4 + 0.1M NaCl solution. Specimen with % Deformation = 11.

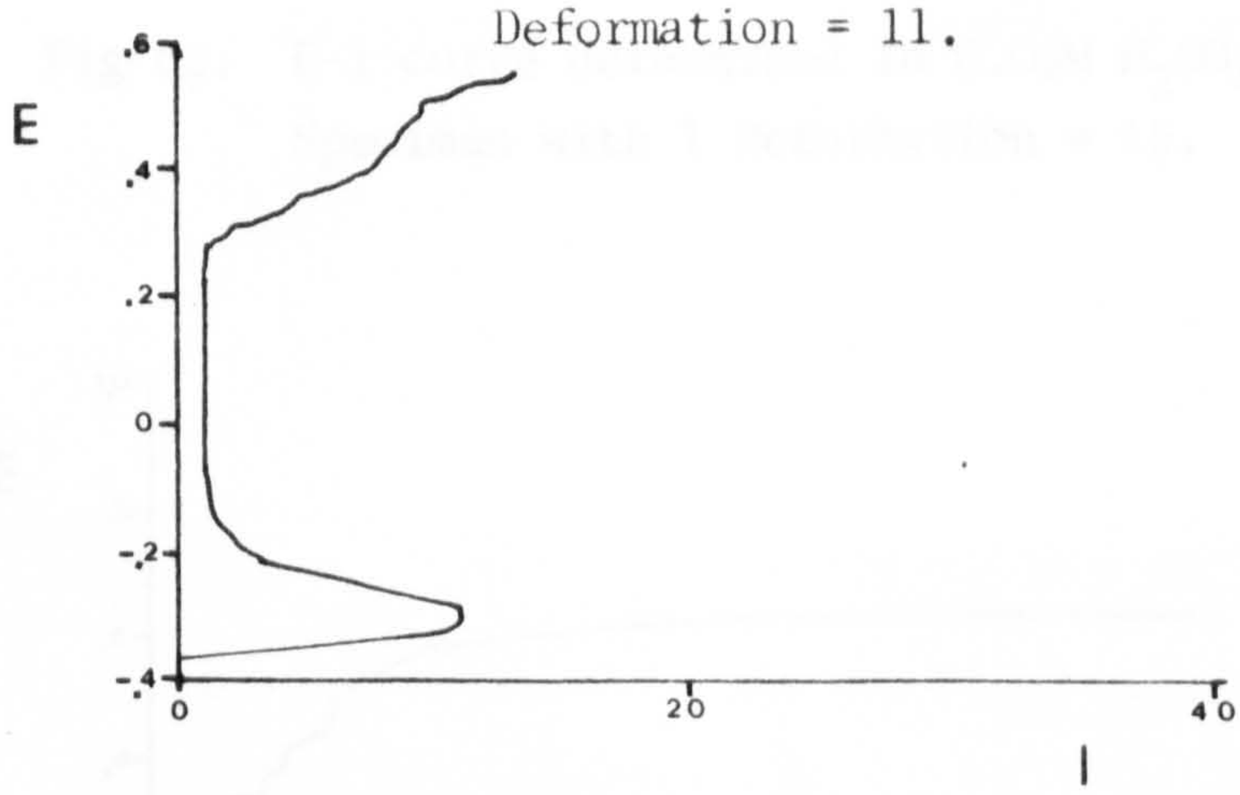

Fig. 60. E-1 curve determined in 0.05M H_2SO_4 + 0.1M NaCl solution. Specimen with % Deformation = 10.

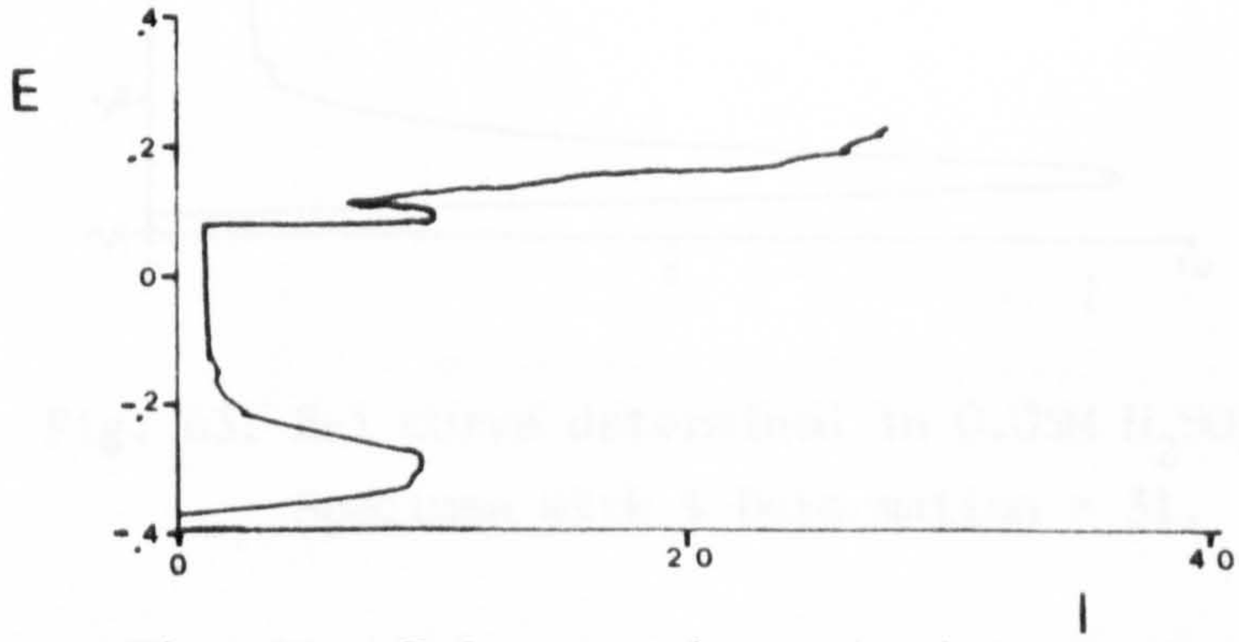

Fig. 61. E-1 curve determined in 0.05M H_2SO_4 + 0.1M Na Cl solution, Specimen with % Deformation = 9.

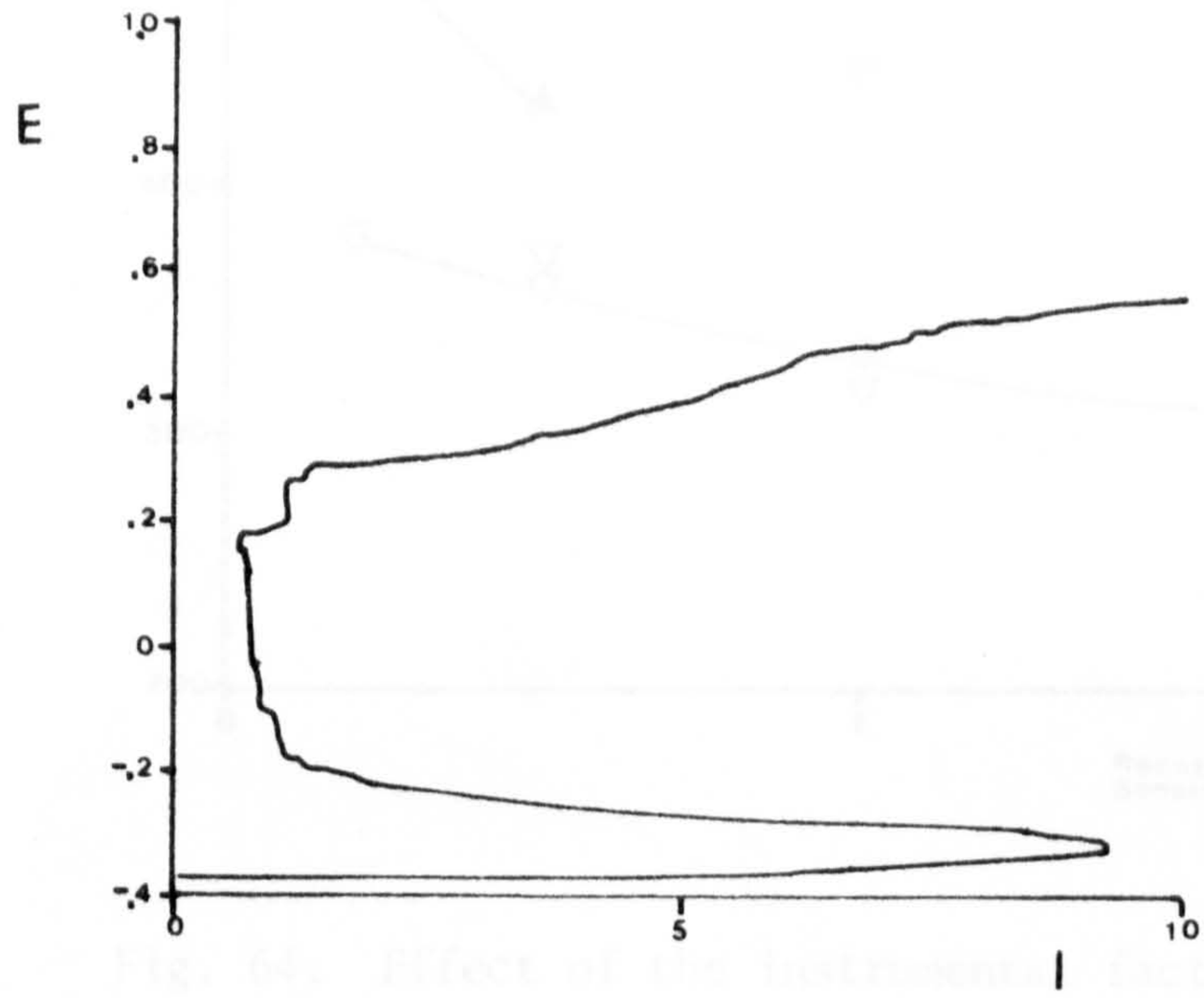

Fig 62. E-i curve determined in 0.05M H_2SO_4 + 0.1M NaCl solution. Specimen with % Deformation = 19.

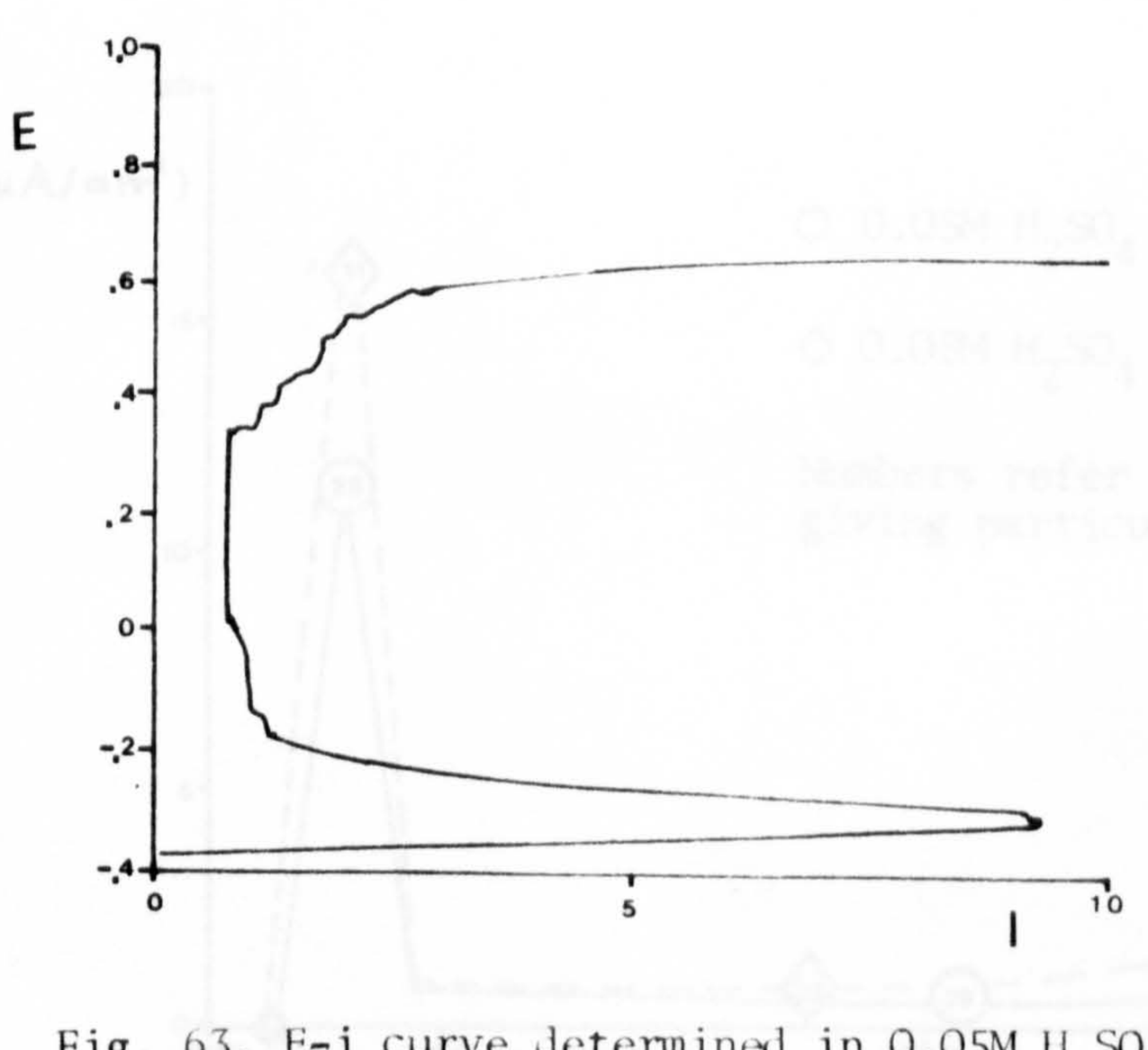

Fig. 63. E-i curve determined in 0.05M H_2SO_4 + 0.1M NaCl solution. Specimen with % Deformation = 31.

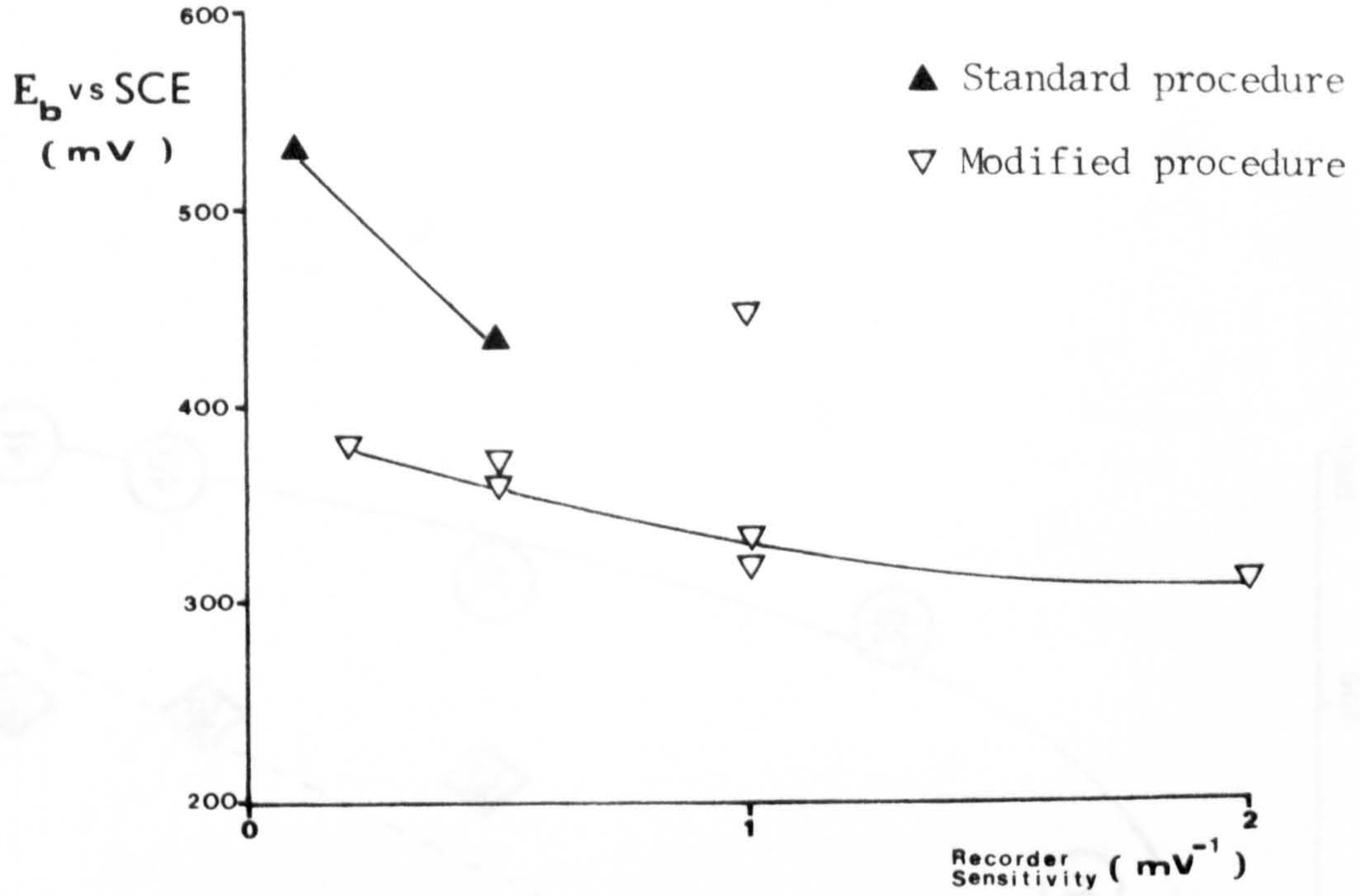

Fig. 64. Effect of the instrumental factor, recorder sensitivity, on the value of the breakdown potential, E_b.

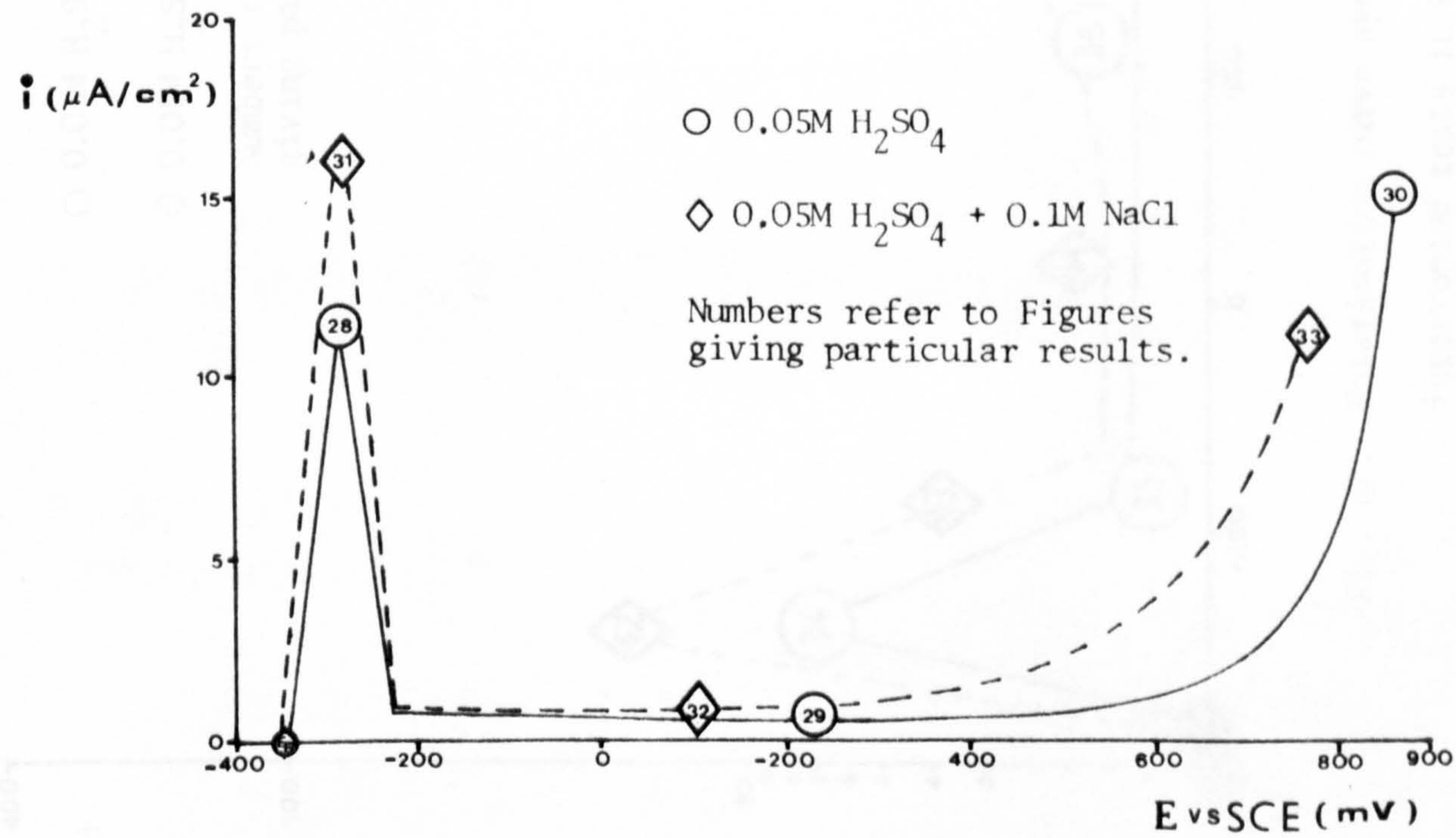

Fig. 65. Polarisation curve synthesized using coordinates of first series of interrupted tests in 0.05M H_2SO_4 and 0.05M H_2SO_4 + 0.1M NaCl.

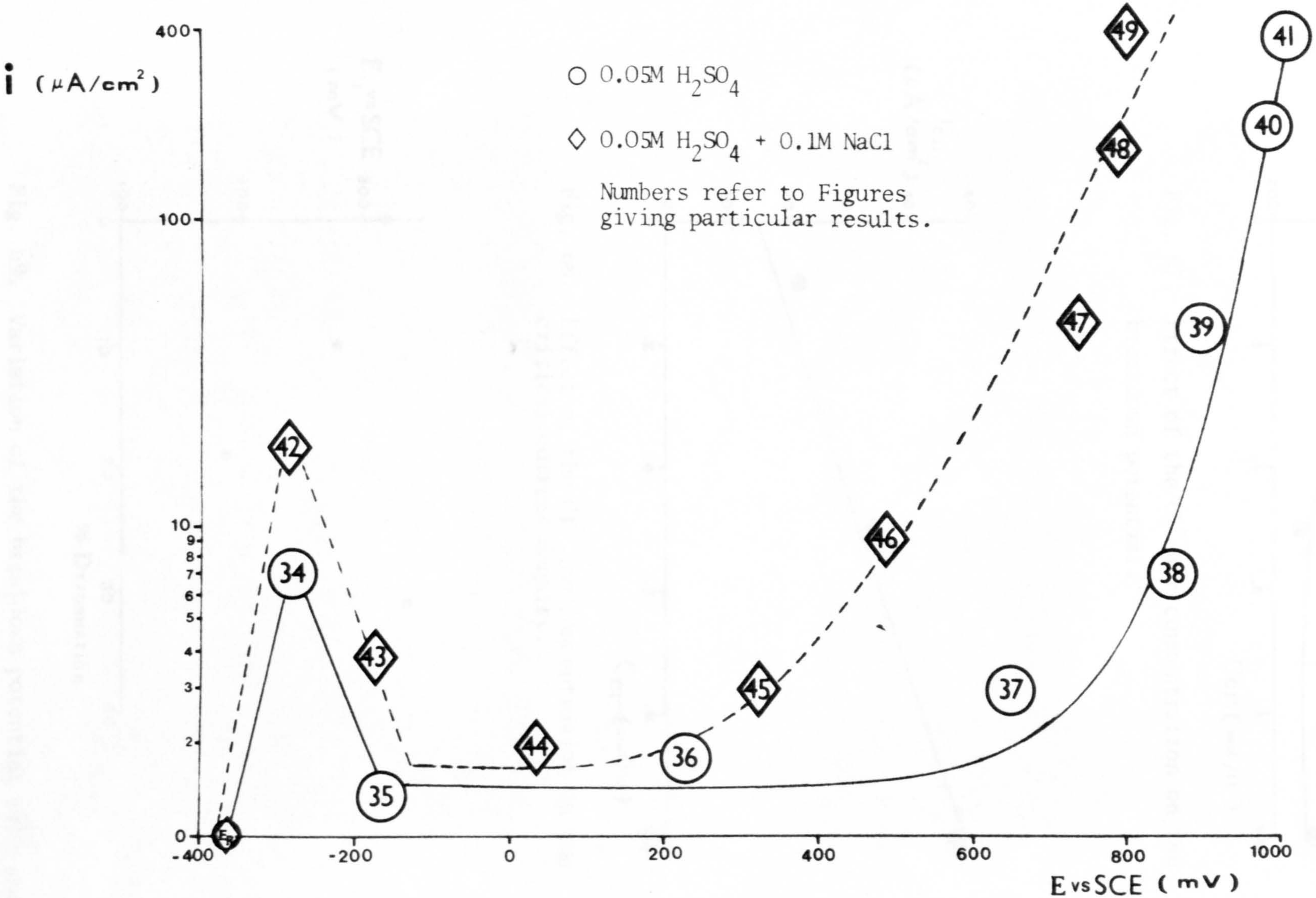

Fig. 66. Polarisation curve synthesized using coordinates of second series of interrupted tests in 0.05M H_2SO_4 and 0.05M H_2SO_4 + 0.1M NaCl.

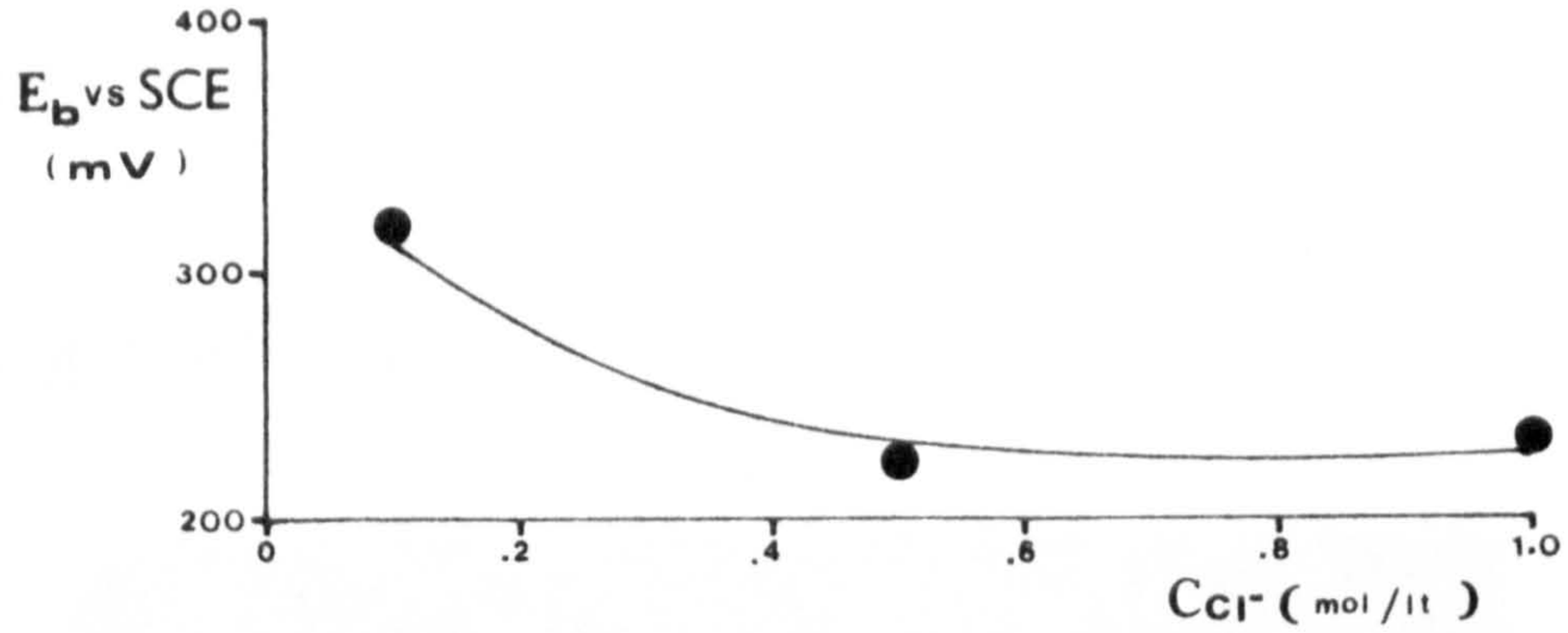

Fig. 67. Effect of the Cl^- ion concentration on the breakdown potential.

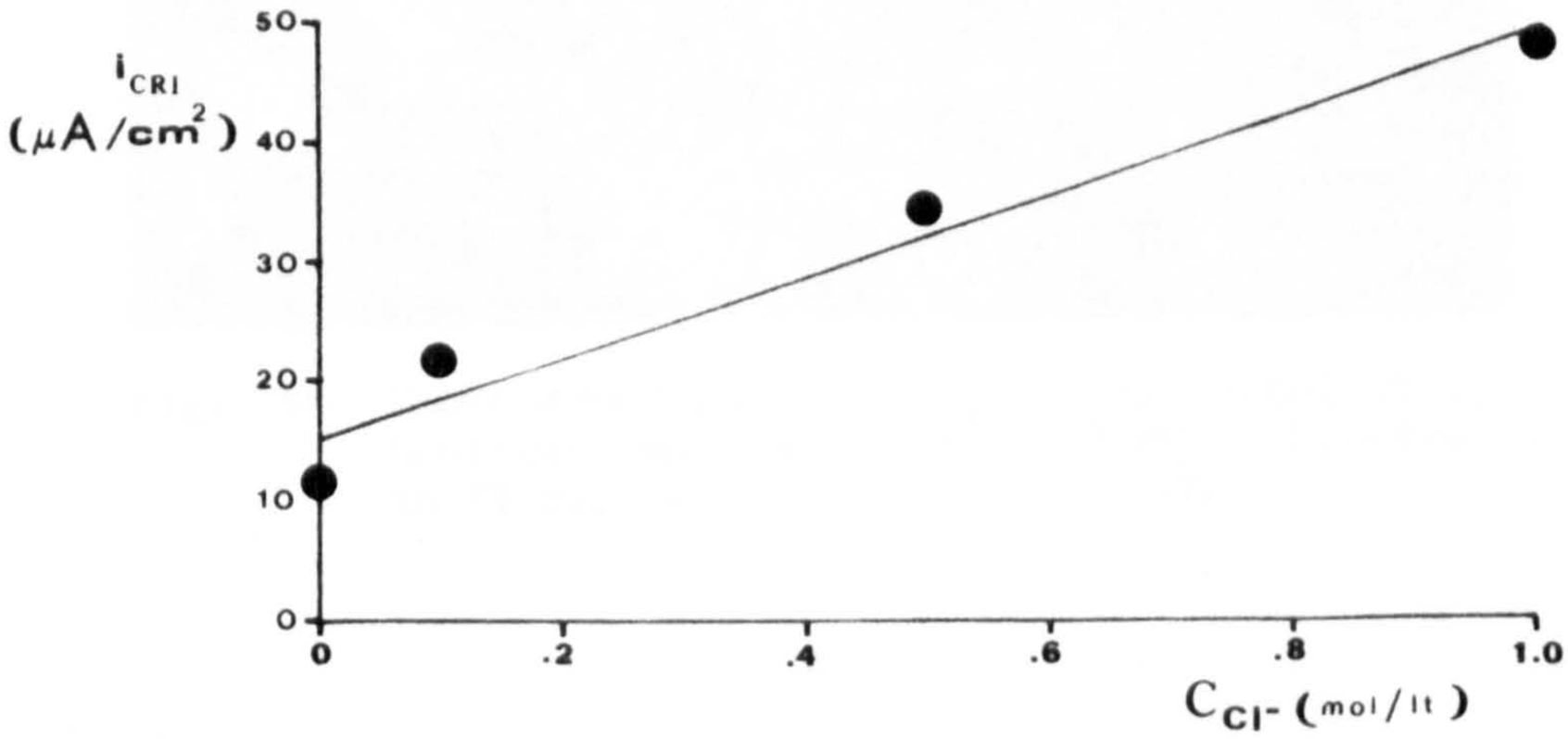

Fig. 68. Effect of the Cl^- ion concentration on the critical current density.

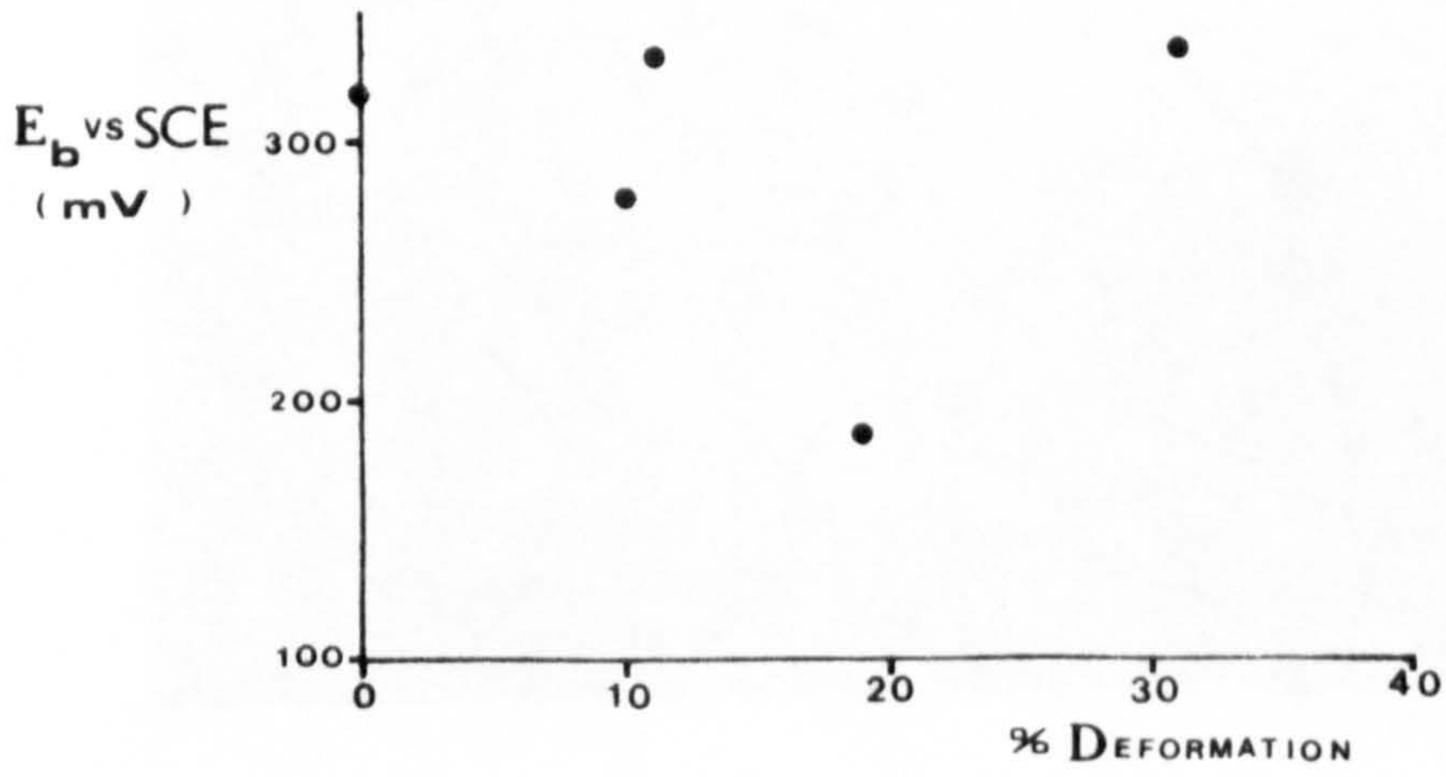

Fig. 69. Variation of the breakdown potential with the amount of cold work as measured as % deformation.

EXAMINATION OF METAL SURFACES.

1. OPTICAL MICROSCOPY

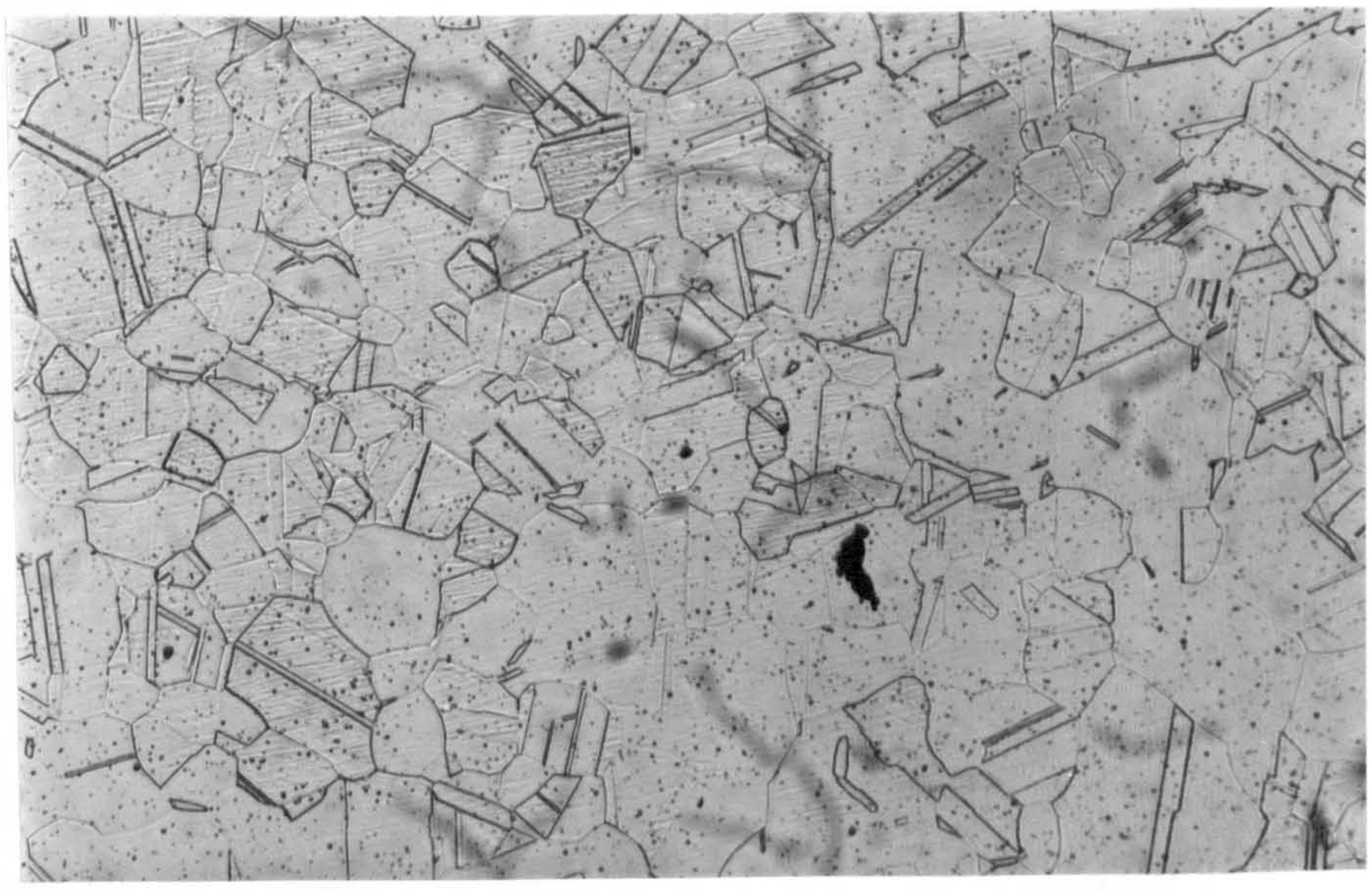

Fig. 70. Microstructure of 316 stainless steel after heat-treatment at 1100°C and WQ. Electro etched in 1% oxalic acid solution x 100

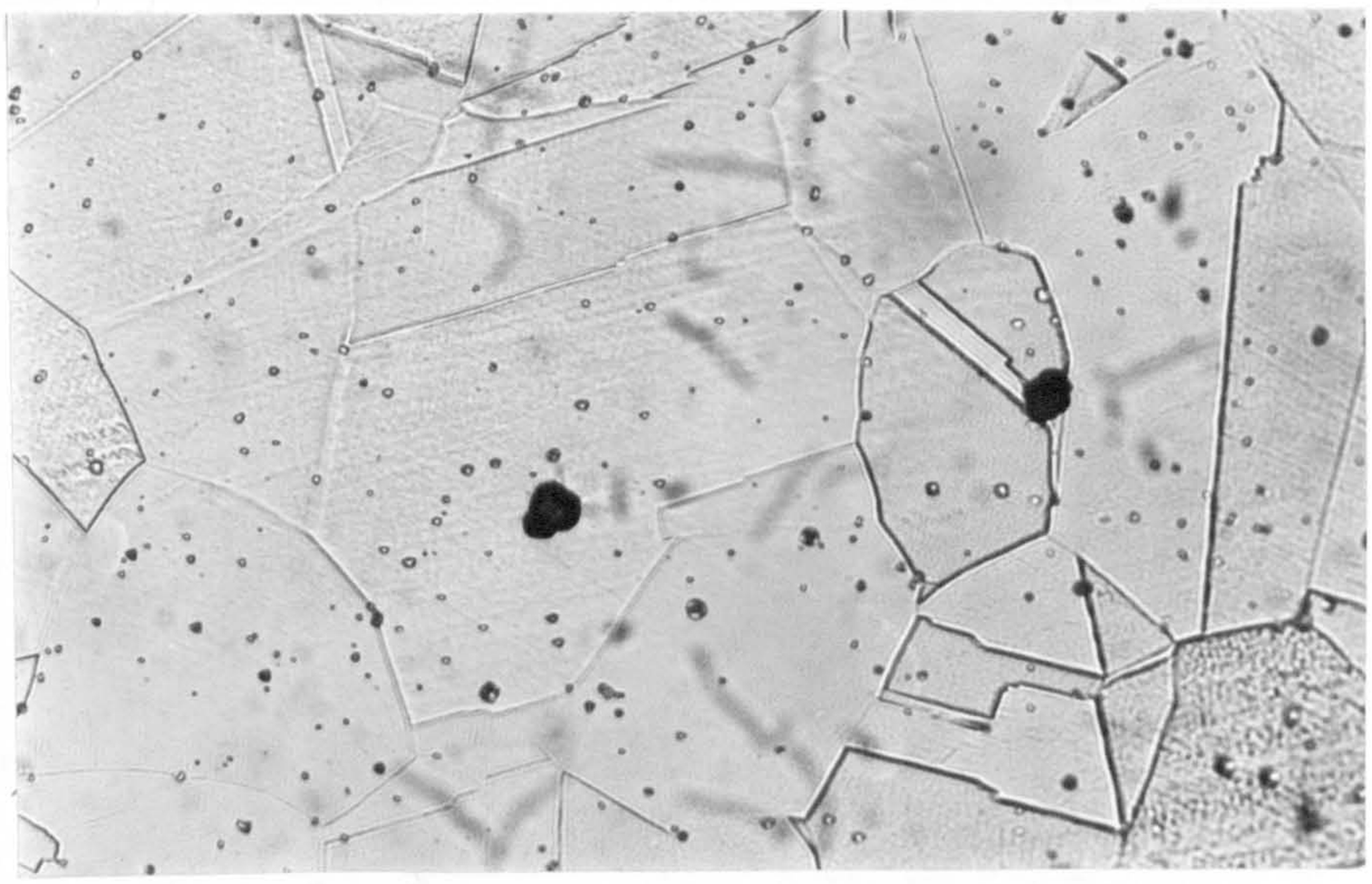

Fig. 71 Detail of the microstructure of 316 stainless steel at higher magnification x 500

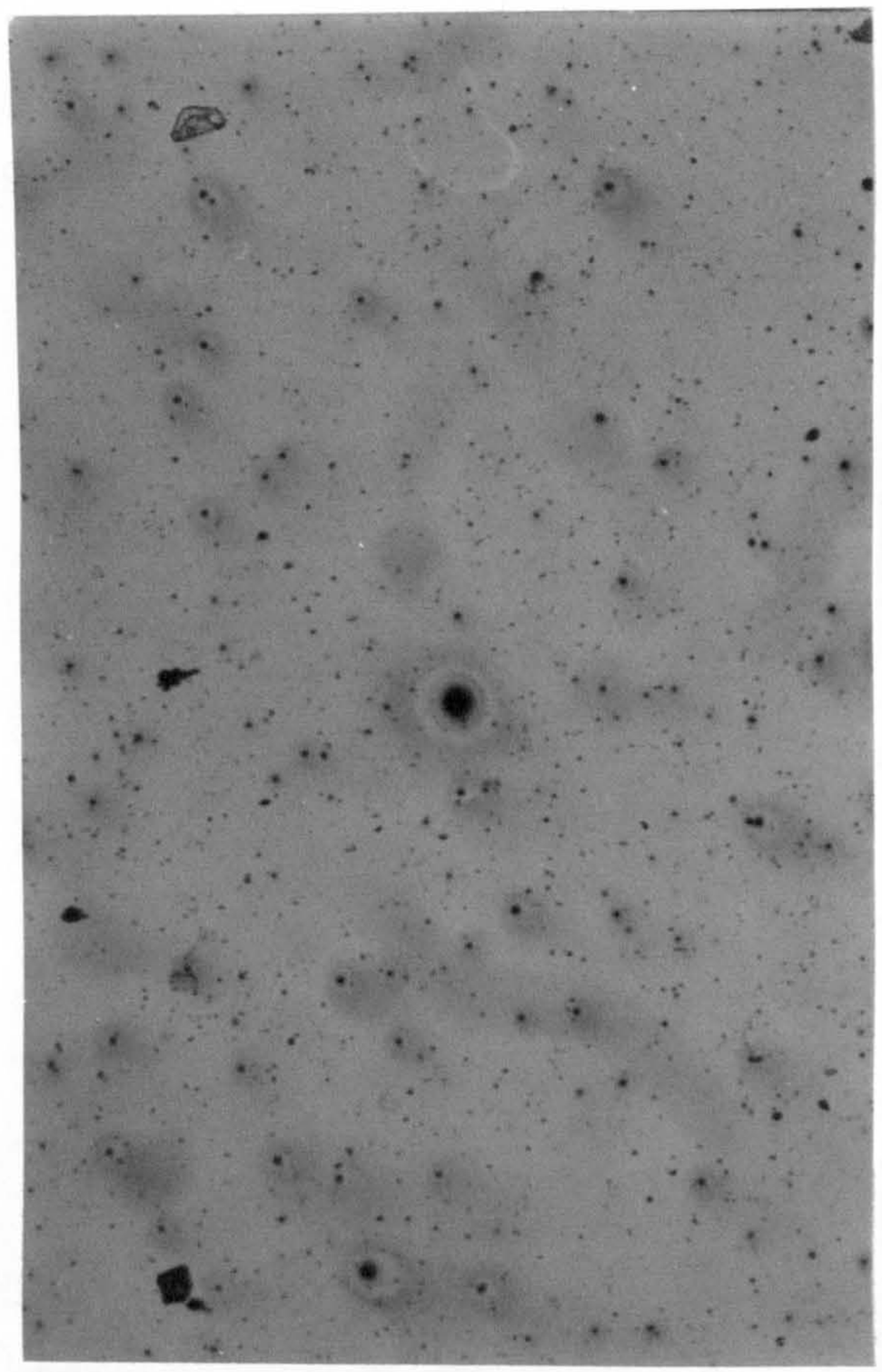

72

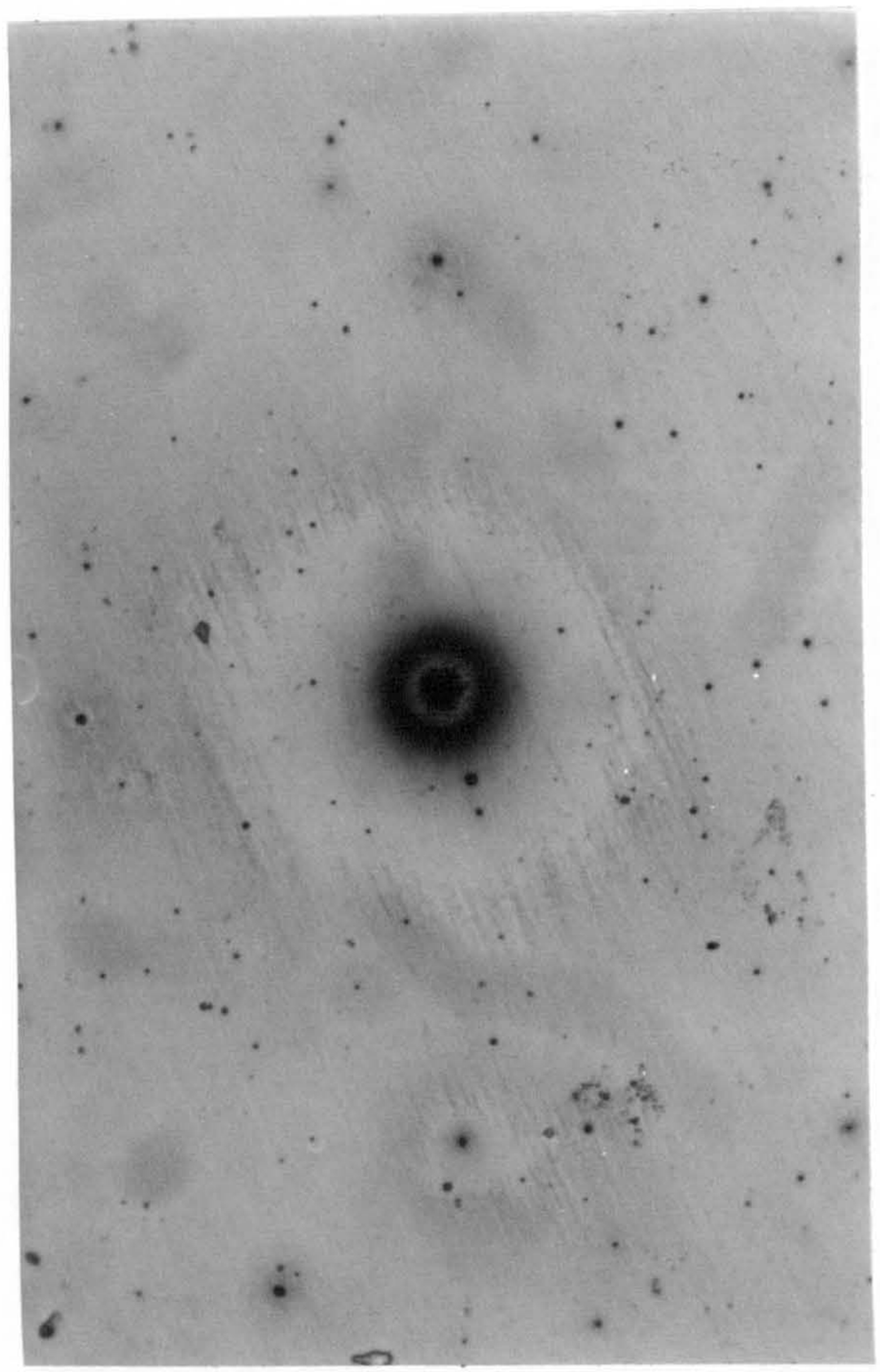

73

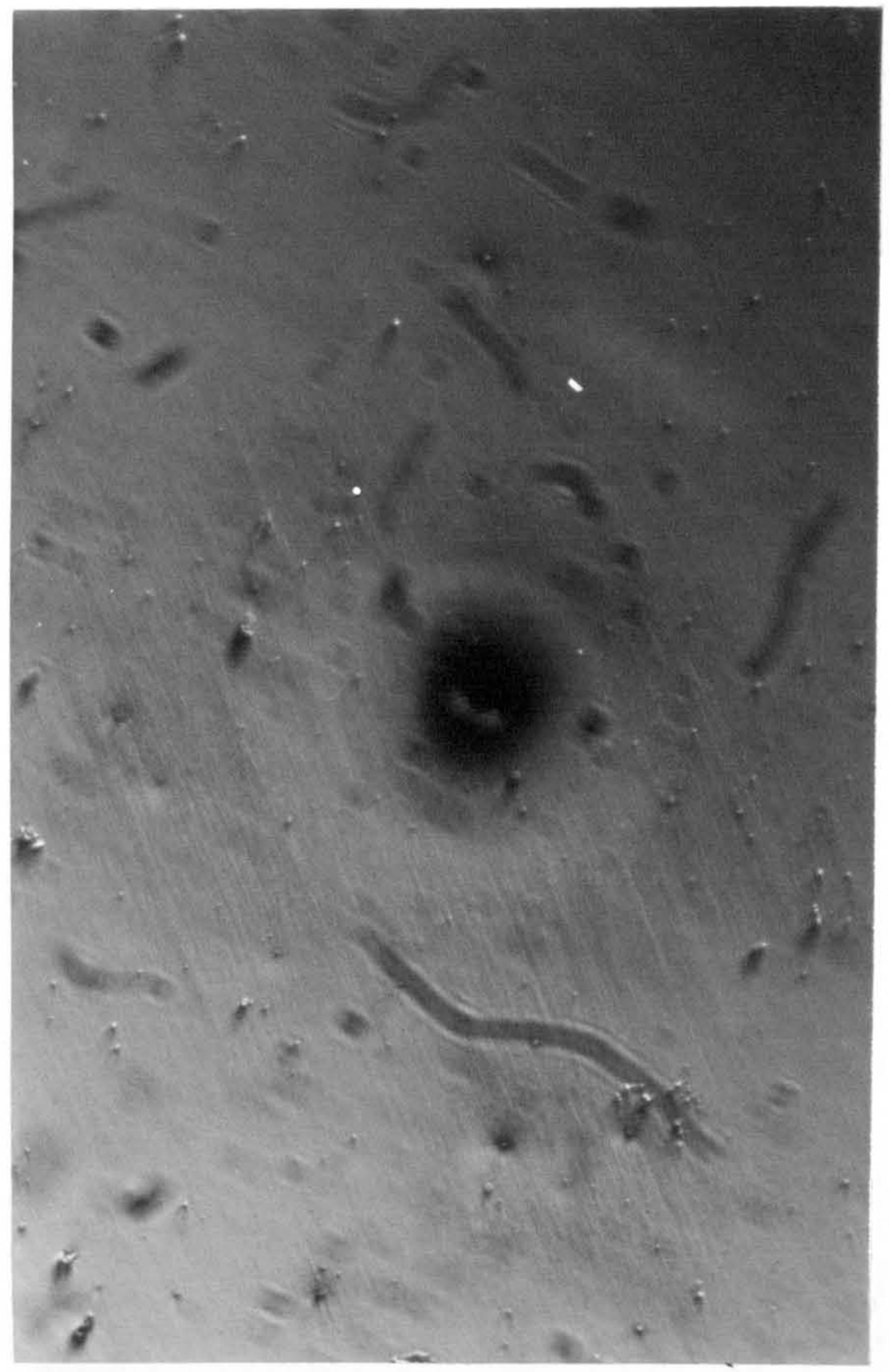

74

Figs 72-73. Micrographs of specimen anodically polarised in 0.05M H_2SO_4 and interrupted at the coordinates (-290, 13)

Fig. 72 x 100

Fig. 73 As Fig 72 x 500

Fig. 74 As Fig. 73 Oblique illumination

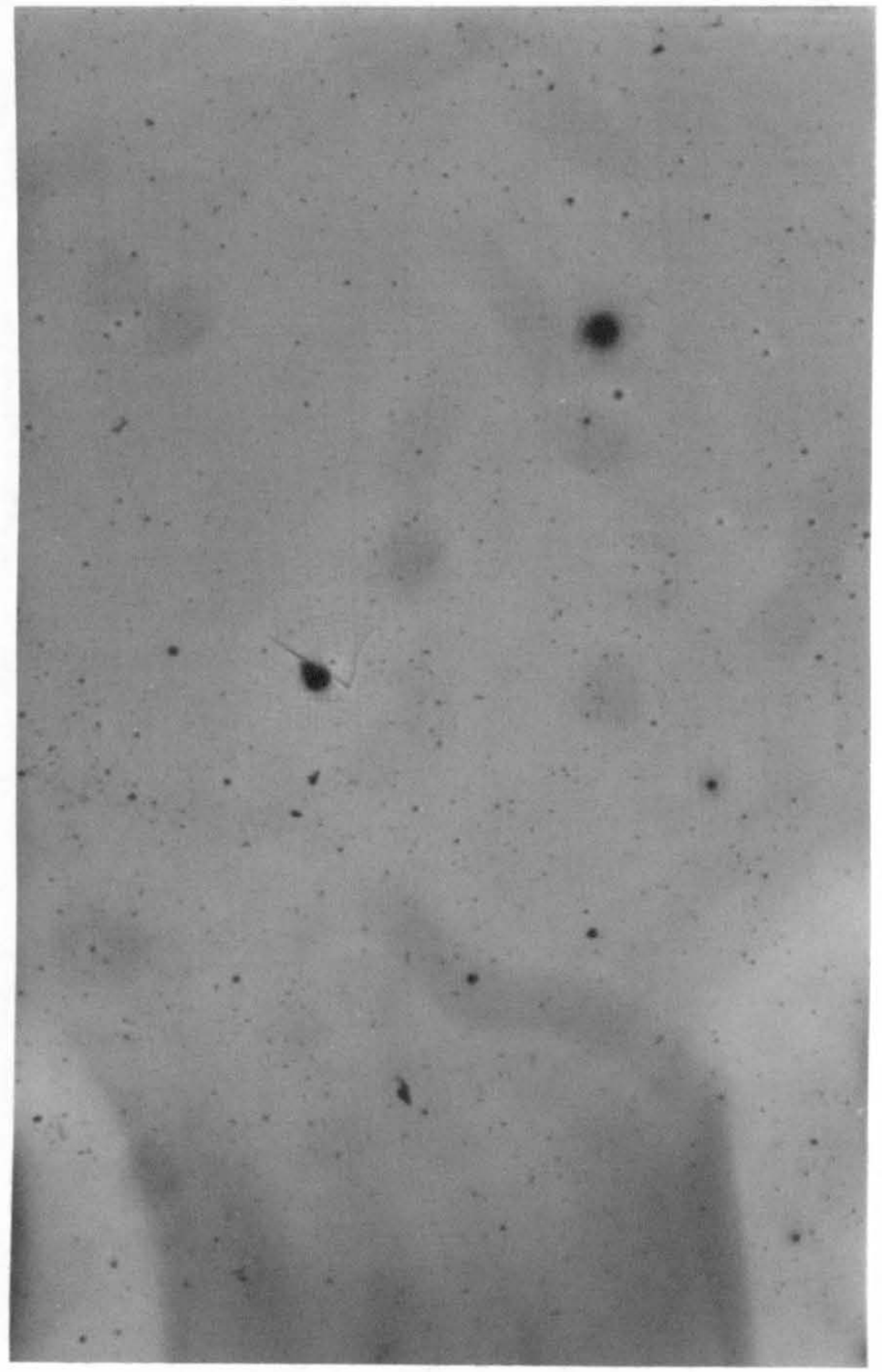

75

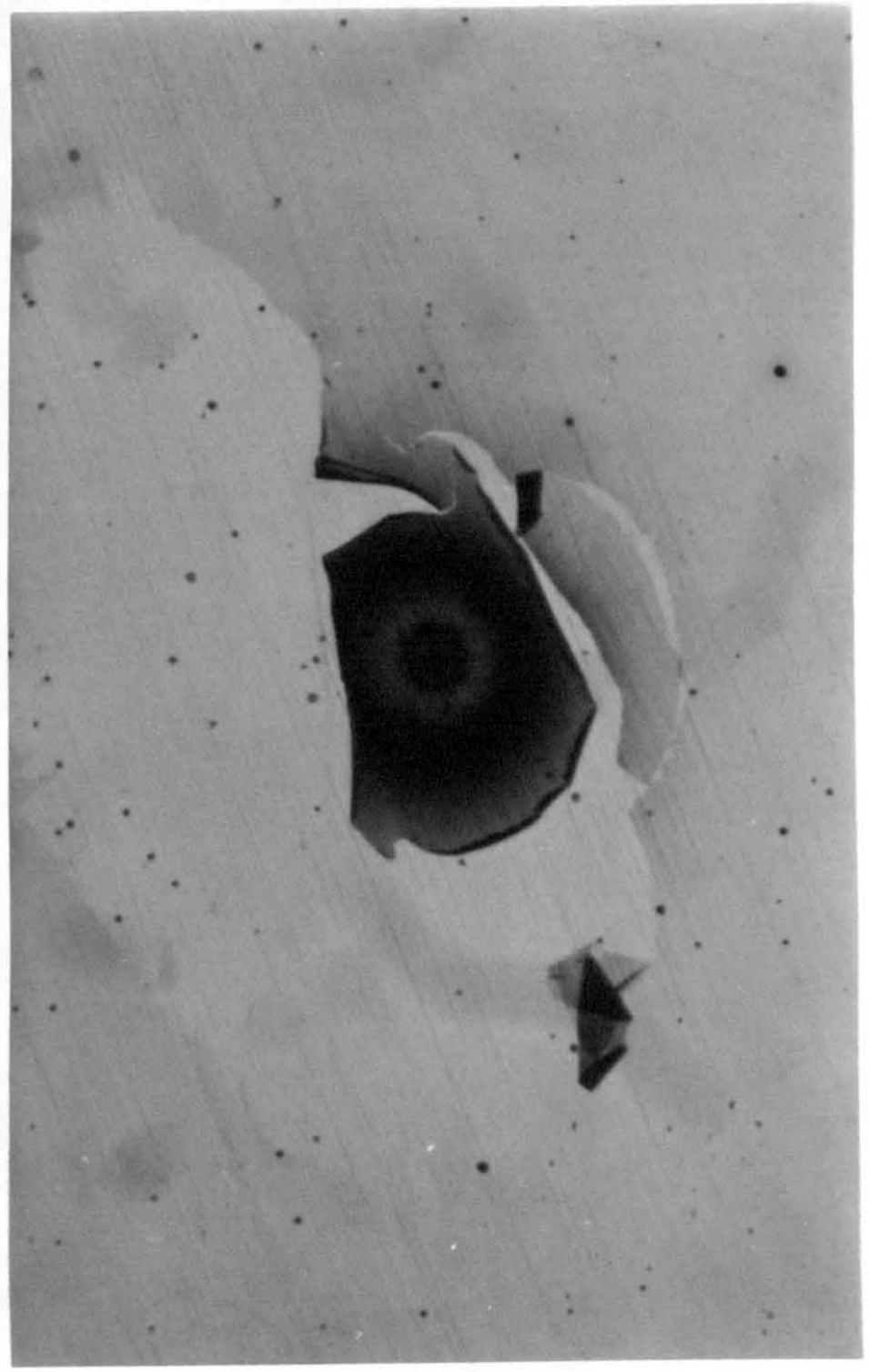

76

77

Figs 75-77. Micrographs of specimen anodically polarised in 0.05 M H_2SO_4 and interrupted at the co ordinate (230, 1.5)

Fig. 72 x 100

Fig. 76 As Fig. 75 x 500

Fig. 77 As Fig. 76
Oblique illumination

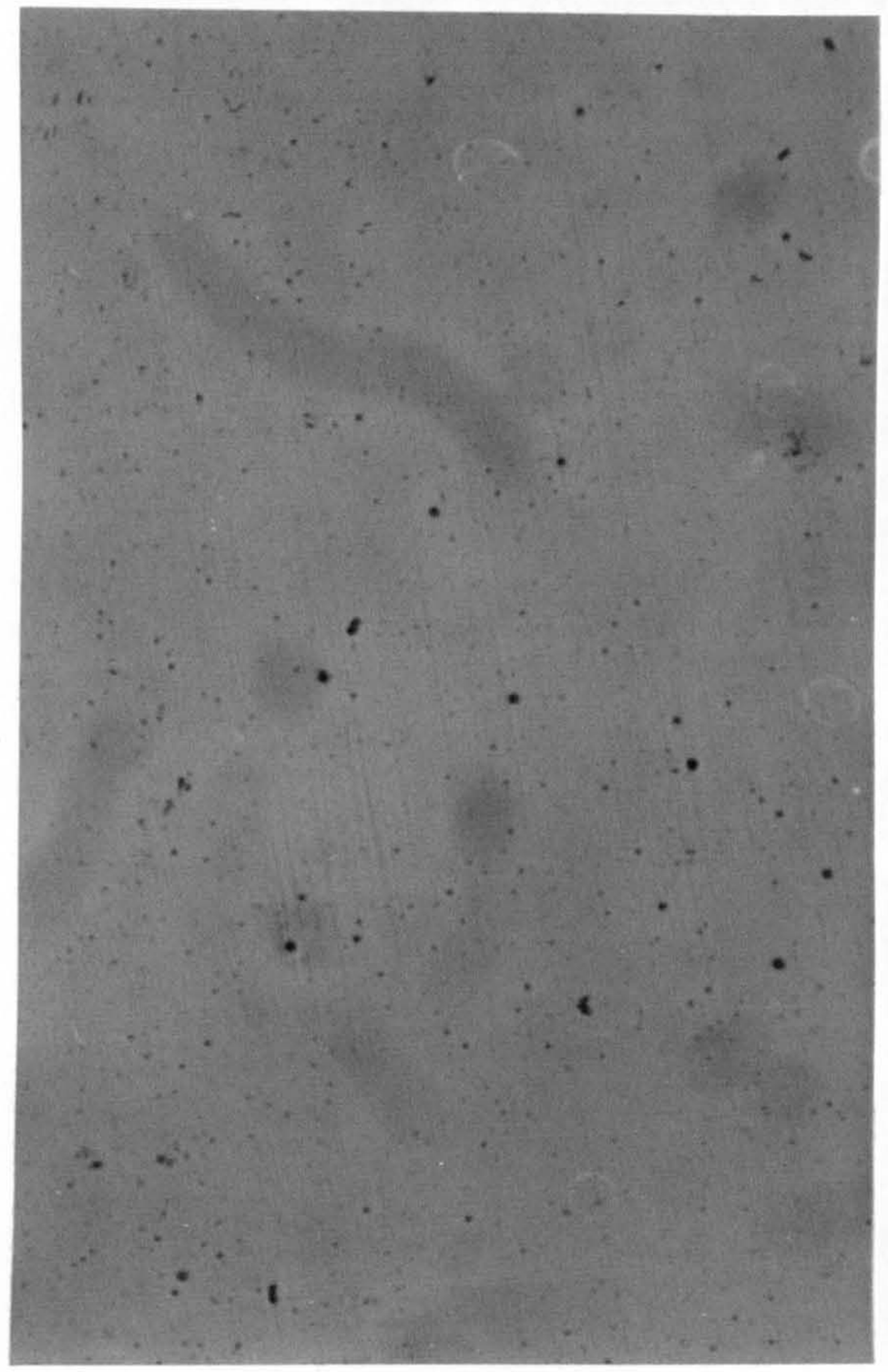

Fig. 78

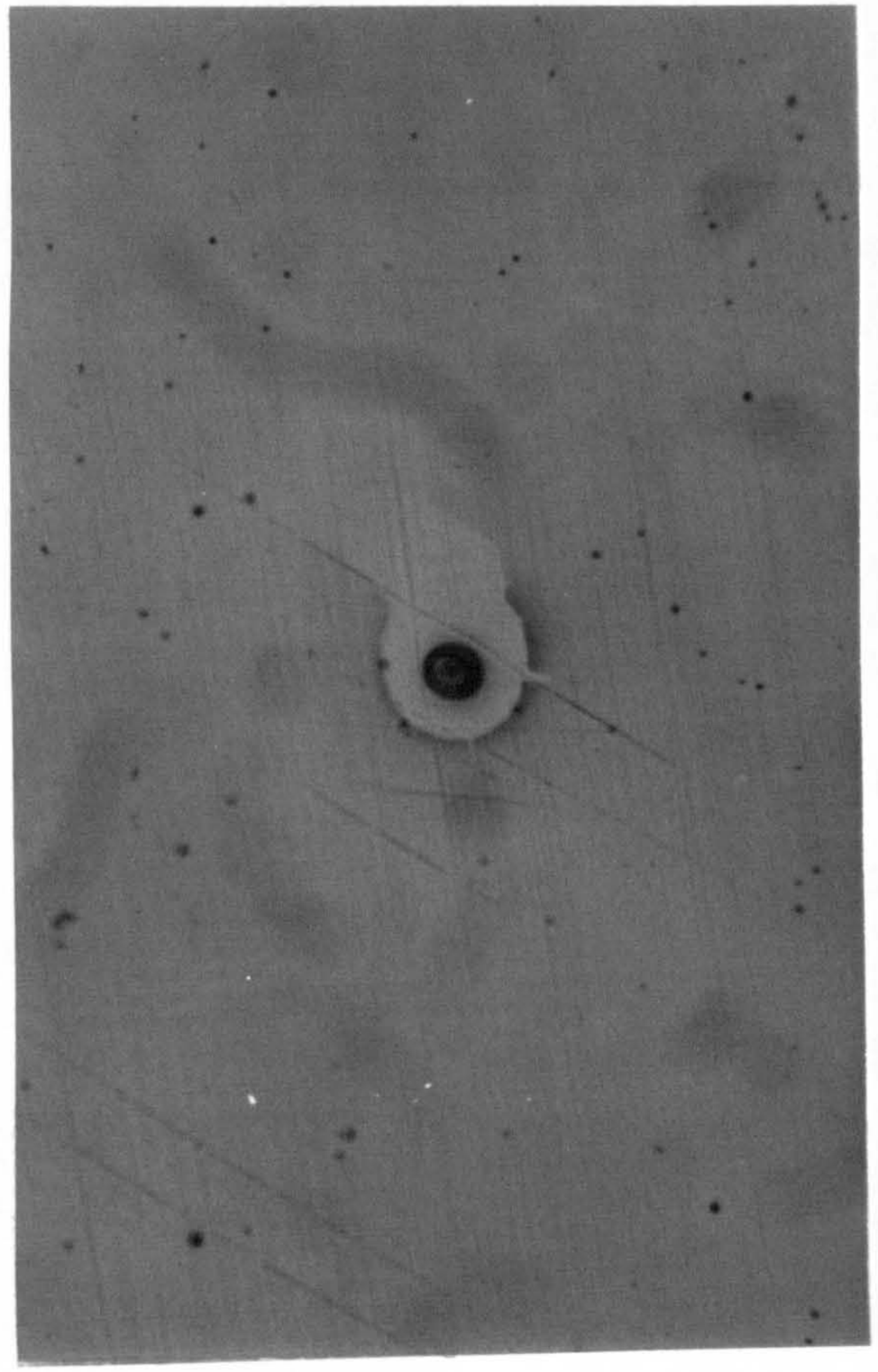

Fig. 79

Fig. 80

Figs. 78-80 Micrographs of specimen anodically polarised in 0.05M H_2SO_4 and interrupted at the co-ordinates (860, 15)

Fig. 78 x 100

Fig. 79 As Fig. 78 x 500

Fig. 80 As Fig. 79
Oblique illumination

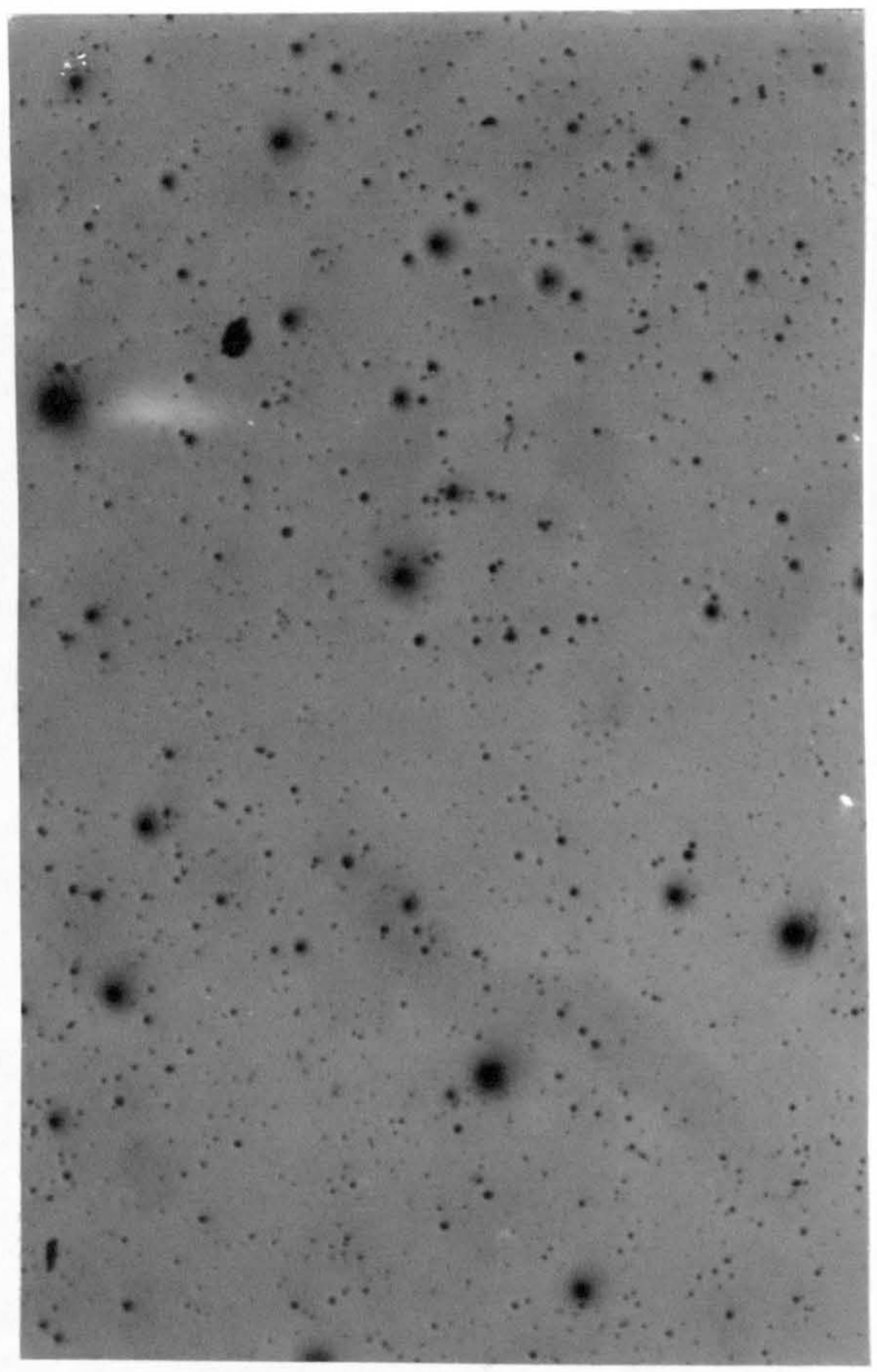

Fig. 81

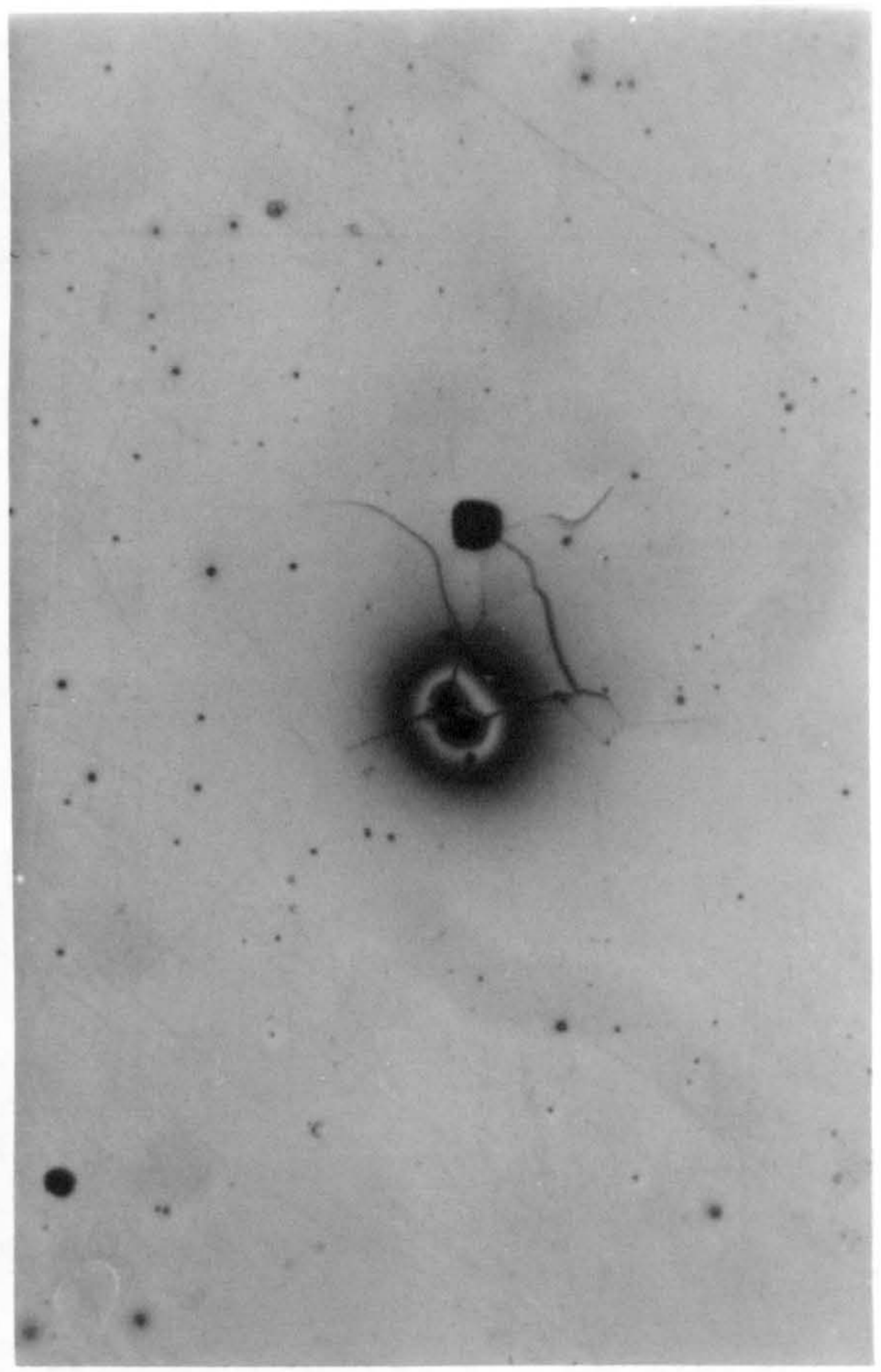

82

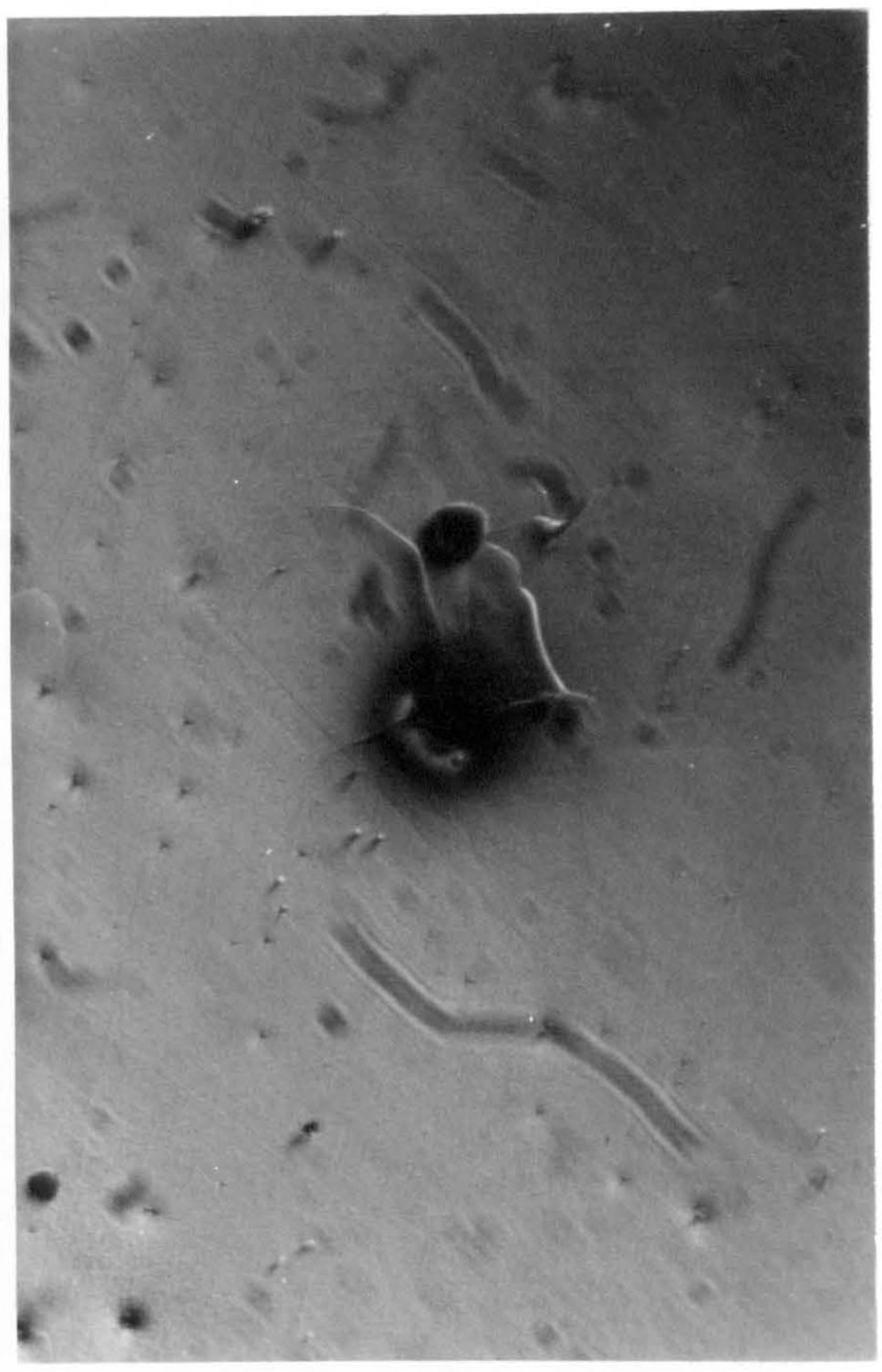

83

Figs 81-83 Micrographs of specimen anodically polarised in 0.05M H_2SO_4 and 0.1M NaCl and interrupted at the coordinates (-284, 17.0)

Fig. 81 x 100

Fig. 82 As Fig. 81 x 500

Fig. 83 As Fig. 81
Oblique illumination

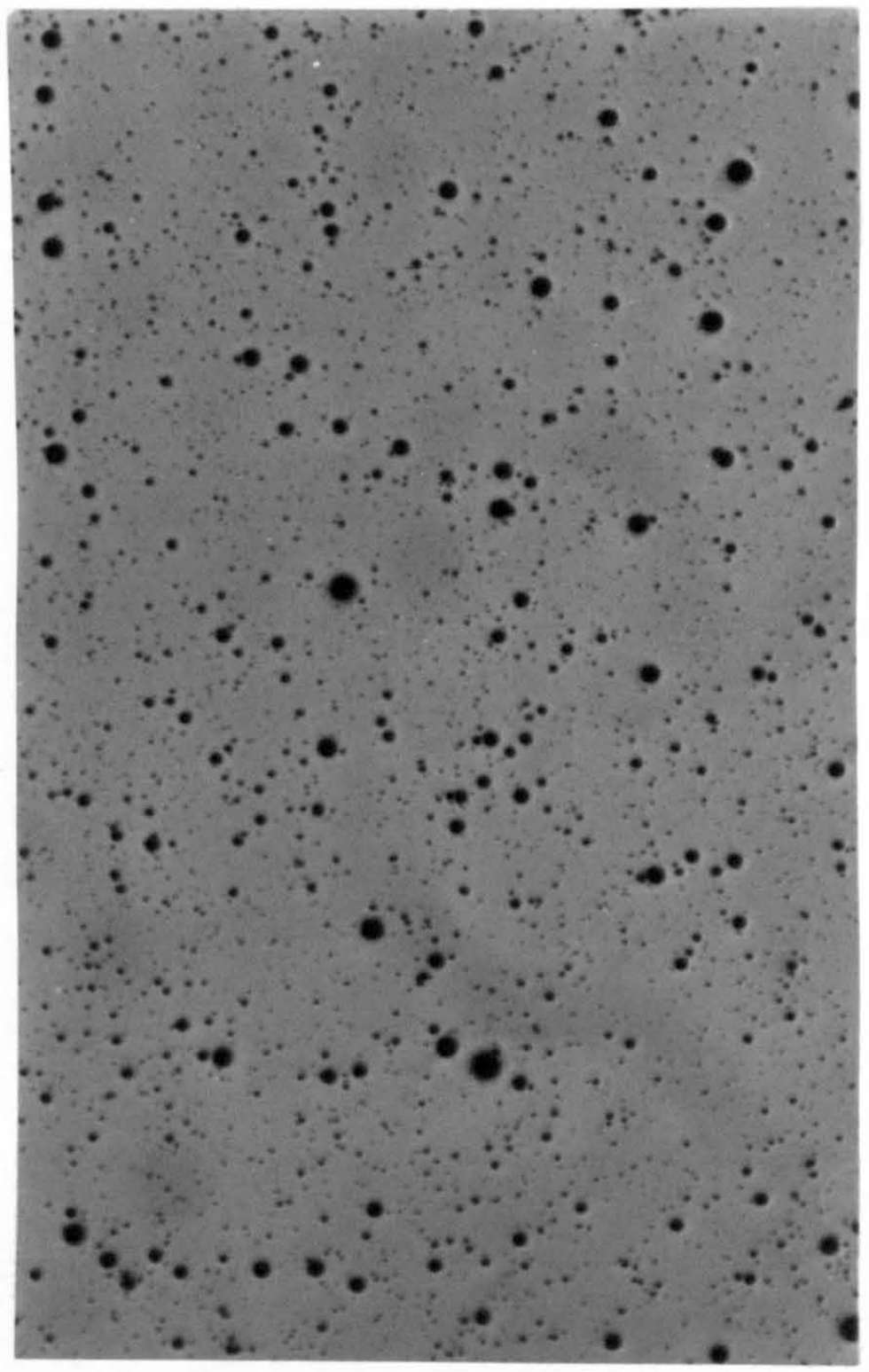

84

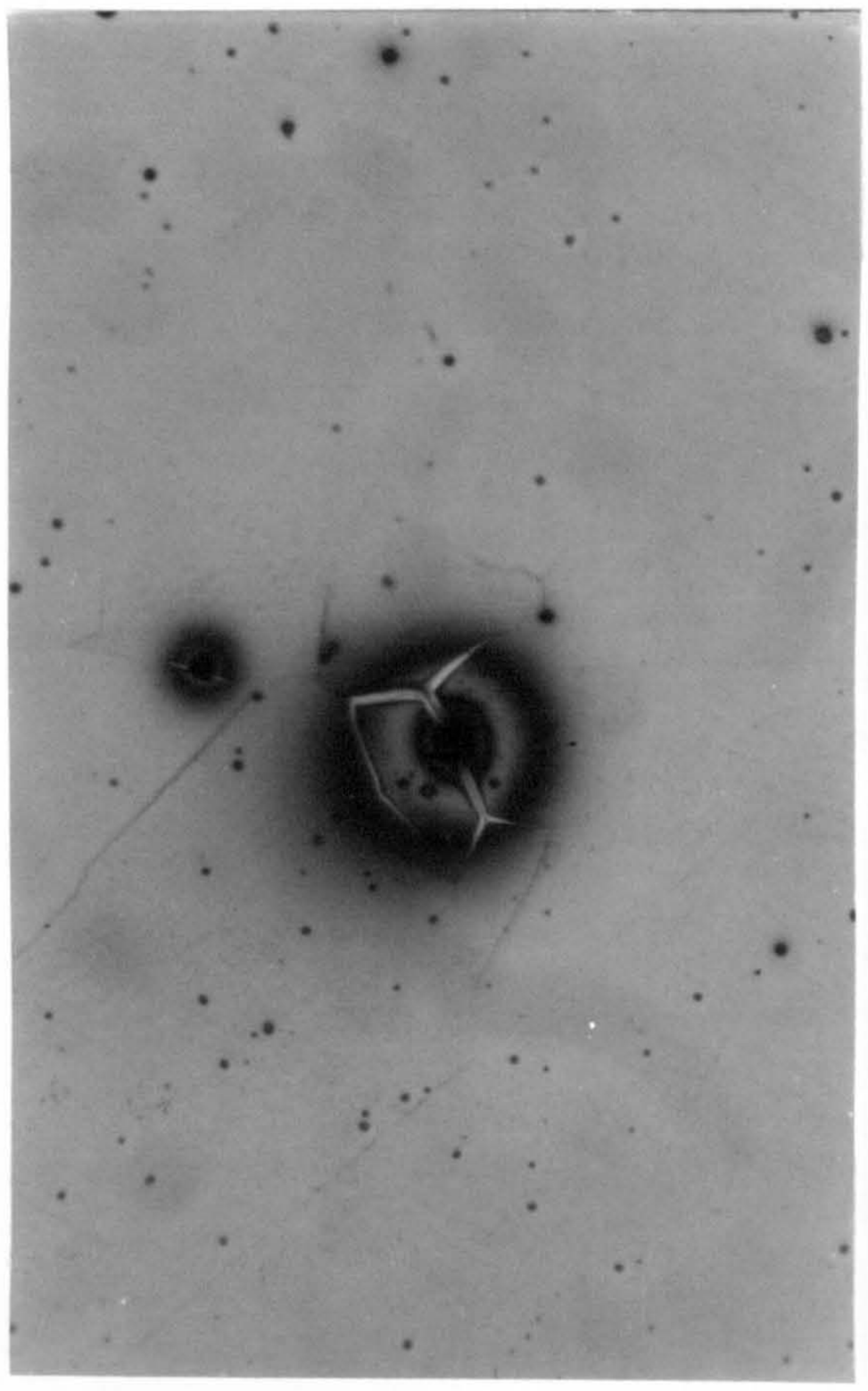

85

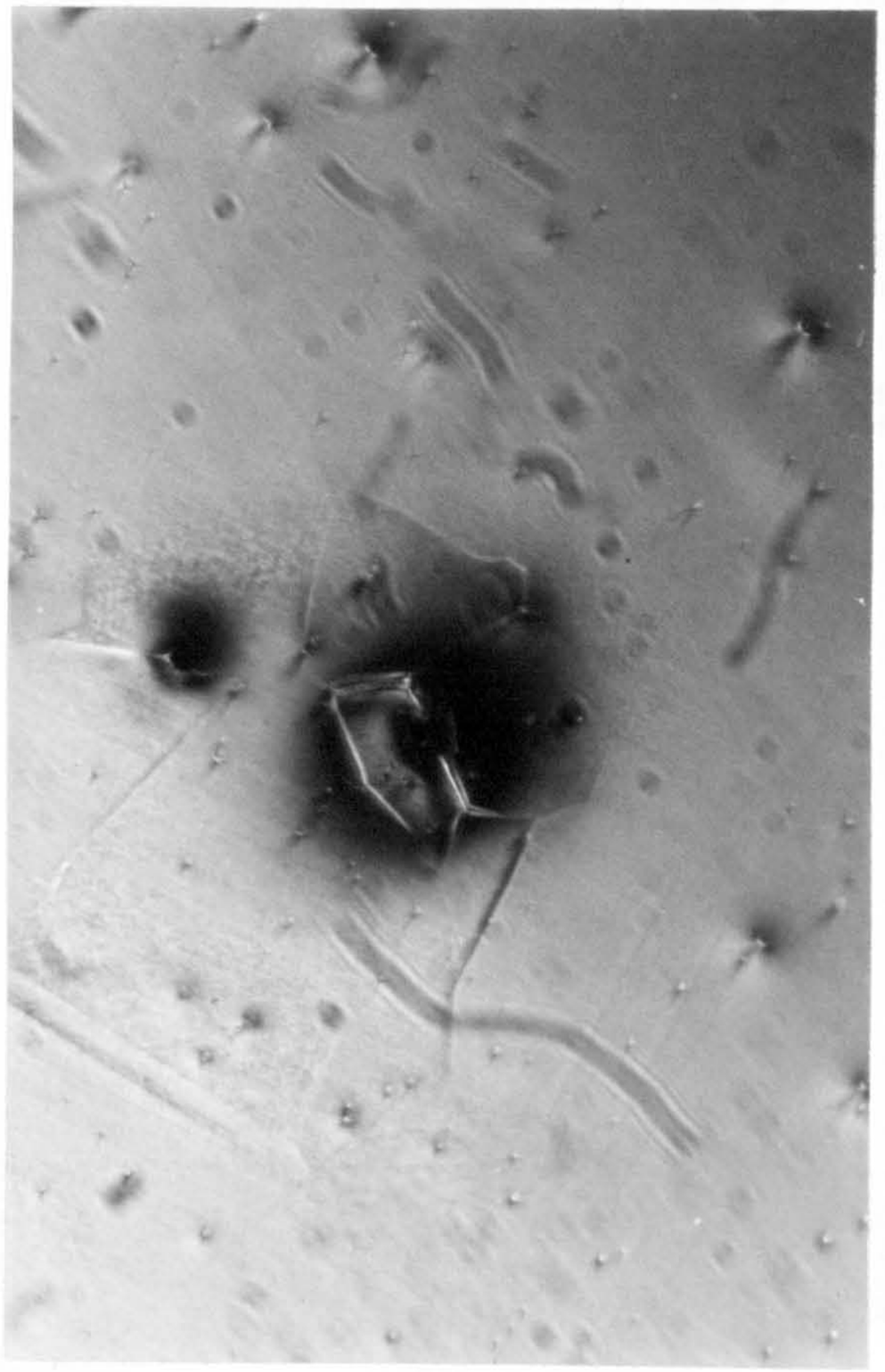

86

Figs. 84-86. Micrographs of specimen anodically polarised in 0.05M H_2SO_4 + 0.1M NaCl. and interrupted at the coordinates (100, 1.5)

Fig. 84 x 50

Fig. 85 As Fig. 84 x 500

Fig. 86 As Fig 85

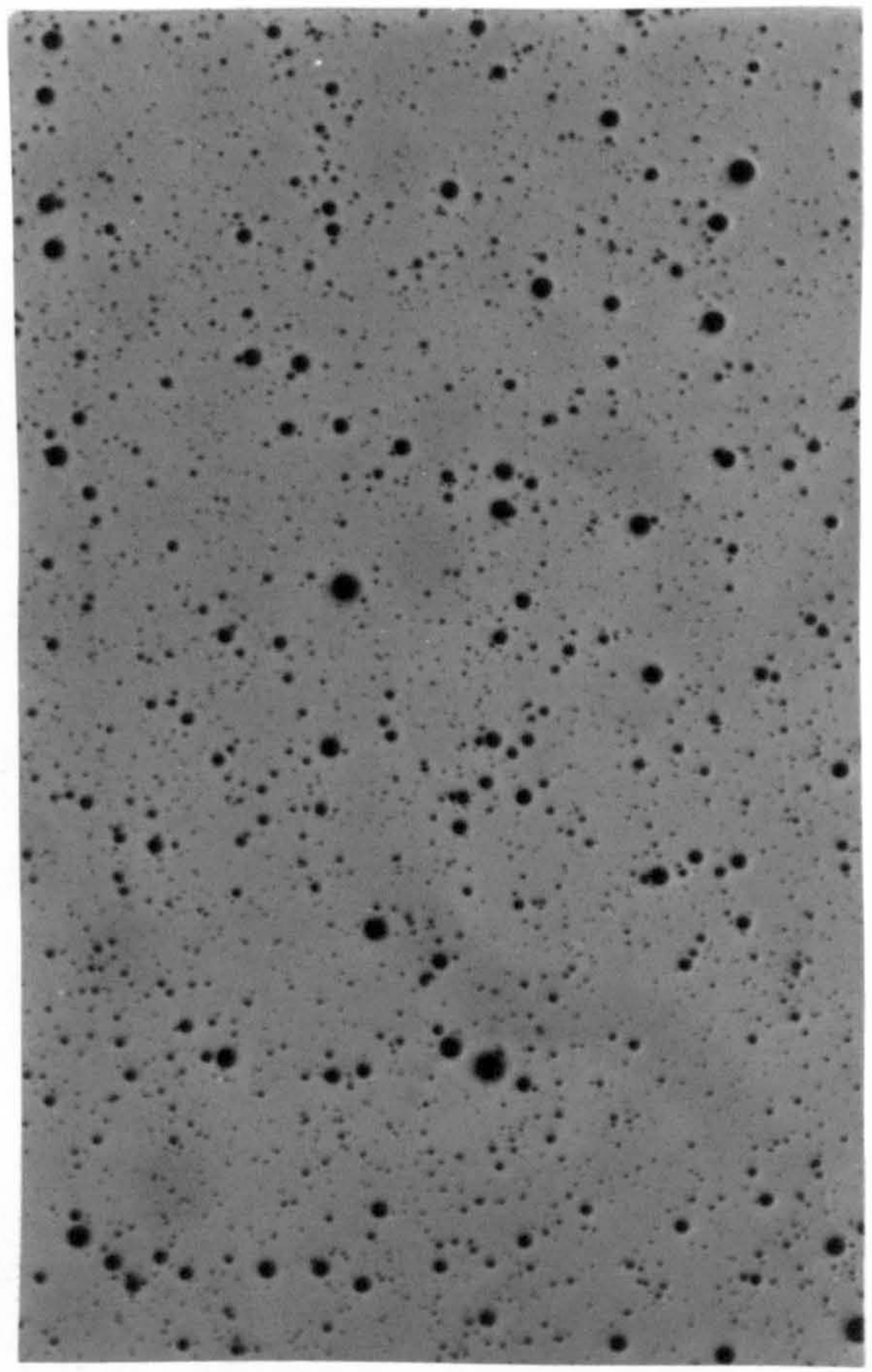

84

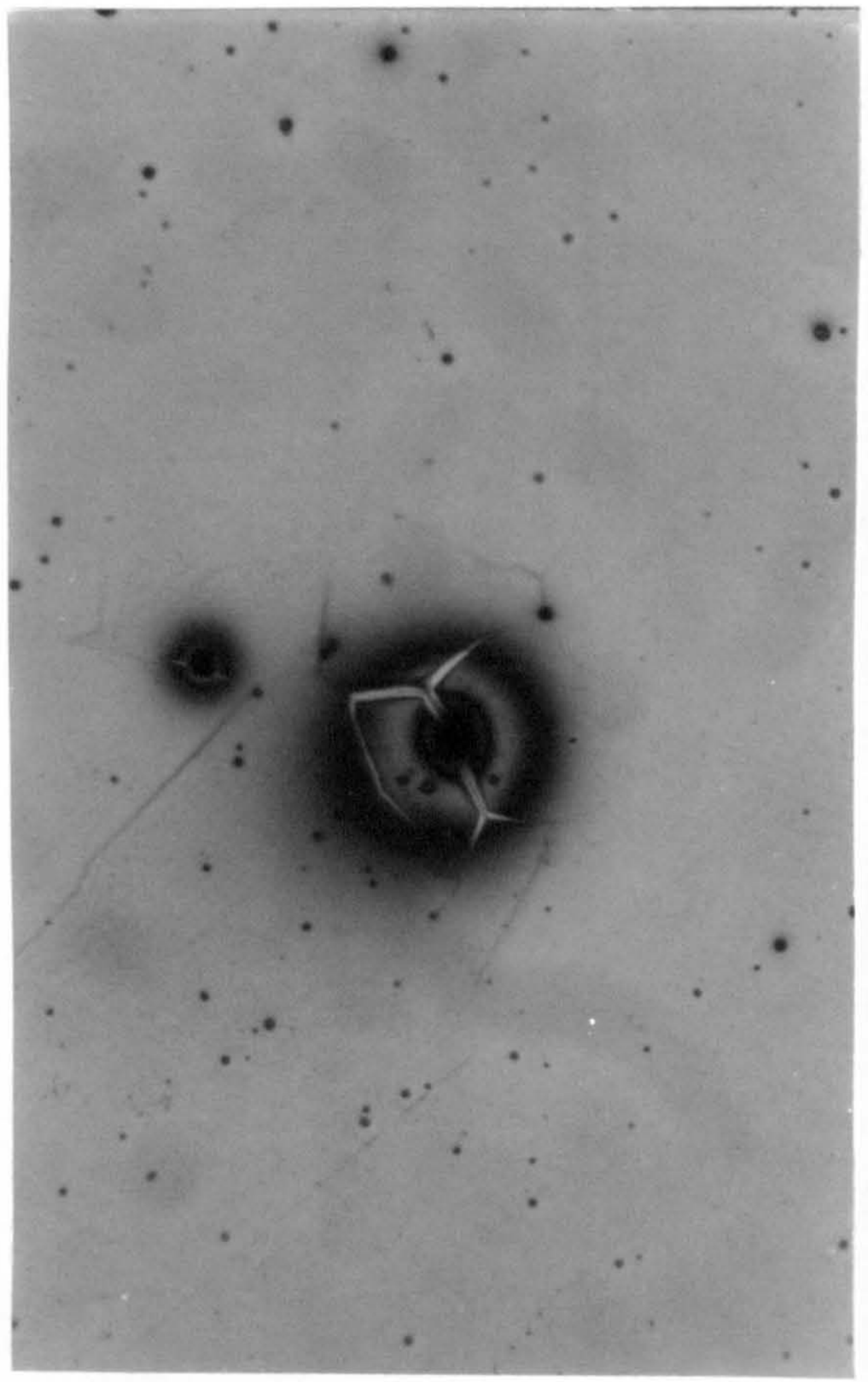

85

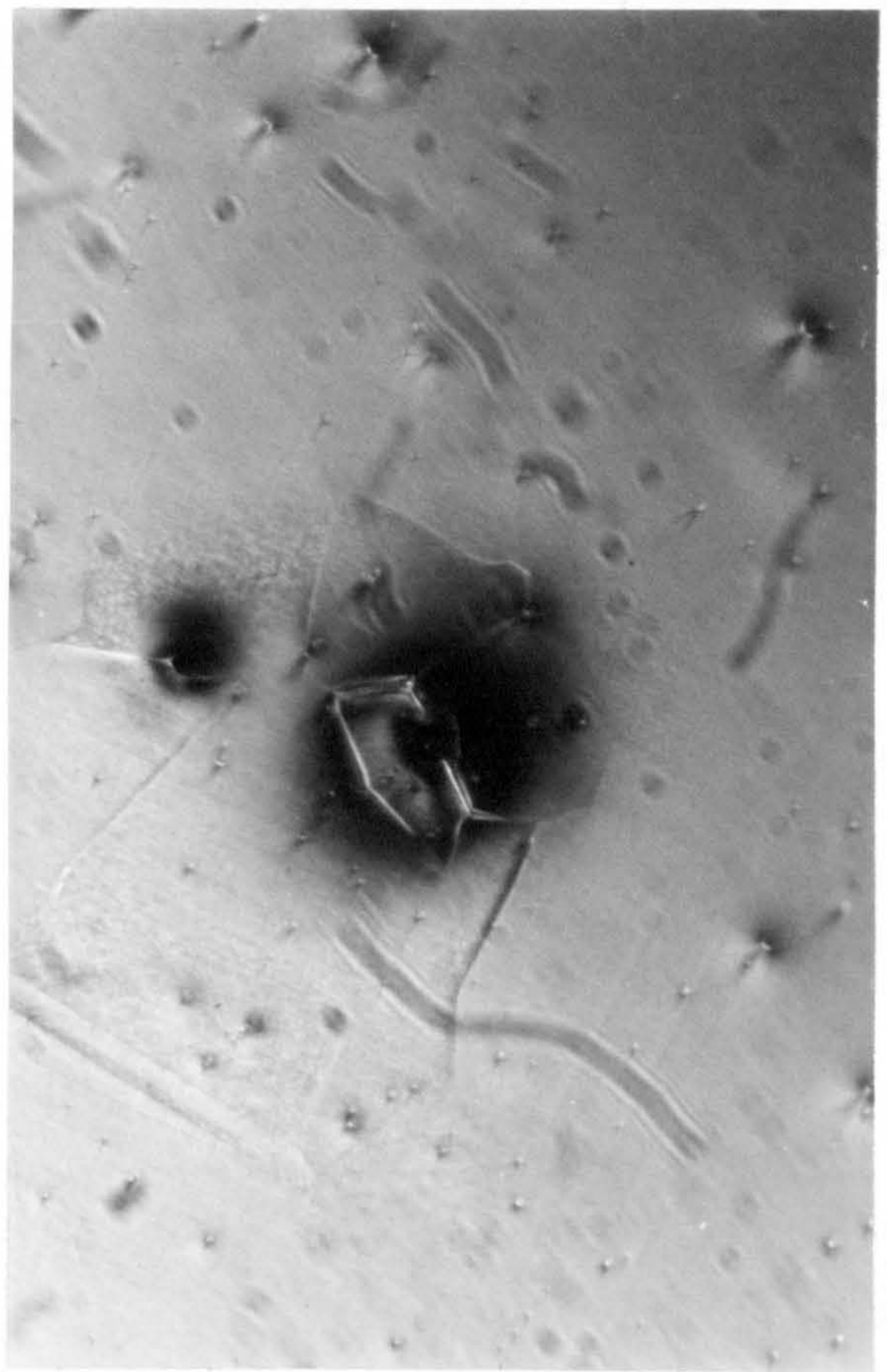

86

Figs. 84-86. Micrographs of specimen anodically polarised in 0.05M H_2SO_4 + 0.1M NaCl. and interrupted at the coordinates (100, 1.5)

Fig. 84 x 50

Fig. 85 As Fig. 84 x 500

Fig. 86 As Fig 85
Oblique illumination

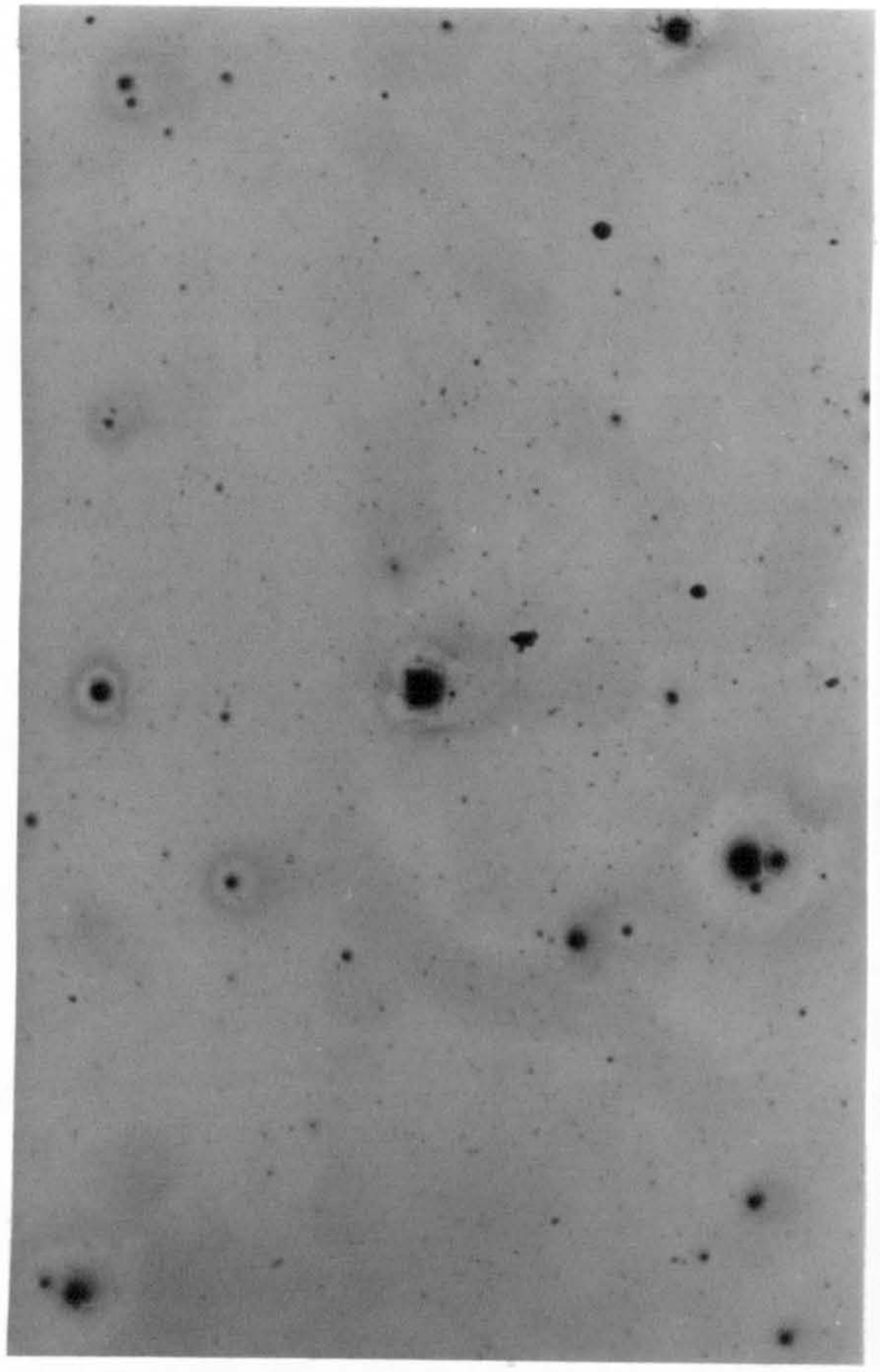

87

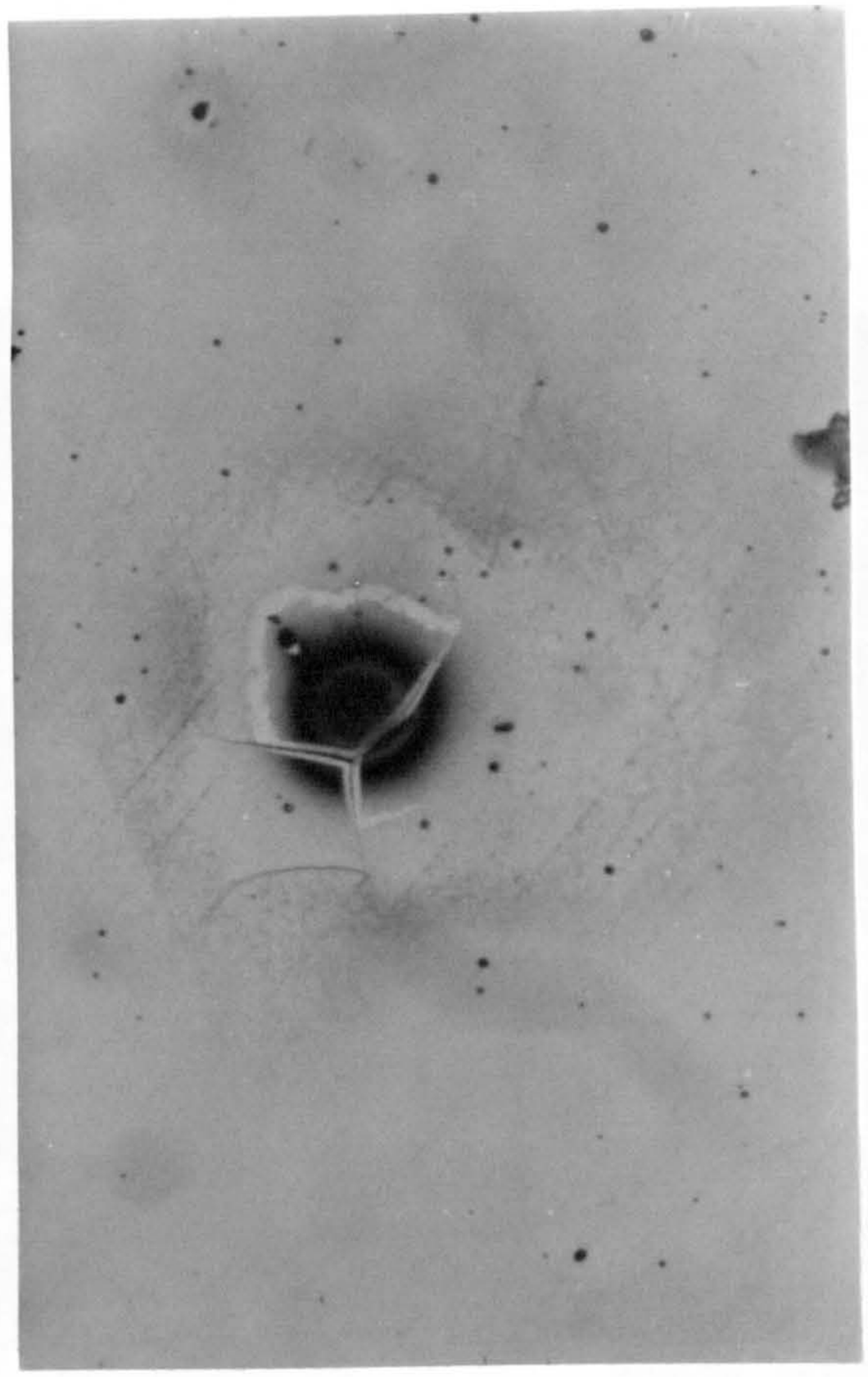

88

89

Figs 87-89 Micrographs of specimen anodically polarised in 0.05M H_2SO_4 + 0.1M NaCl and interrupted at the coordinates (768, 12)

Fig. 87 x 100

Fig. 88 As Fig. 87 x 500

Fig. 89 As Fig. 88
Oblique illumination

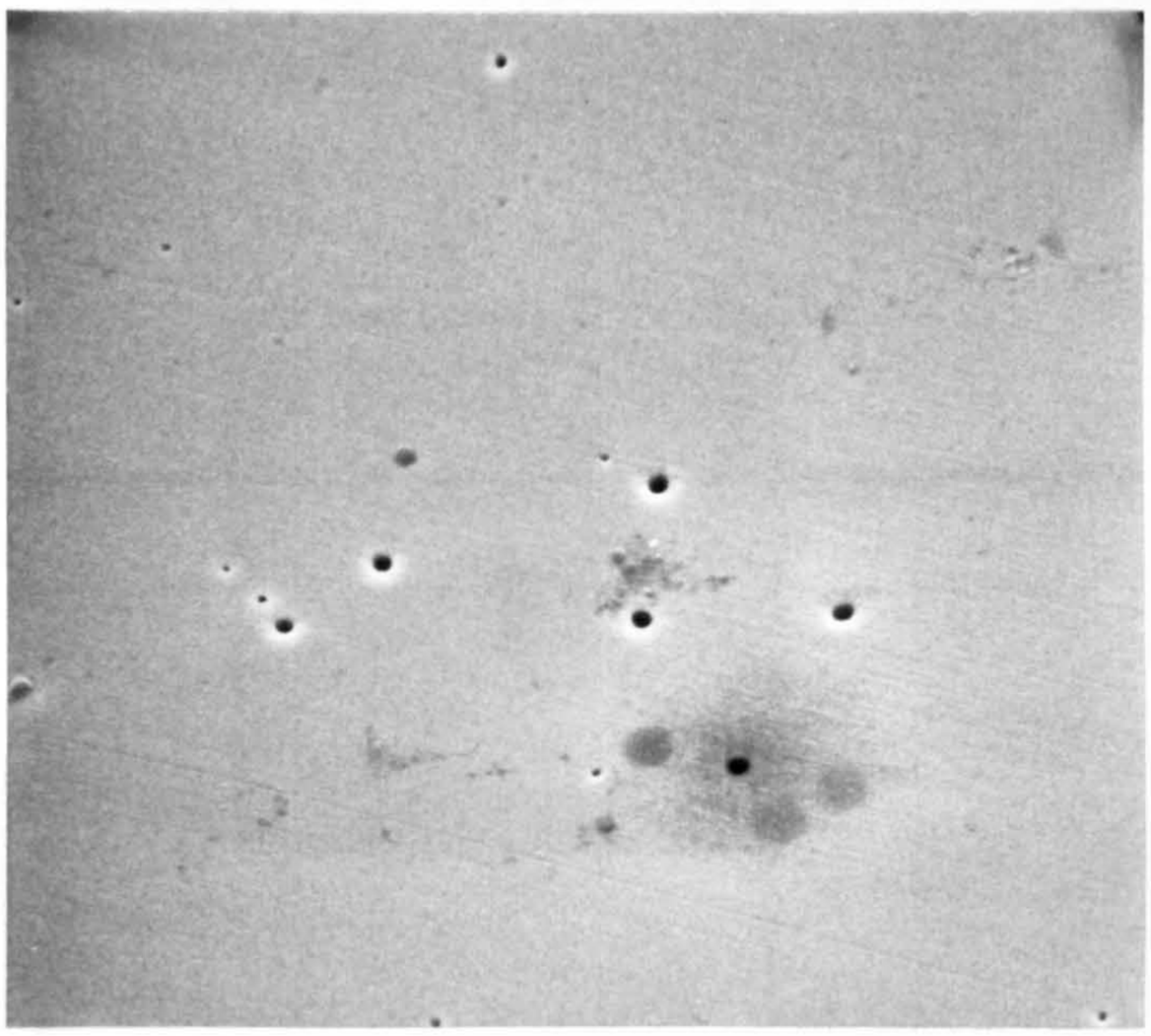

Fig. 90. Micrograph of specimen anodically polarised in 0.05M H_2SO_4 and interrupted at the coordinates (-290, 13) Active range. x2K

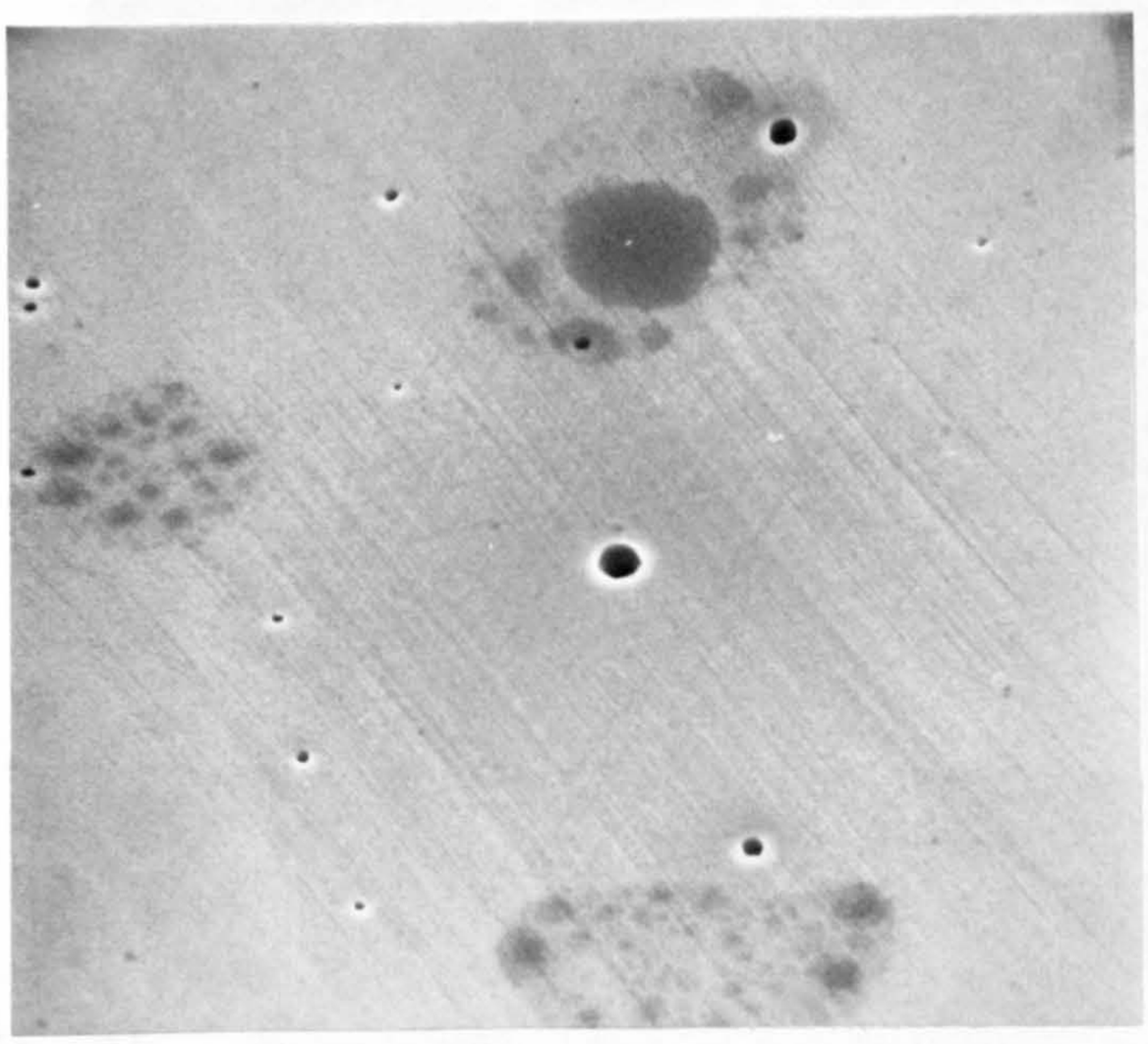

Fig. 91. Micrograph of specimen anodically polarised in 0.05M H_2SO_4 and interrupted at the coordinates (230, 1.5). Passive range. 2K

Fig. 92. As Fig. 91 showing a inclusion. 5K undergoing dissolution.

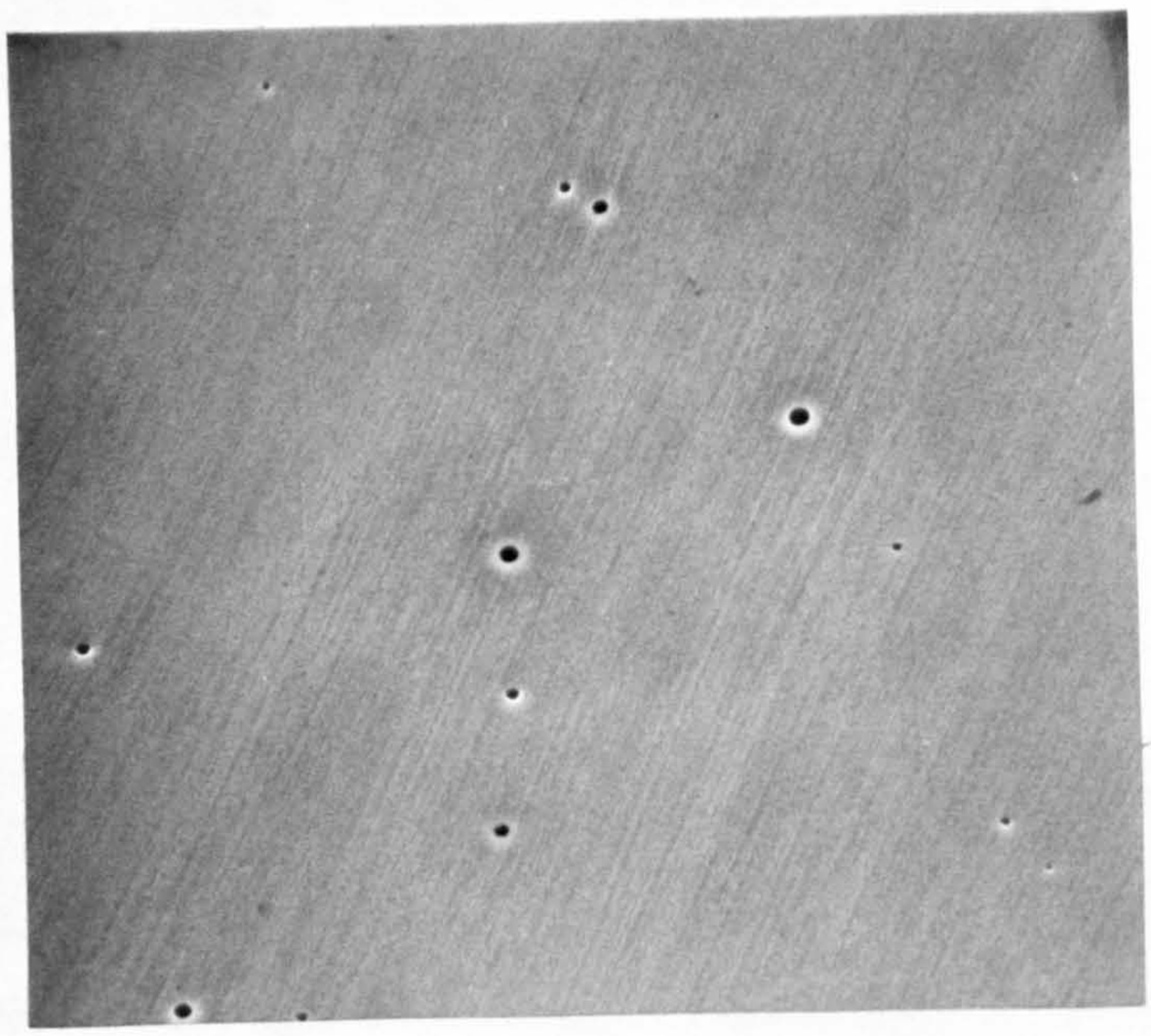

Fig. 93. Micrograph of specimen anodically polarised in 0.05M H_2SO_4 and interrupted at the coordinates (860, 15). Transpassive range. 2K.

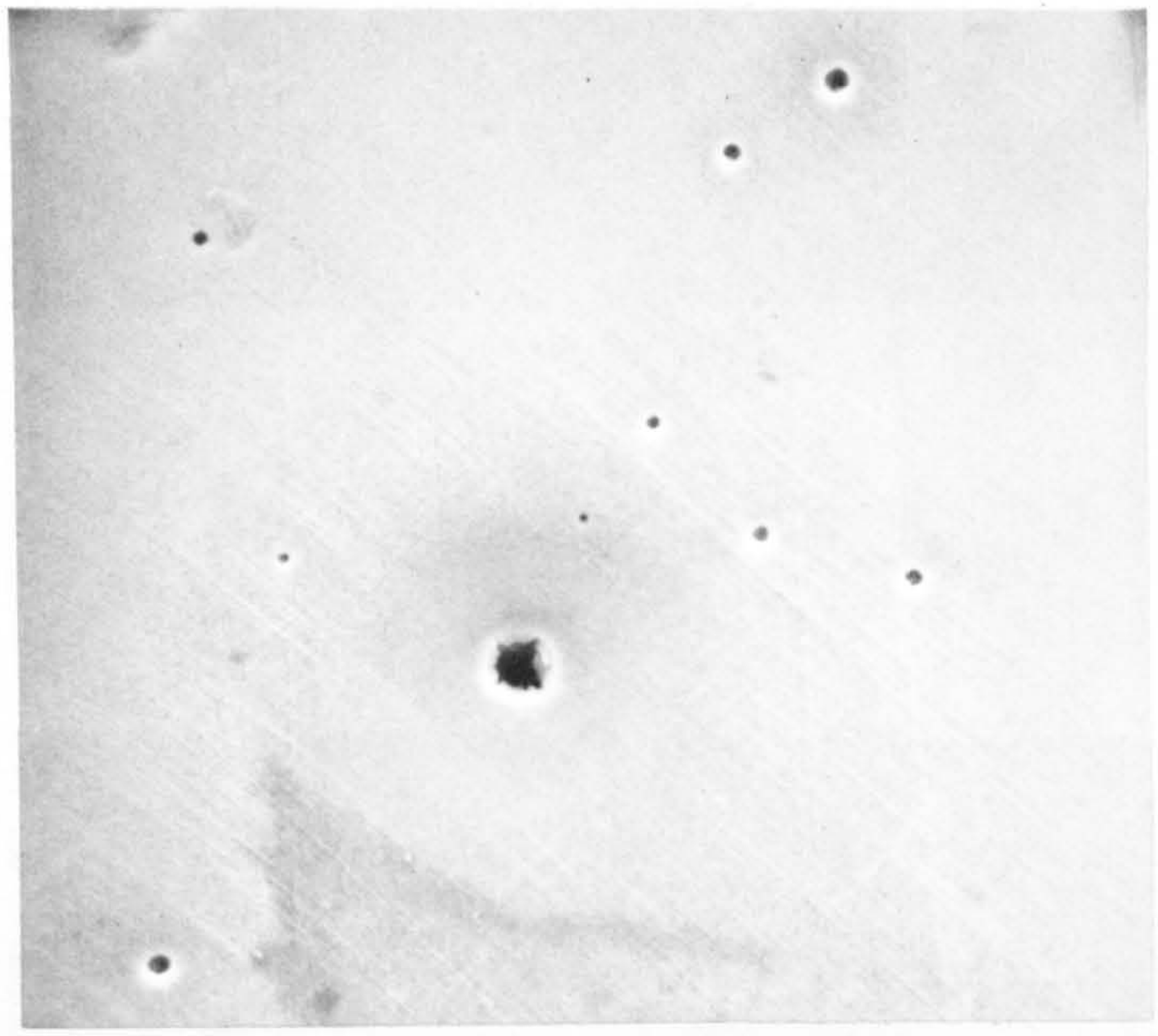

Fig. 94. Micrograph of specimen anodically polarised in 0.05M H_2SO_4 + 0.1M NaCl and interrupted at the coordinates (-284, 17.0) Active range. 2K.

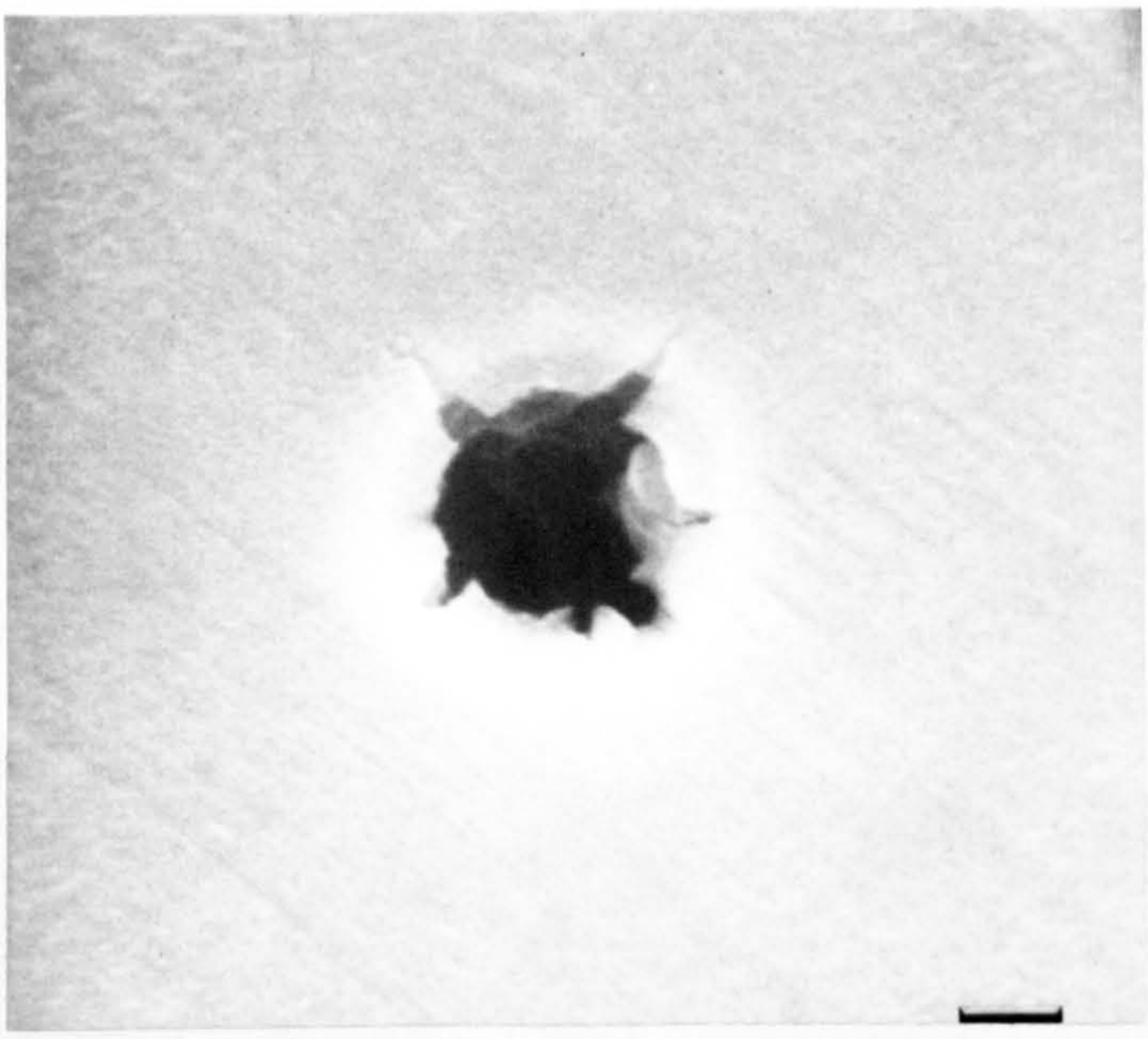

Fig. 95. As Fig. 94. Close view of a pit-site. 5K.

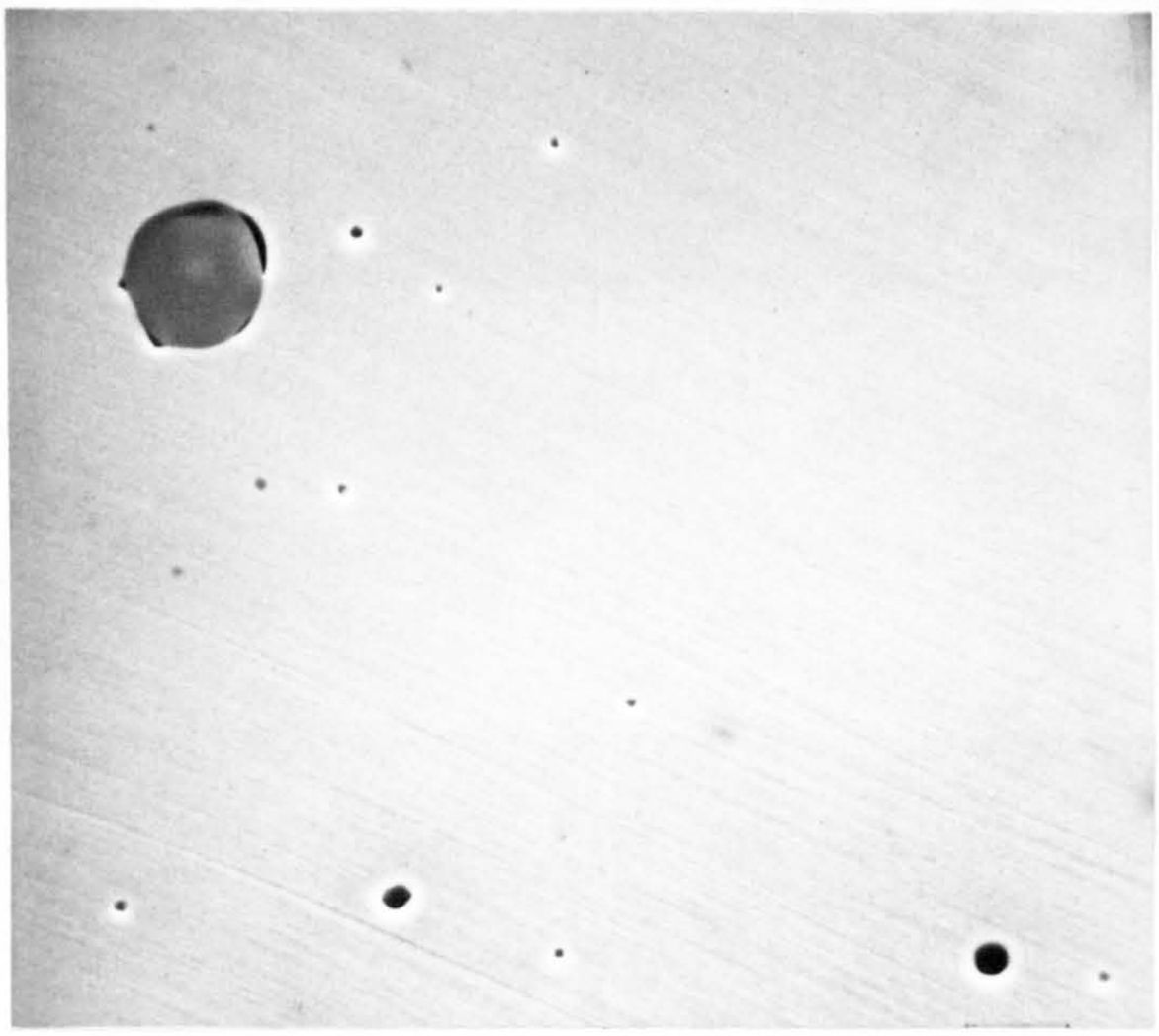

Fig. 96. Micrograph of specimen anodically polarised in 0.05M H_2SO_4 + 0.1M NaCl and interrupted at the coordinate (100, 1.5). Passive range. 2K.

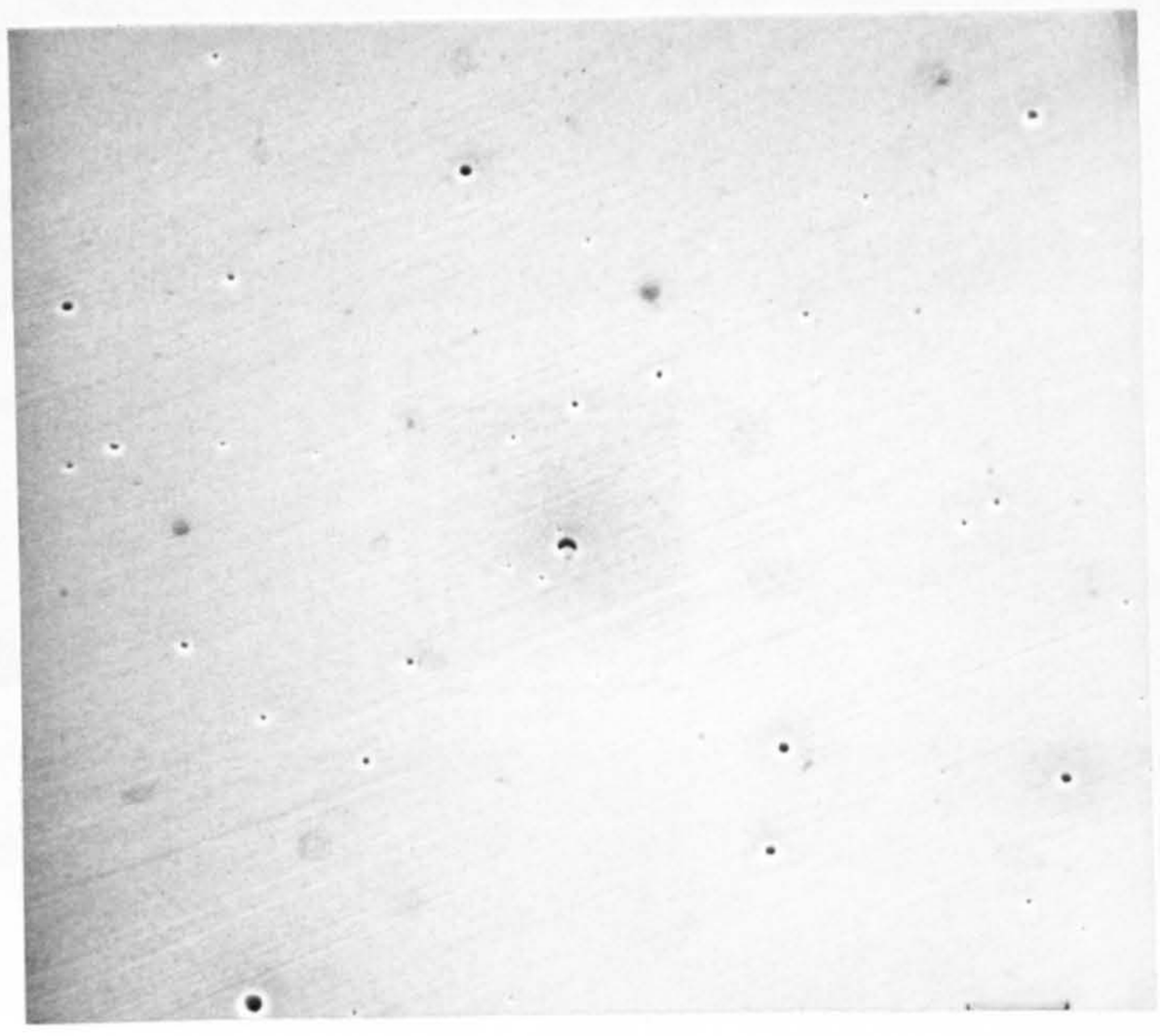

Fig. 97. Micrograph of specimen anodically polarised in 0.05M H_2SO_4 + 0.1M NaCl and interrupted at the coordinate (768, 12). Pitting range. 1K.

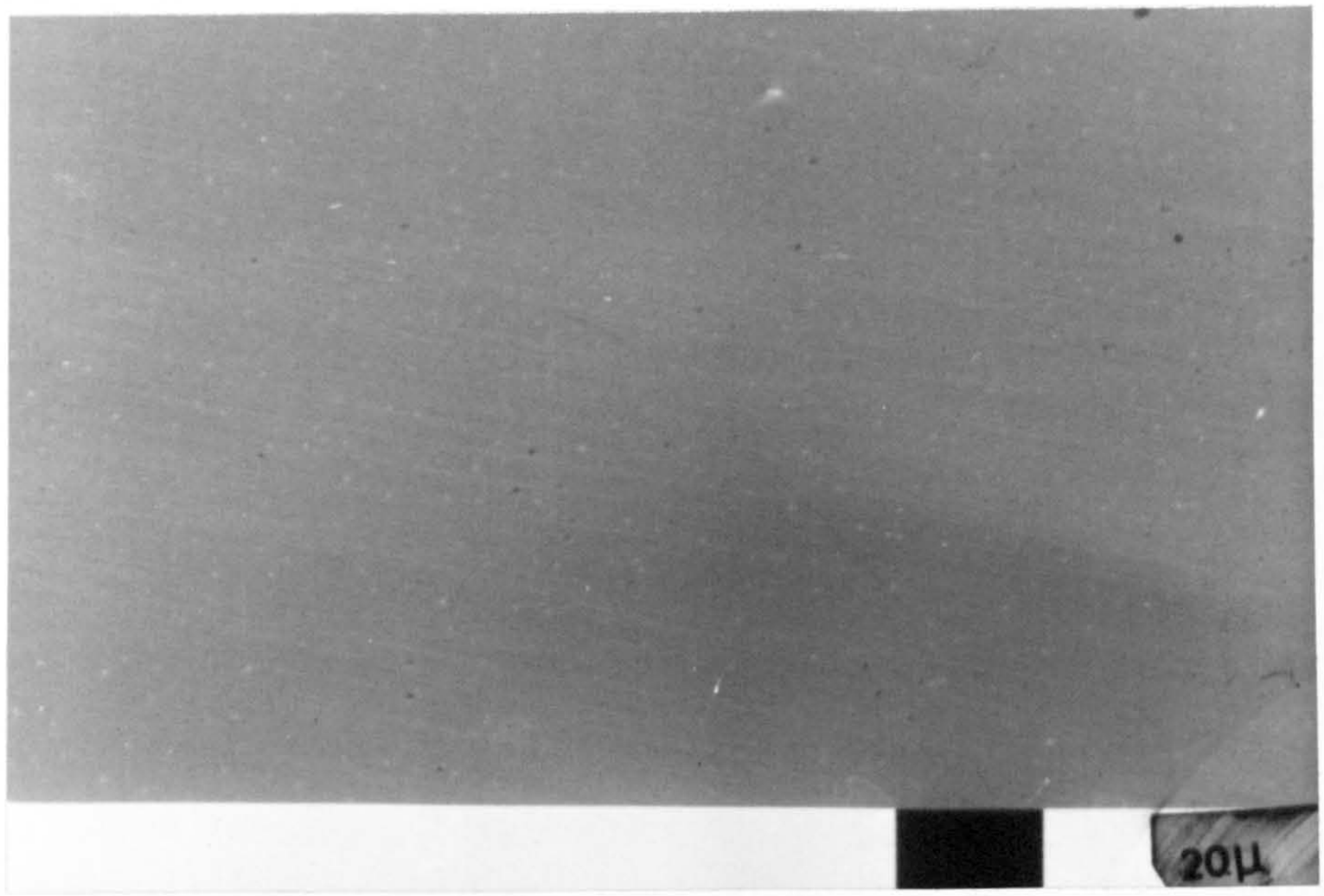

Fig. 98. Micrograph of a polished surface prior to immersion in a test solution. 1K.

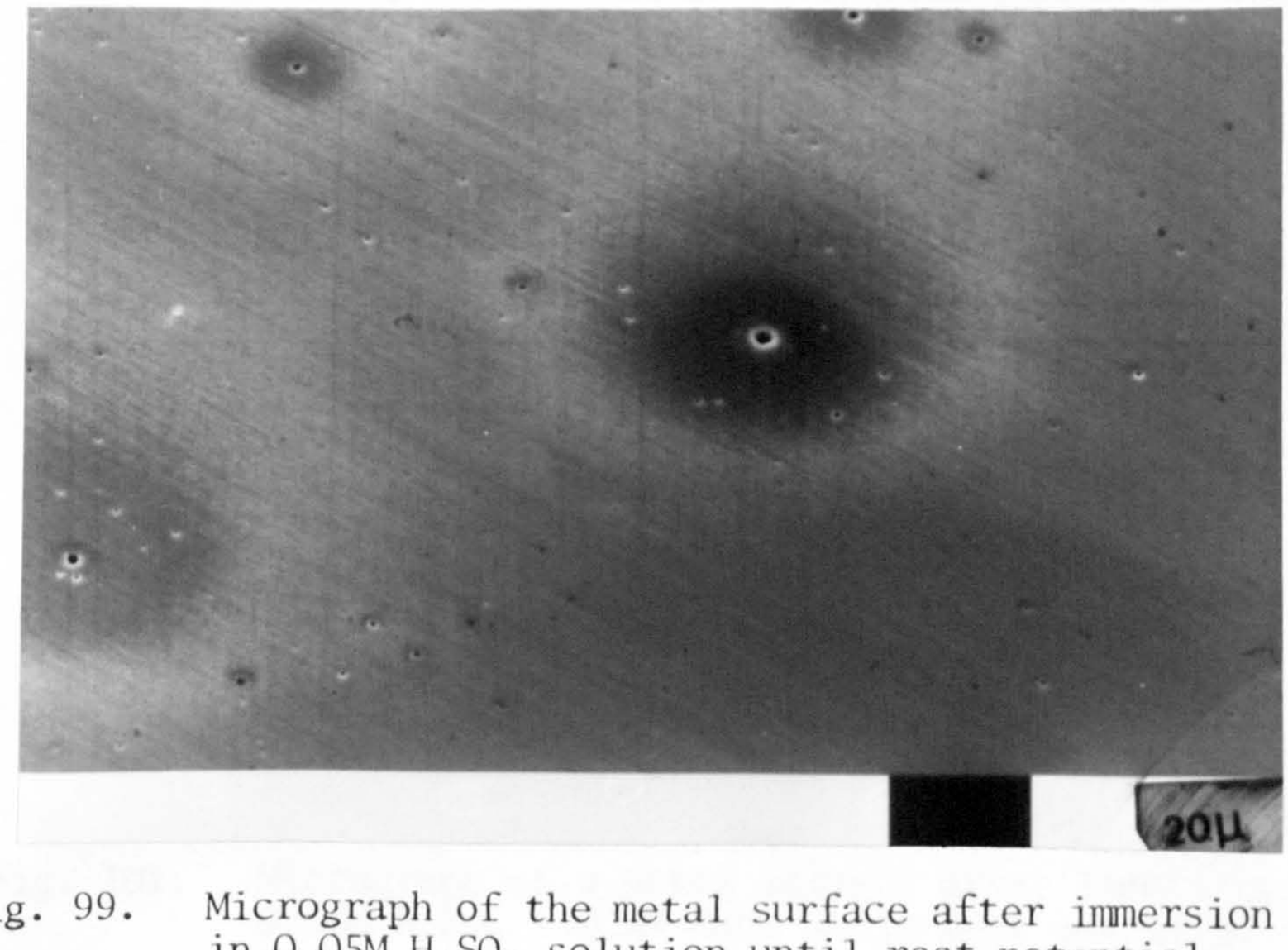

Fig. 99. Micrograph of the metal surface after immersion in 0.05M H_2SO_4 solution until rest potential measurement, ^tE_R. 1K.

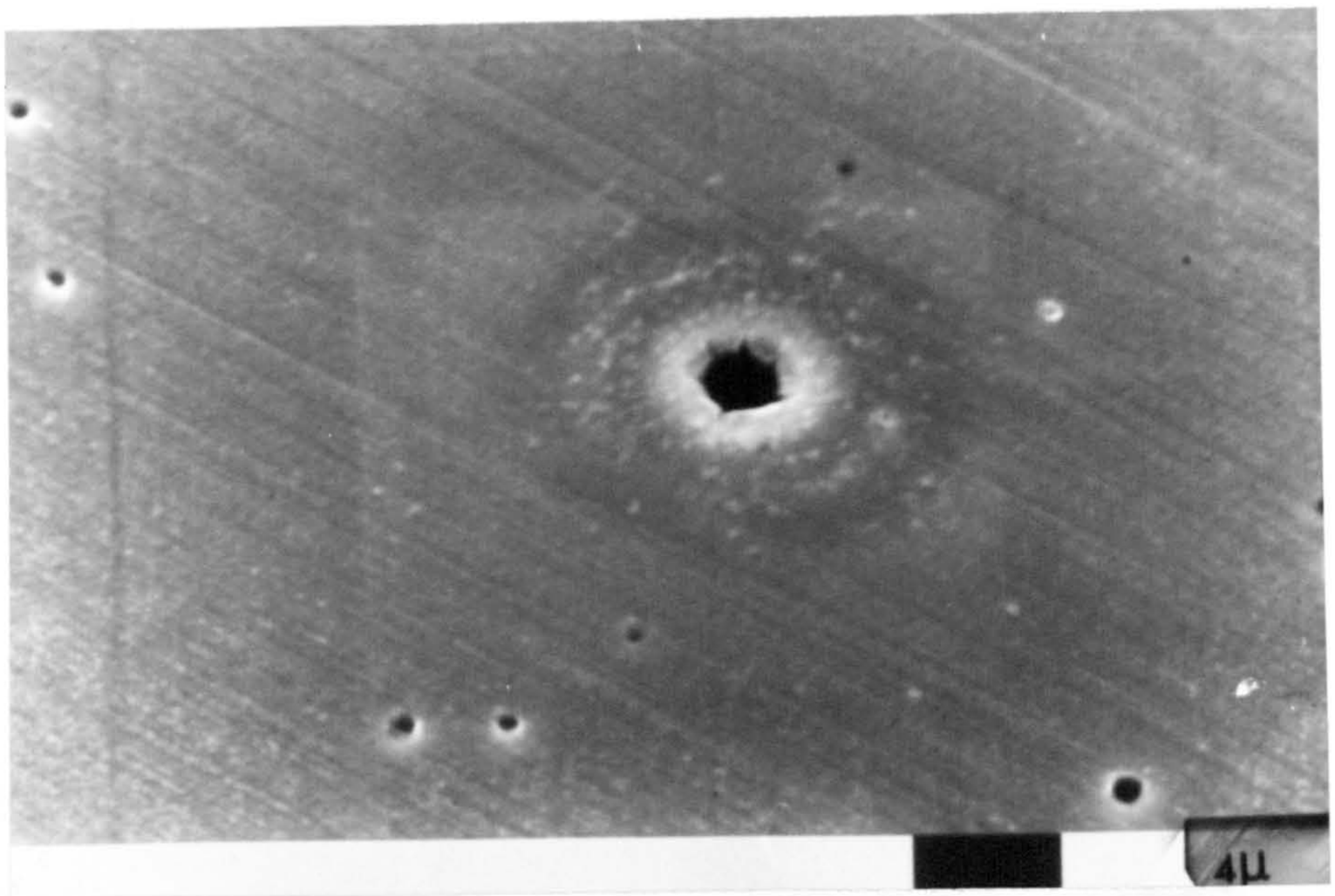

Fig. 100. As Fig. 99, close view of a pit-site. 5K.

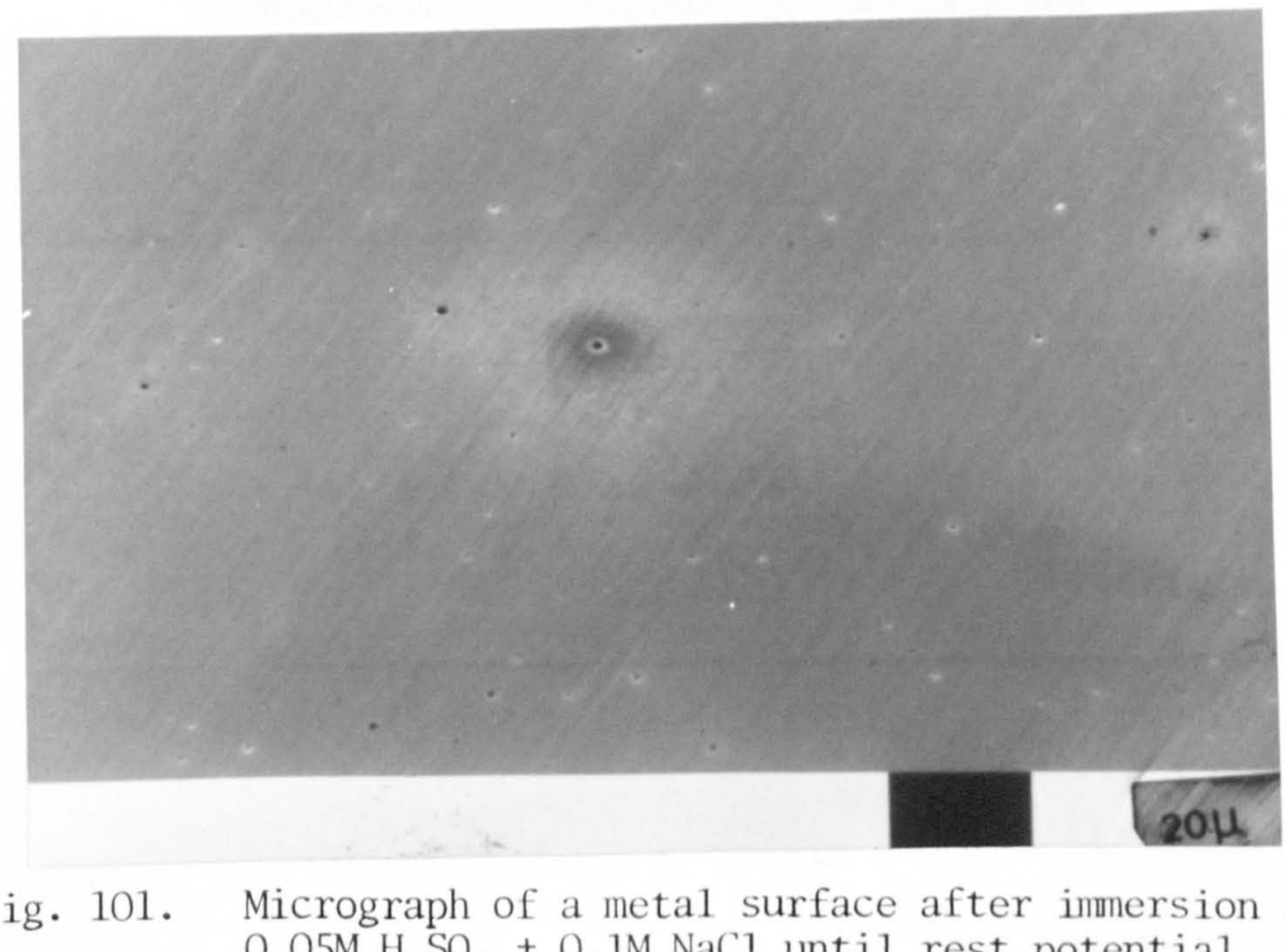

Fig. 101. Micrograph of a metal surface after immersion in 0.05M H_2SO_4 + 0.1M NaCl until rest potential measurement. 1K.

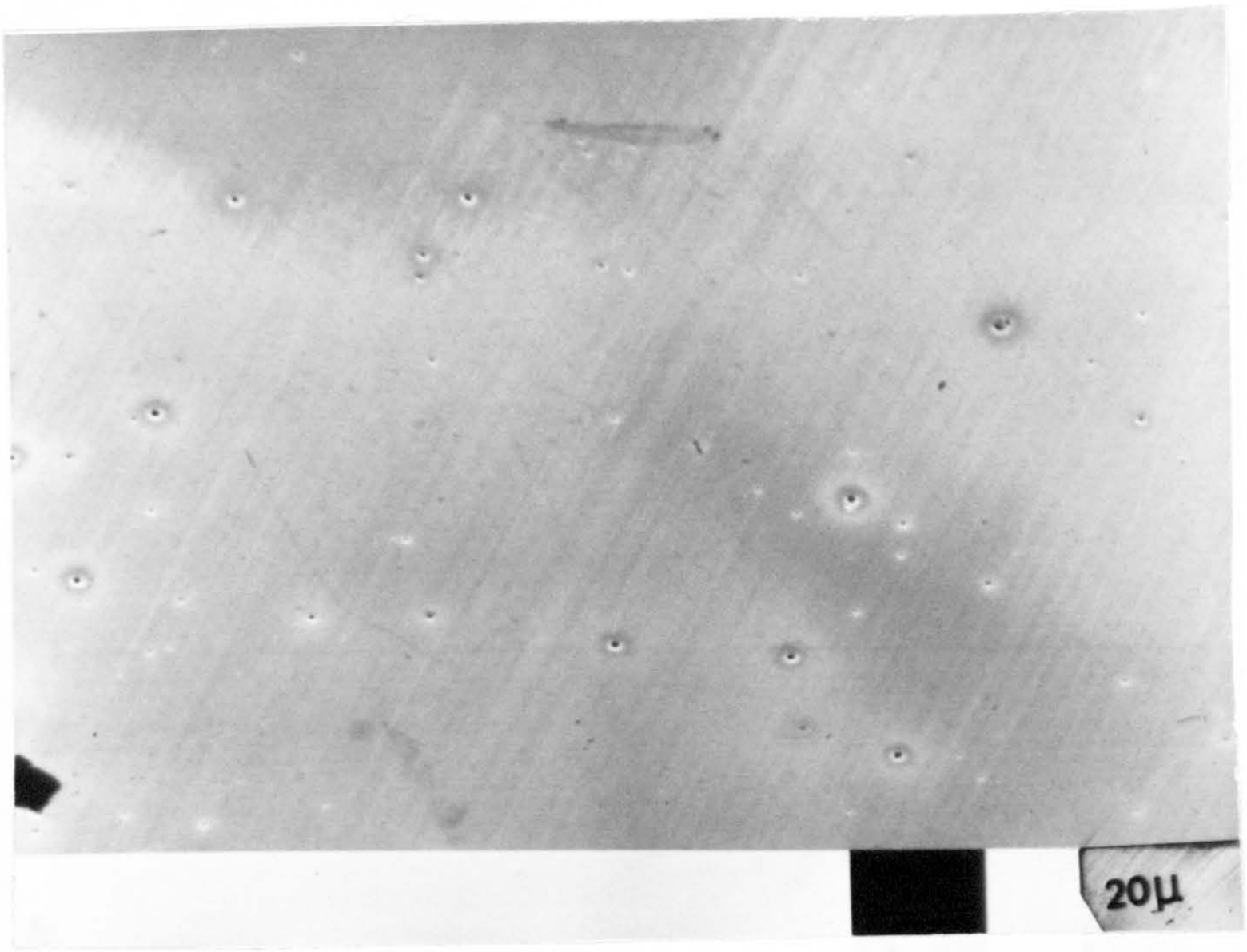

Fig. 102. Example of the micrographs used for the pit-site counting in specimens tested in 0.05M H_2SO_4 solutions. Actual size. 1K.

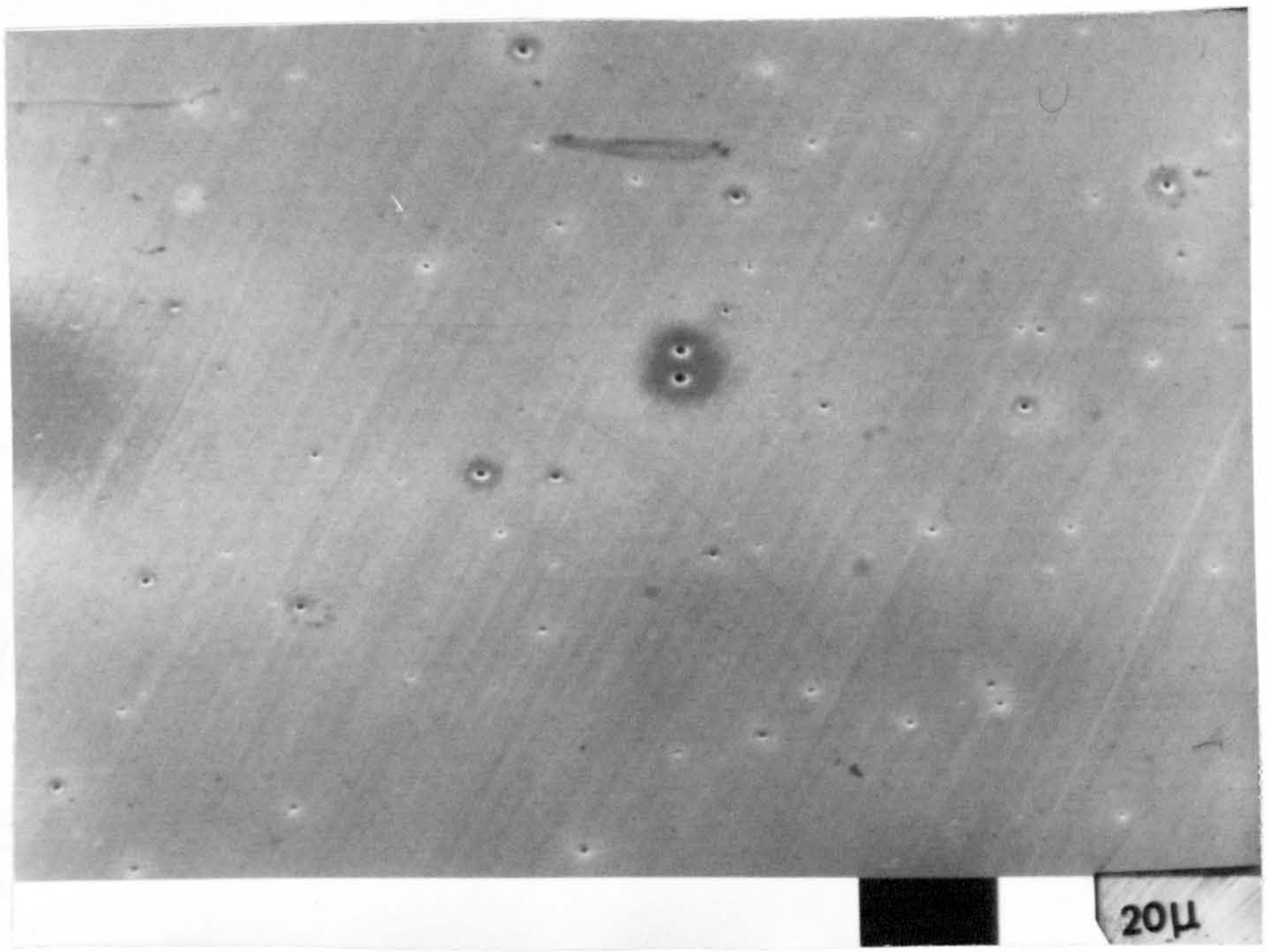

Fig. 103. Example of the micrographs used for the pit-site countings in specimens tested in 0.05M H_2SO_4 + 0.1M NaCl Actual size. 1K.

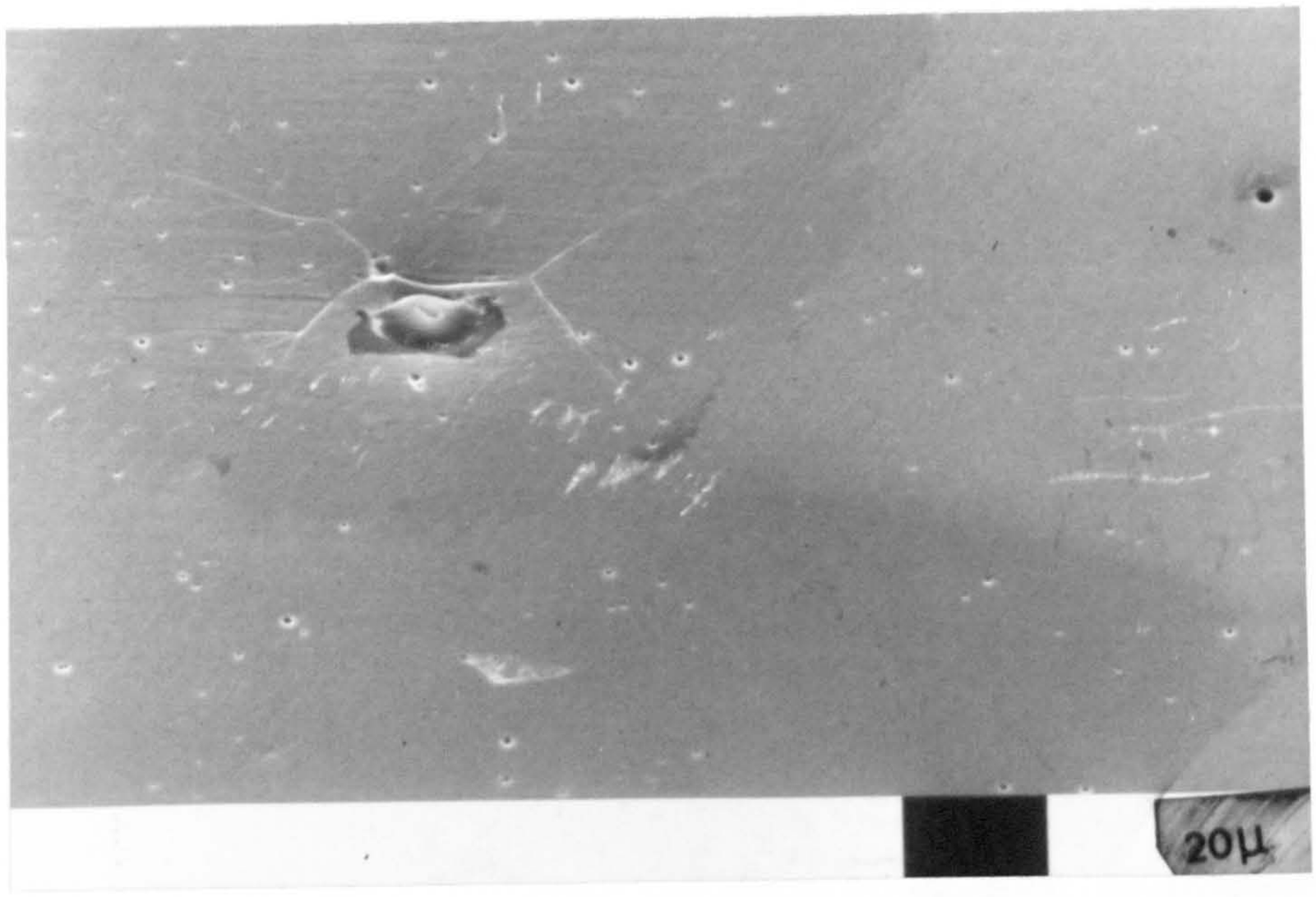

Fig. 104. Micrograph of specimen anodically polarised in 0.05M H_2SO_4 and interrupted at the coordinates (1000, 400). Initial formation of etch-pattern in the transpassive range. 1K.

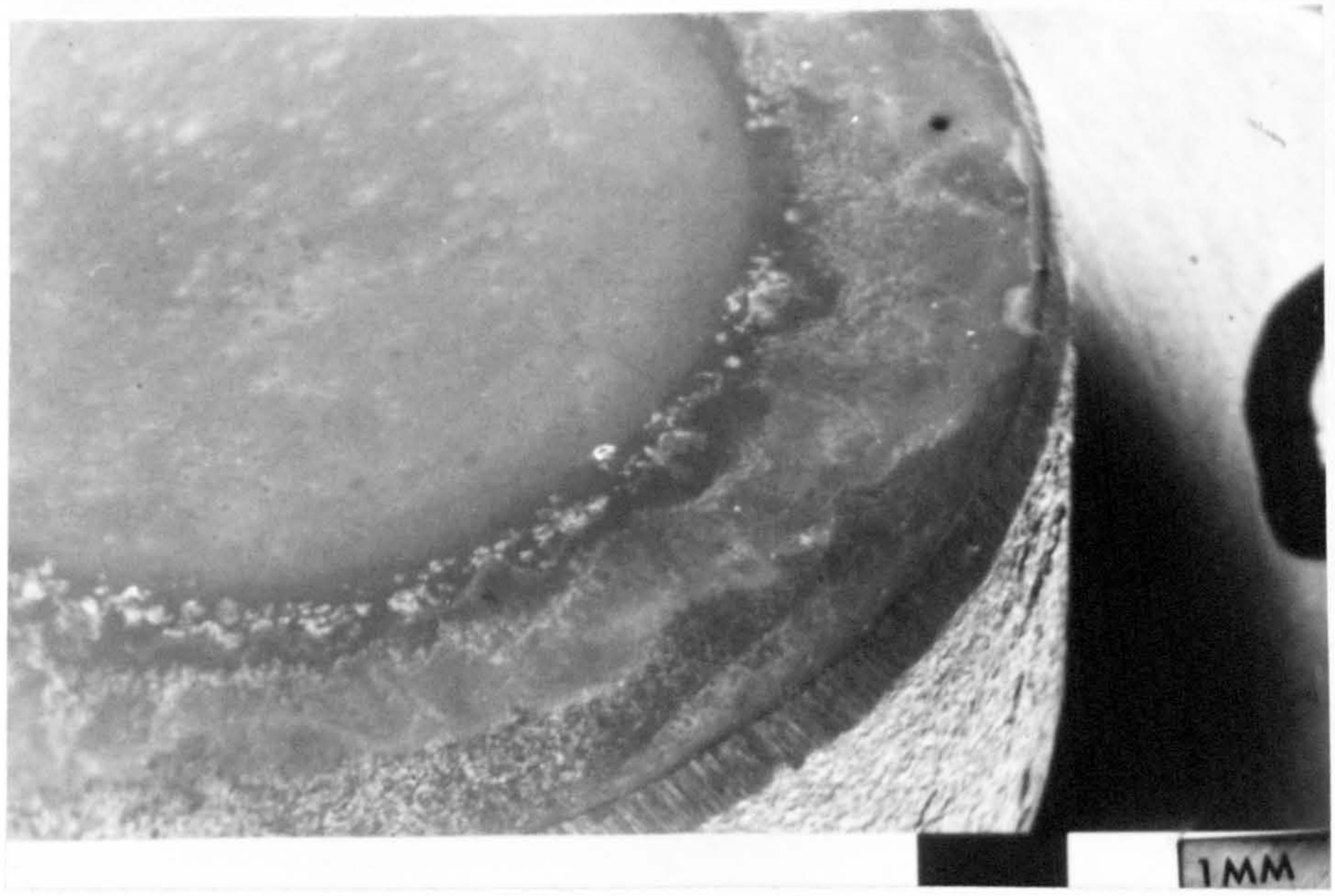

Fig. 105. Micrograph of specimen anodically polarised in 0.05M H_2SO_4 + 0.1M NaCl and interrupted at the coordinates (790, 400). Pitting range. General view of the surface. 50X.

Fig. 106. As Fig. 105. Closer view of the surface area covered by the gasket. Feature A typical cervice morphology. Feature B, pits well developed. Feature C, general dissolution areas. x200.

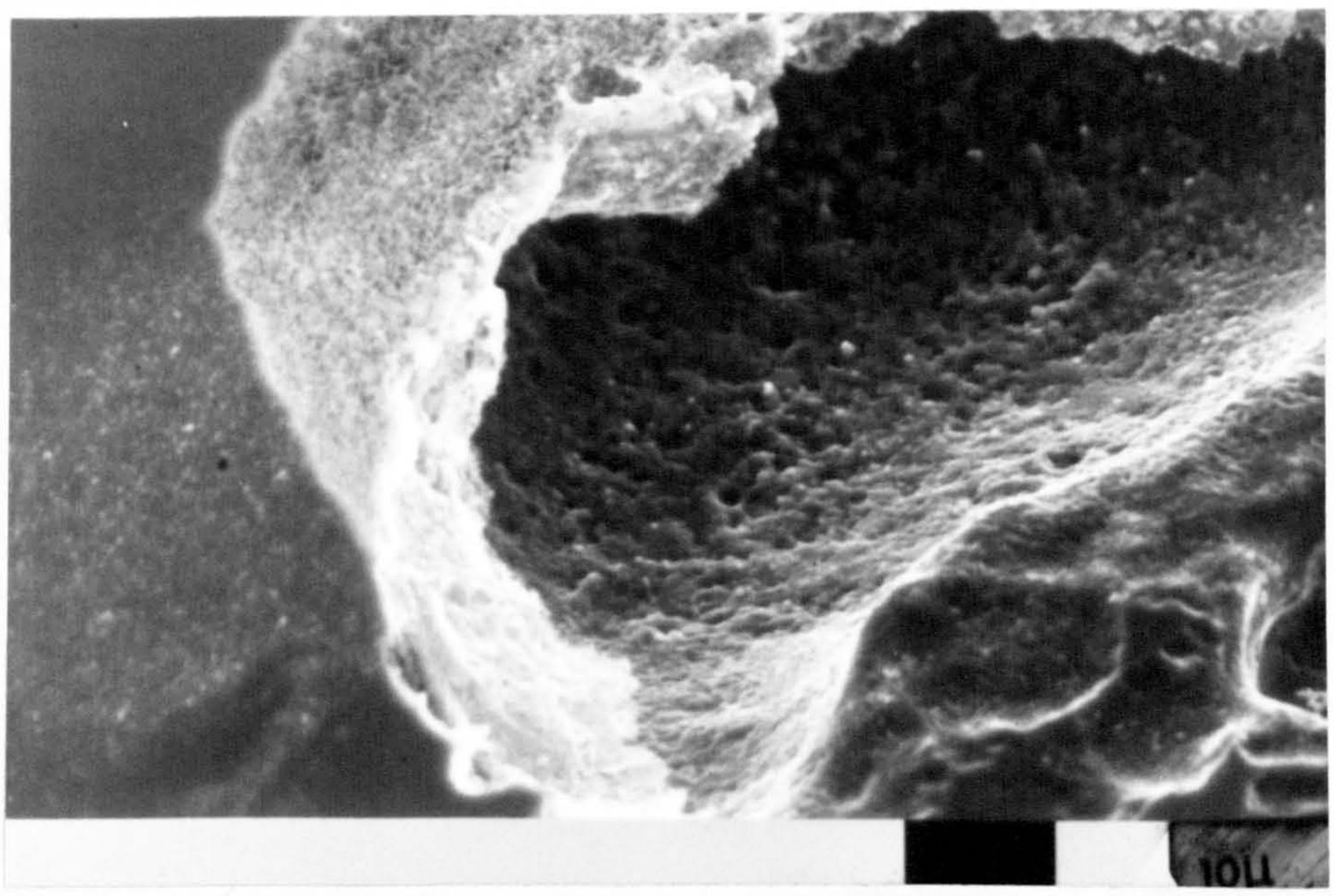

Fig. 107. Close view of feature A in Fig. 106. 2K.

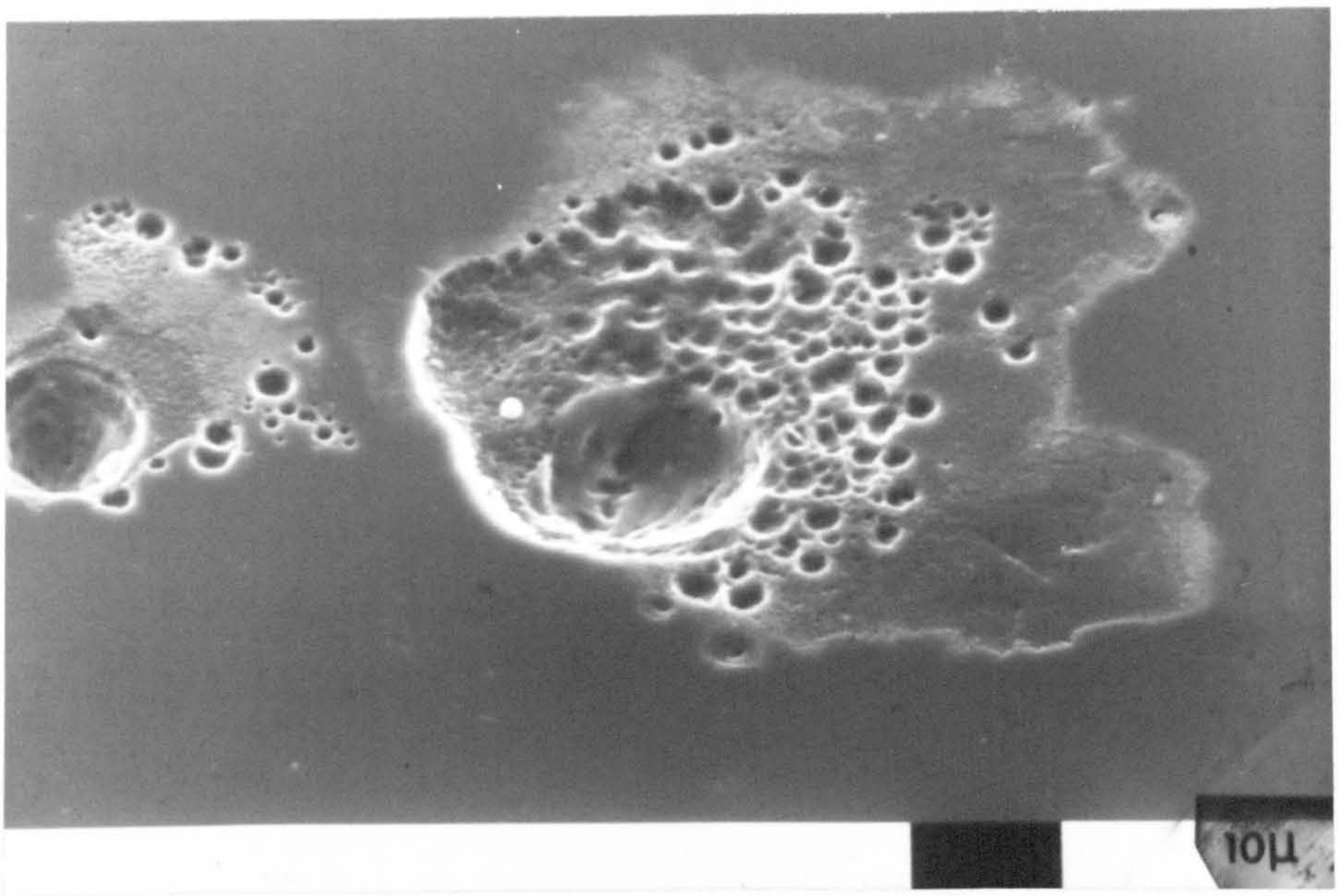

Fig. 108. Close view of feature B in Fig. 106. 2K.

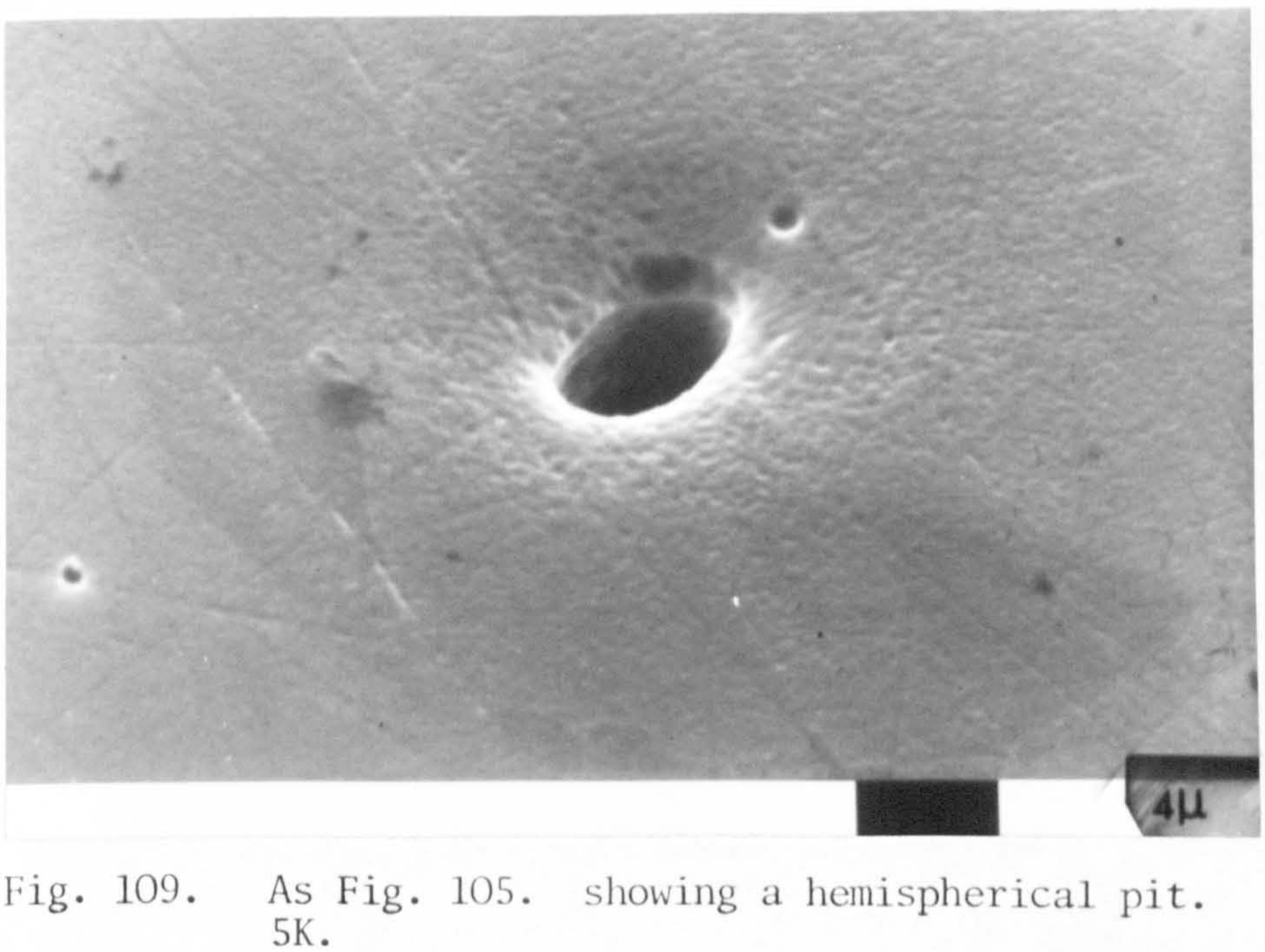

Fig. 109. As Fig. 105. showing a hemispherical pit. 5K.

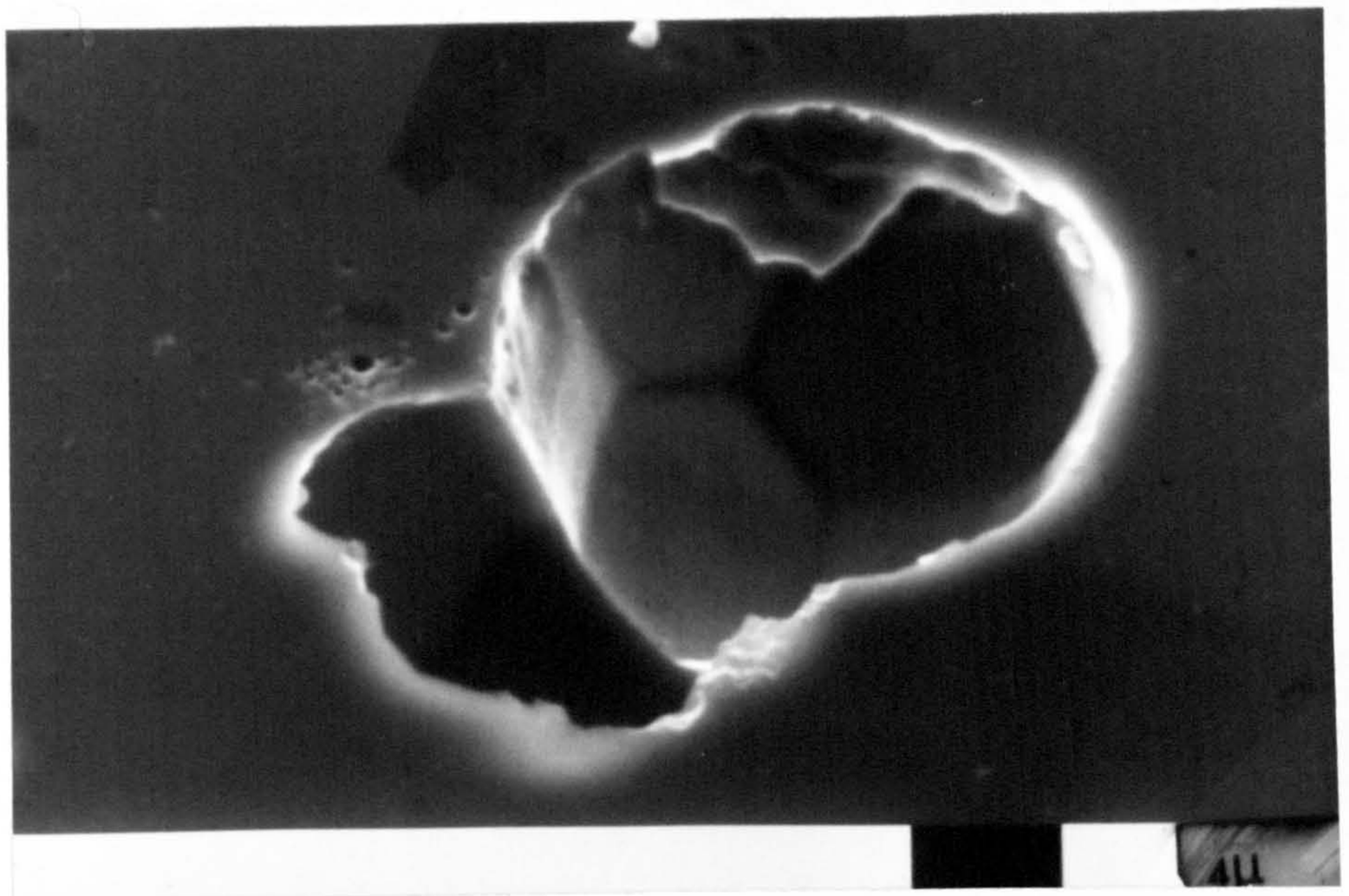

Fig. 110. As Fig. 105. showing a crystallographic pit. x5K.

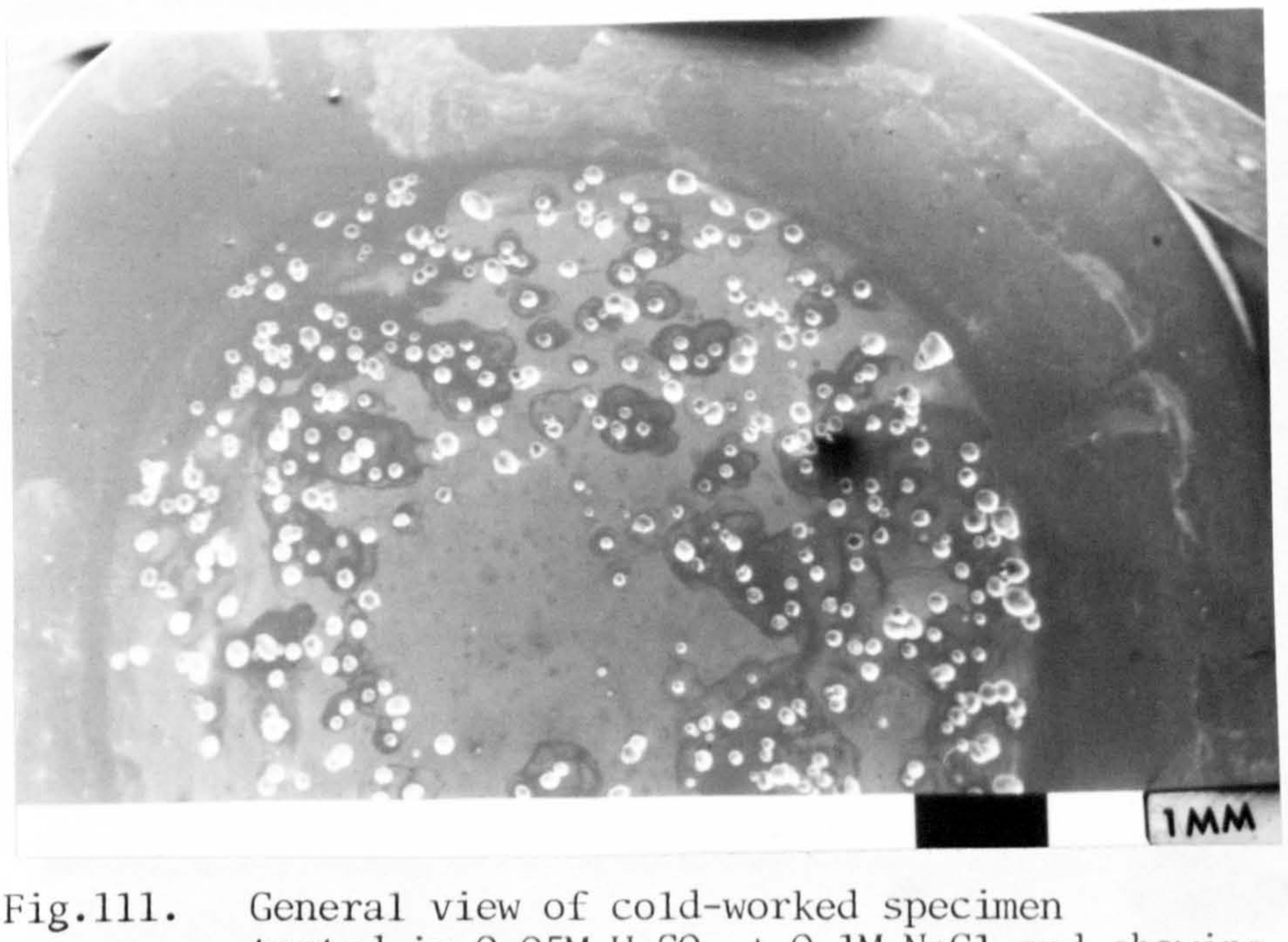

Fig.111. General view of cold-worked specimen tested in 0.05M H_2SO_4 + 0.1M NaCl and showing a severe localised attack on the surface. x50.

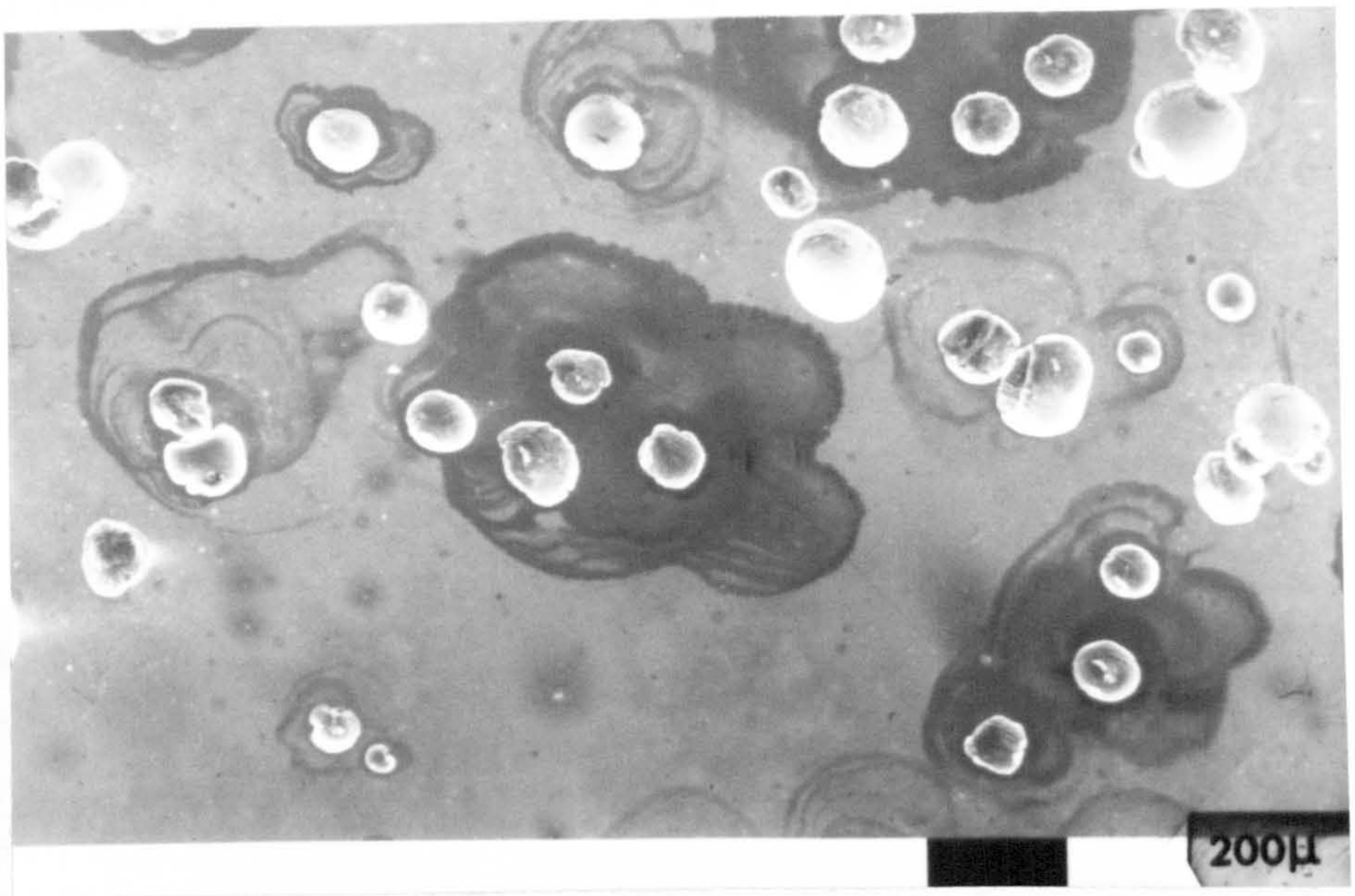

Fig. 112. As Fig. 111. Closer view showing polished an non-polished pits. x500.

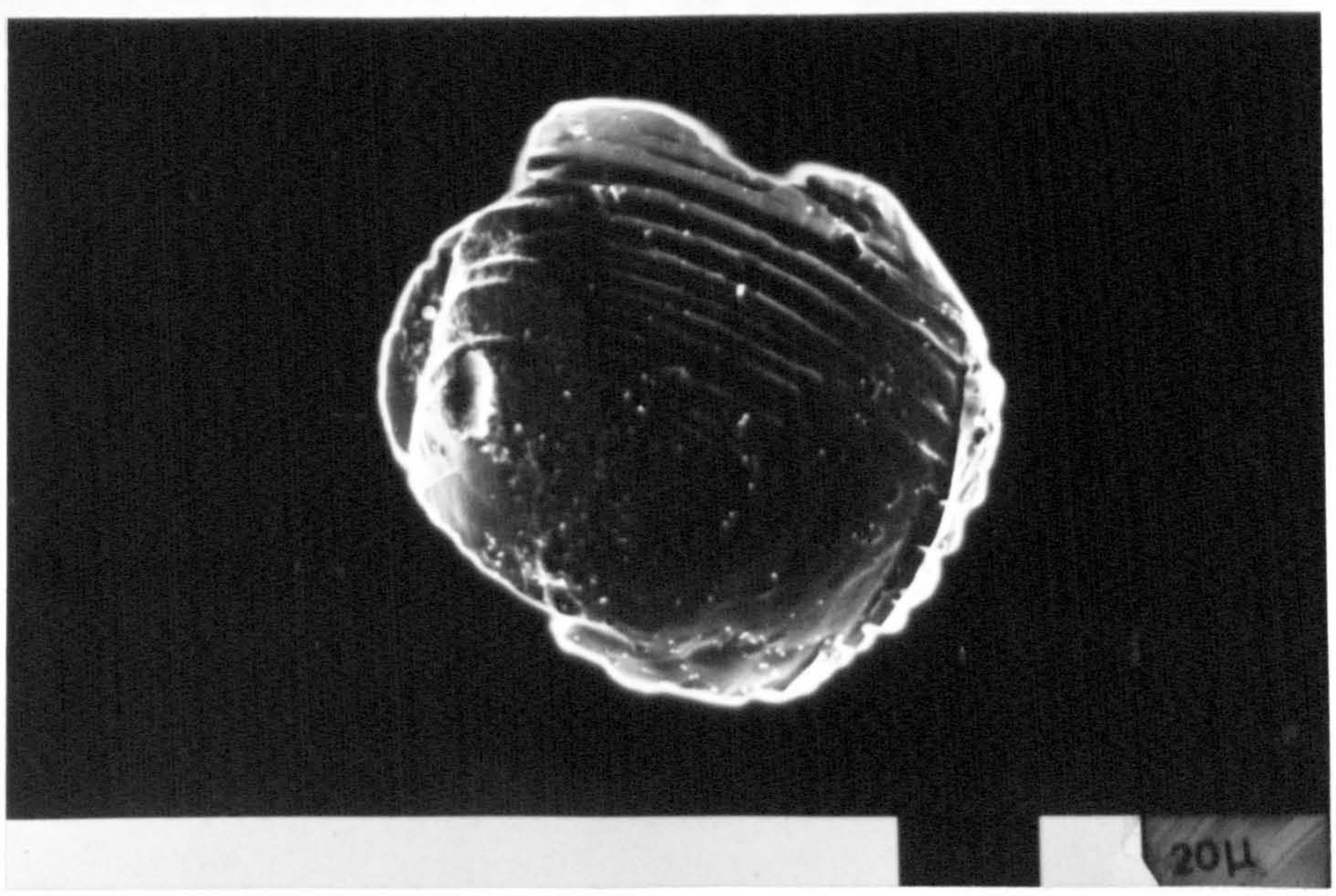

Fig. 113. As Fig. 111. Close view of a non-polished pit showing striations. x1K.

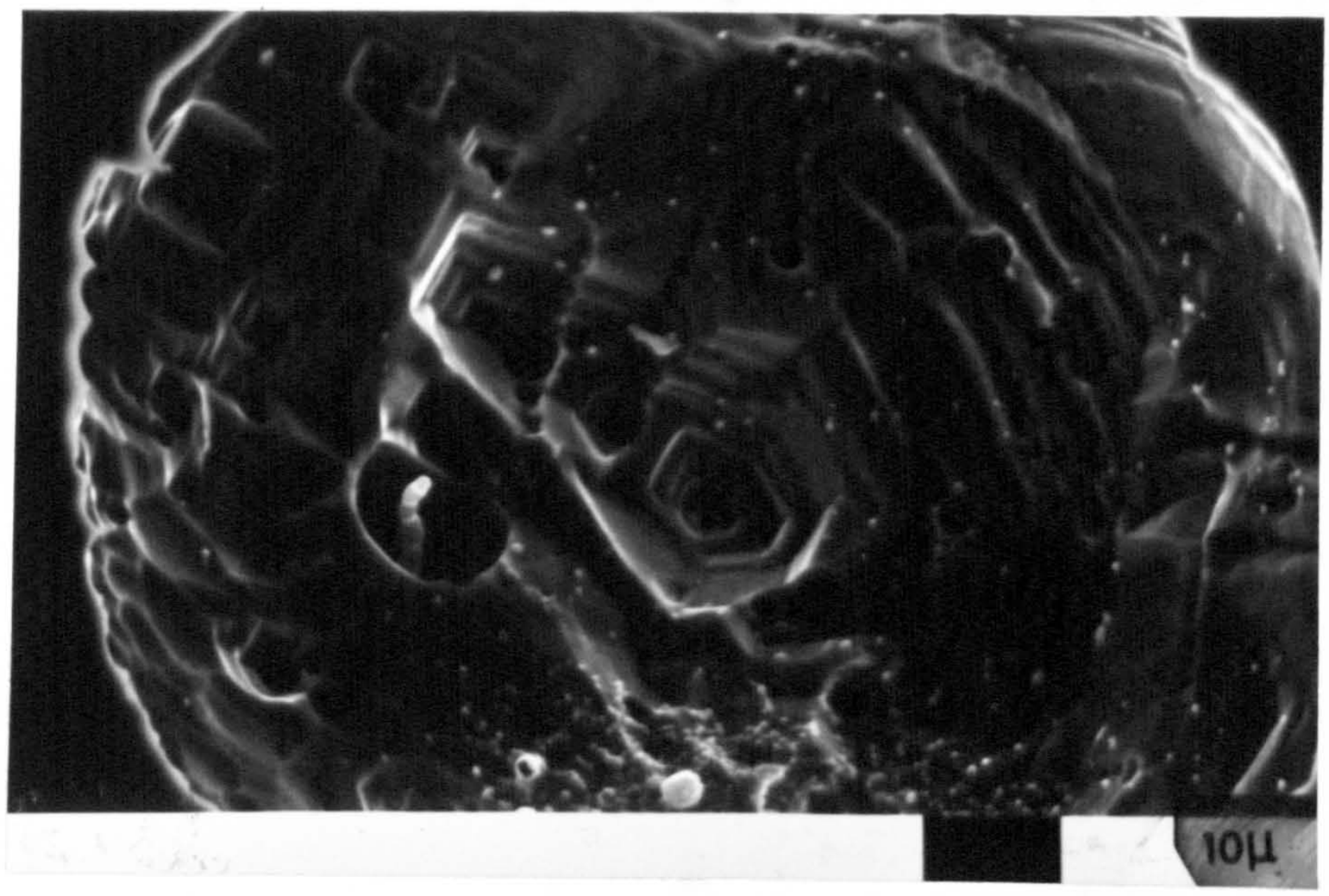

Fig. 114. As Fig. 111. Close view of a non-polished pit showing crystallographic propagation of the dissolution process. x2K.

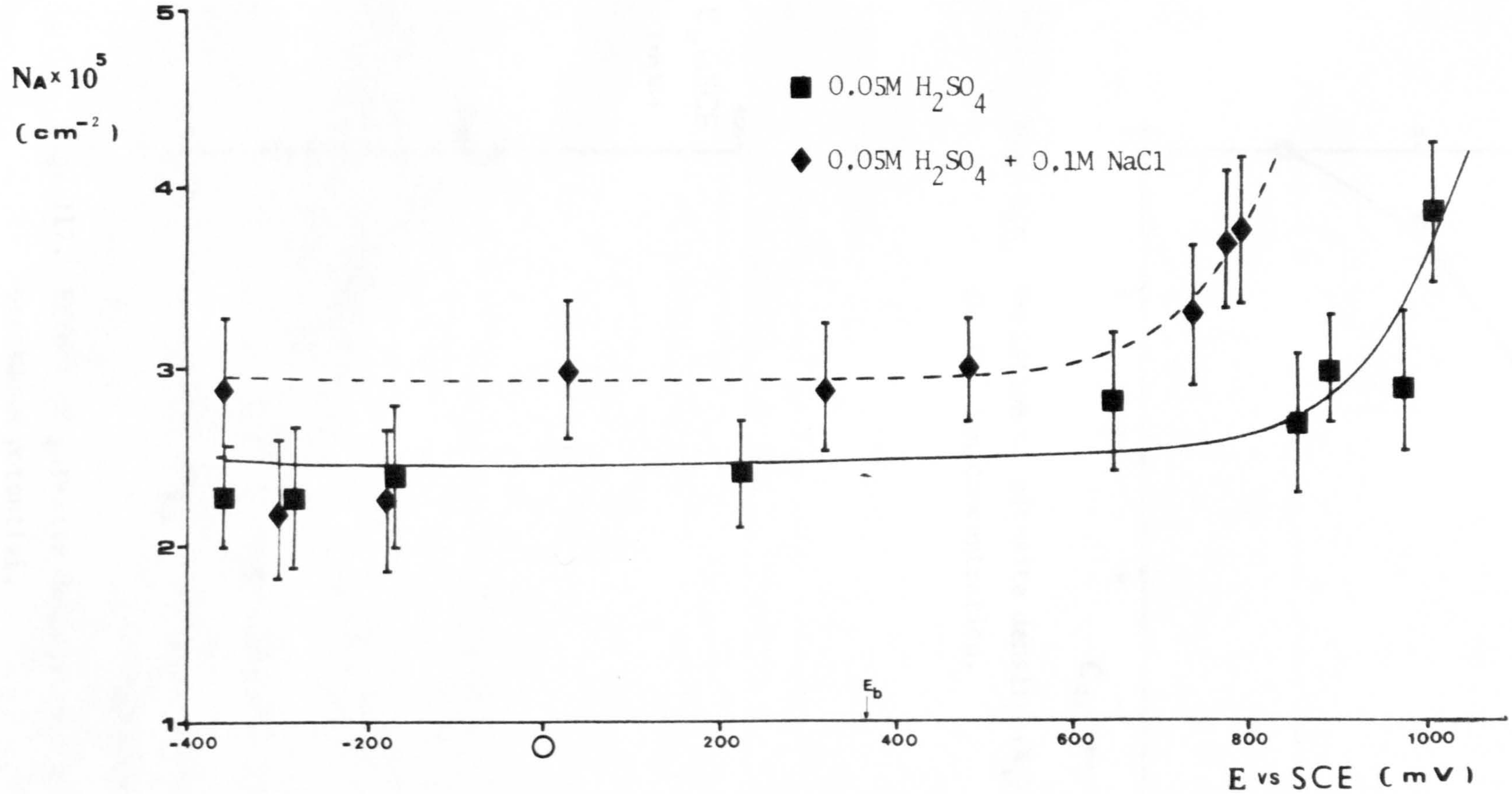

Fig. 115. Variation of pit-site density (N_A) with the metal-electrode potential.

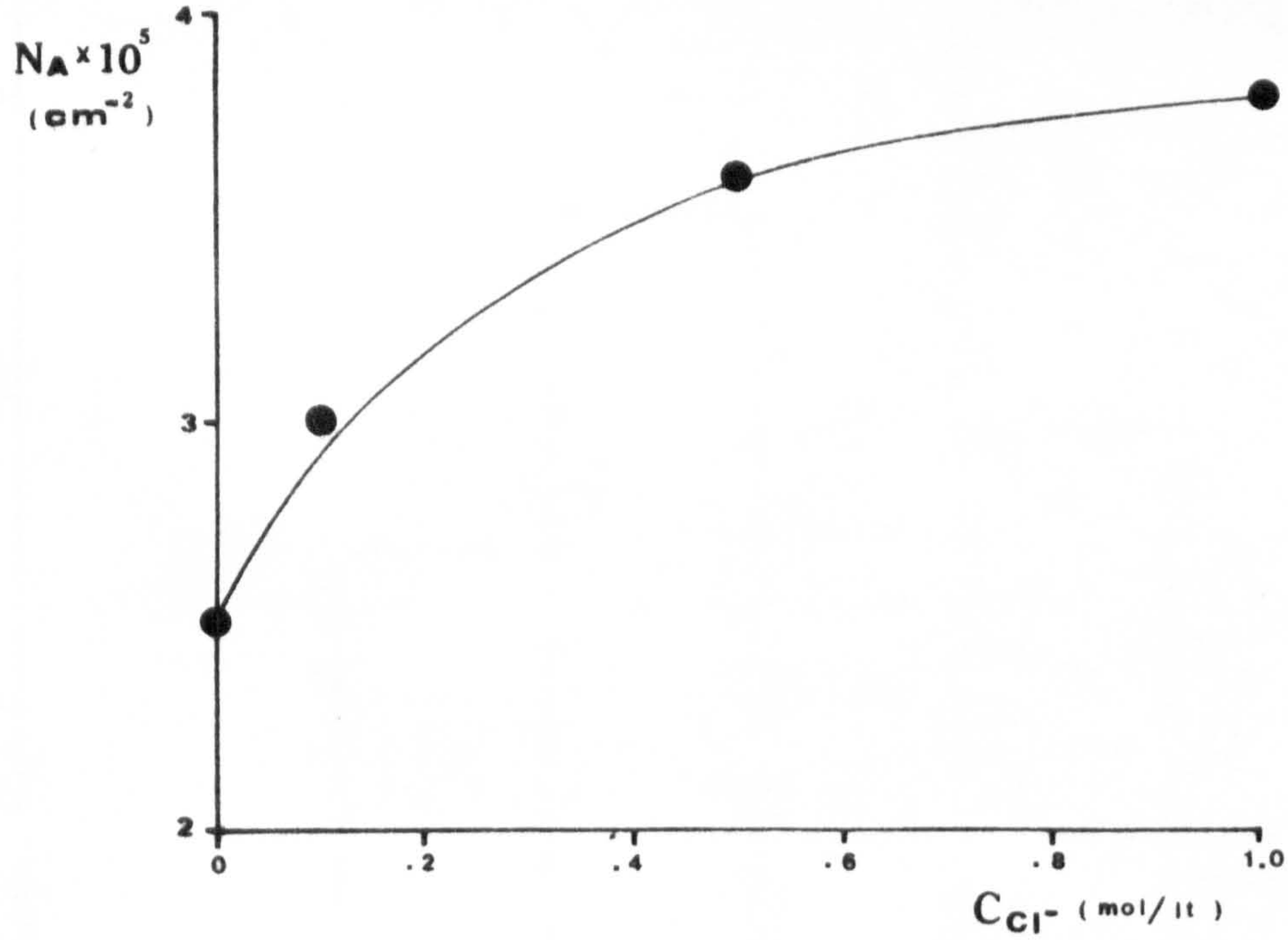

Fig. 116, Variation of pit-site density (N_A) with the Cl^- ion concentration.

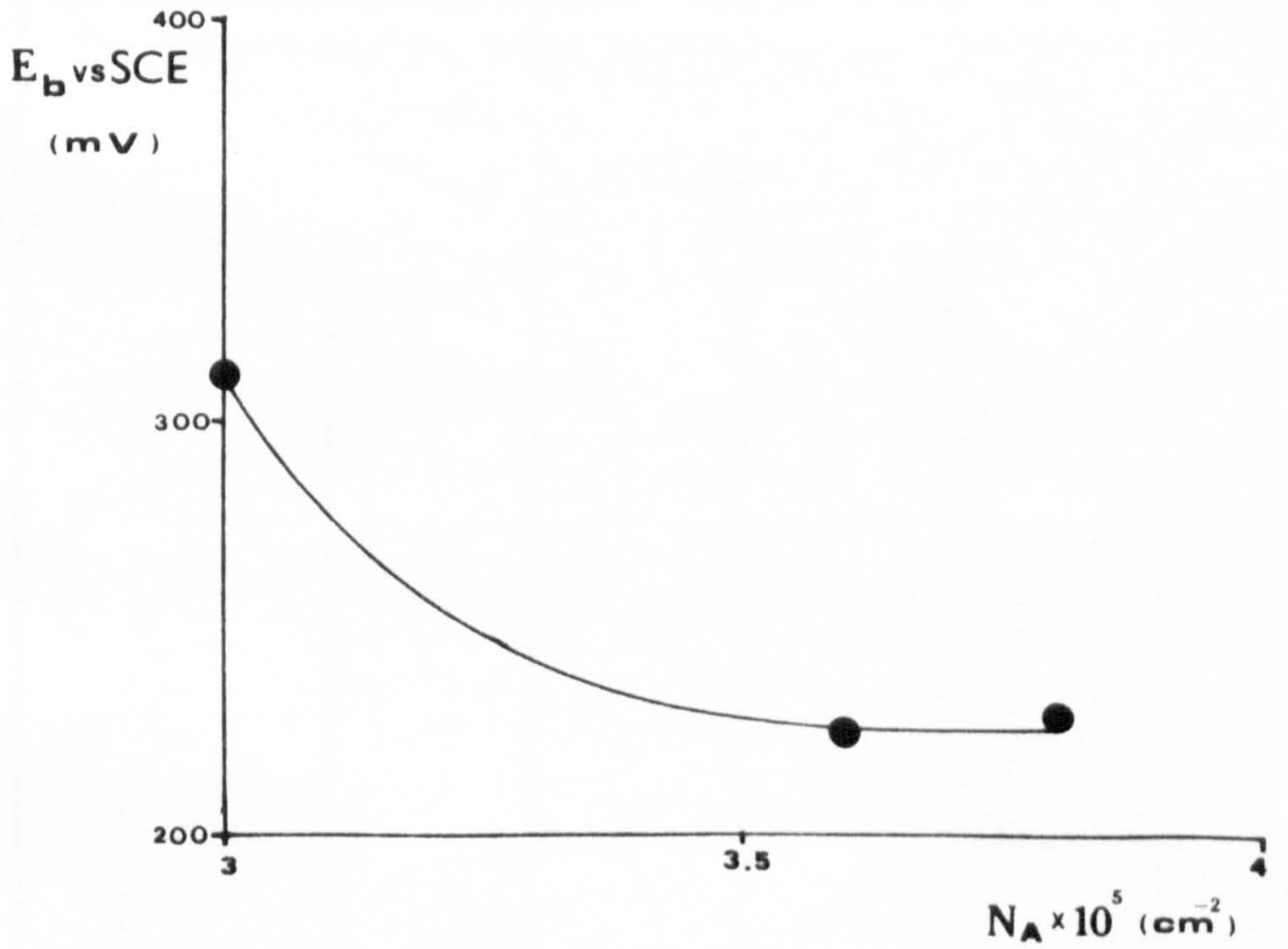

Fig. 117. Effect of pit-site density (N_A) on the breakdown potential.

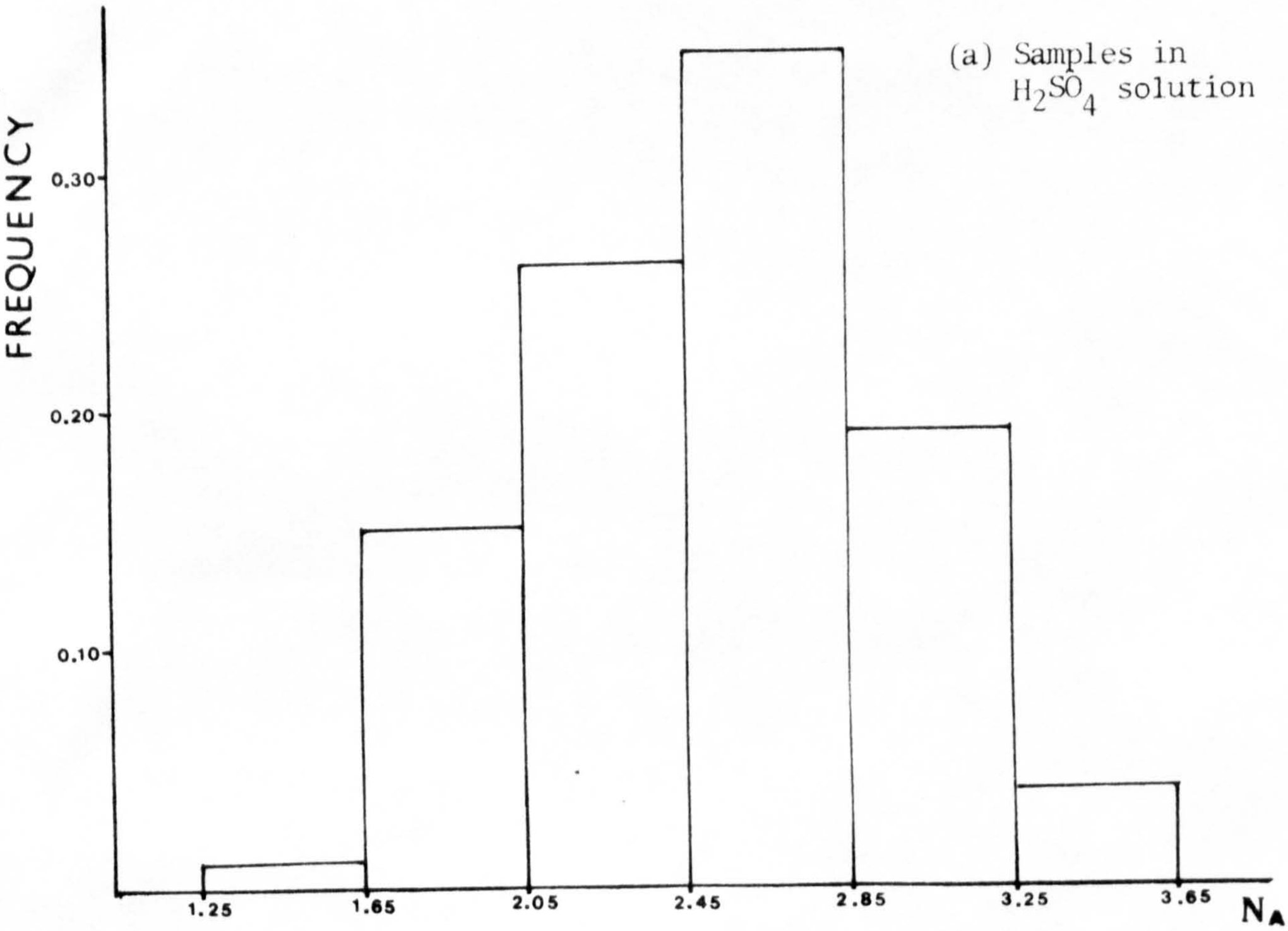

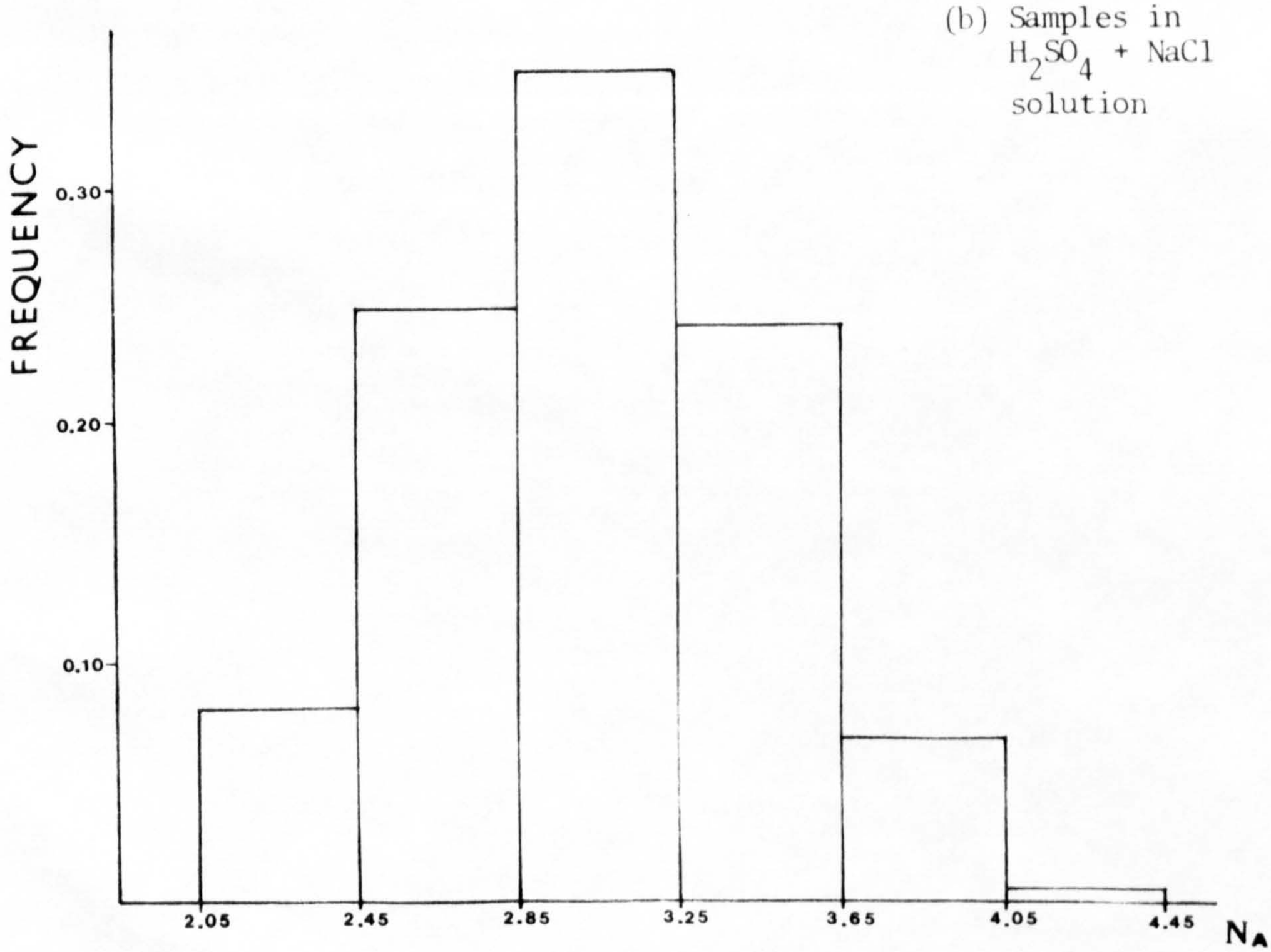

Figs. 118 a and b. Histograms for samples conforming with the null hypothesis in the variance analysis.